US 20110312683A1

(19) **United States**

(12) **Patent Application Publication**

Silverbrook et al.

(10) **Pub. No.: US 2011/0312683 A1**

(43) **Pub. Date: Dec. 22, 2011**

(54) **MICROFLUIDIC TEST MODULE FOR INTERFACING WITH TABLET COMPUTER**

(75) Inventors: **Kia Silverbrook**, Rozelle (AU); **Alireza Moini**, Rozelle (AU); **Mehdi Azimi**, Rozelle (AU)

(73) Assignee: **Geneasys Pty Ltd**

(21) Appl. No.: **13/149,985**

(22) Filed: **Jun. 1, 2011**

Related U.S. Application Data

(60) Provisional application No. 61/356,018, filed on Jun. 17, 2010, provisional application No. 61/437,686, filed on Jan. 30, 2011.

Publication Classification

(51) **Int. Cl.**

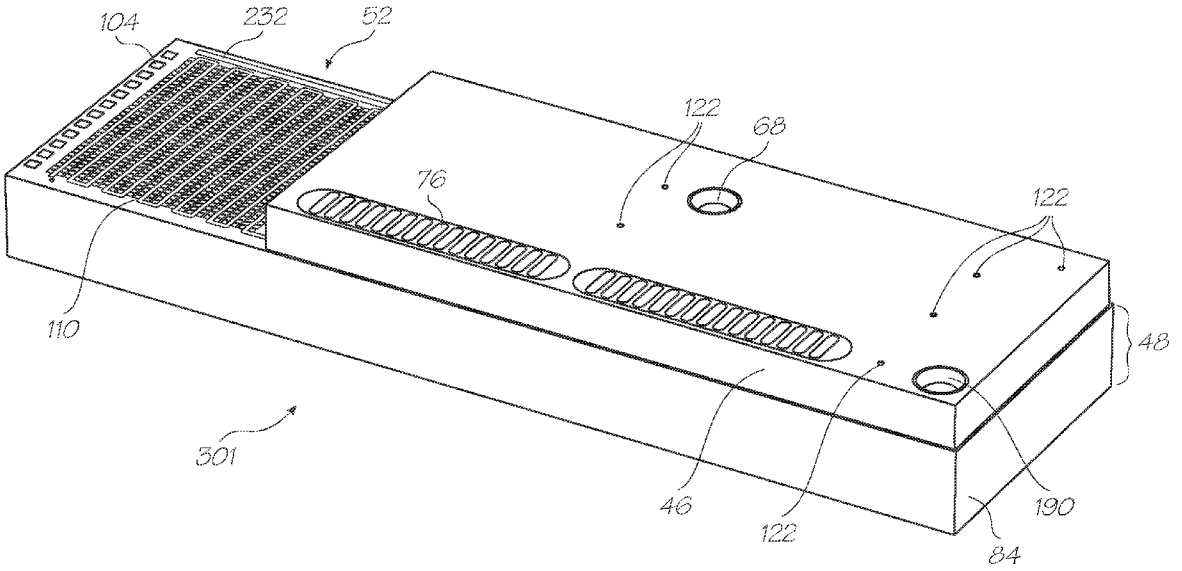
C40B 60/12 (2006.01)

C12M 1/40 (2006.01)

(52) **U.S. Cl.** **506/39**; 435/287.2

(57) **ABSTRACT**

A microfluidic test module for analyzing a sample fluid and communicating test results to a tablet computer, the microfluidic test module having an outer casing with a receptacle for receiving the sample, functional sections for processing and analyzing the sample, a communication interface for communication with the tablet computer, and, a controller for operative control of the communication interface.



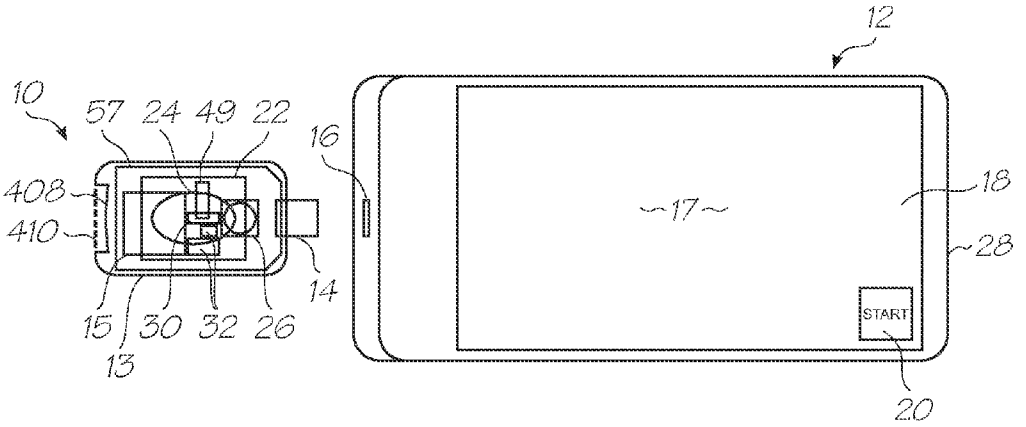

12
10
57
24
49
22
16
408
410
17
18
28
14
START
20
15
13
30
32
26

FIG. 1

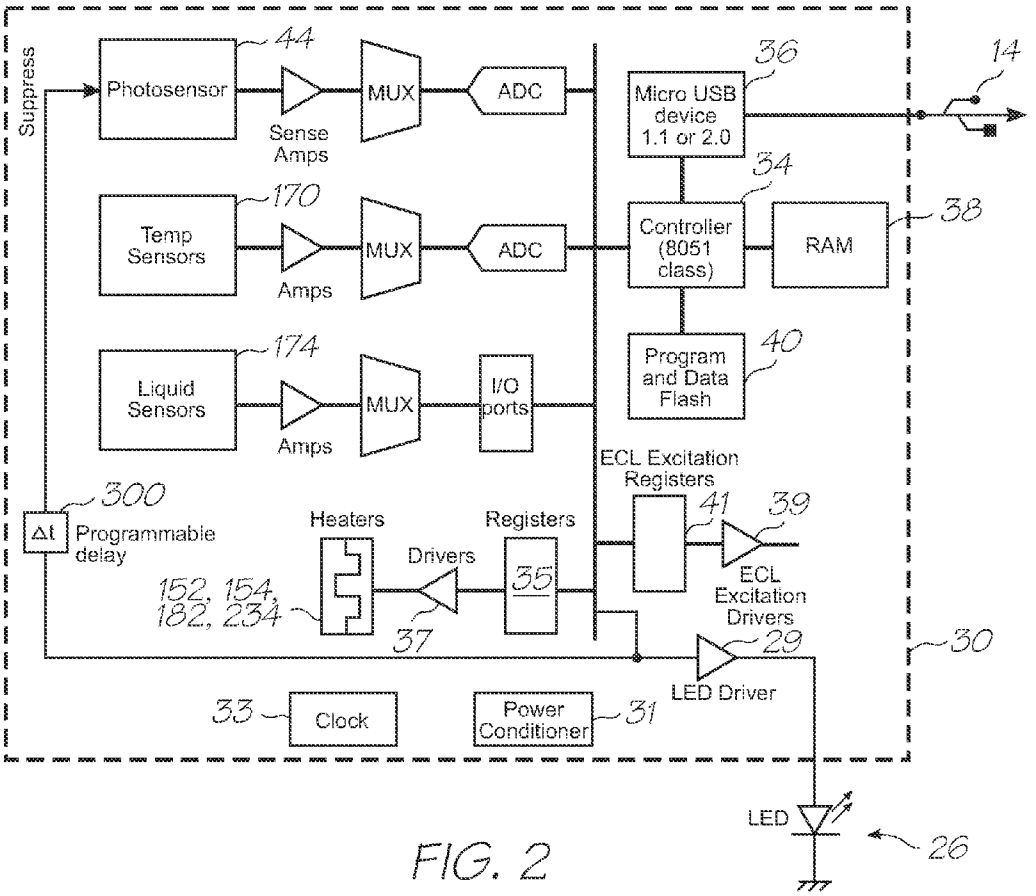

Suppress
Photosensor
44
Sense Amps
MUX
ADC
Micro USB device 1.1 or 2.0
36
14
Temp Sensors
170
Amps
34
Controller (8051 class)
RAM
38
Liquid Sensors
174
I/O ports
Program and Data Flash
40
ECL Excitation Registers
41
39
300
Δt
Programmable delay
Heaters
Registers
Drivers
35
152, 154, 182, 234
37
ECL Excitation Drivers
29
30
LED Driver
33
Clock
Power Conditioner
31
LED
26

FIG. 2

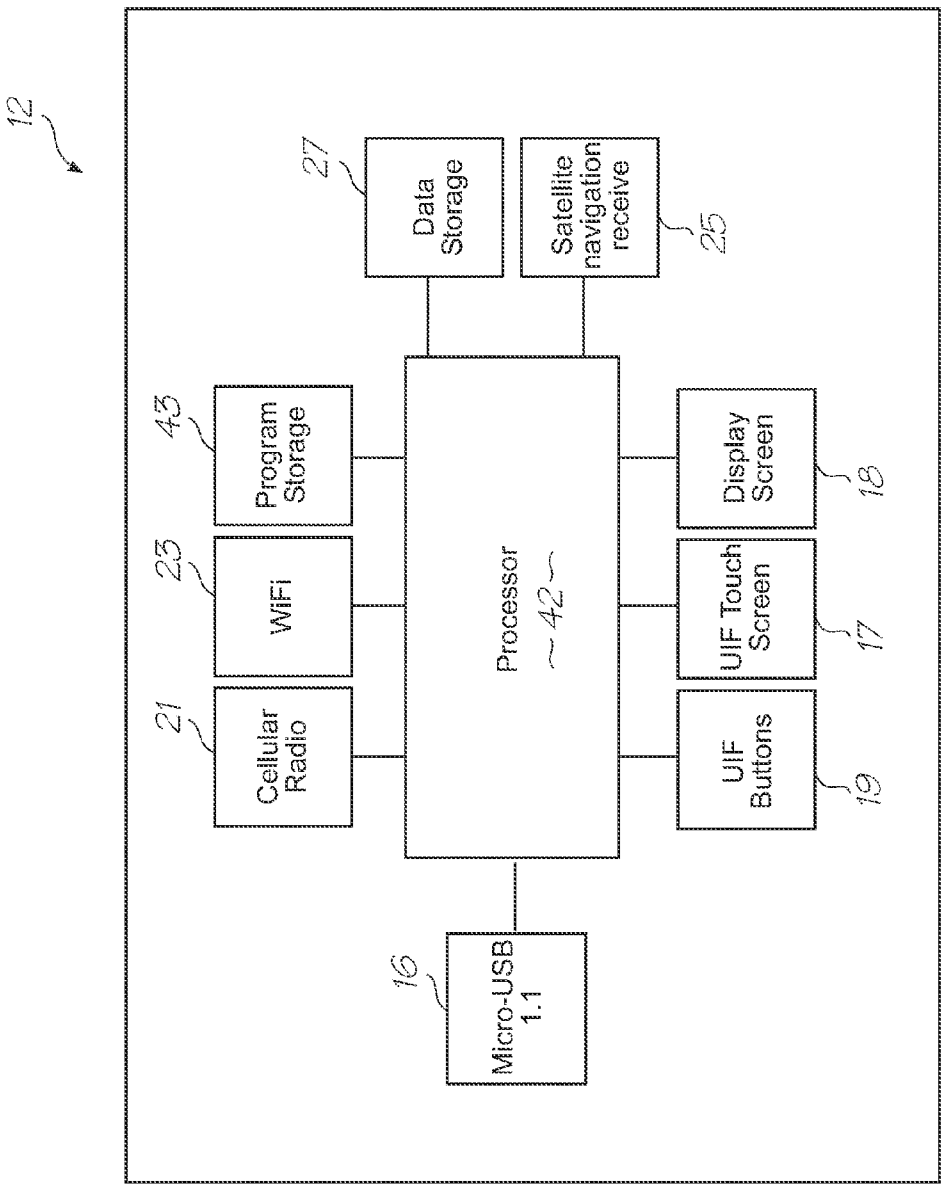

12
27
Data Storage
Satellite navigation receive
25
43
Program Storage
23
WiFi
21
Cellular Radio
Processor
42
Display Screen
18
UIF Touch Screen
17
UIF Buttons
19
16
Micro-USB 1.1

FIG. 3

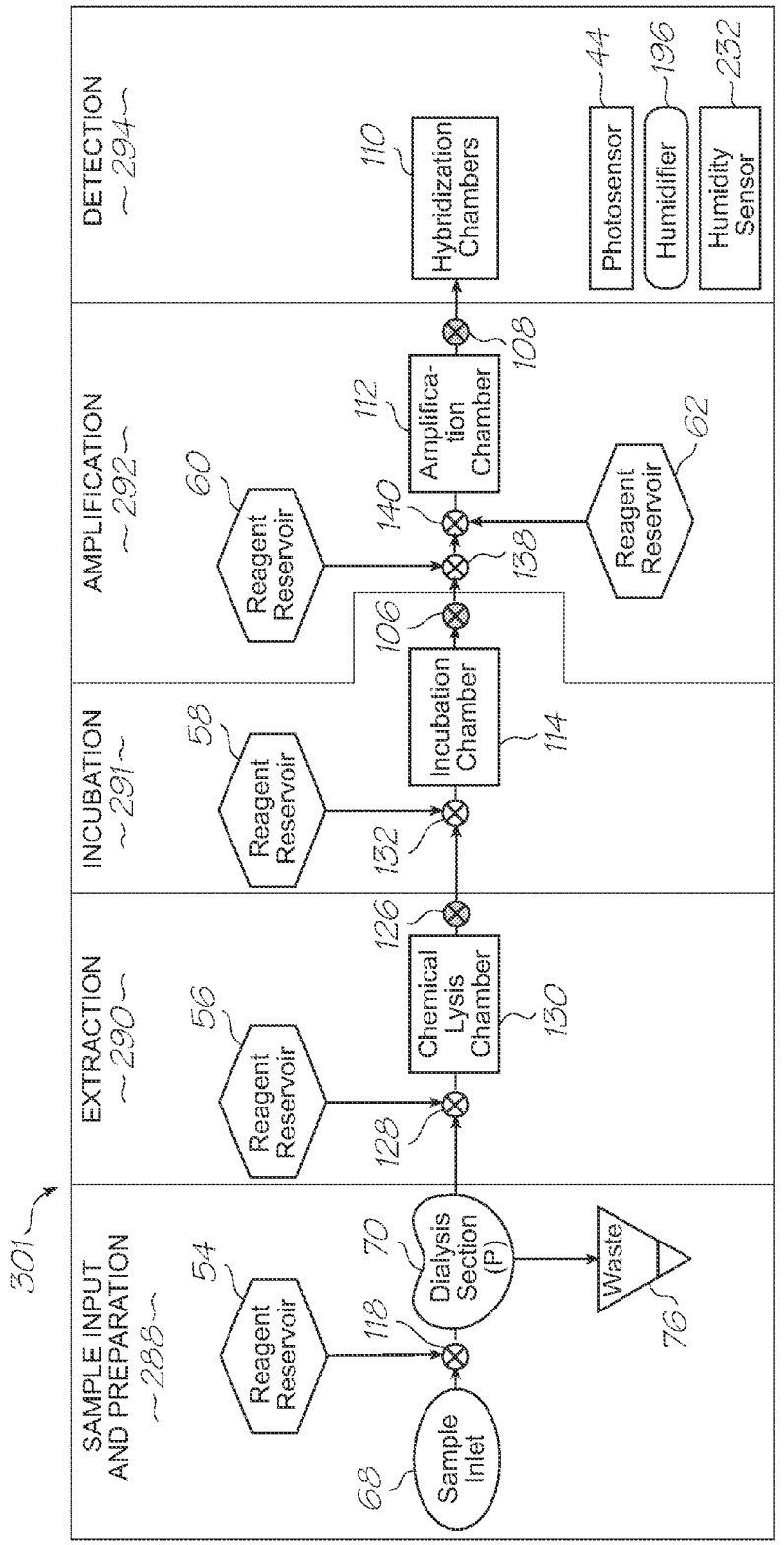

301
SAMPLE INPUT AND PREPARATION ~286~
EXTRACTION ~290~
INCUBATION ~291~
AMPLIFICATION ~292~
DETECTION ~294~
Sample Inlet
68
Reagent Reservoir
54
118
Dialysis Section (P)
70
Waste
76
Reagent Reservoir
56
128
Chemical Lysis Chamber
130
126
Reagent Reservoir
58
132
Incubation Chamber
114
106
Reagent Reservoir
60
140
Amplification Chamber
112
138
Reagent Reservoir
62
108
Hybridization Chambers
110
Photosensor
44
Humidifier
196
Humidity Sensor
232
KEY
⊗ Surface tension valve
⊗ Boiling - initiated valve
⊗ Thermal bend actuator valve
⊕ Fault tolerant valve array
P Pathogen target
L Leukocyte target

FIG. 4

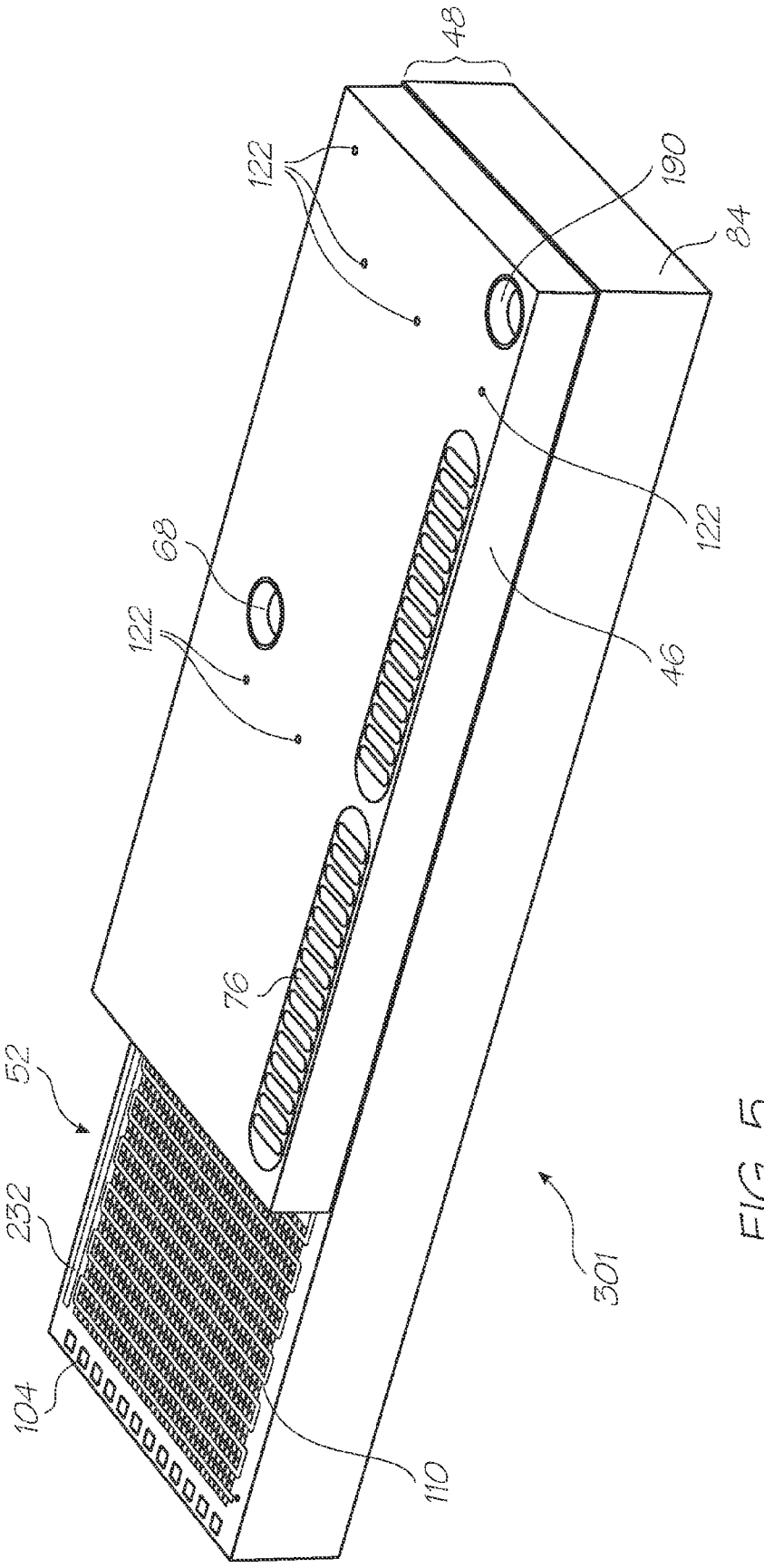


FIG. 5

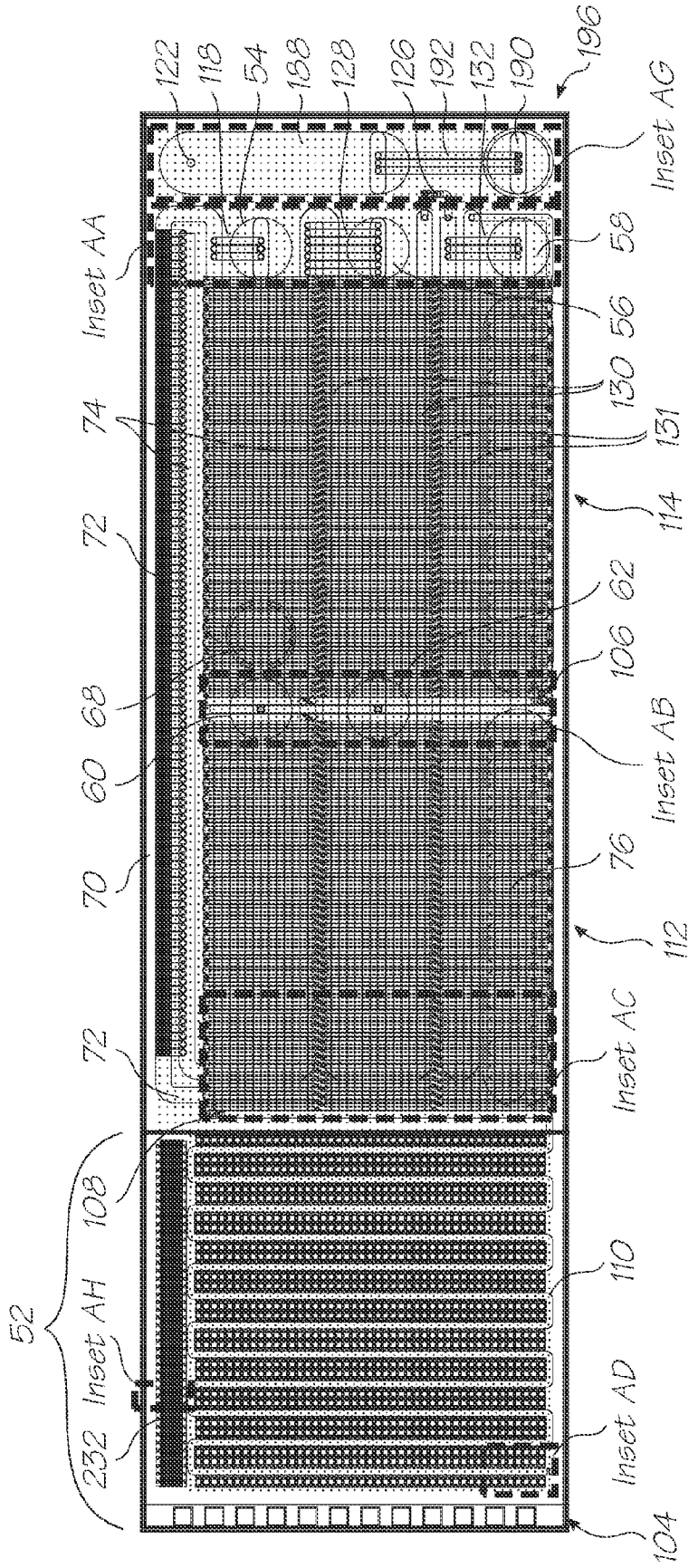

122
118
54
138
128
126
192
132
190
196
Inset AG
58
56
130
131
114
62
106
Inset AB
76
112
Inset AC
72
74
72
68
60
70
52
108
Inset AH
232
110
Inset AD
104

FIG. 6

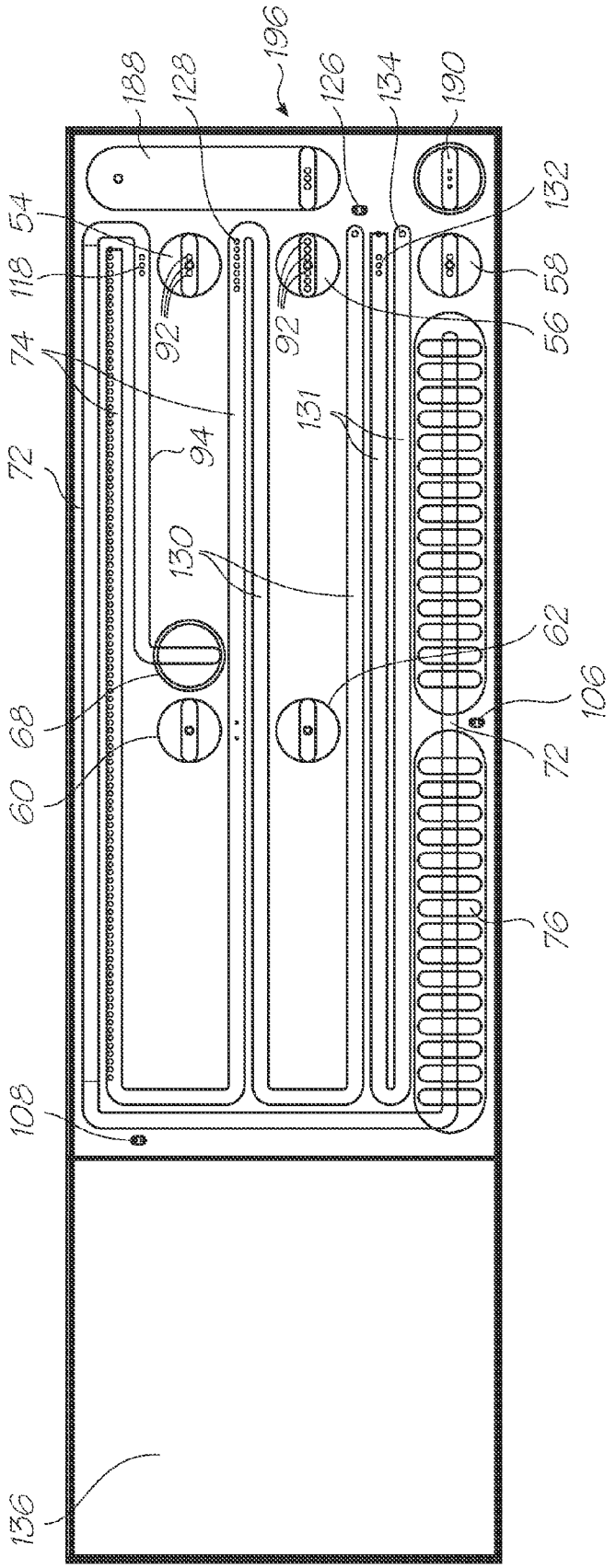

196
188
128
126
134
190
132
54
118
92
92
58
56
74
94
131
72
130
62
106
68
72
60
76
108
136

FIG. 7

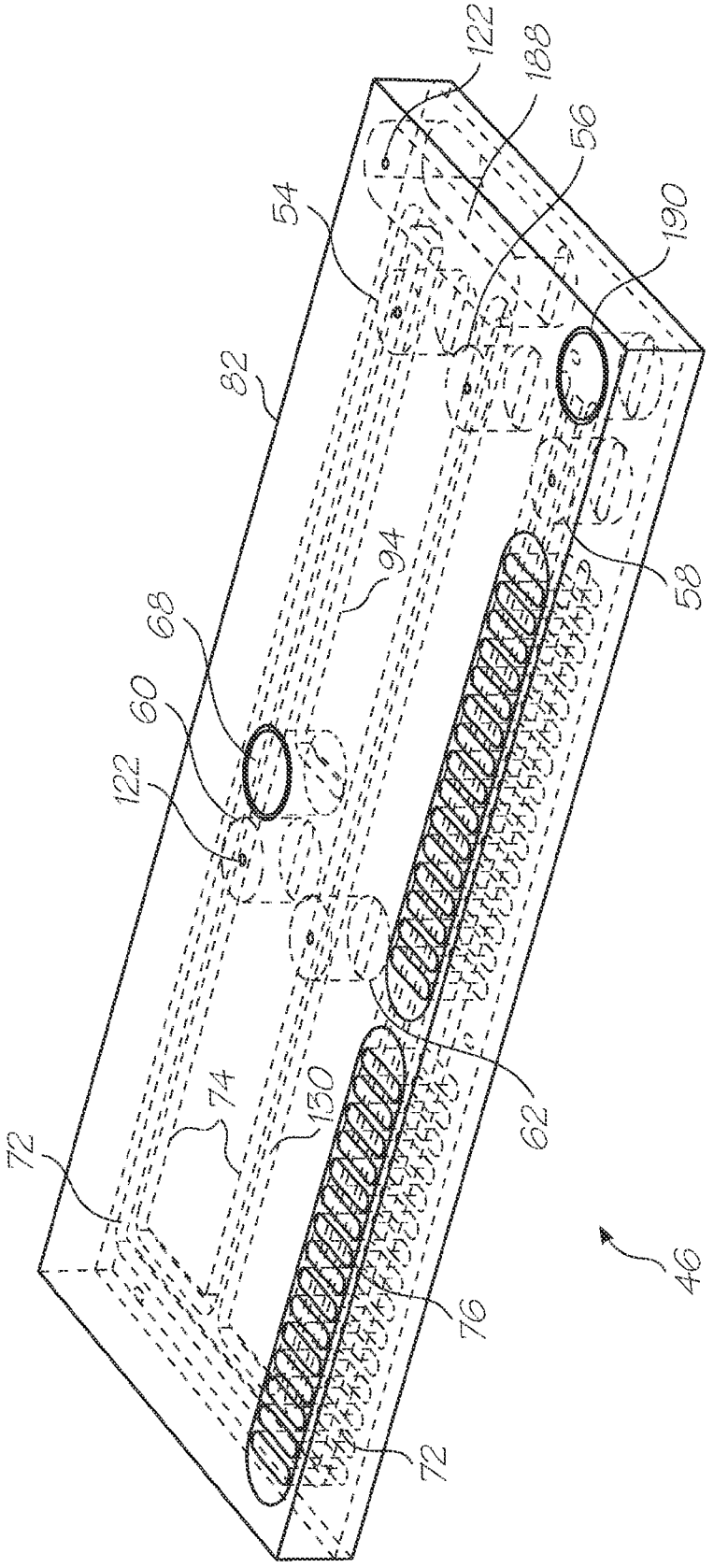


FIG. 8

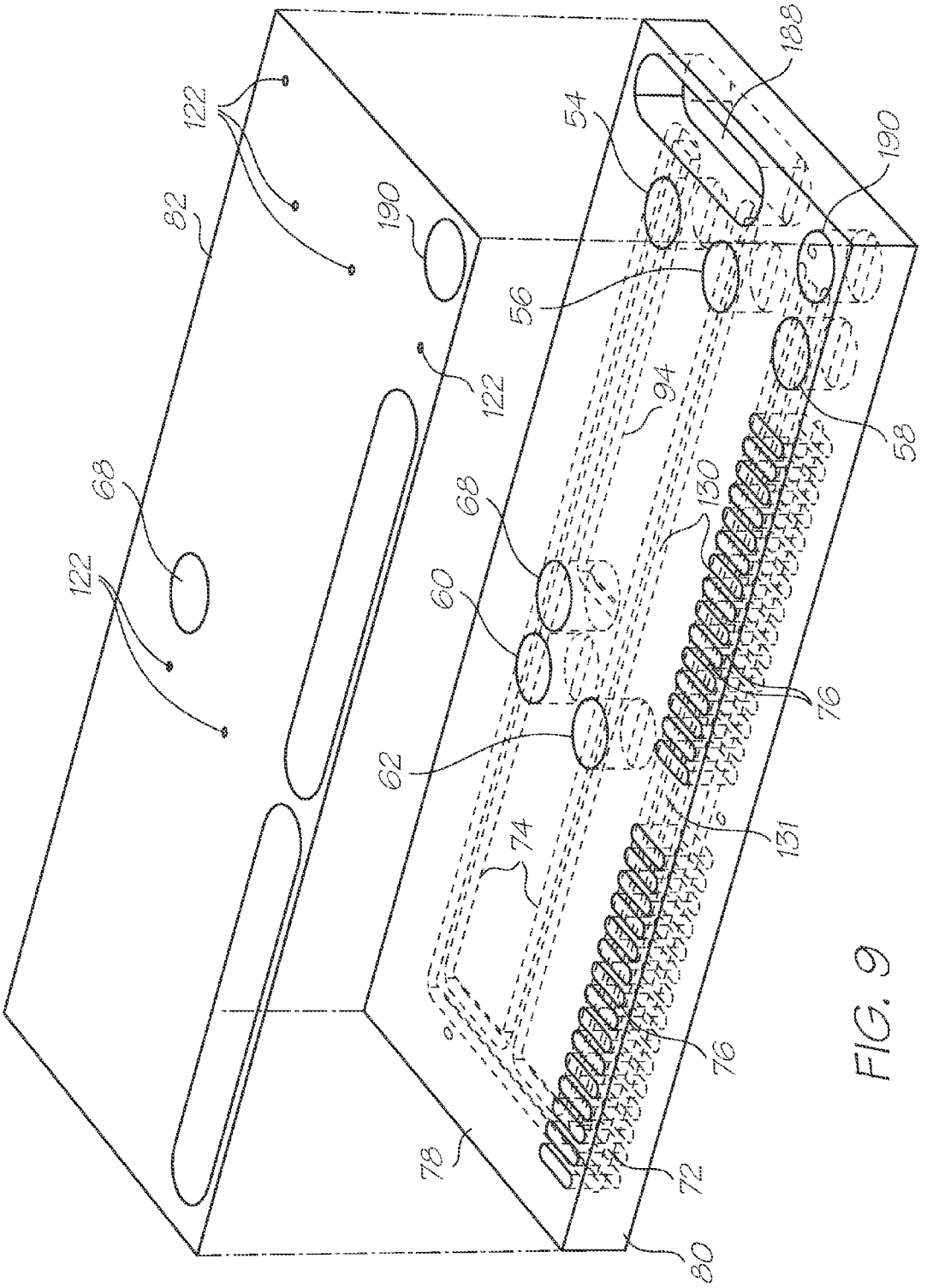

122
82
190
54
188
190
56
122
94
58
68
68
122
60
130
62
76
74
131
76
78
72
80

FIG. 9

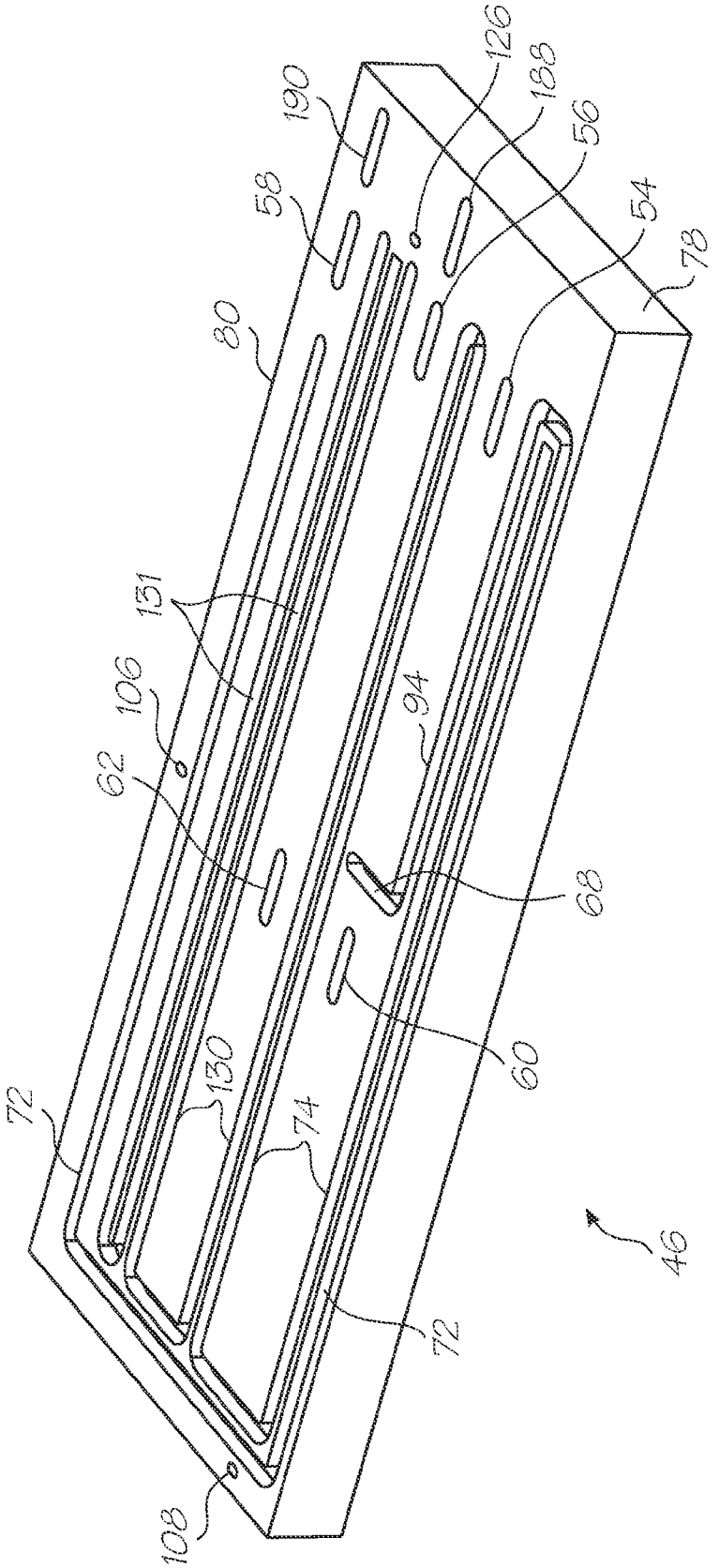


FIG. 10

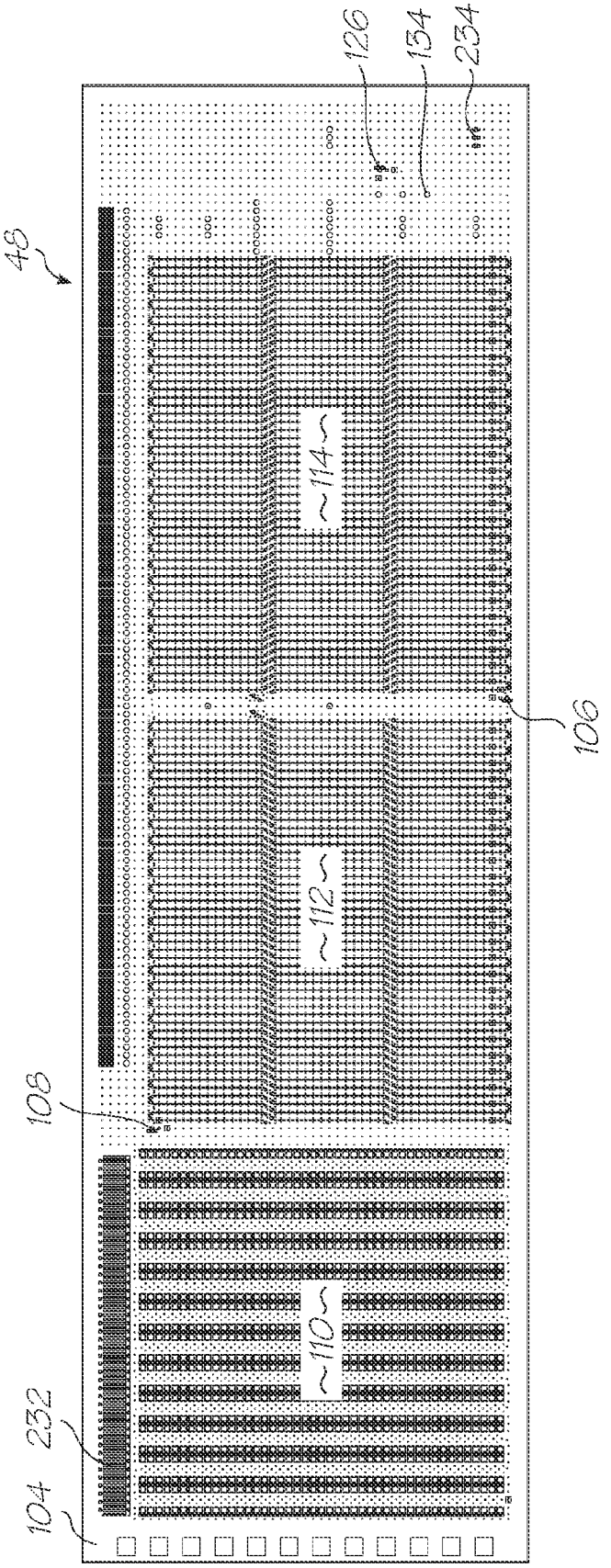


FIG. 11

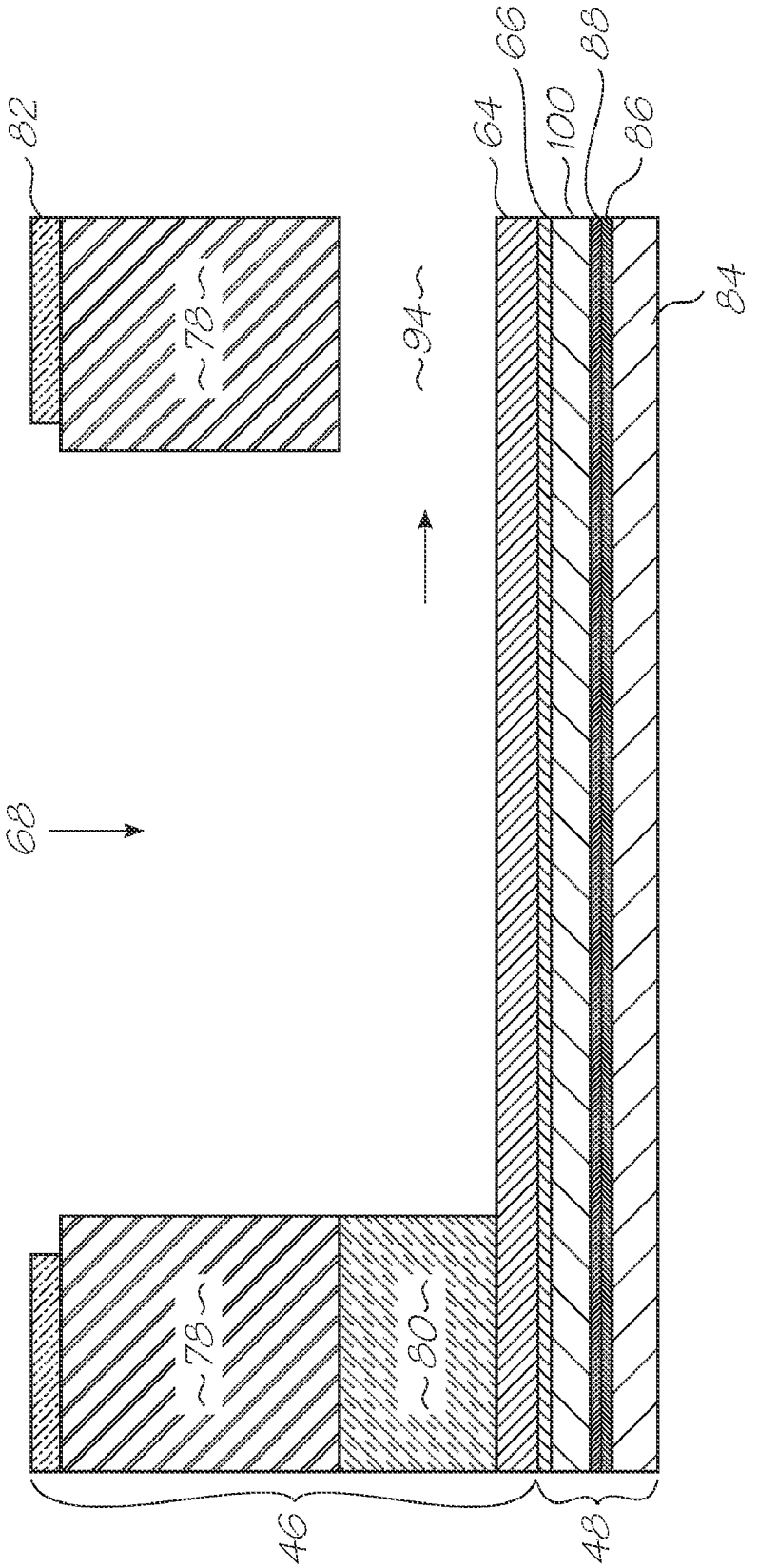


FIG. 12

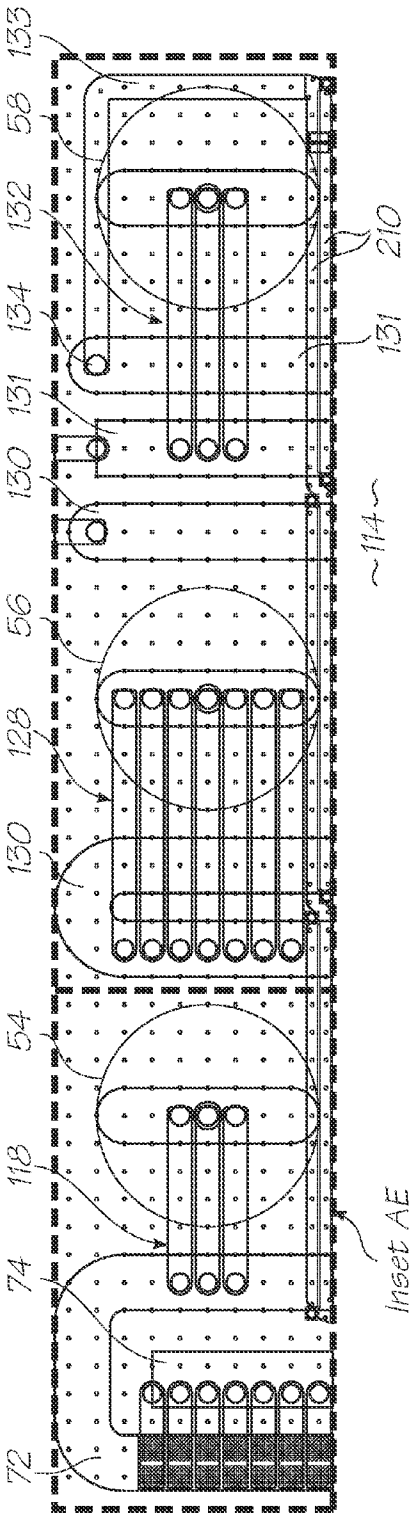


FIG. 13 (Inset AA)

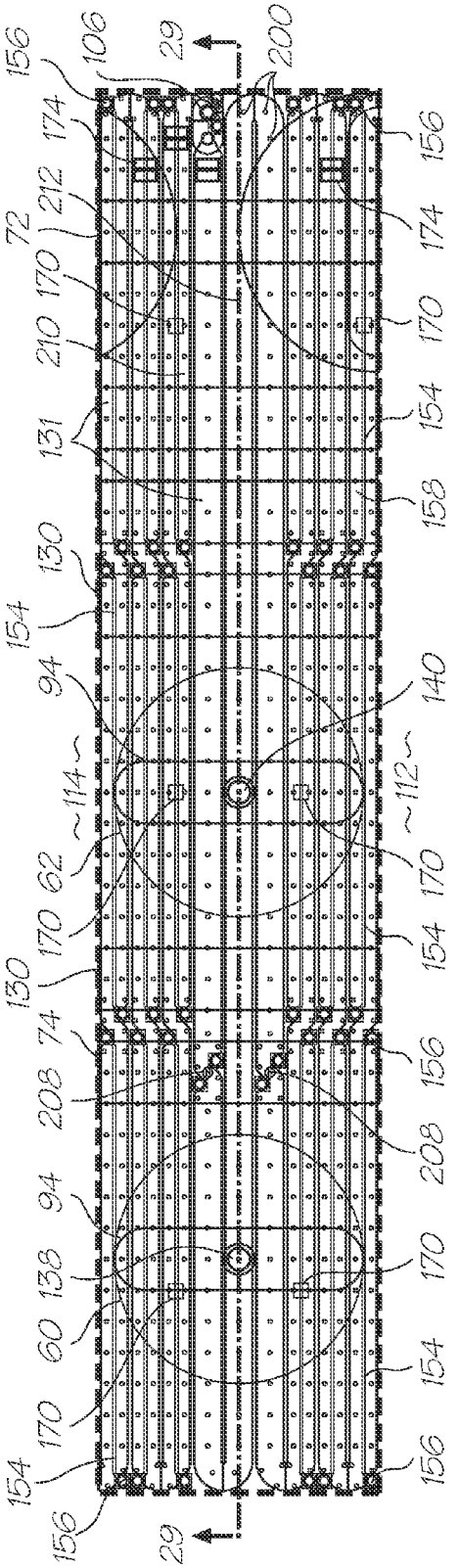


FIG. 14 (Inset AB)

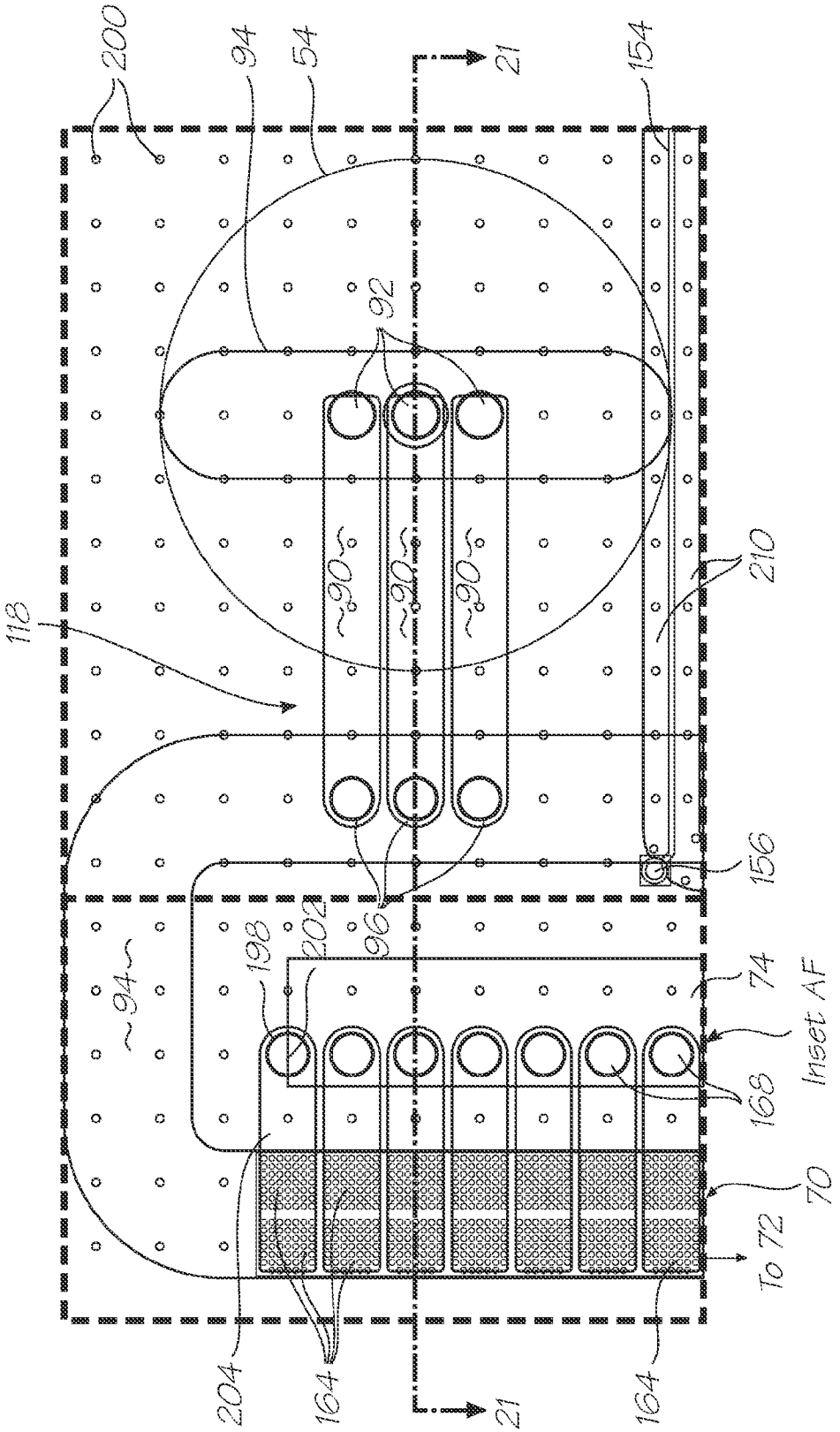


FIG. 15 (Inset AE)

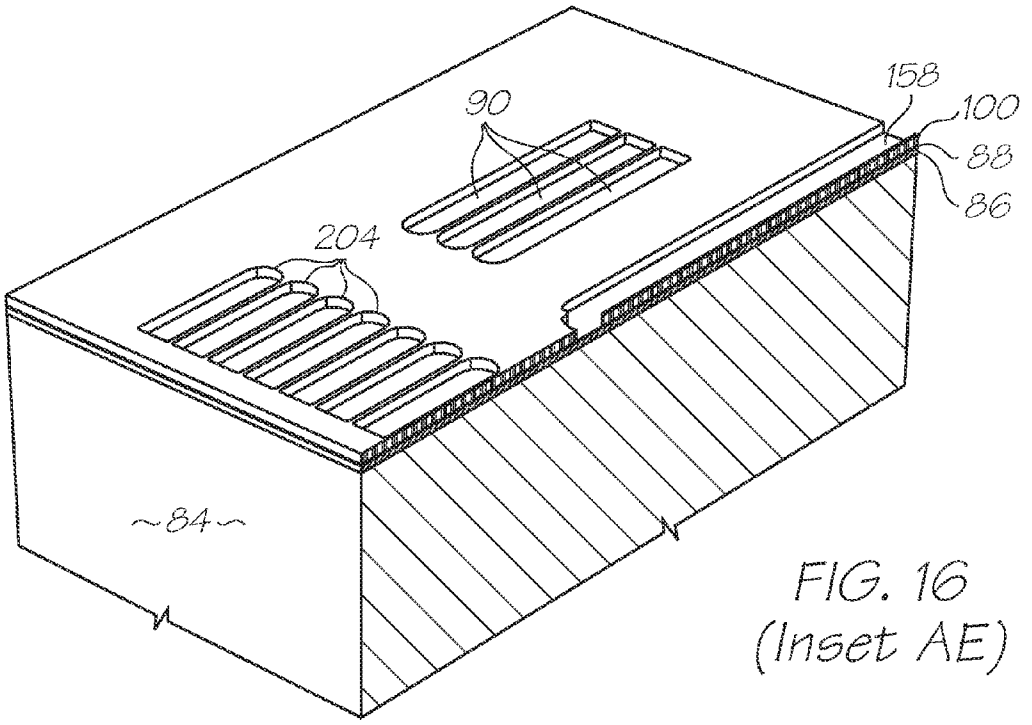


FIG. 16
(Inset AE)

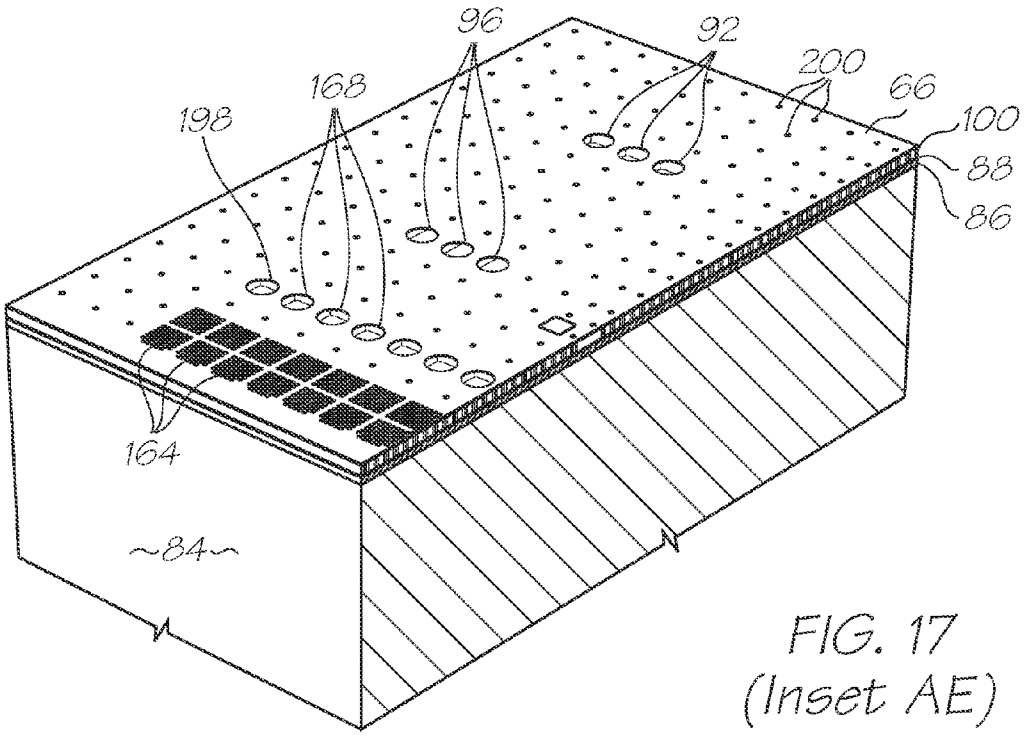


FIG. 17
(Inset AE)

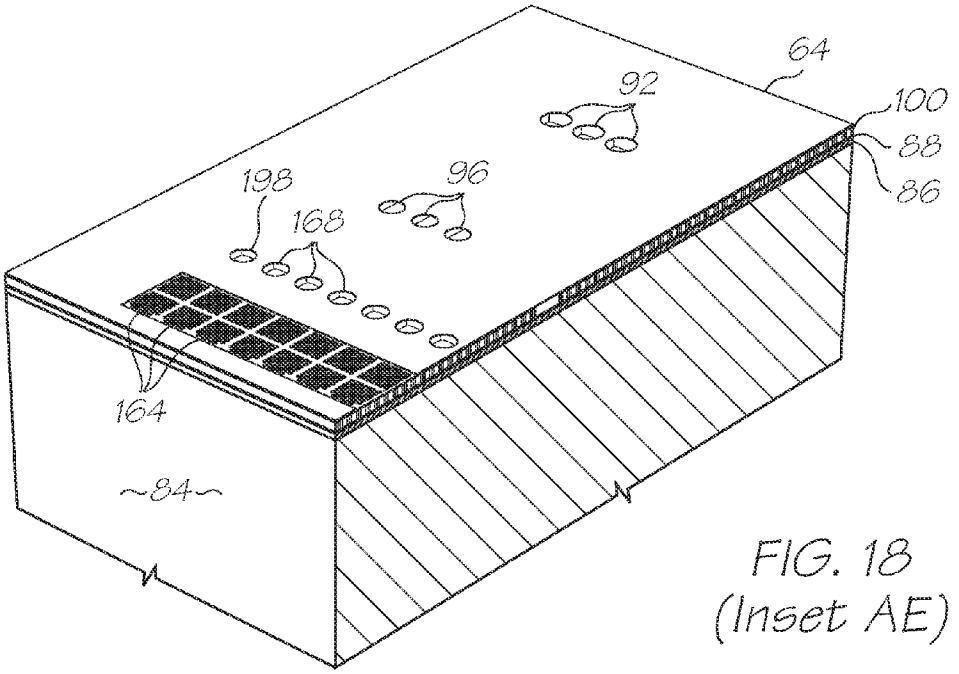


FIG. 18
(Inset AE)

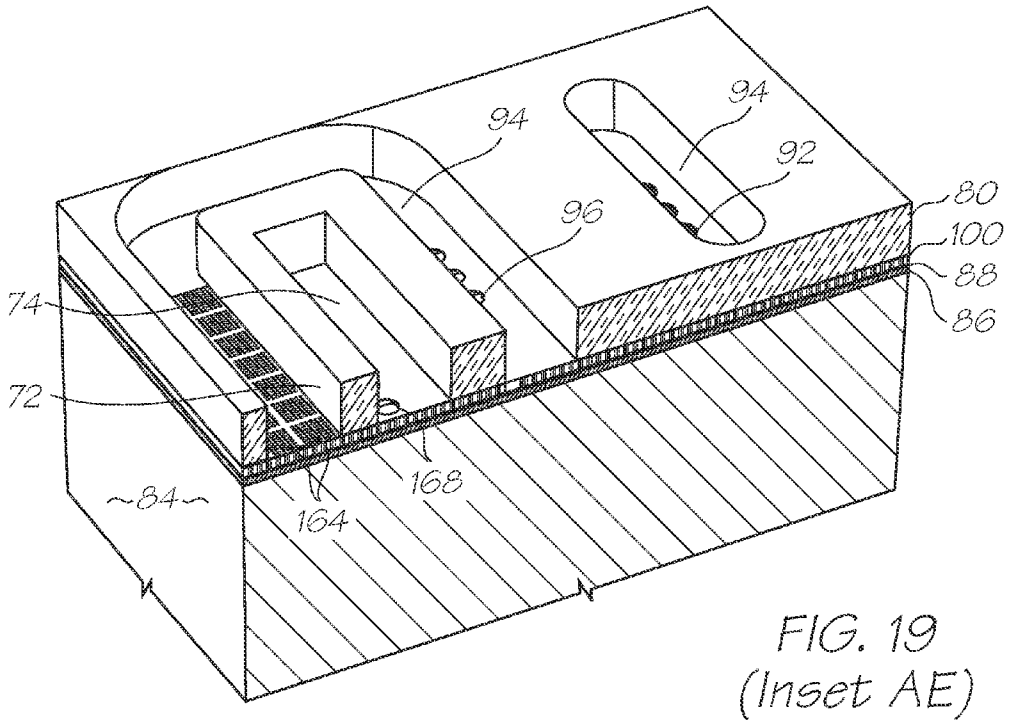


FIG. 19
(Inset AE)

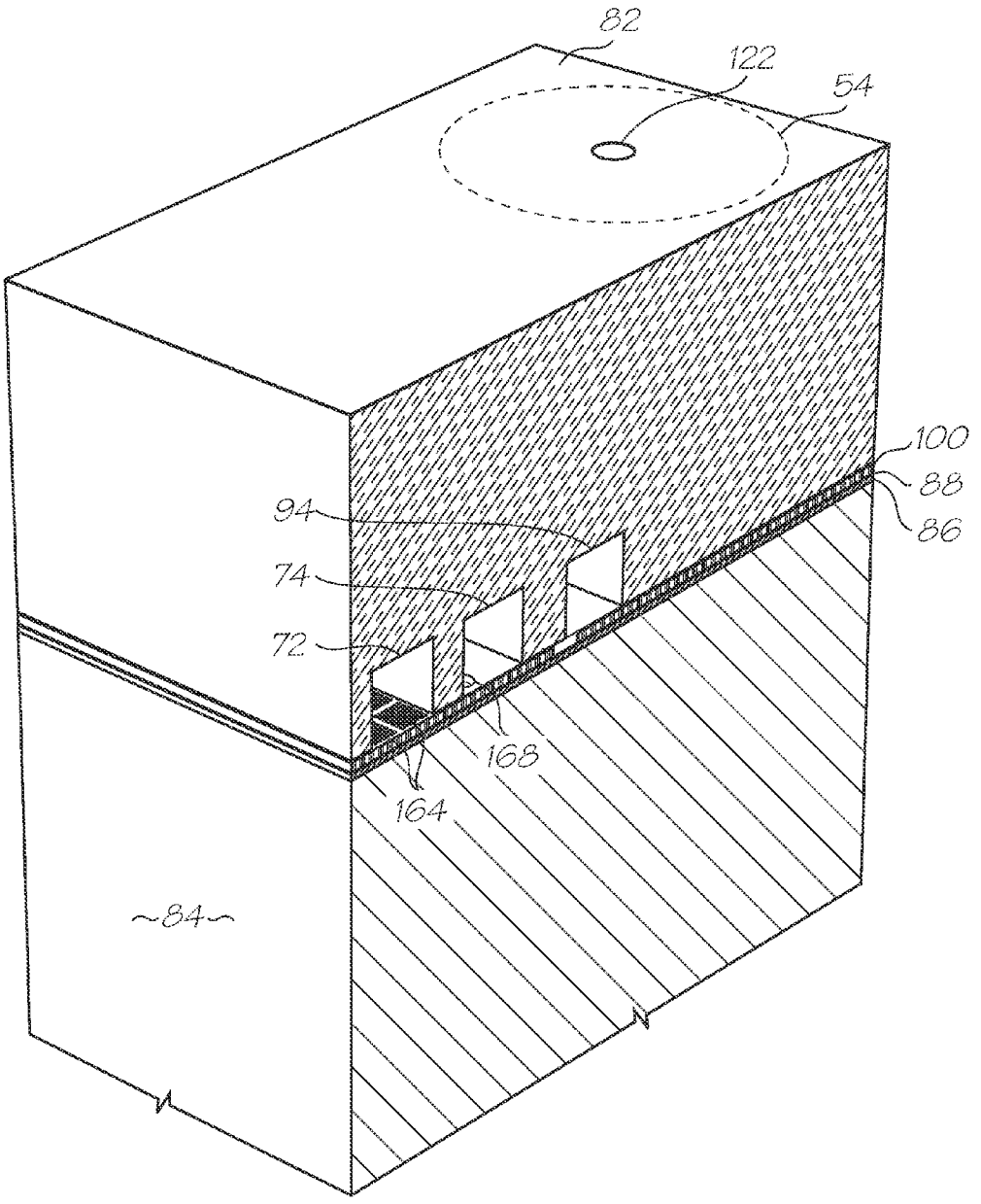


FIG. 20
(Inset AE)

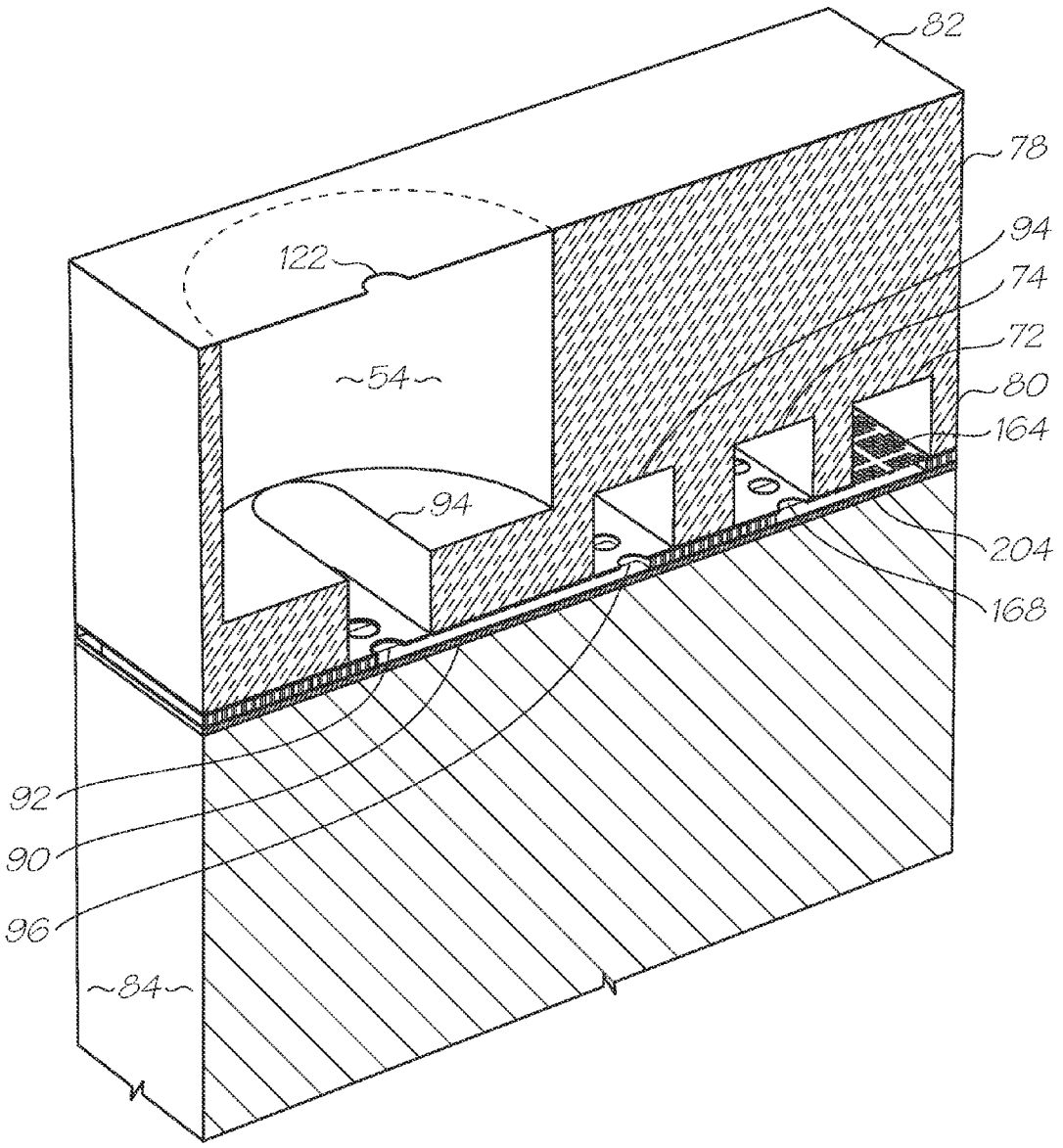


FIG. 21
(Inset AE)

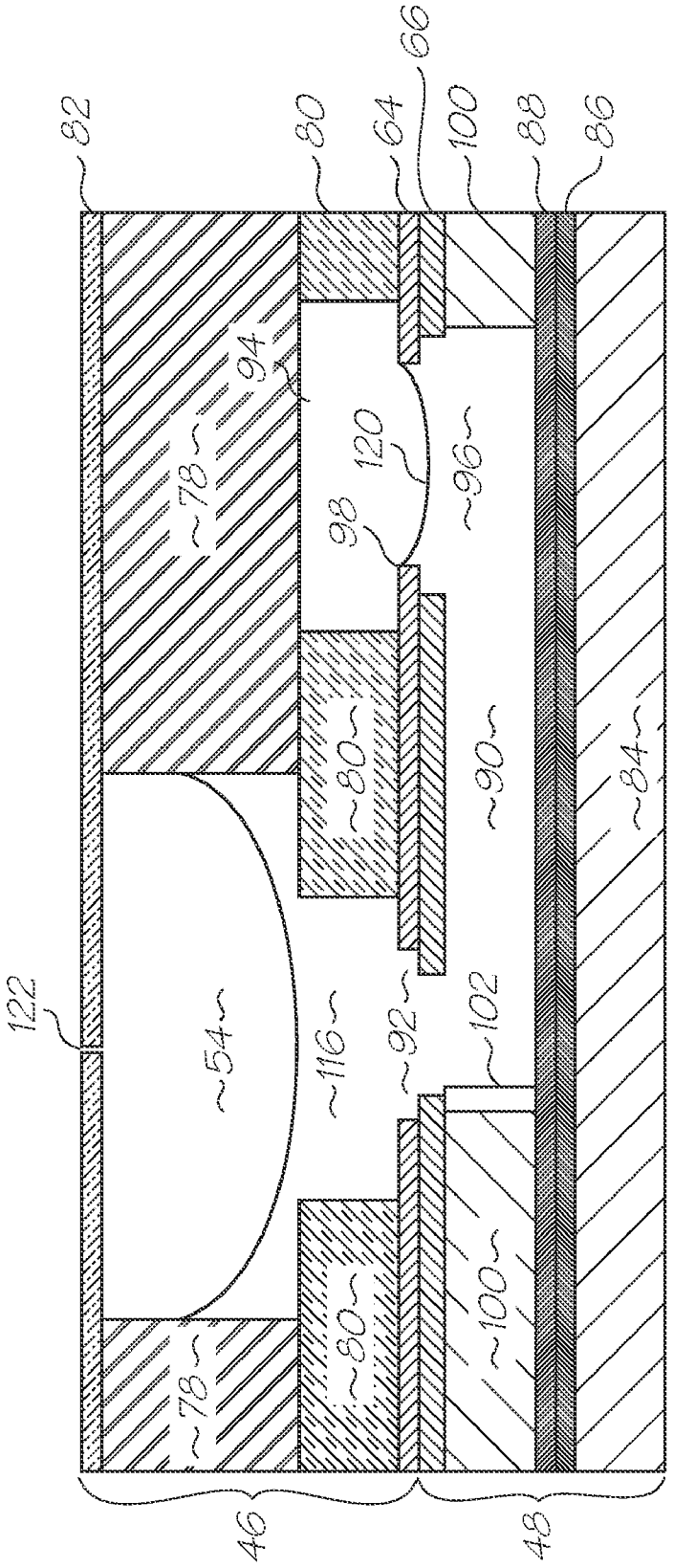

82
80
64
66
100
88
86
94
78
120
98
96
80
90
84
122
54
116
92
102
80
100
78
46
48

FIG. 22

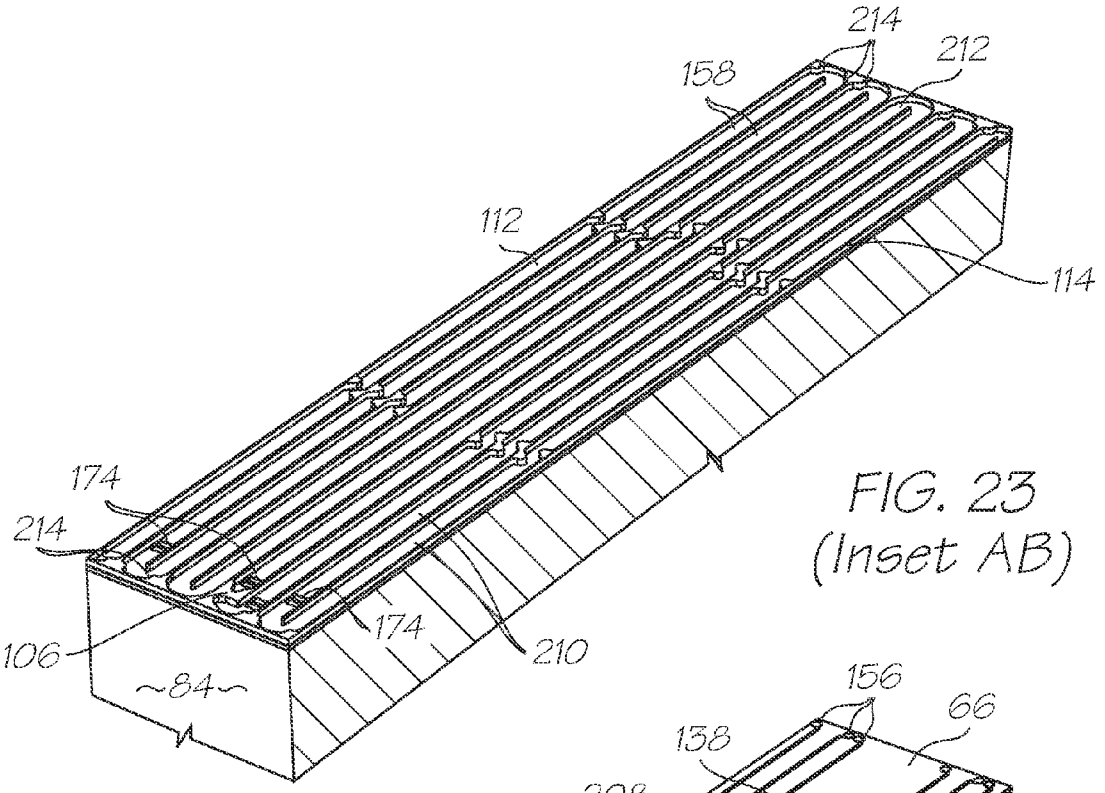


FIG. 23
(Inset AB)

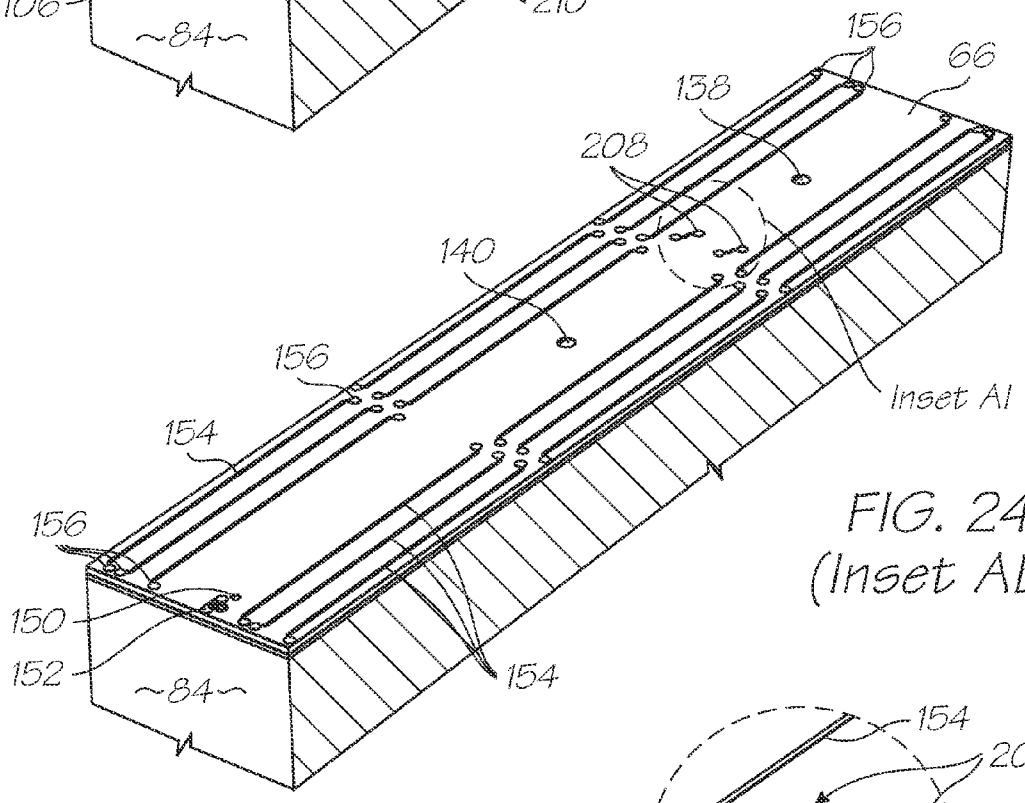


FIG. 24
(Inset AB)

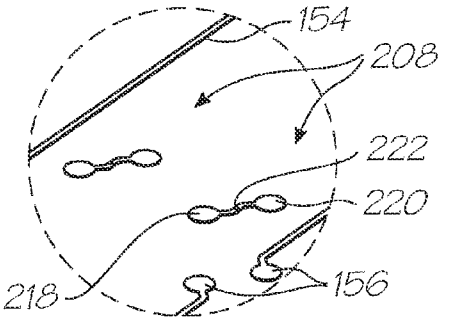


FIG. 25
(Inset AI)

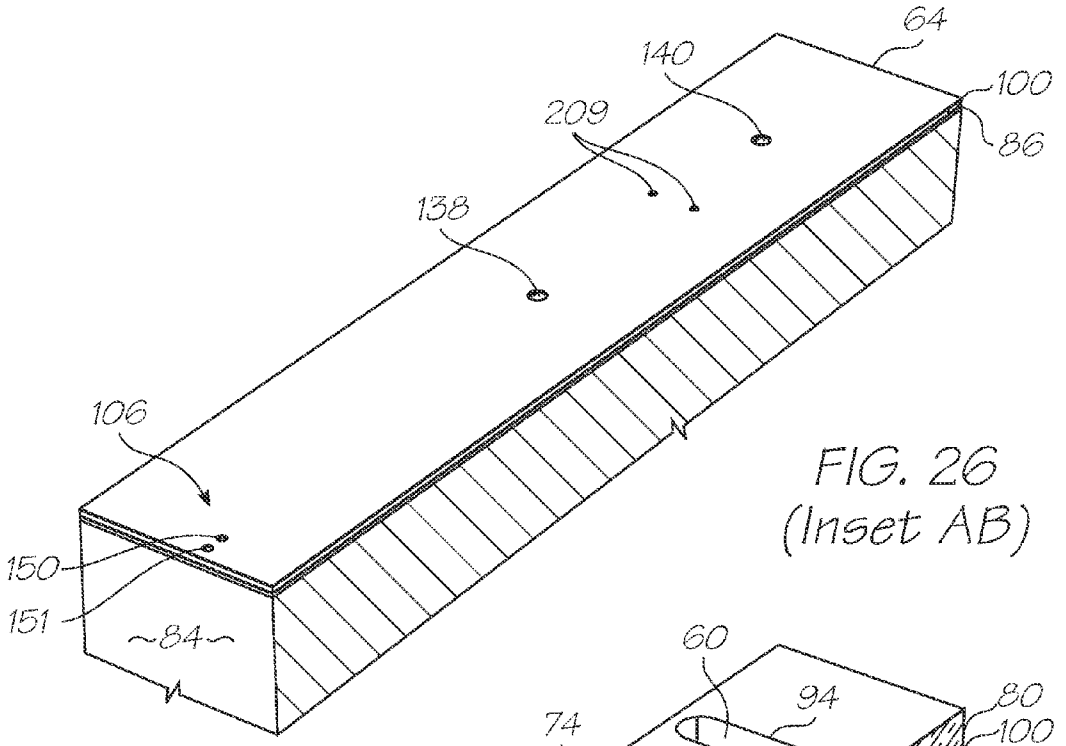


FIG. 26
(Inset AB)

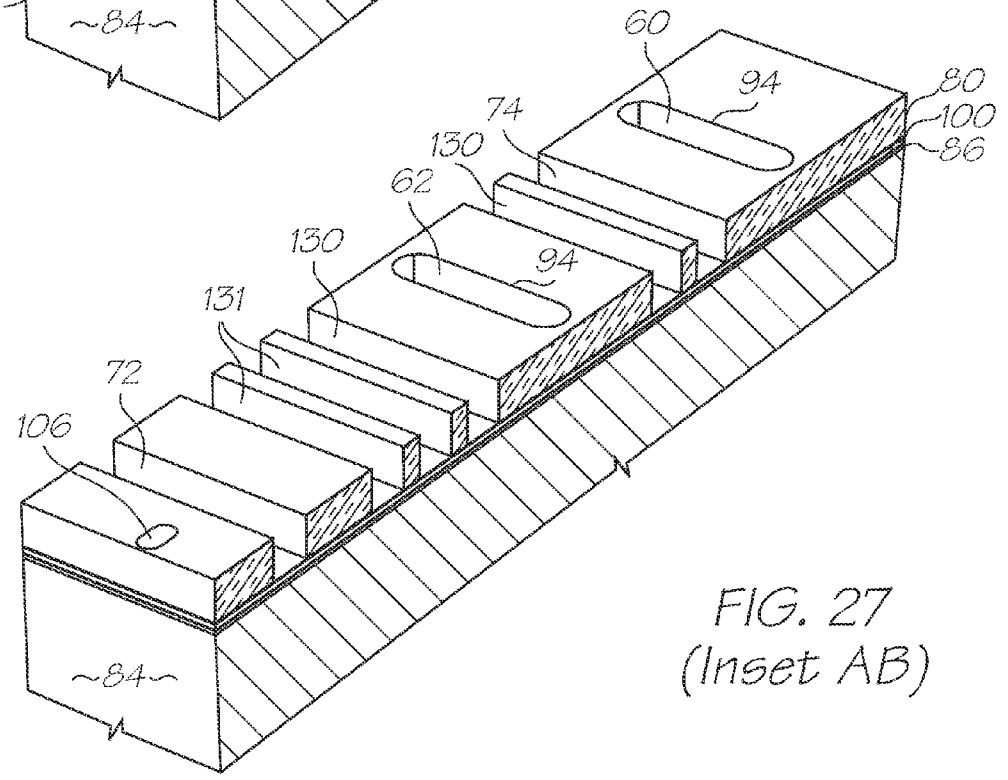


FIG. 27
(Inset AB)

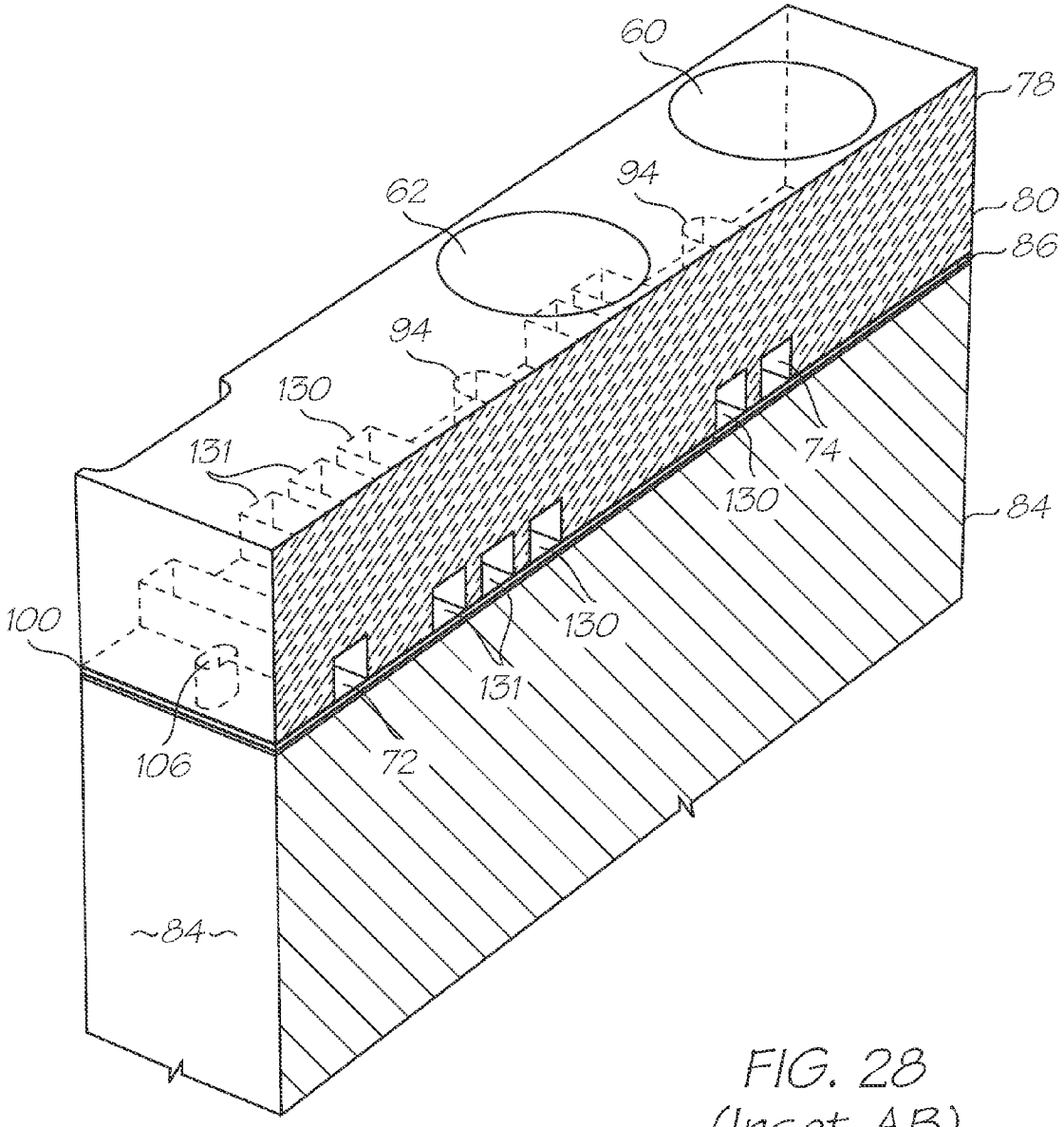


FIG. 28
(Inset AB)

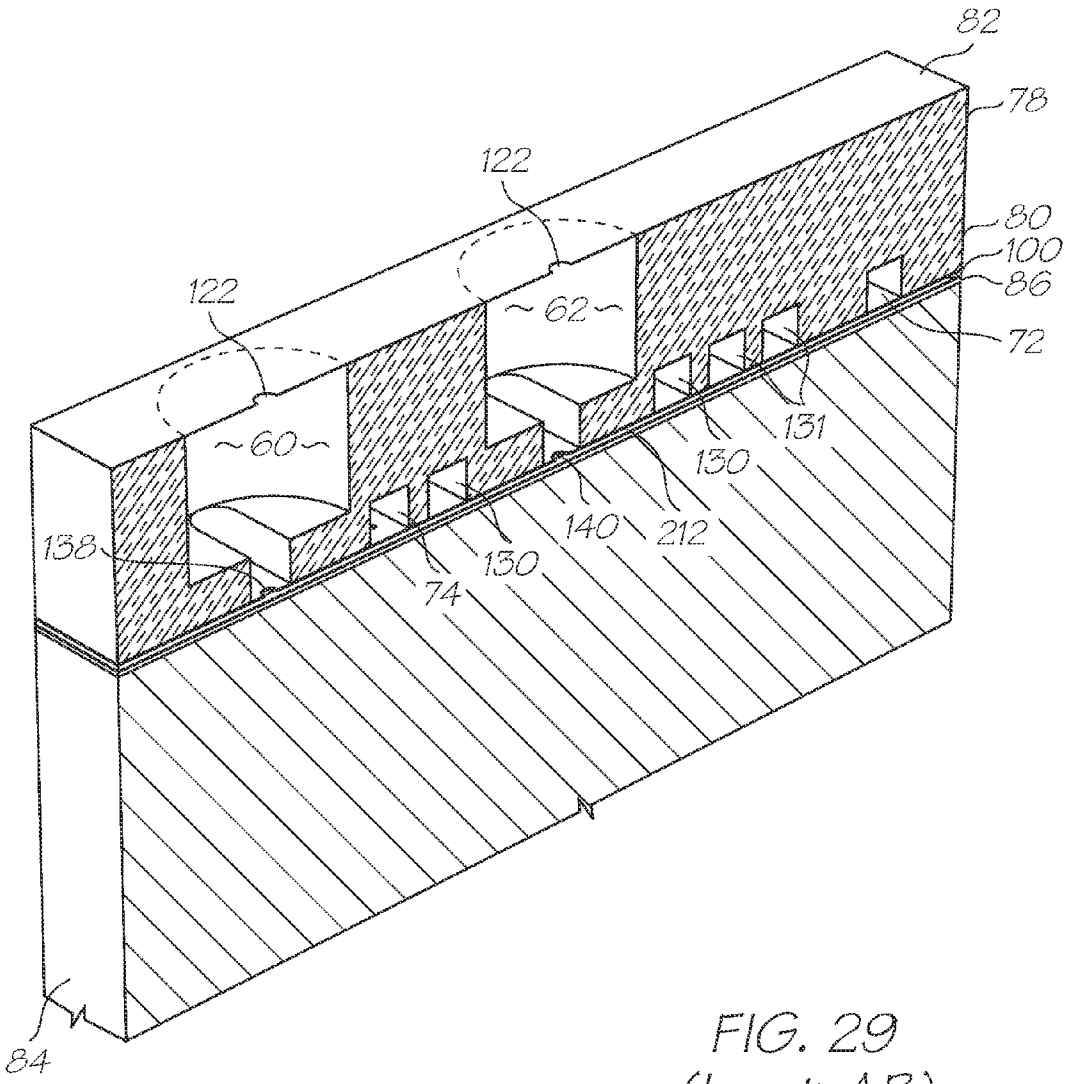


FIG. 29
(Inset AB)

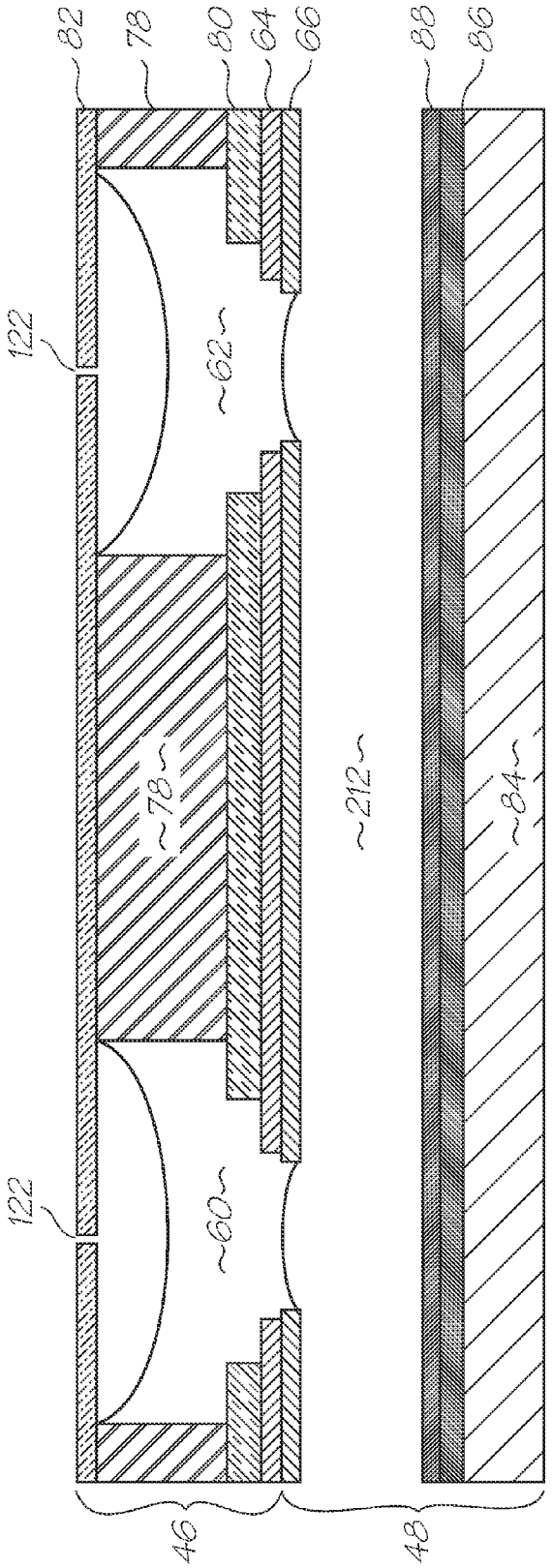

82
78
80
64
66
88
86
122
62
78
212
84
122
60
46
48

FIG. 30

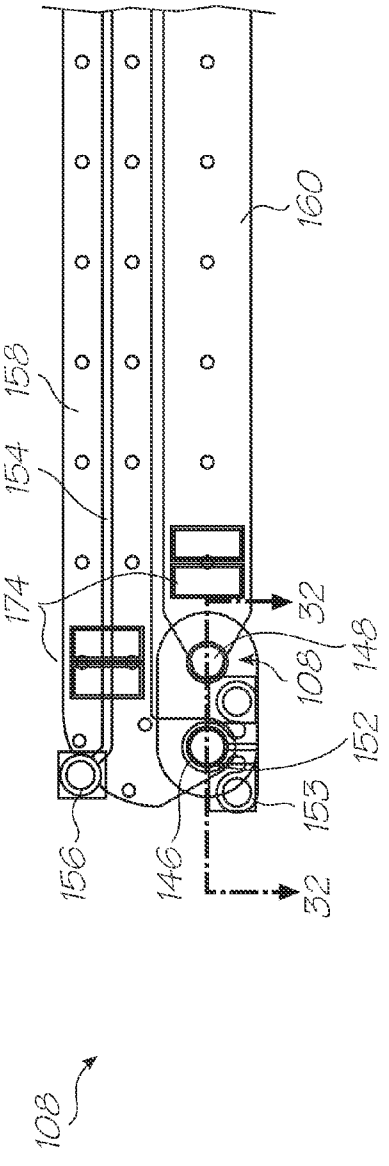

160
158
154
174
32
148
108
152
153
156
146
32
108

FIG. 31

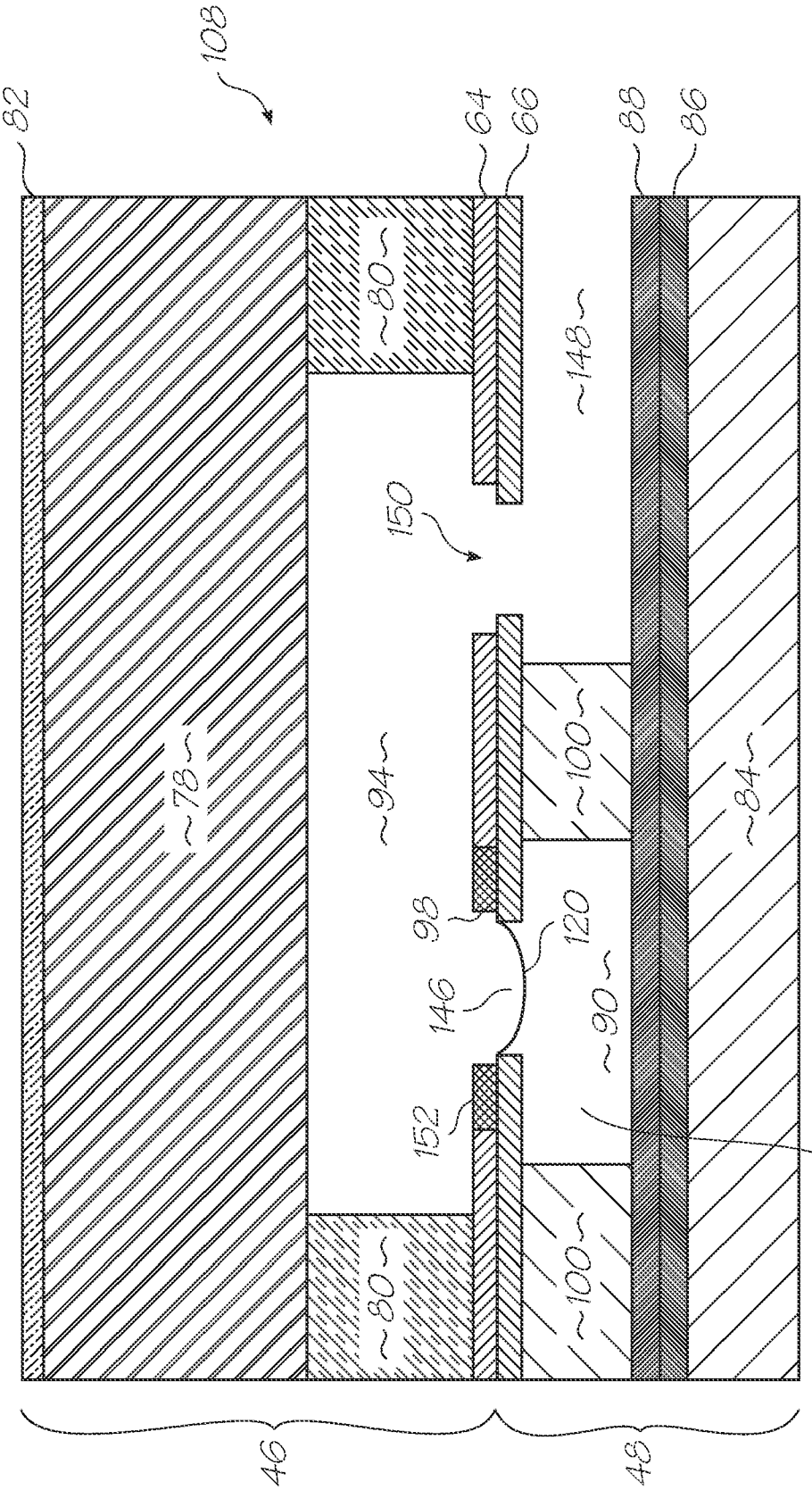

108
82
64
66
88
86
80
148
150
78
94
100
84
98
120
146
90
152
119
80
100
46
48

FIG. 32

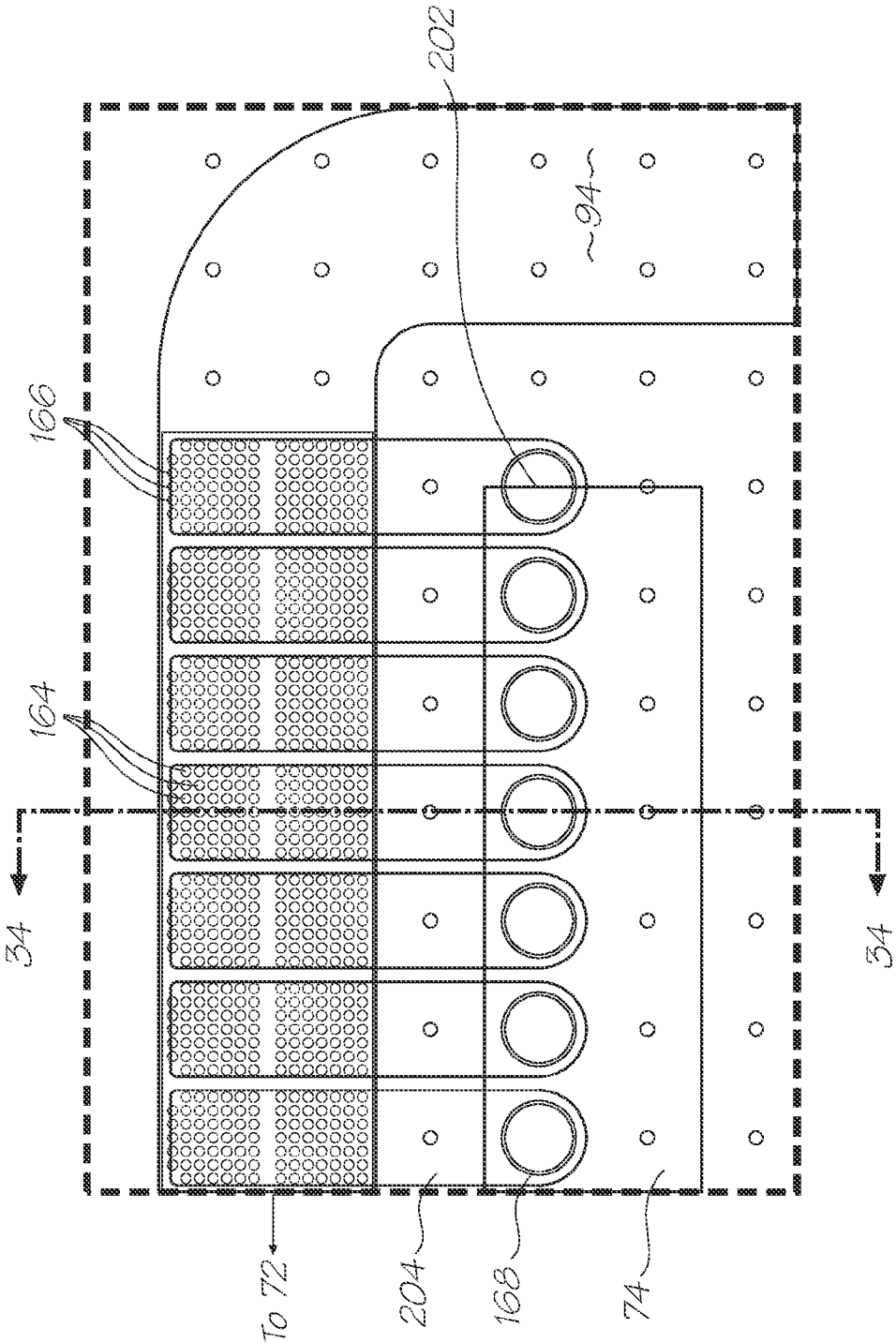


FIG. 33 (Inset AF)

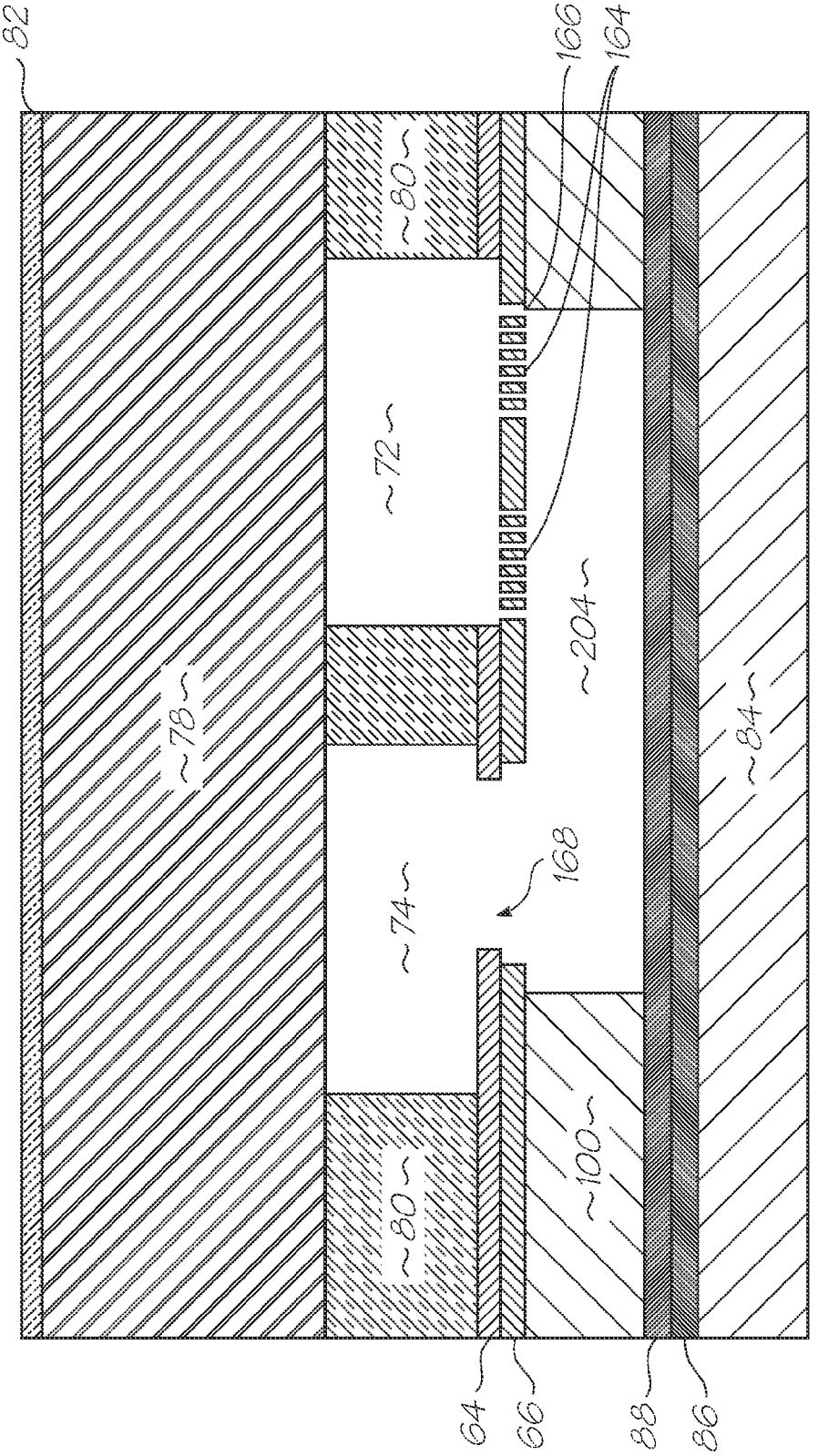


FIG. 34

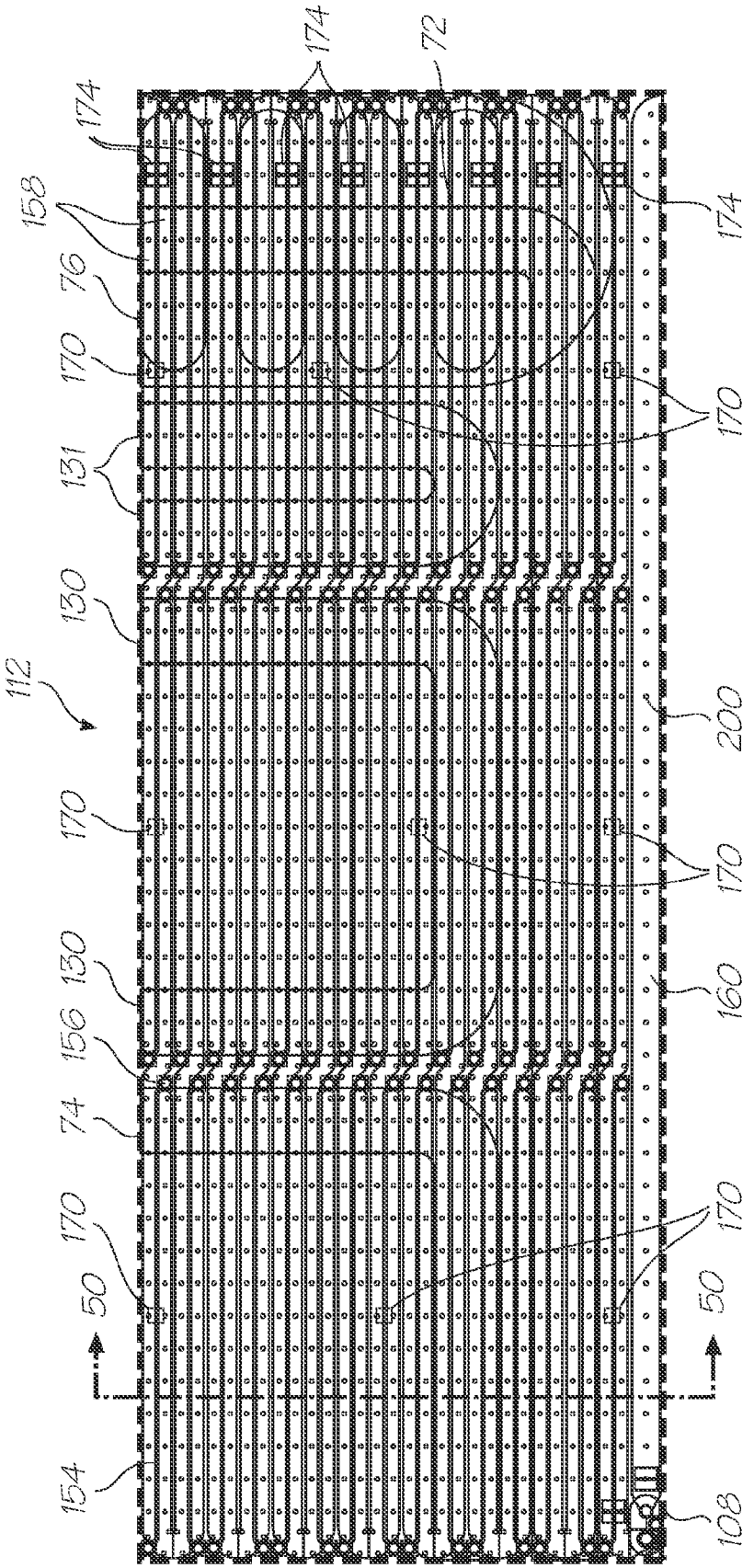


FIG. 35 (Inset AC)

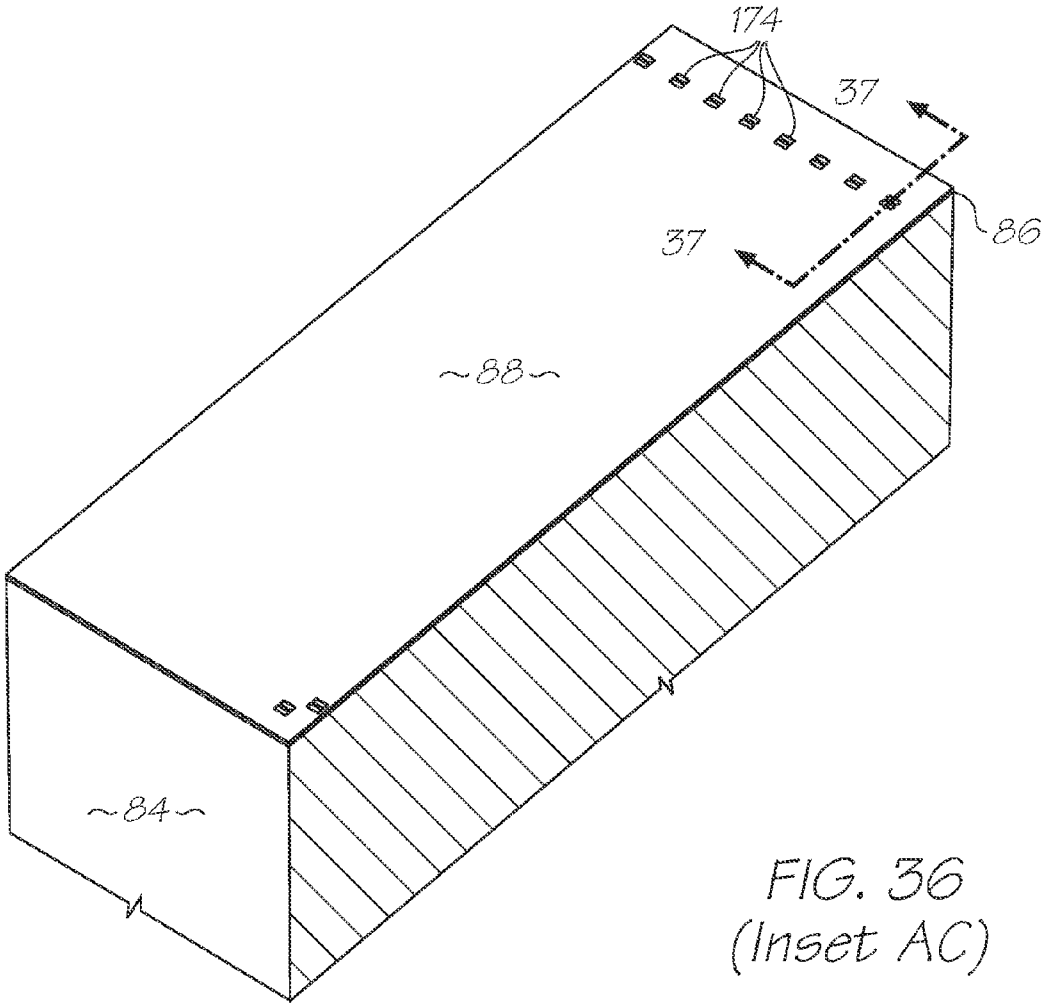


FIG. 36
(Inset AC)

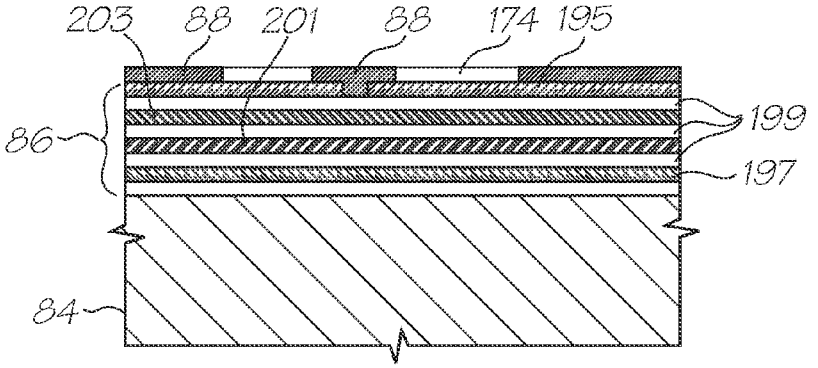


FIG. 37

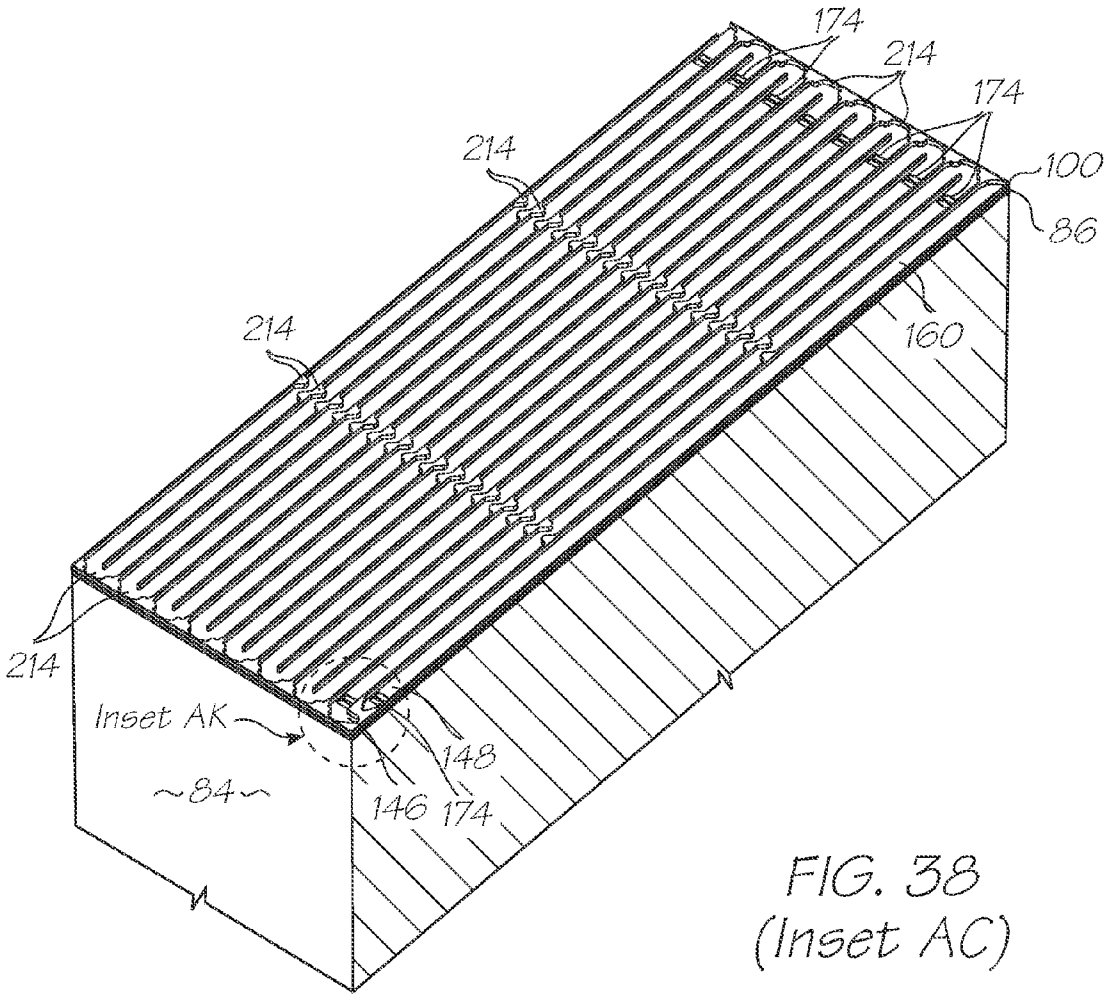


FIG. 38
(Inset AC)

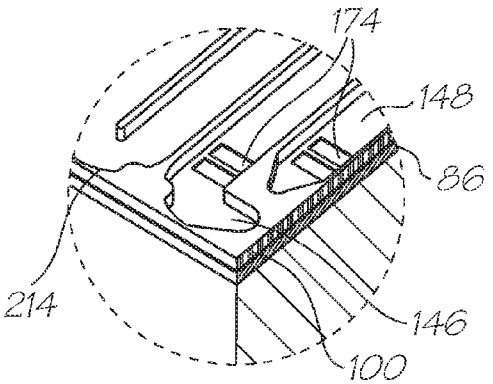


FIG. 39
(Inset AK)

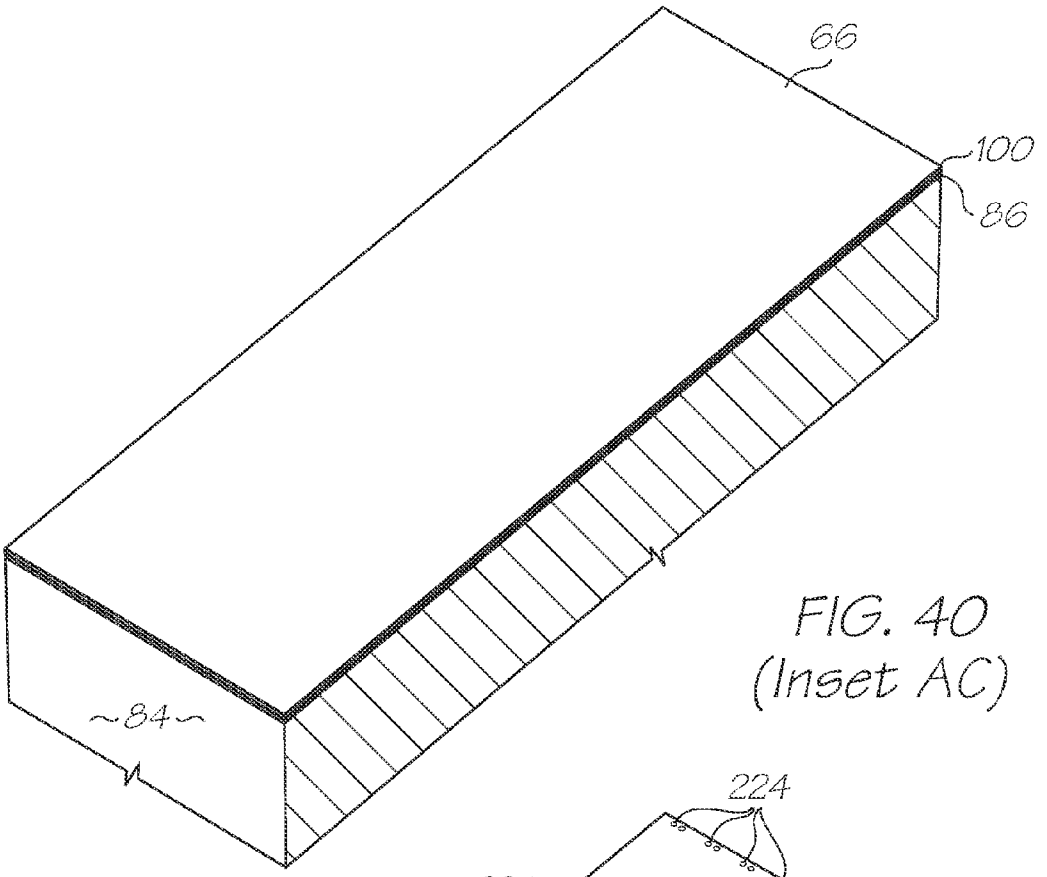


FIG. 40
(Inset AC)

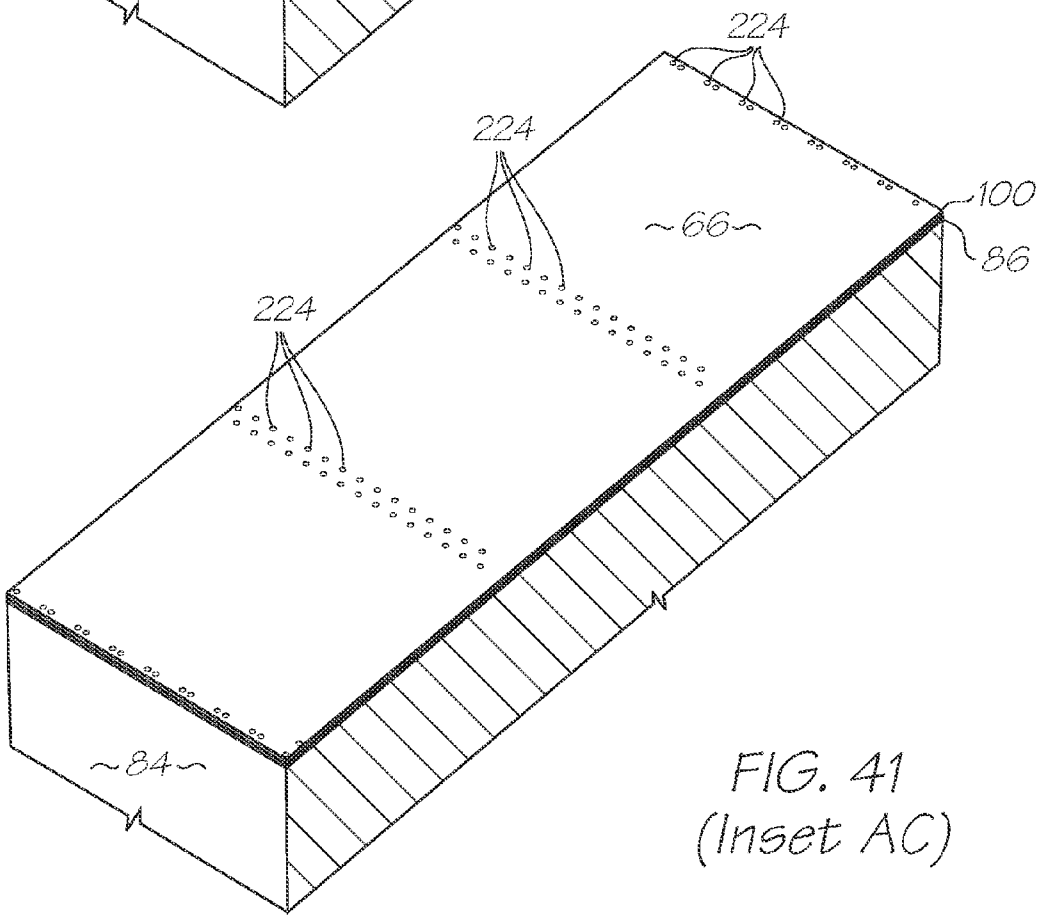


FIG. 41
(Inset AC)

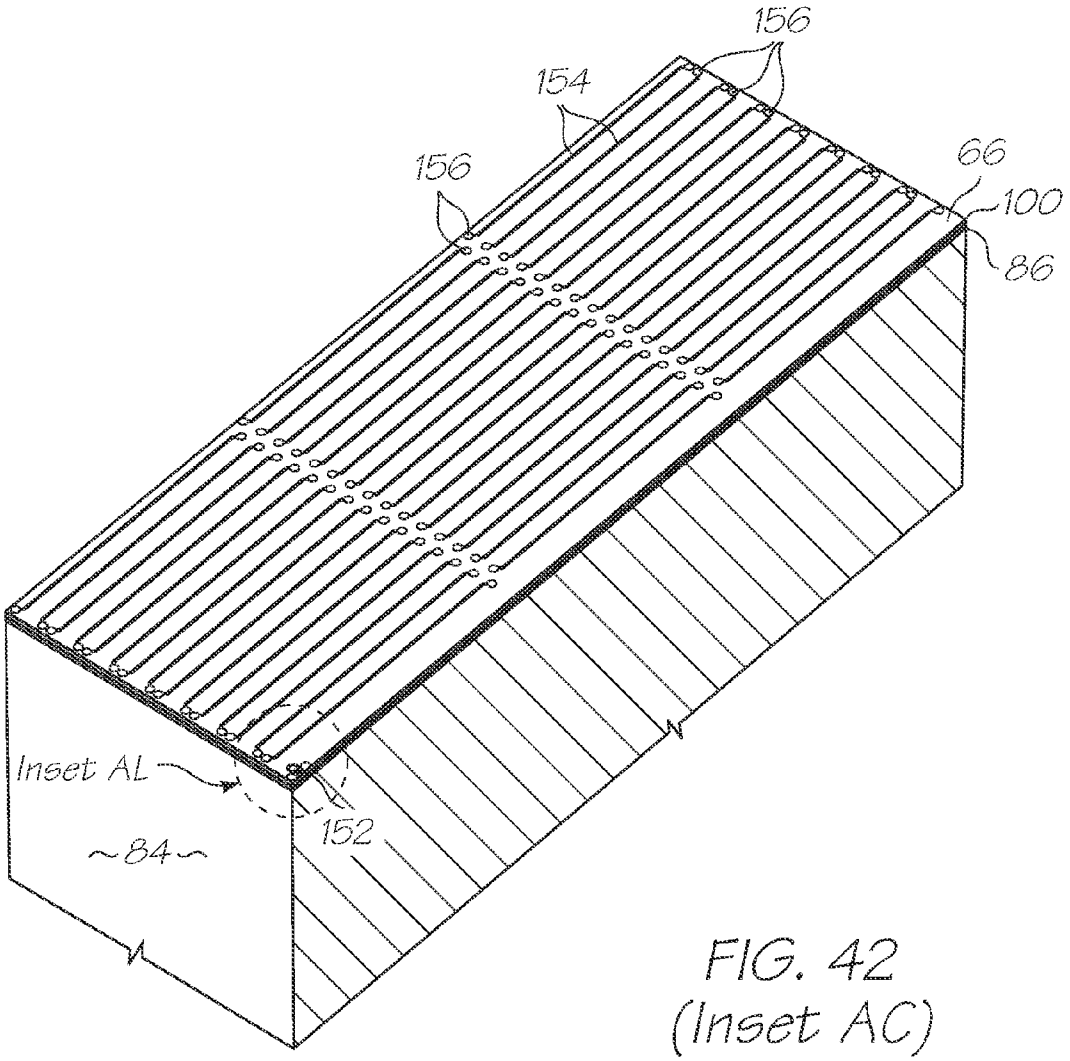


FIG. 42
(Inset AC)

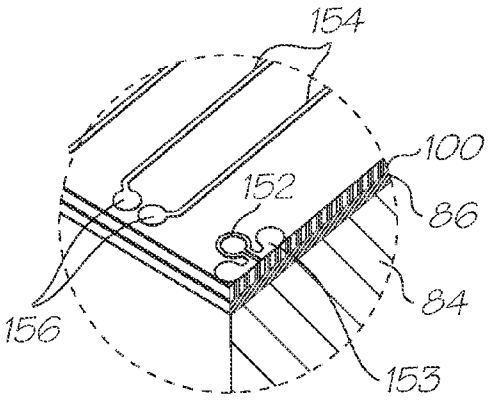


FIG. 43
(Inset AL)

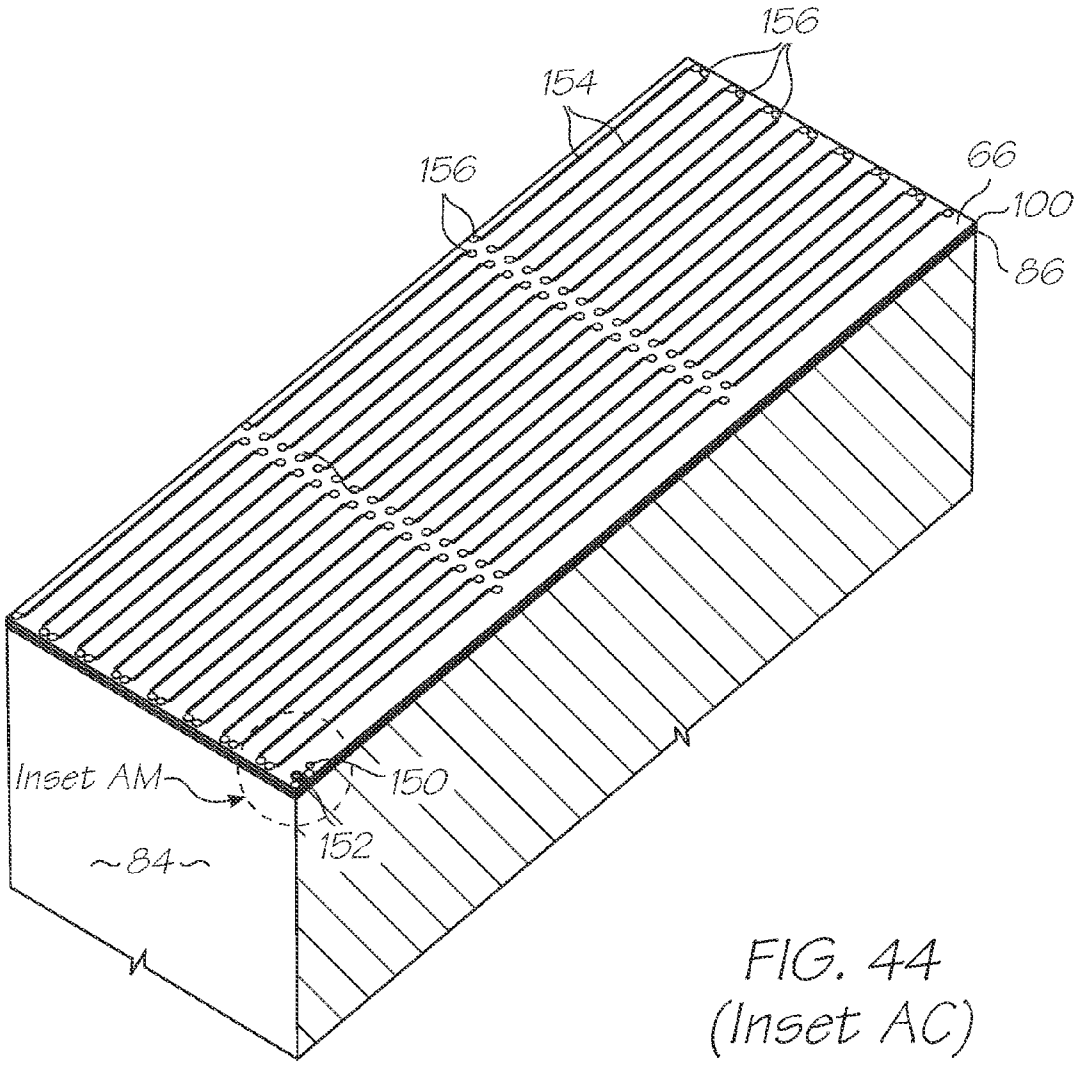


FIG. 44
(Inset AC)

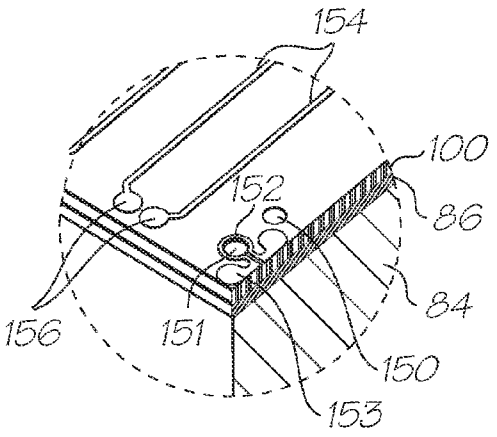


FIG. 45
(Inset AM)

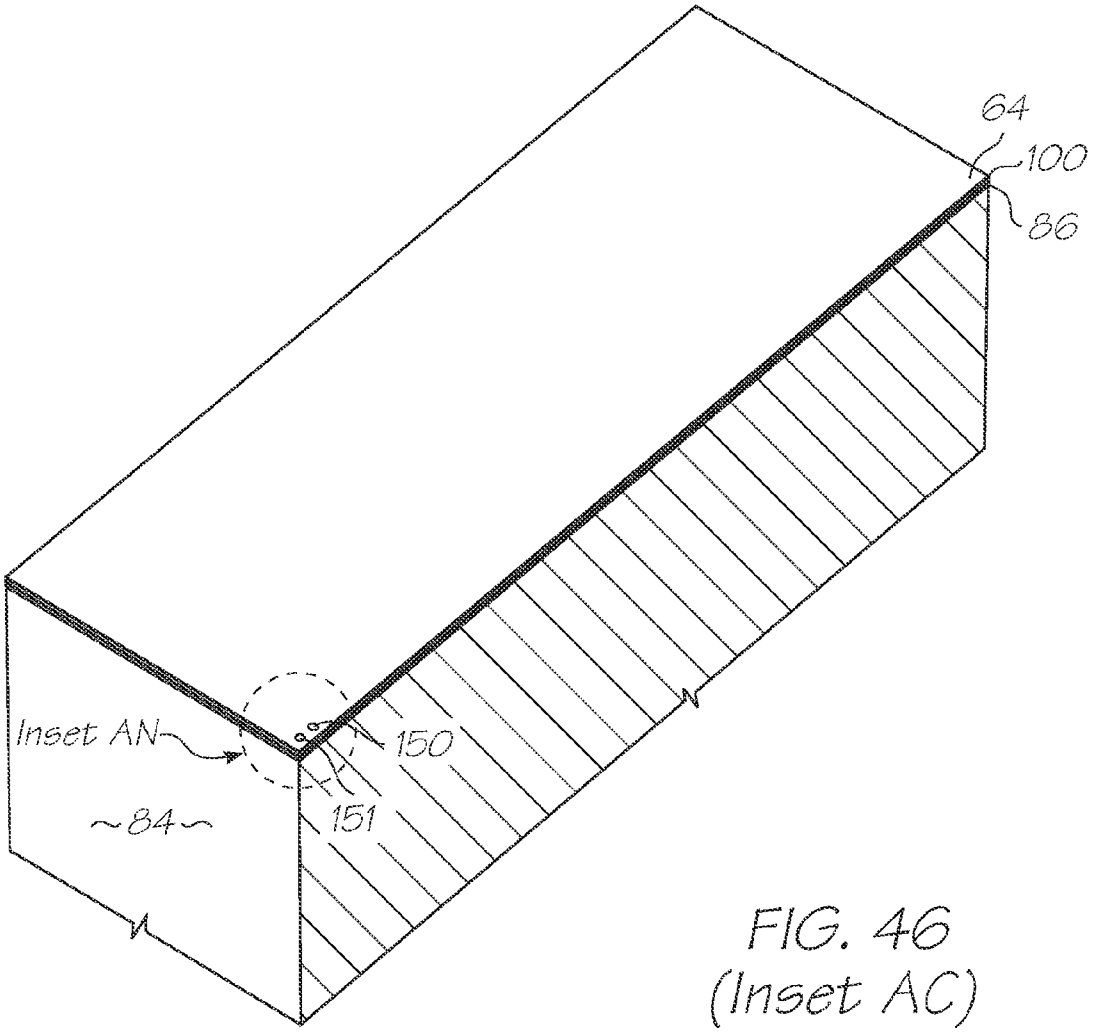


FIG. 46
(Inset AC)

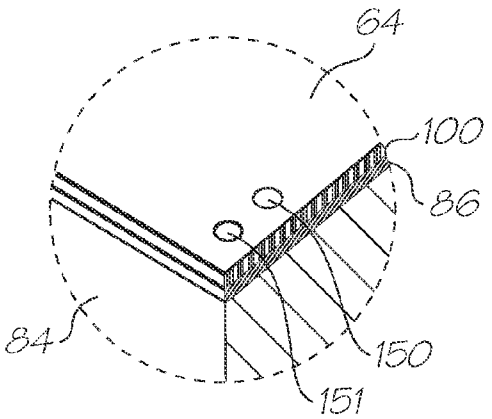


FIG. 47
(Inset AN)

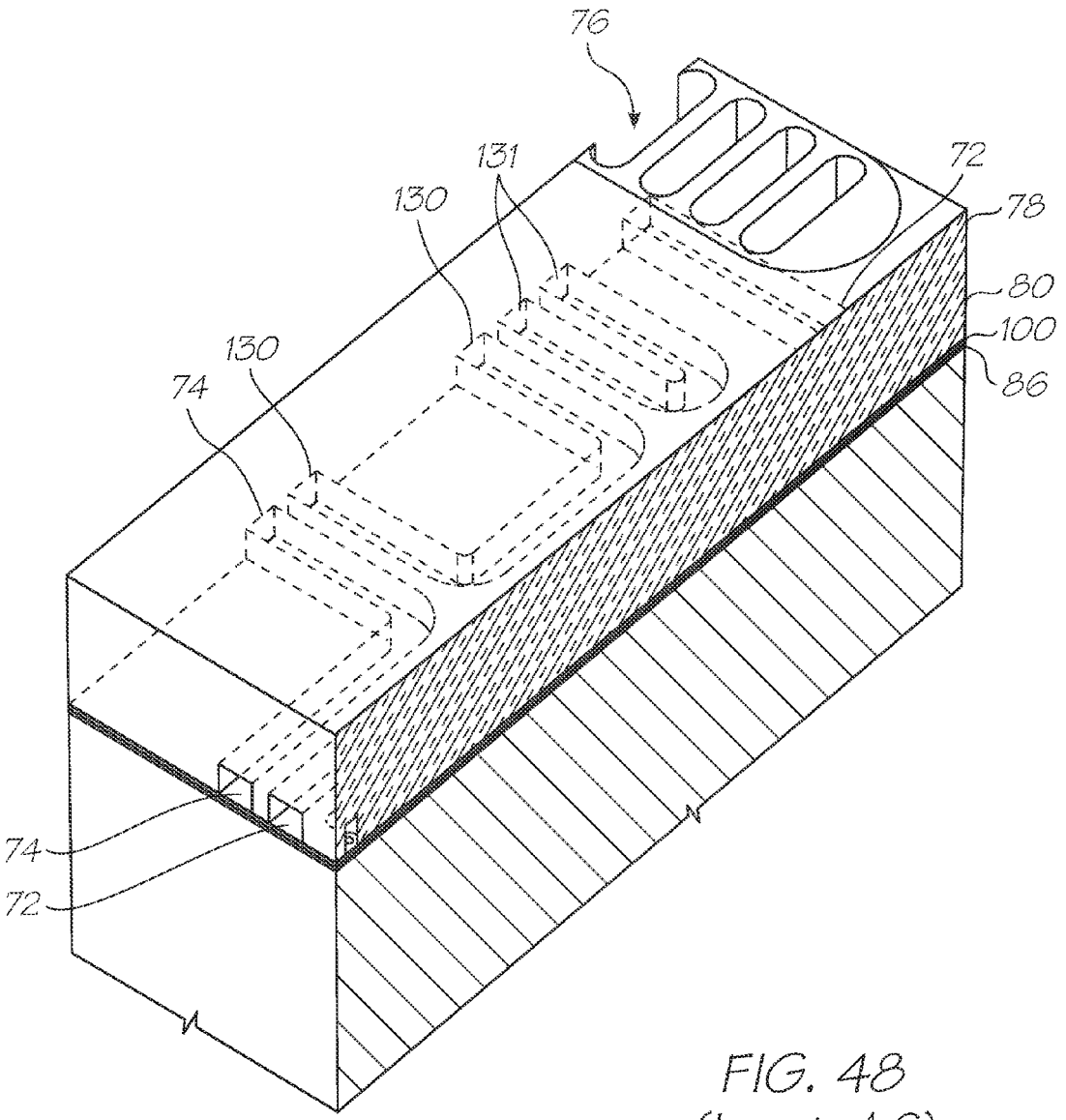


FIG. 48
(Inset AC)

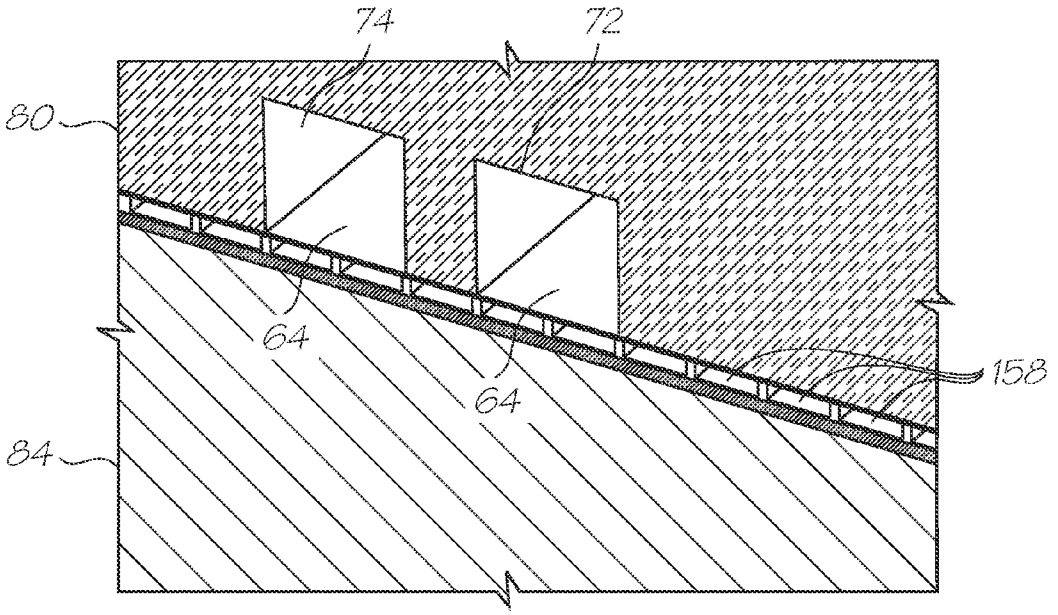


FIG. 49
(Inset AC)

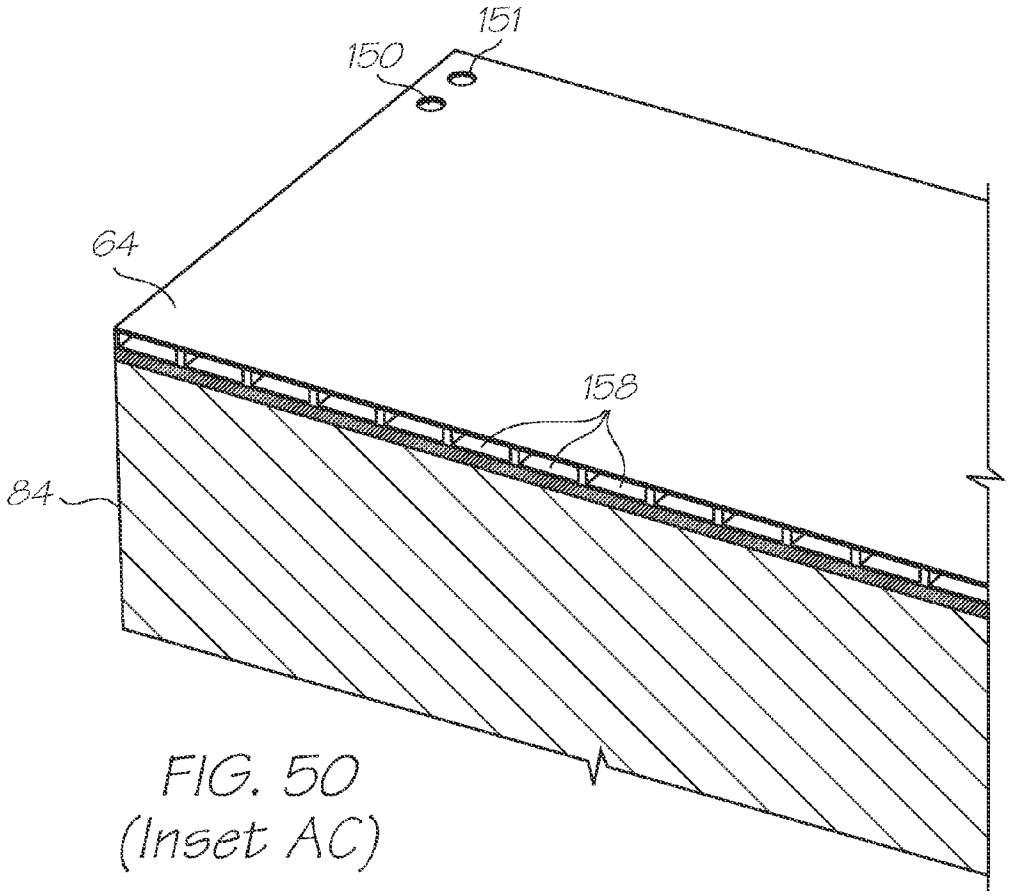


FIG. 50
(Inset AC)

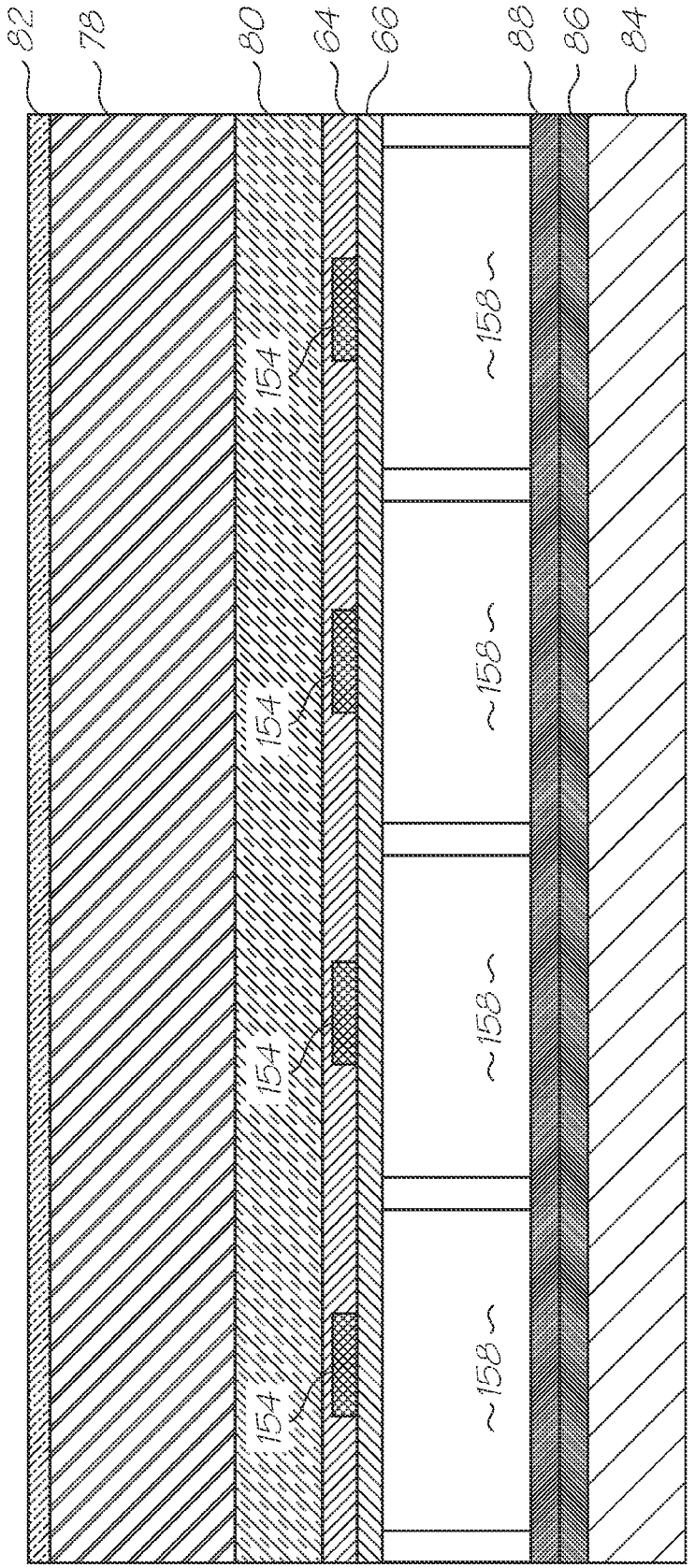


FIG. 51

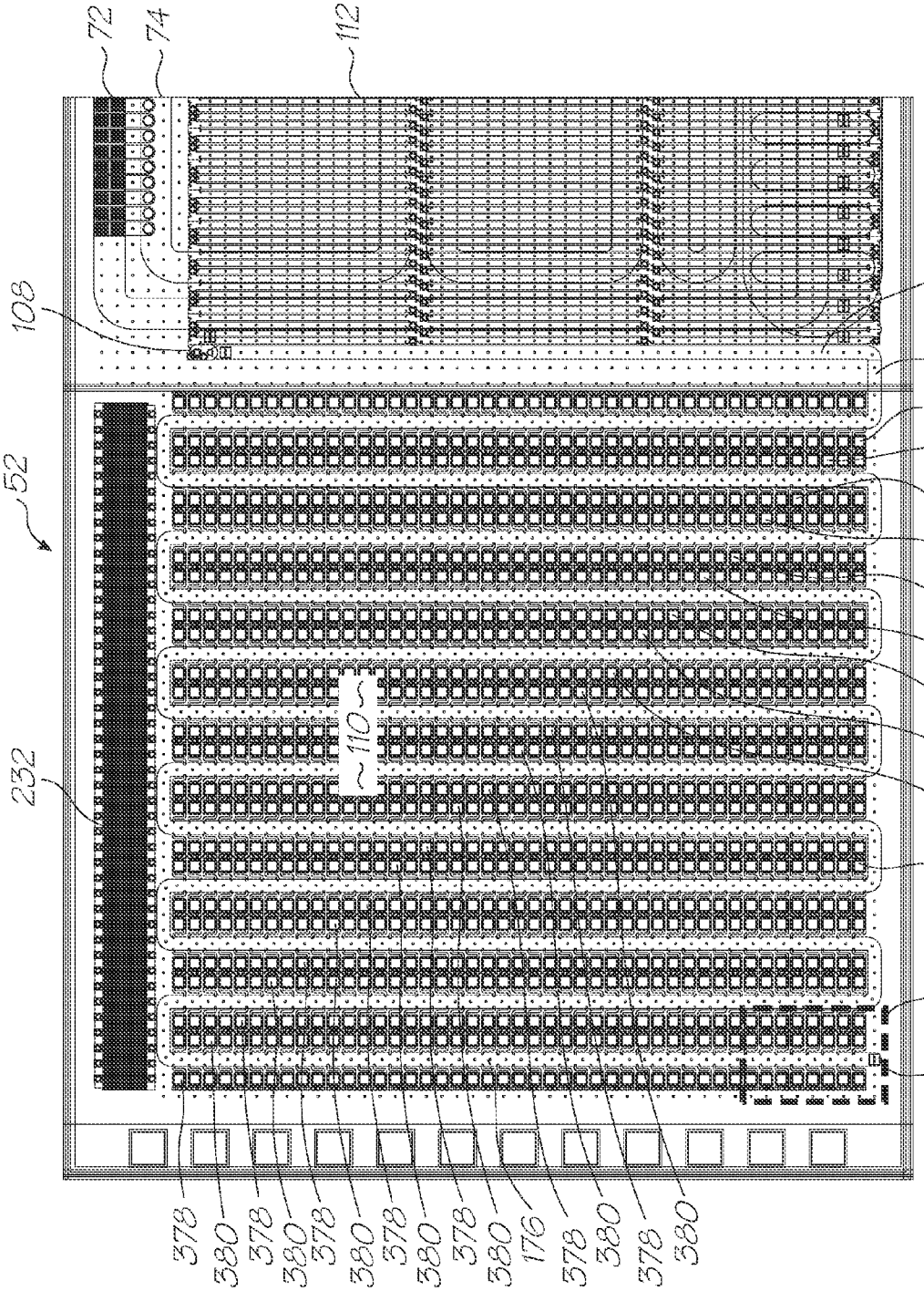


FIG. 52

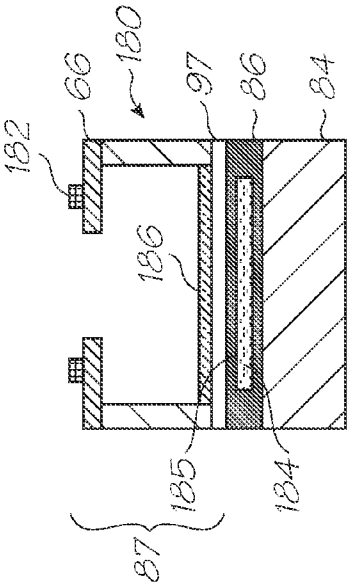


FIG. 54

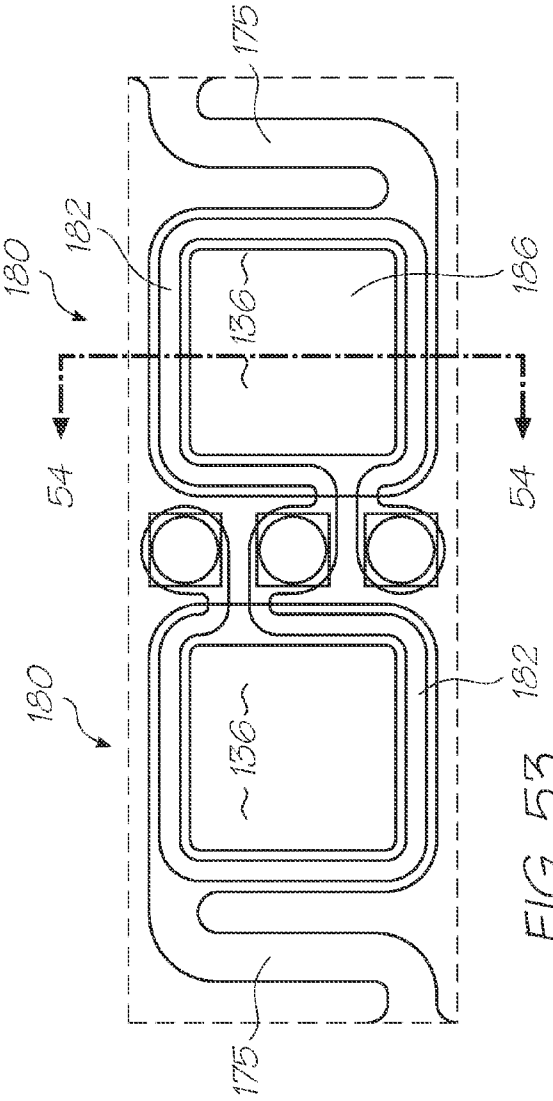


FIG. 53

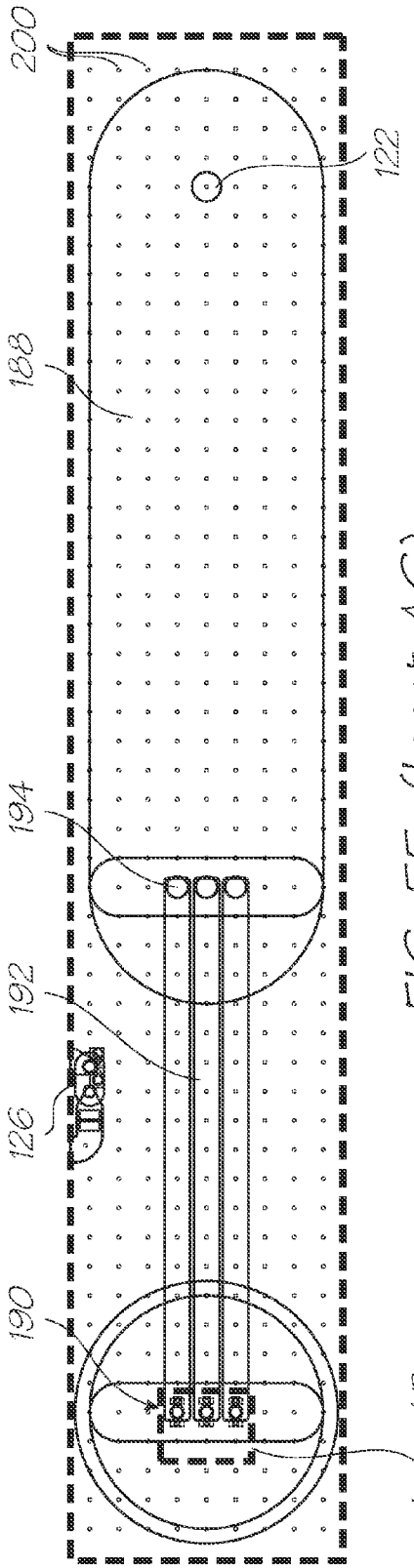


FIG. 55 (Inset AG)

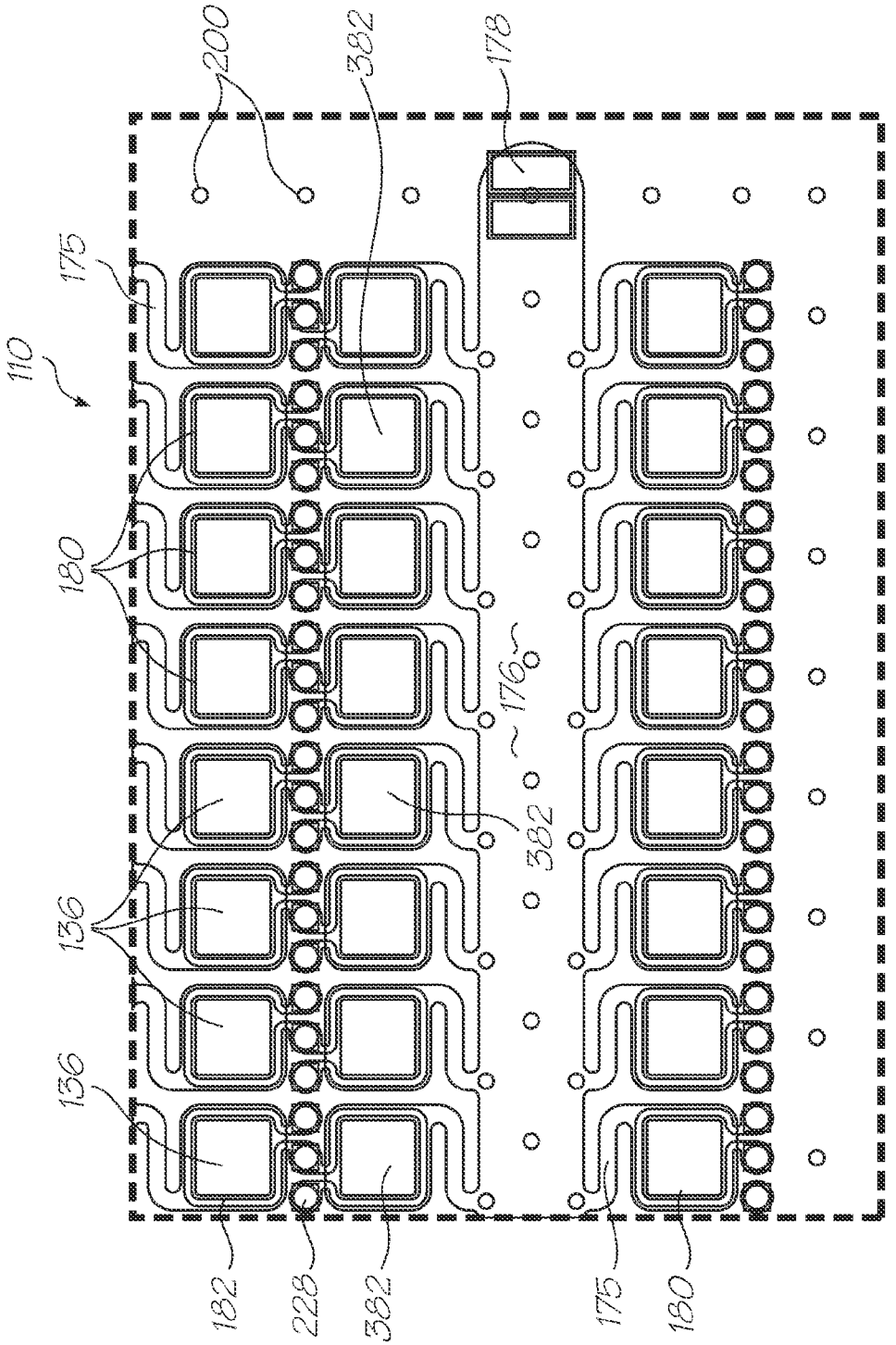


FIG. 56 (Inset AD)

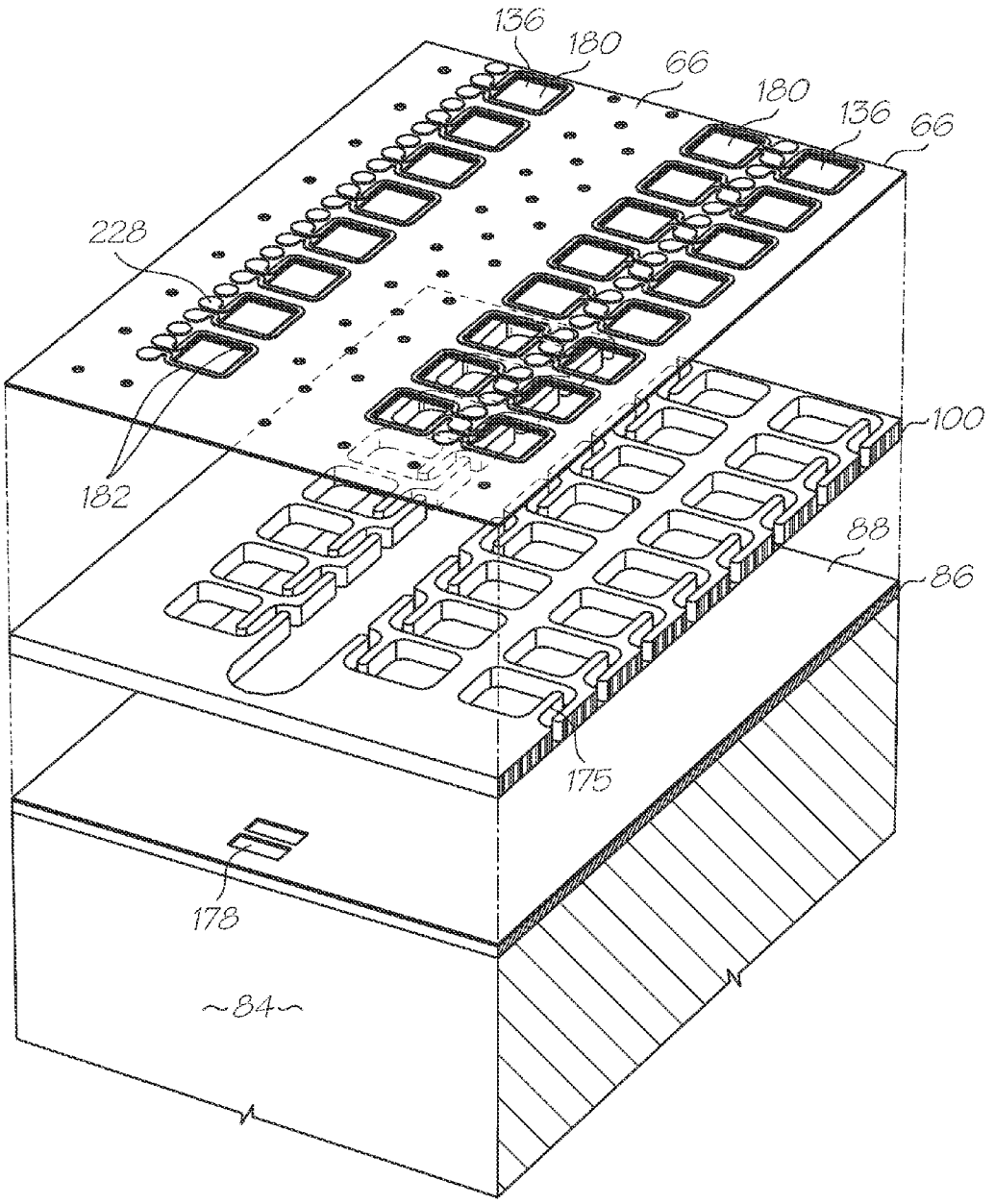


FIG. 57 (Inset AD)

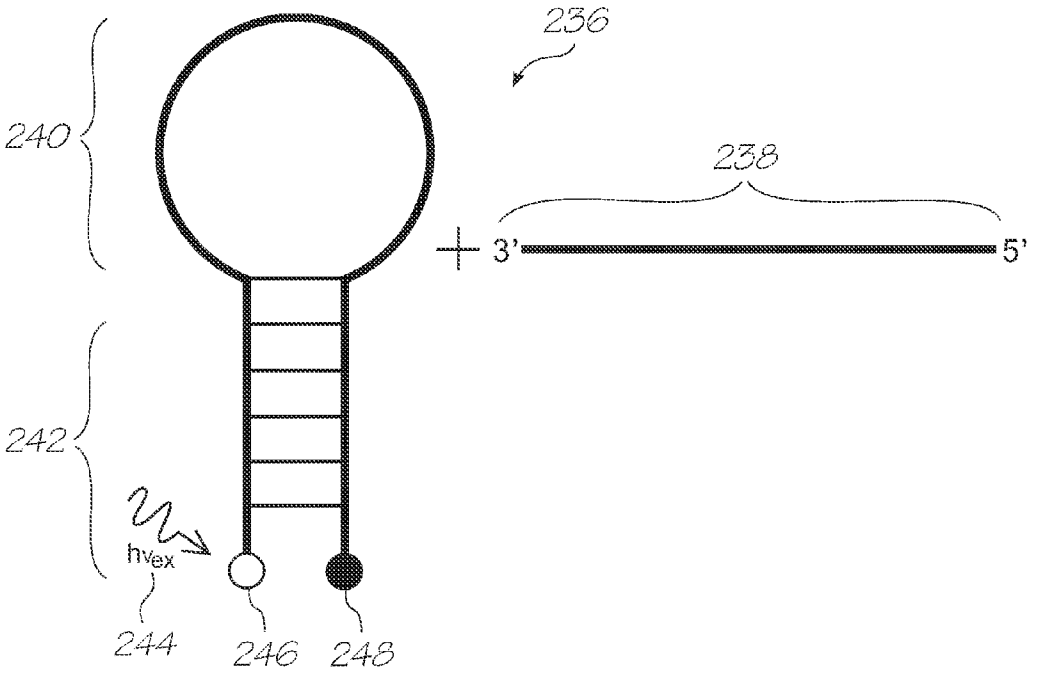


FIG. 58
(PRIOR ART)

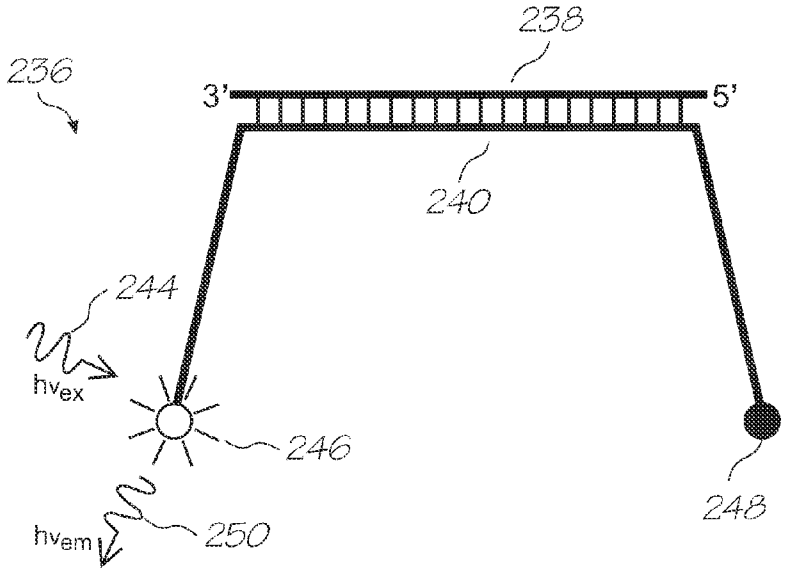


FIG. 59
(PRIOR ART)

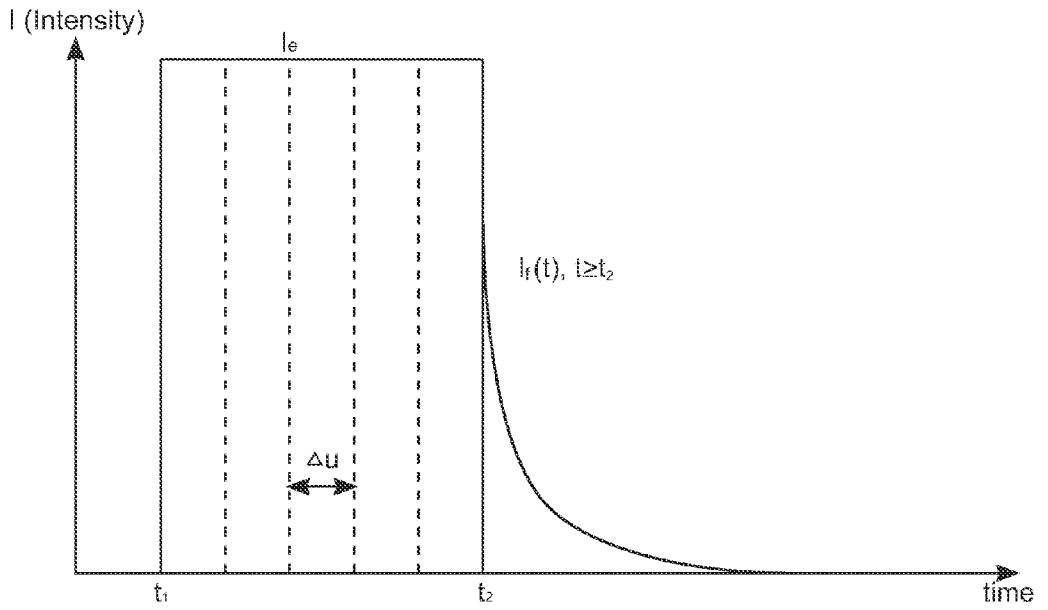

I (Intensity)
I_e
$I_f(t)$, $t \geq t_2$
Δu
t_1
t_2
time

FIG. 60

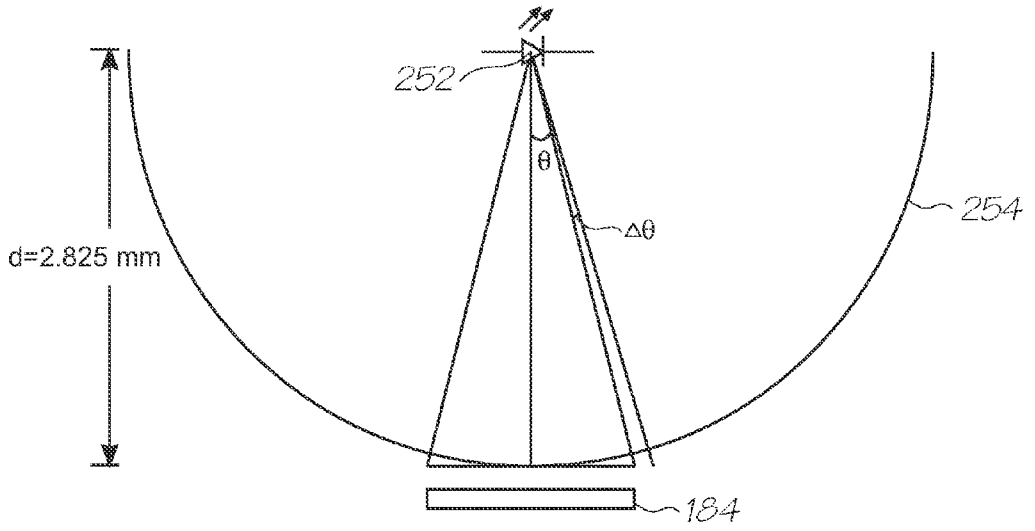

252
θ
Δθ
254
d=2.825 mm
184

FIG. 61

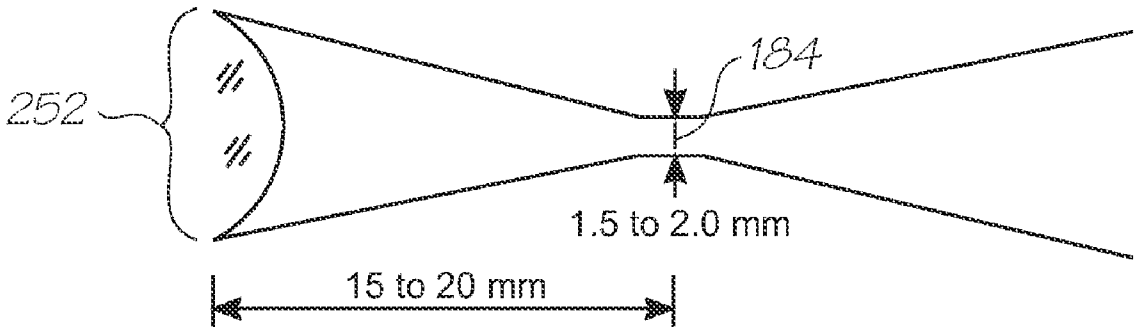


FIG. 62

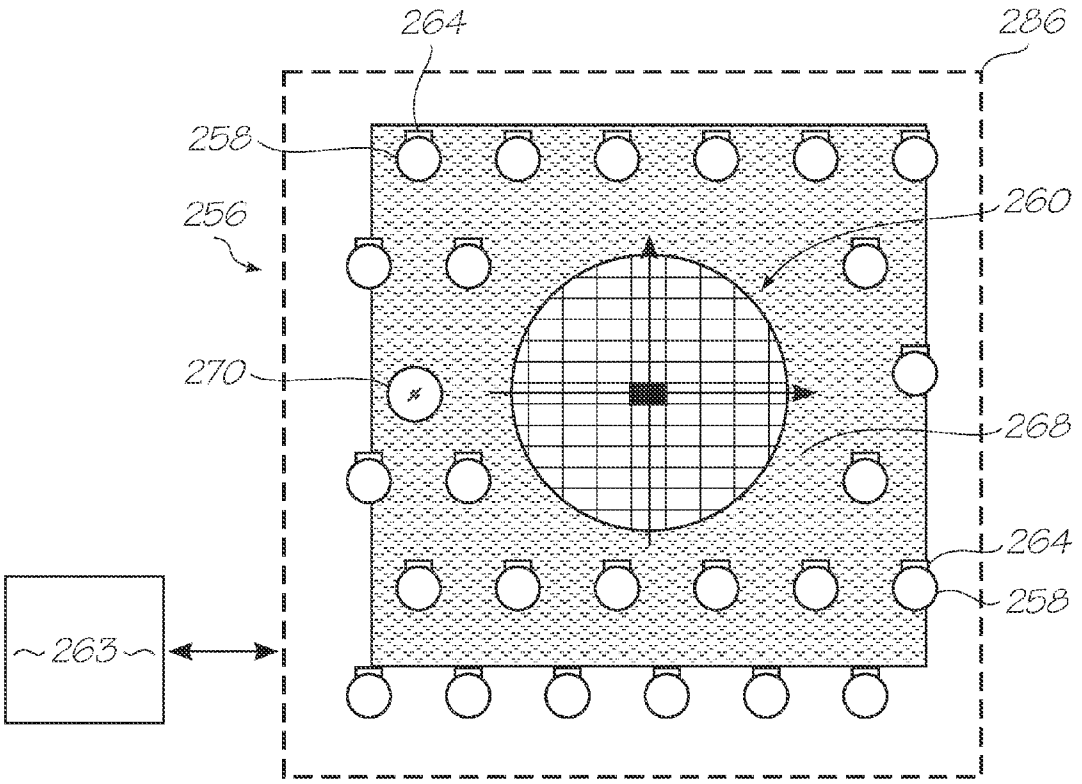


FIG. 63

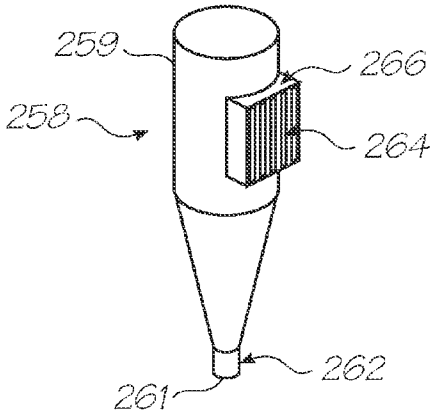


FIG. 64

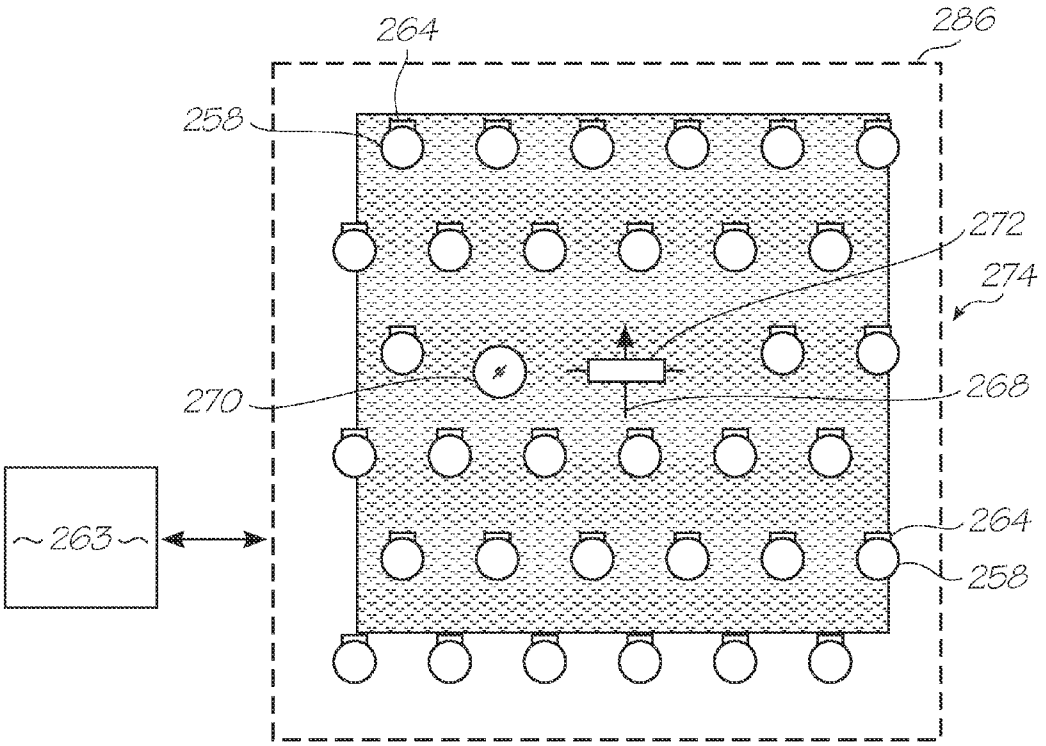

264
286
258
272
274
270
268
263
264
258

FIG. 65

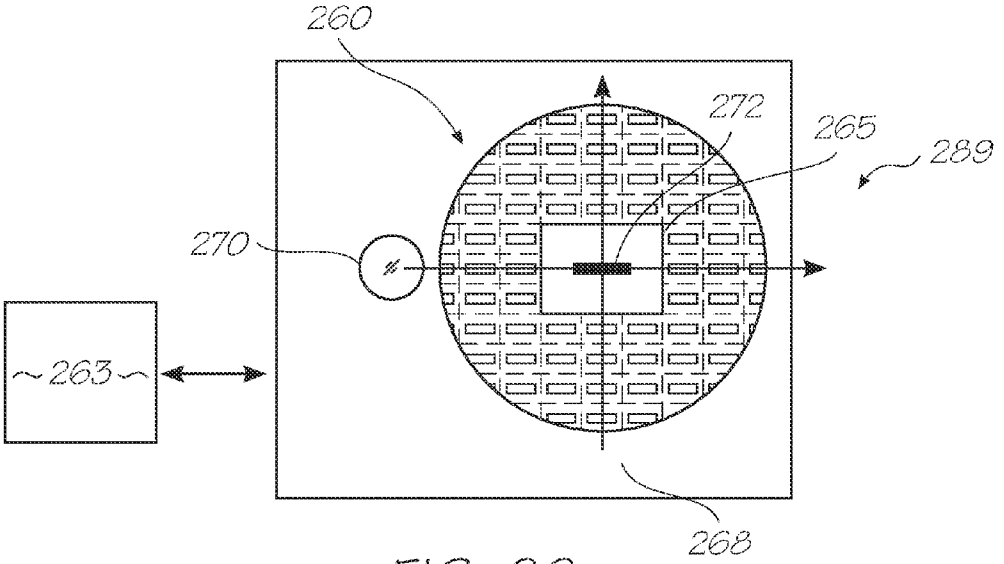

260
272
265
289
270
263
268

FIG. 66

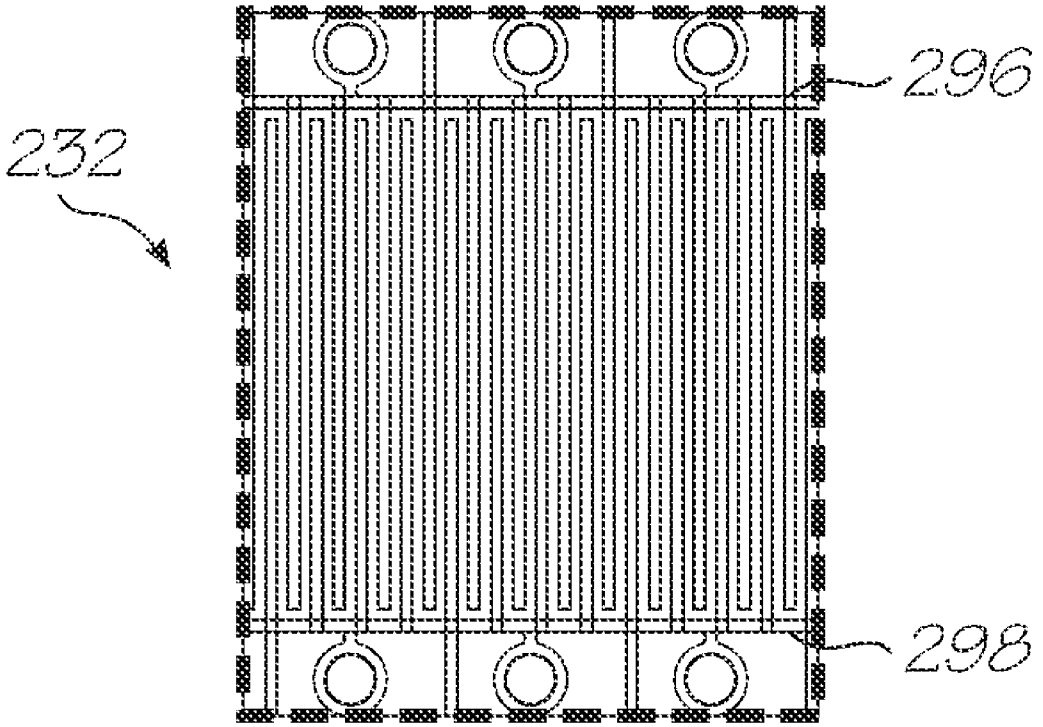


FIG. 67
(Inset AH)

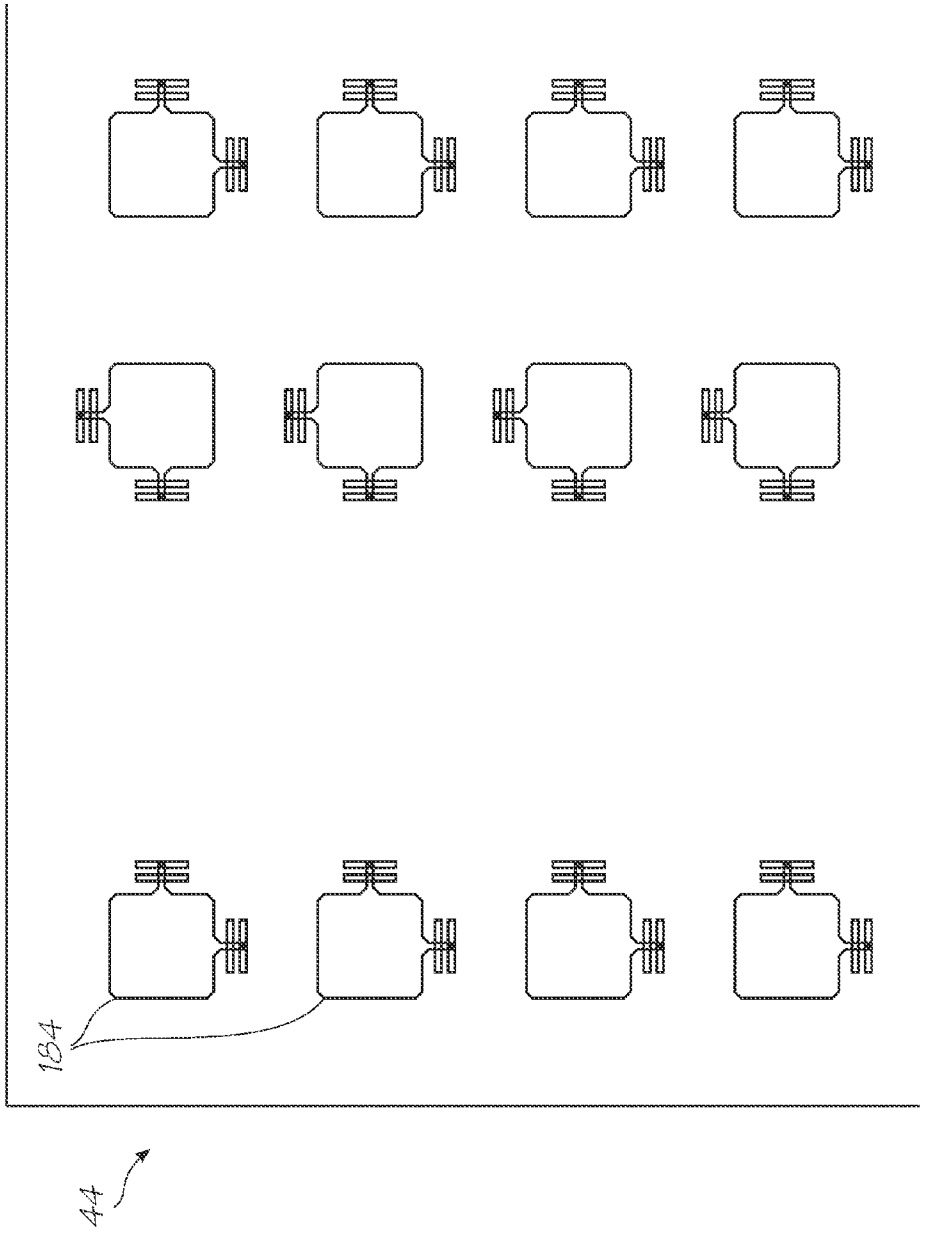


FIG. 68

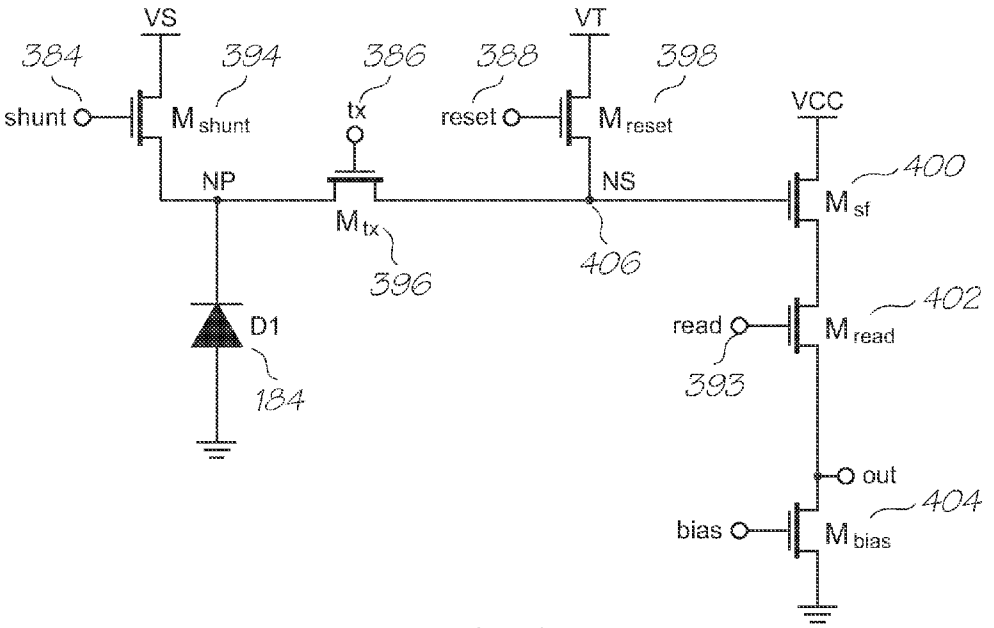

VS
VT
384
394
386
388
398
shunt
M shunt
tx
reset
M reset
VCC
NP
NS
400
M sf
M tx
396
406
D1
184
read
M read
402
393
out
bias
M bias
404

FIG. 69

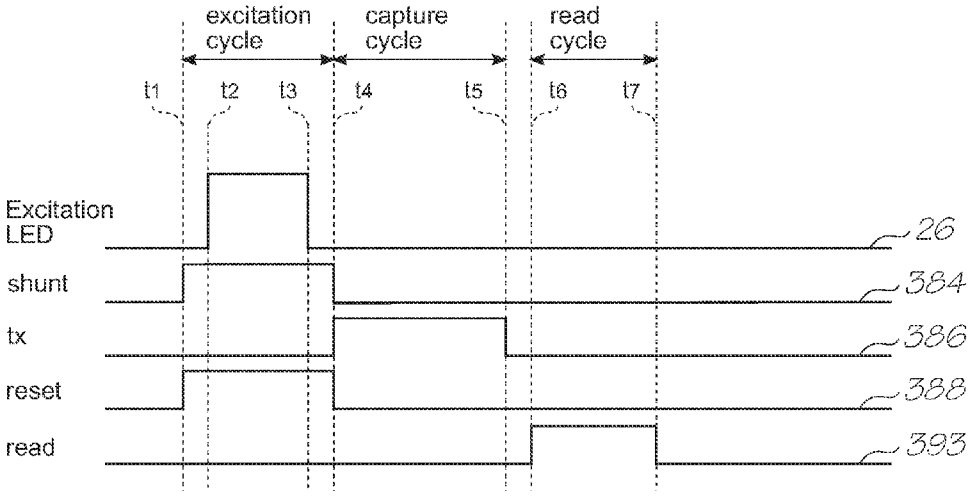

excitation cycle
capture cycle
read cycle
t1
t2
t3
t4
t5
t6
t7
Excitation LED
26
shunt
384
tx
386
reset
388
read
393

FIG. 70

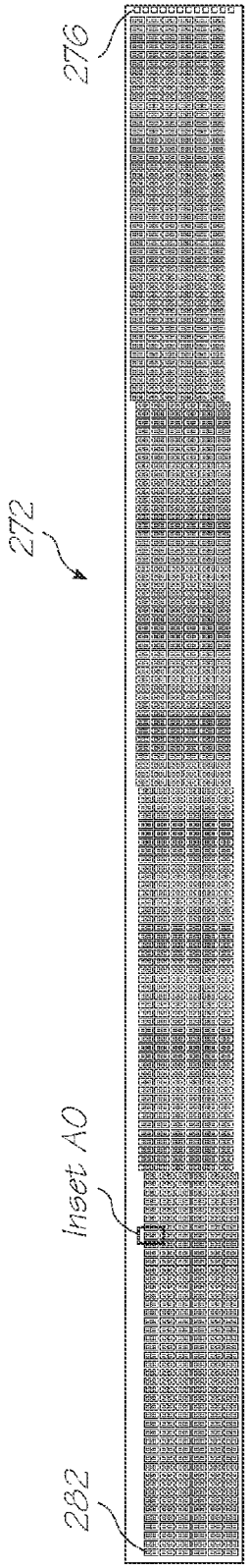


FIG. 71

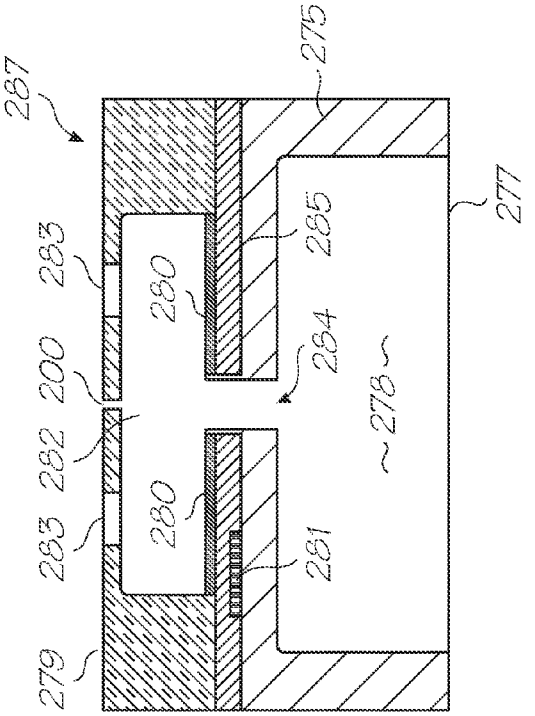


FIG. 73

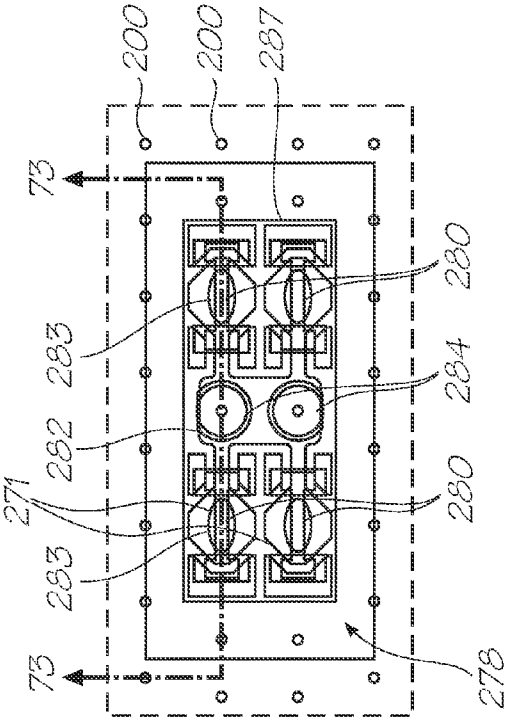


FIG. 72 (Inset A0)

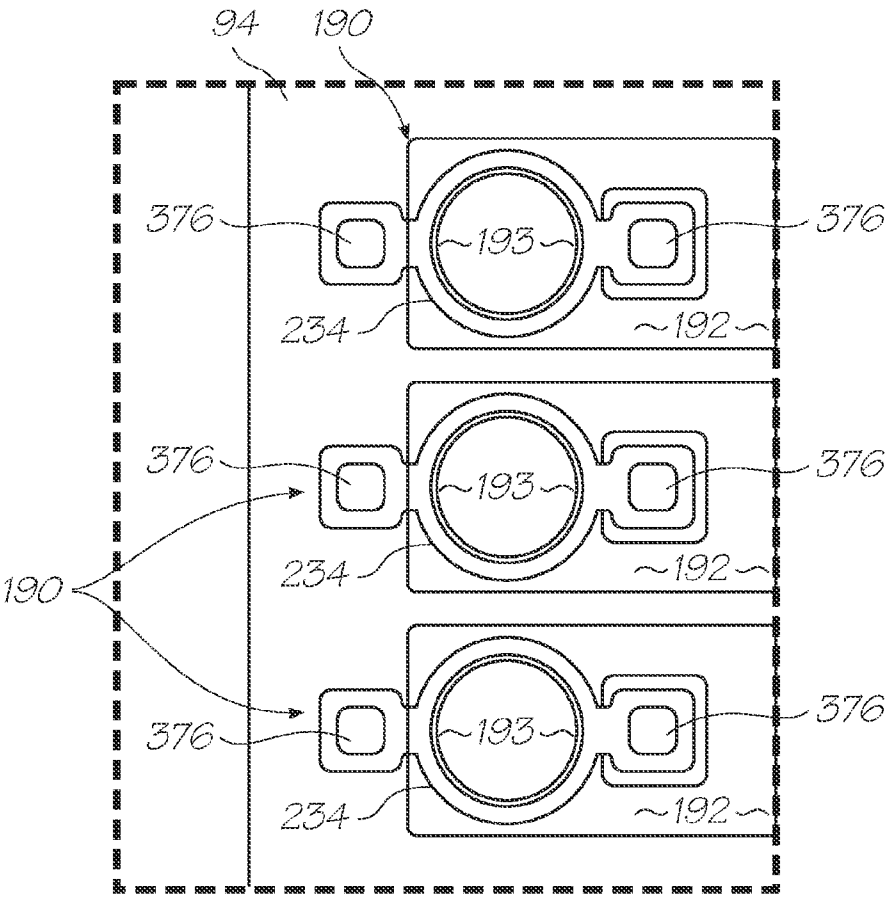


FIG. 74 (Inset AP)

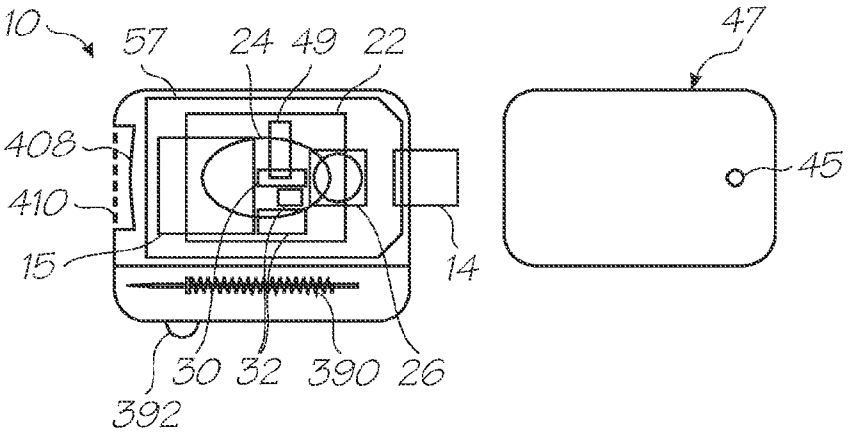


FIG. 77

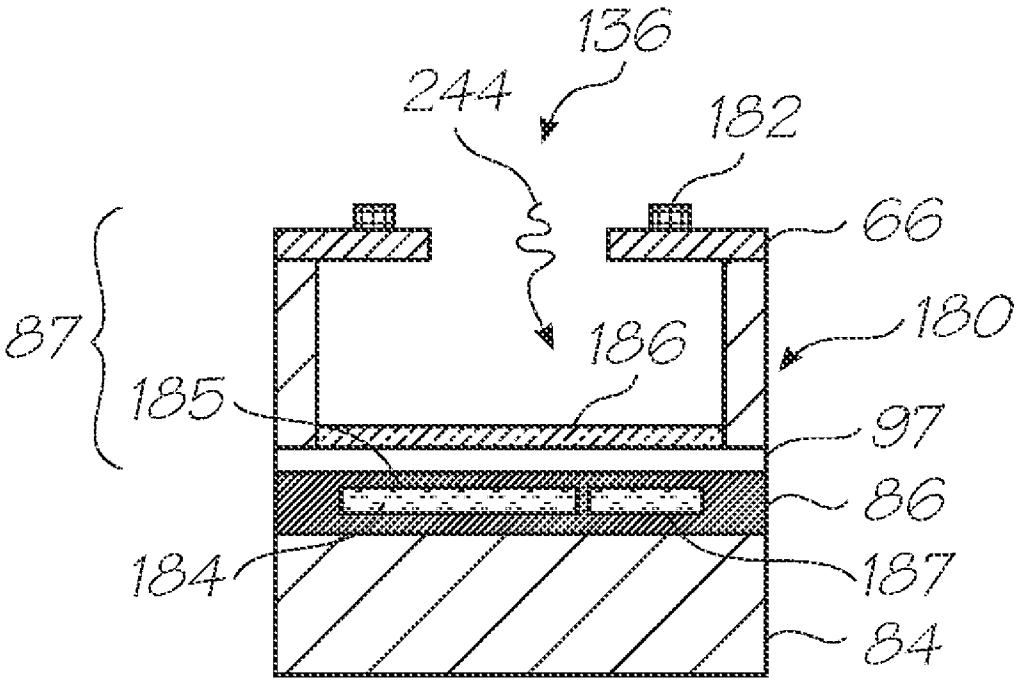


FIG. 75

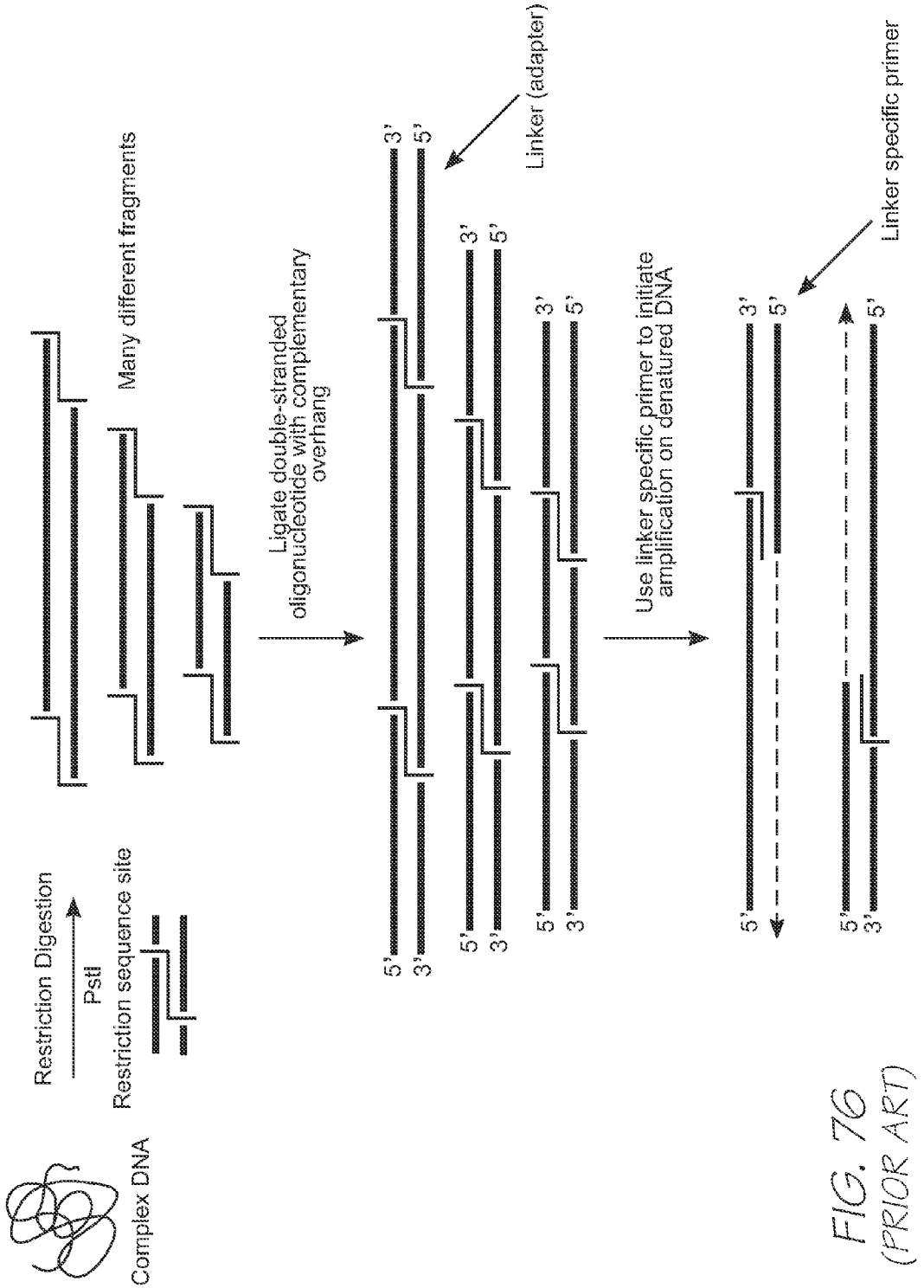


FIG. 76
(PRIOR ART)

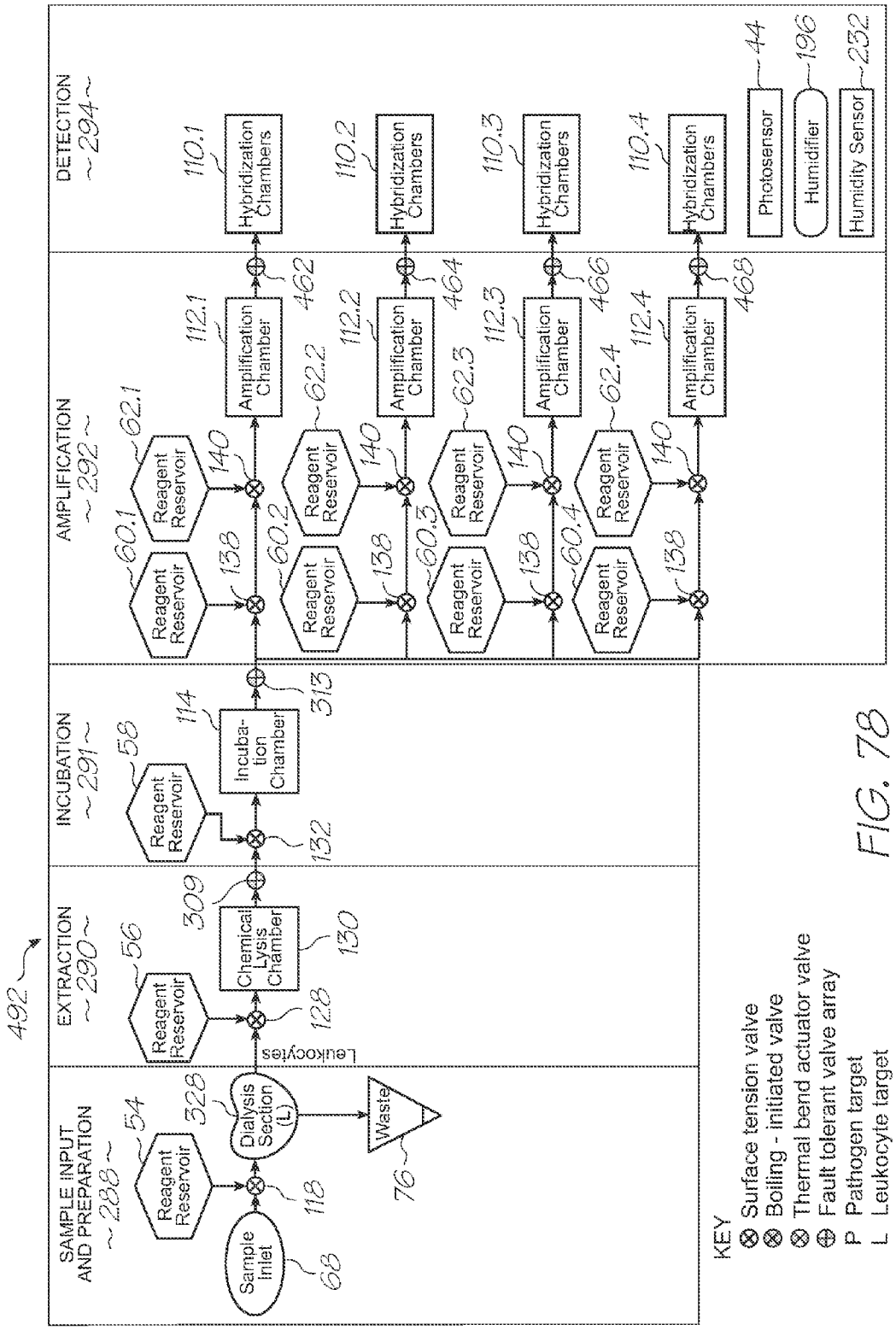

492
SAMPLE INPUT AND PREPARATION
~228~
EXTRACTION
~290~
INCUBATION
~291~
AMPLIFICATION
~292~
DETECTION
~294~
Sample Inlet
68
Reagent Reservoir
54
118
328
Dialysis Section (L)
Waste
76
Leukocytes
Reagent Reservoir
56
128
Chemical Lysis Chamber
130
309
Reagent Reservoir
58
132
Incubation Chamber
114
313
Reagent Reservoir
60.1
62.1
Reagent Reservoir
60.2
62.2
Reagent Reservoir
60.3
62.3
Reagent Reservoir
60.4
62.4
138
140
Amplification Chamber
112.1
112.2
112.3
112.4
462
464
466
468
Hybridization Chambers
110.1
110.2
110.3
110.4
Photosensor
44
Humidifier
196
Humidity Sensor
232
KEY
⊗ Surface tension valve
⊗ Boiling - initiated valve
⊗ Thermal bend actuator valve
⊕ Fault tolerant valve array
P Pathogen target
L Leukocyte target

FIG. 78

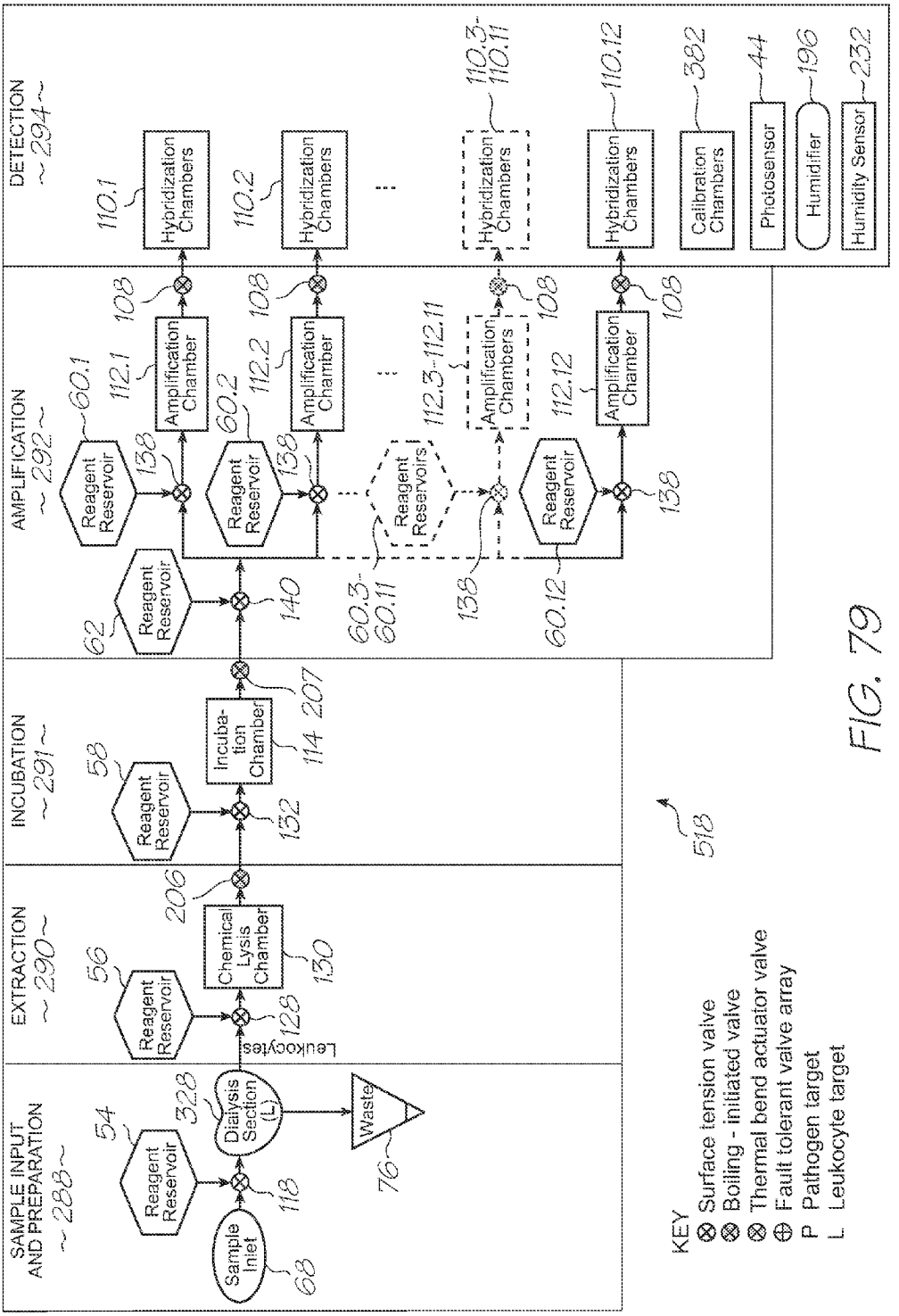

SAMPLE INPUT AND PREPARATION ~288~
EXTRACTION ~290~
INCUBATION ~291~
AMPLIFICATION ~292~
DETECTION ~294~
Sample Inlet
Reagent Reservoir
Dialysis Section (L)
Waste
Leukocytes
Chemical Lysis Chamber
Incubation Chamber
Amplification Chamber
Reagent Reservoirs
Amplification Chambers
Hybridization Chambers
Calibration Chambers
Photosensor
Humidifier
Humidity Sensor
KEY
Surface tension valve
Boiling - initiated valve
Thermal bend actuator valve
Fault tolerant valve array
P Pathogen target
L Leukocyte target

FIG. 79

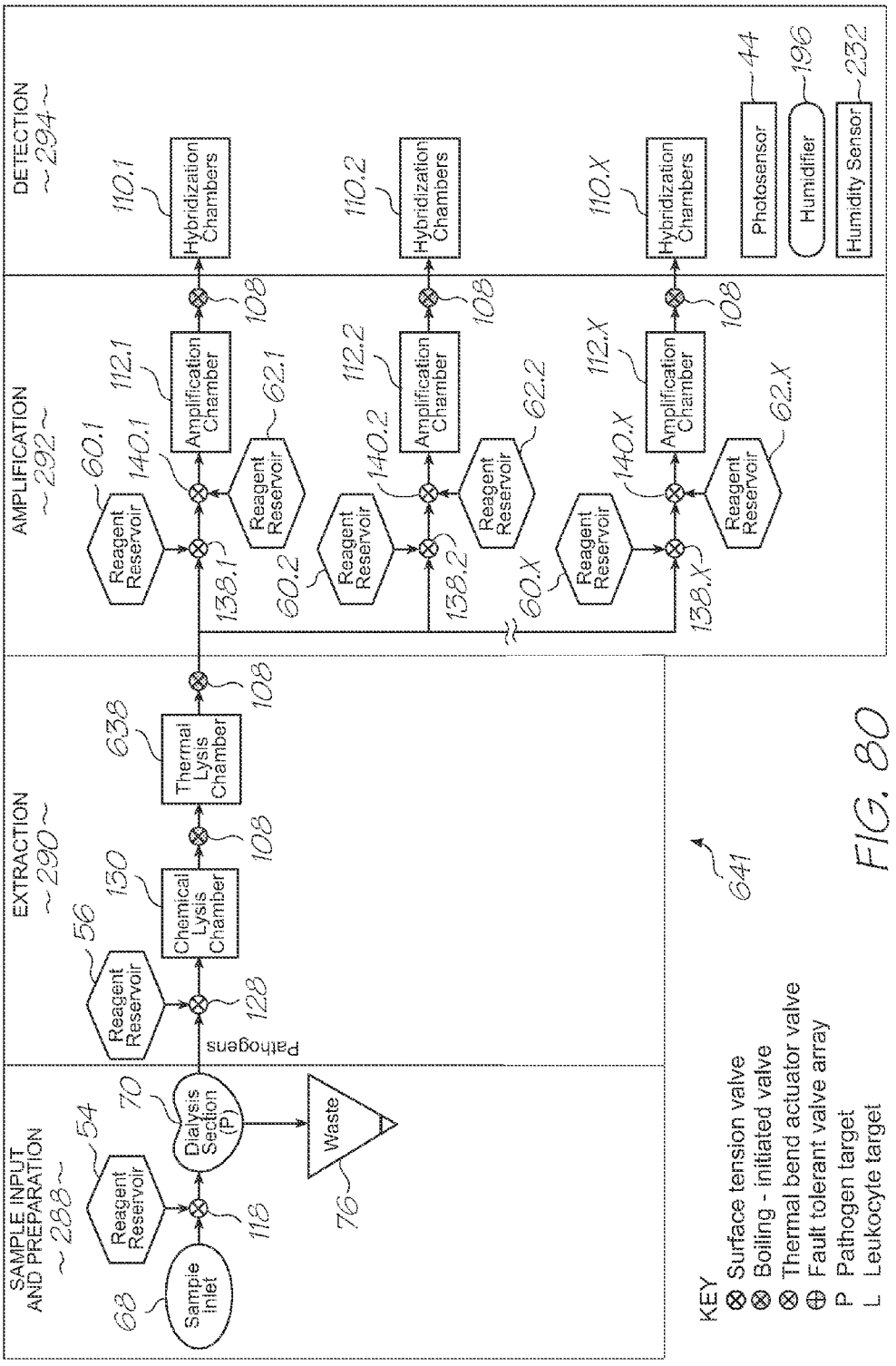

SAMPLE INPUT AND PREPARATION
~288~
EXTRACTION
~290~
AMPLIFICATION
~292~
DETECTION
~294~
Sample Inlet
Reagent Reservoir
Dialysis Section (P)
Waste
Pathogens
Chemical Lysis Chamber
Thermal Lysis Chamber
Amplification Chamber
Hybridization Chambers
Photosensor
Humidifier
Humidity Sensor
KEY
Surface tension valve
Boiling - initiated valve
Thermal bend actuator valve
Fault tolerant valve array
P Pathogen target
L Leukocyte target

FIG. 80

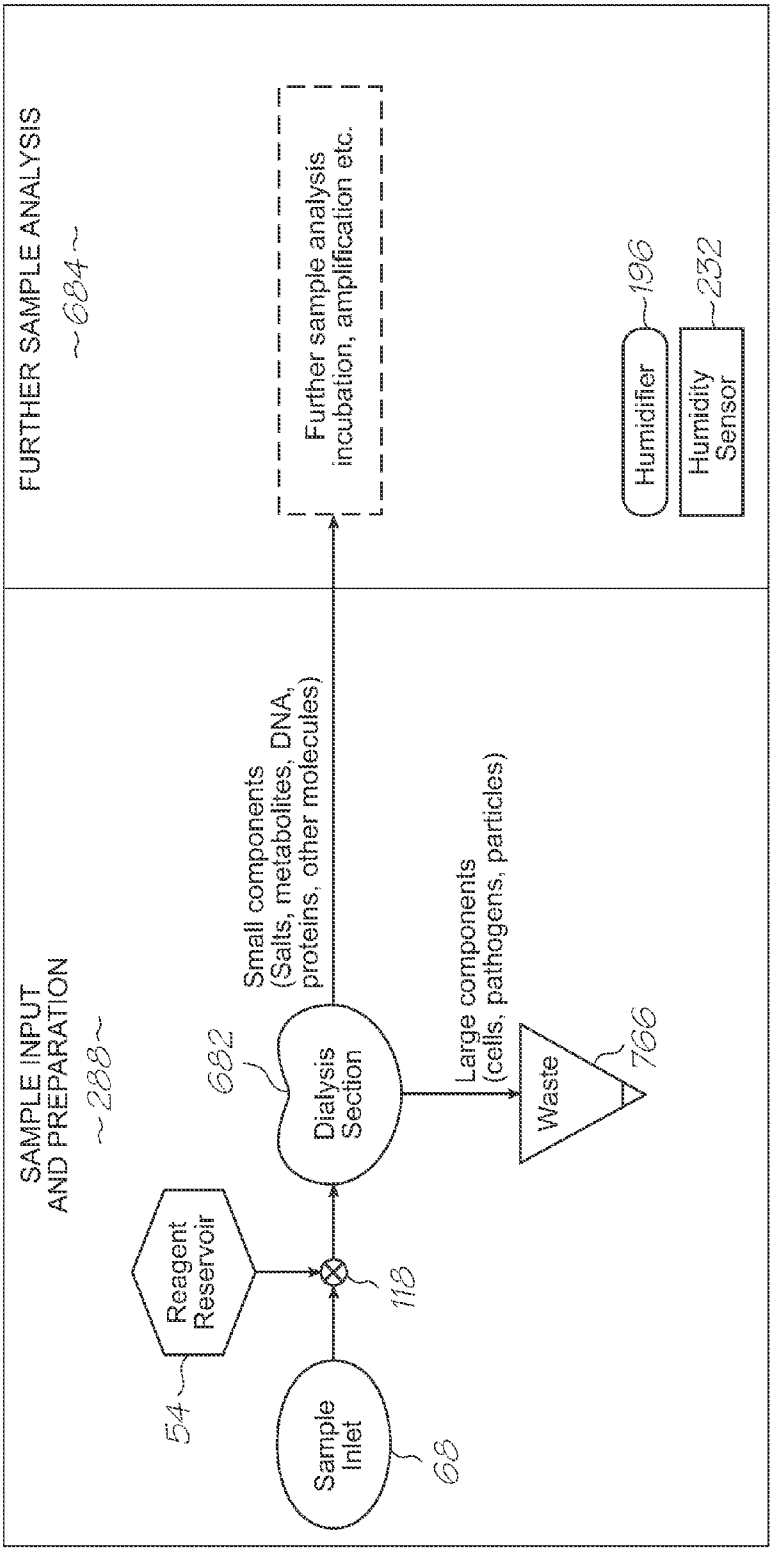

SAMPLE INPUT AND PREPARATION
~238~
FURTHER SAMPLE ANALYSIS
~684~
Sample Inlet
68
Reagent Reservoir
54
118
682
Dialysis Section
Small components (Salts, metabolites, DNA, proteins, other molecules)
Large components (cells, pathogens, particles)
Waste
766
Further sample analysis incubation, amplification etc.
Humidifier
196
Humidity Sensor
232
671
KEY
Surface tension valve
Boiling - initiated valve
Thermal bend actuator valve
Fault tolerant valve array
P Pathogen target
L Leukocyte target

FIG. 81

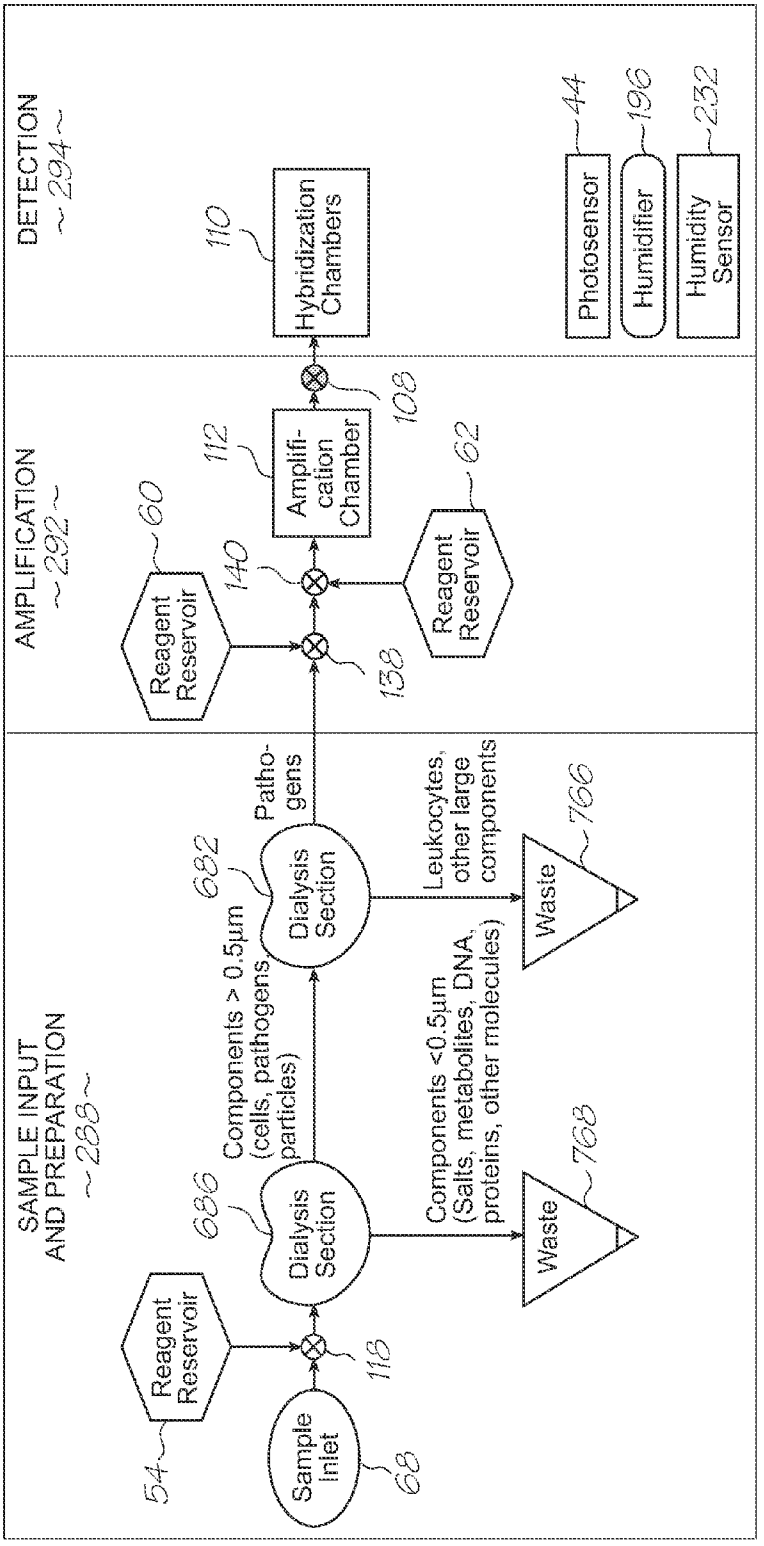

SAMPLE INPUT AND PREPARATION
~288~
AMPLIFICATION
~292~
DETECTION
~294~
Reagent Reservoir
54
Sample Inlet
68
118
Dialysis Section
686
Components > 0.5μm (cells, pathogens, particles)
Components <0.5μm (Salts, metabolites, DNA, proteins, other molecules)
Waste
768
Dialysis Section
682
Patho-gens
Leukocytes, other large components
Waste
766
138
Reagent Reservoir
60
140
Reagent Reservoir
62
112
Amplifi-cation Chamber
108
110
Hybridization Chambers
Photosensor
44
Humidifier
196
Humidity Sensor
232
KEY
Surface tension valve
Boiling - initiated valve
Thermal bend actuator valve
Fault tolerant valve array
P Pathogen target
L Leukocyte target
675

FIG. 82

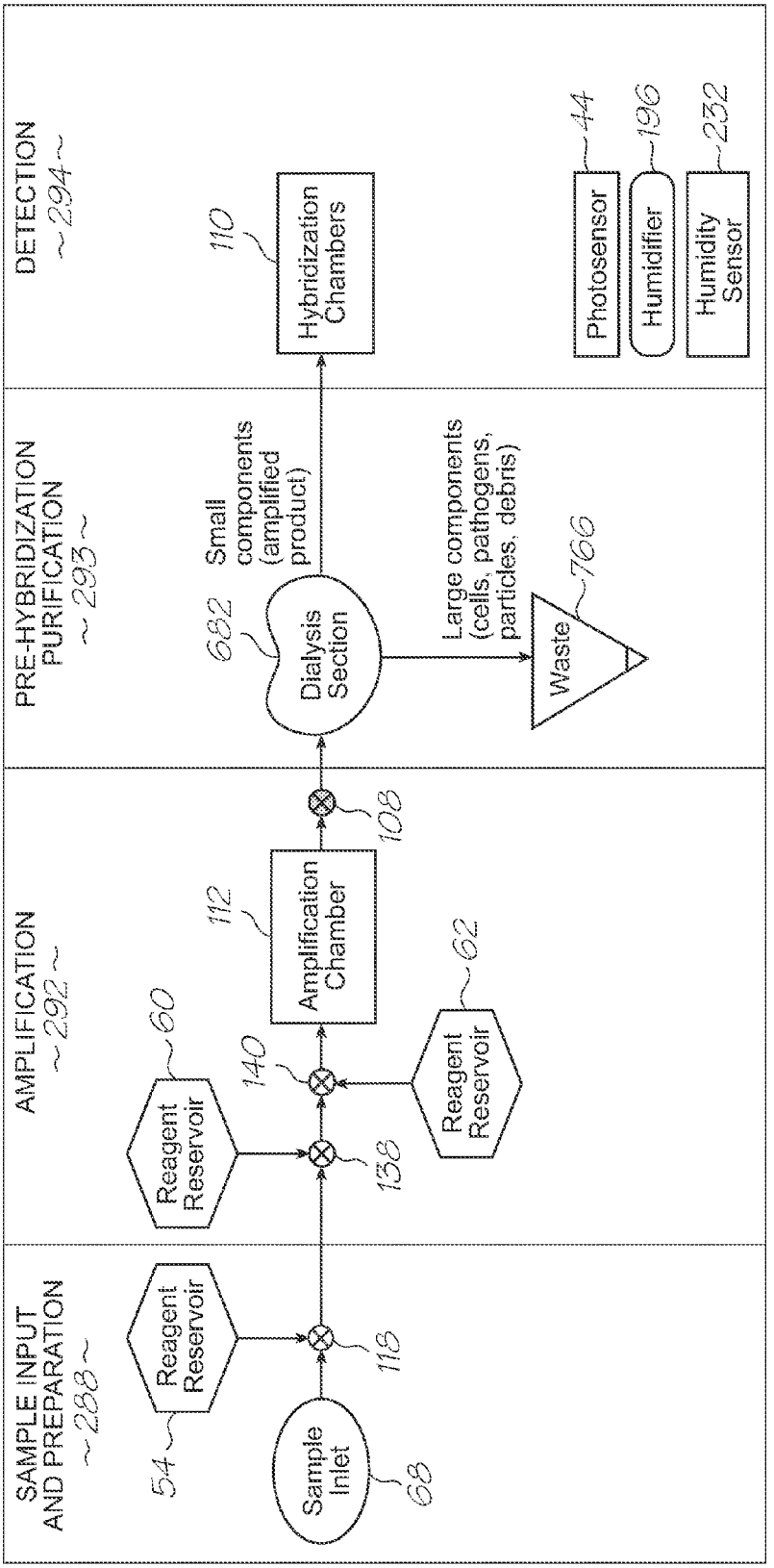

SAMPLE INPUT AND PREPARATION ~288~
AMPLIFICATION ~292~
PRE-HYBRIDIZATION PURIFICATION ~293~
DETECTION ~294~
Reagent Reservoir
54
Sample Inlet
68
116
Reagent Reservoir
60
138
140
Amplification Chamber
112
108
Reagent Reservoir
62
682
Dialysis Section
Small components (amplified product)
Large components (cells, pathogens, particles, debris)
Waste
766
110
Hybridization Chambers
Photosensor
44
Humidifier
196
Humidity Sensor
232
674
KEY
⊗ Surface tension valve
⊗ Boiling - initiated valve
⊗ Thermal bend actuator valve
⊕ Fault tolerant valve array
P Pathogen target
L Leukocyte target

FIG. 83

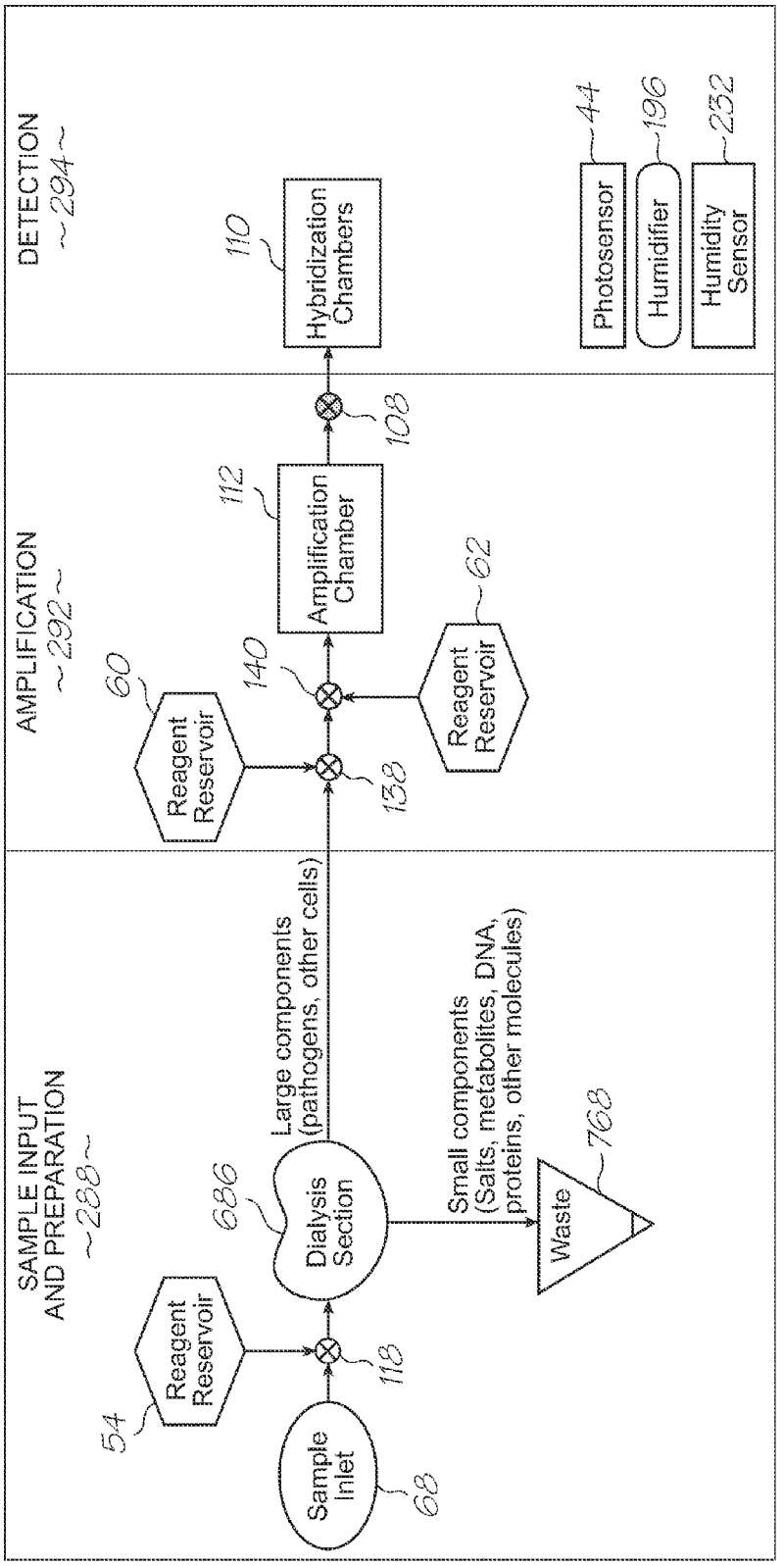

SAMPLE INPUT AND PREPARATION
~238~
AMPLIFICATION
~292~
DETECTION
~294~
54
Reagent Reservoir
68
Sample Inlet
118
686
Dialysis Section
Large components (pathogens, other cells)
Small components (Salts, metabolites, DNA, proteins, other molecules)
768
Waste
60
Reagent Reservoir
140
138
112
Amplification Chamber
108
110
Hybridization Chambers
62
Reagent Reservoir
44
Photosensor
196
Humidifier
232
Humidity Sensor
677
KEY
⊗ Surface tension valve
⊗ Boiling - initiated valve
⊗ Thermal bend actuator valve
⊕ Fault tolerant valve array
P Pathogen target
L Leukocyte target

FIG. 84

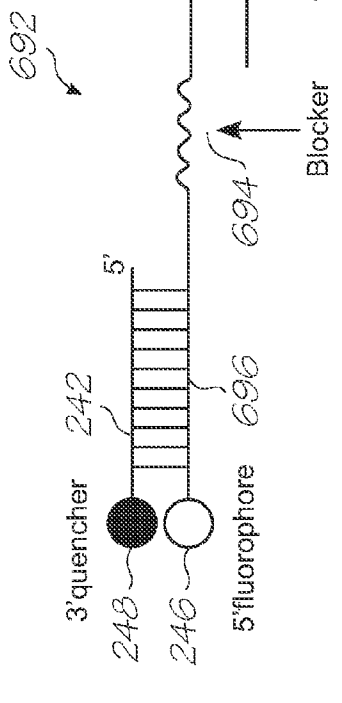


FIG. 85
(PRIOR ART)

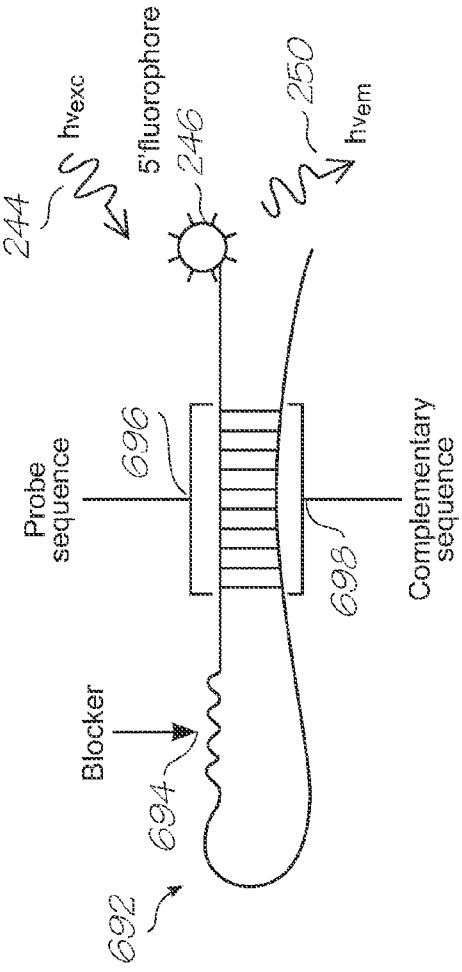
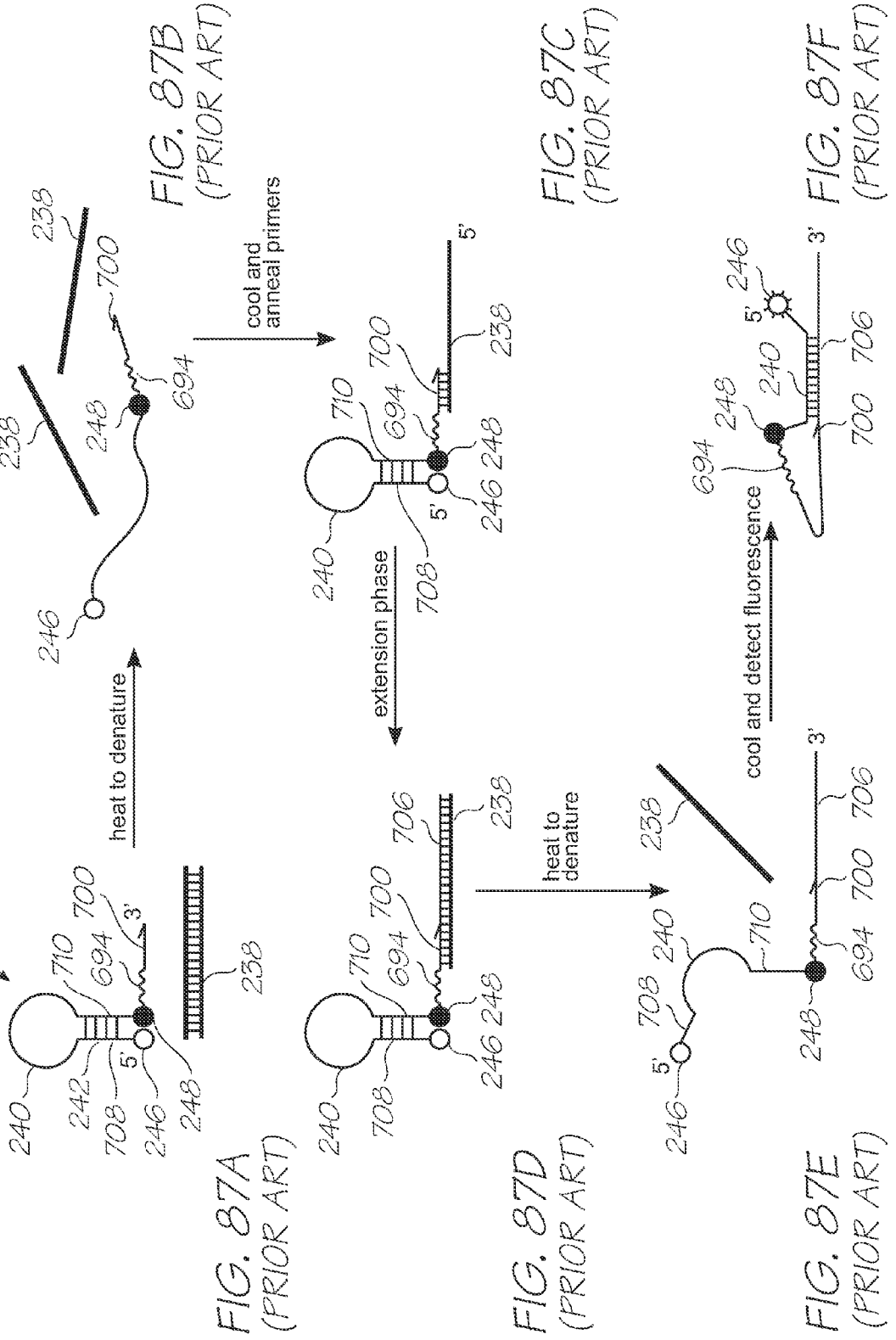


FIG. 86
(PRIOR ART)


704
710
700
694
3'
240
242
708
5'
246
248
238
heat to denature
238
700
694
248
246
FIG. 87A
(PRIOR ART)
FIG. 87B
(PRIOR ART)
cool and
anneal primers
710
700
694
5'
238
240
708
246 248
extension phase
FIG. 87C
(PRIOR ART)
706
700
694
710
240
708
246 248
heat to
denature
238
FIG. 87D
(PRIOR ART)
cool and detect fluorescence
246
5'
3'
248
240
706
694
700
FIG. 87E
(PRIOR ART)
FIG. 87F
(PRIOR ART)

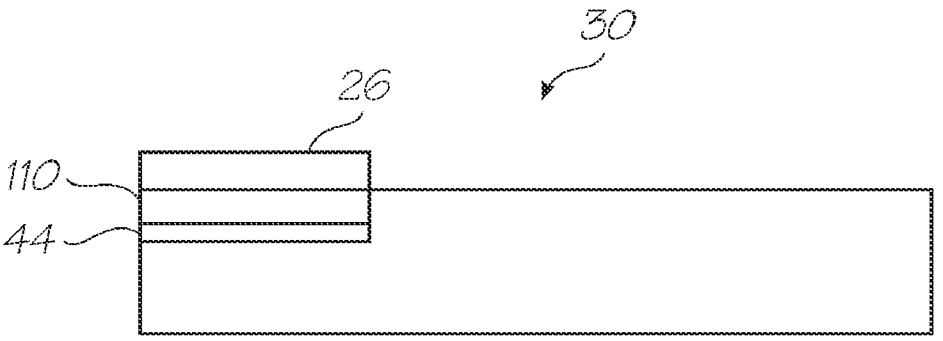


FIG. 88

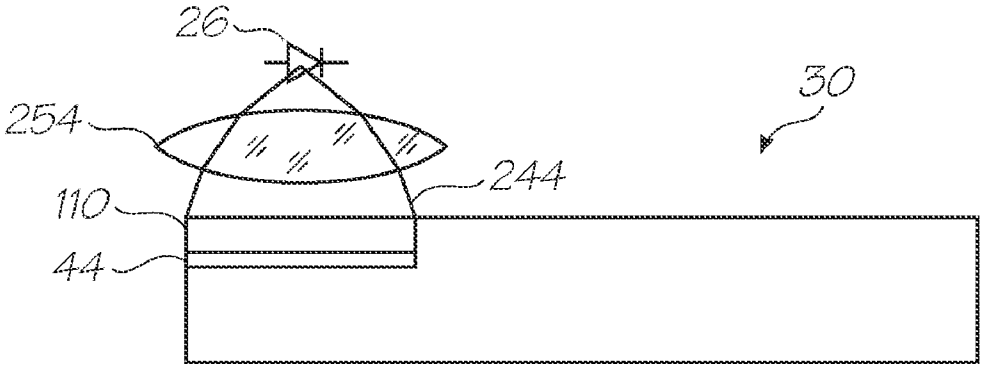


FIG. 89

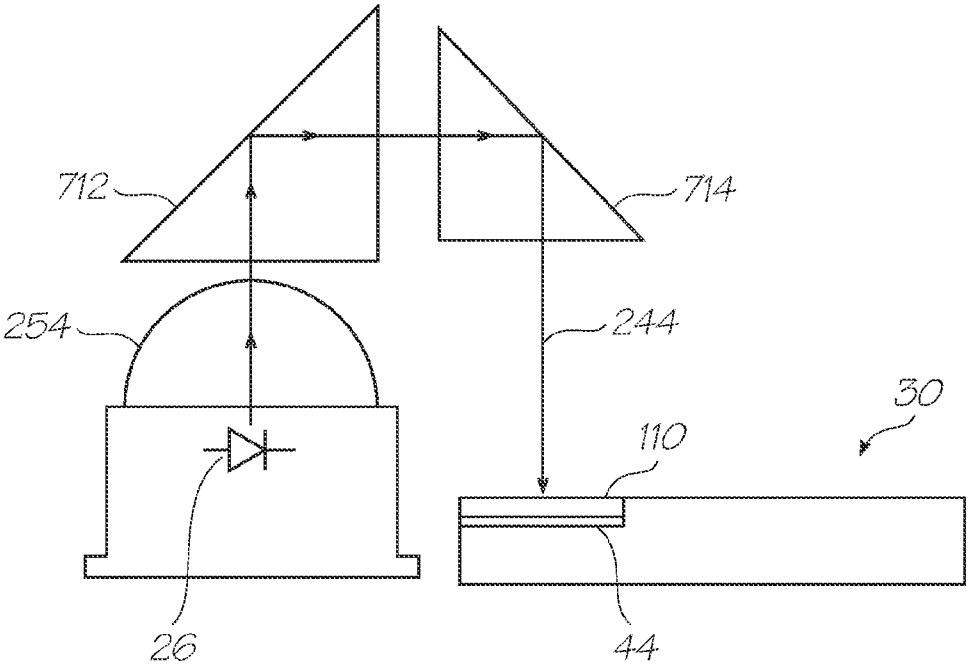


FIG. 90

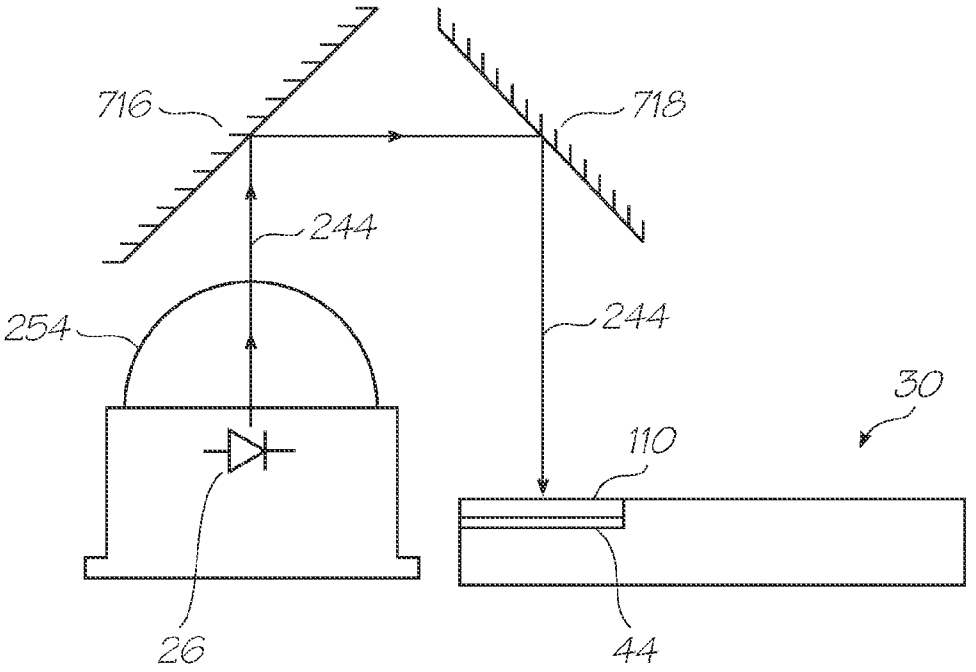
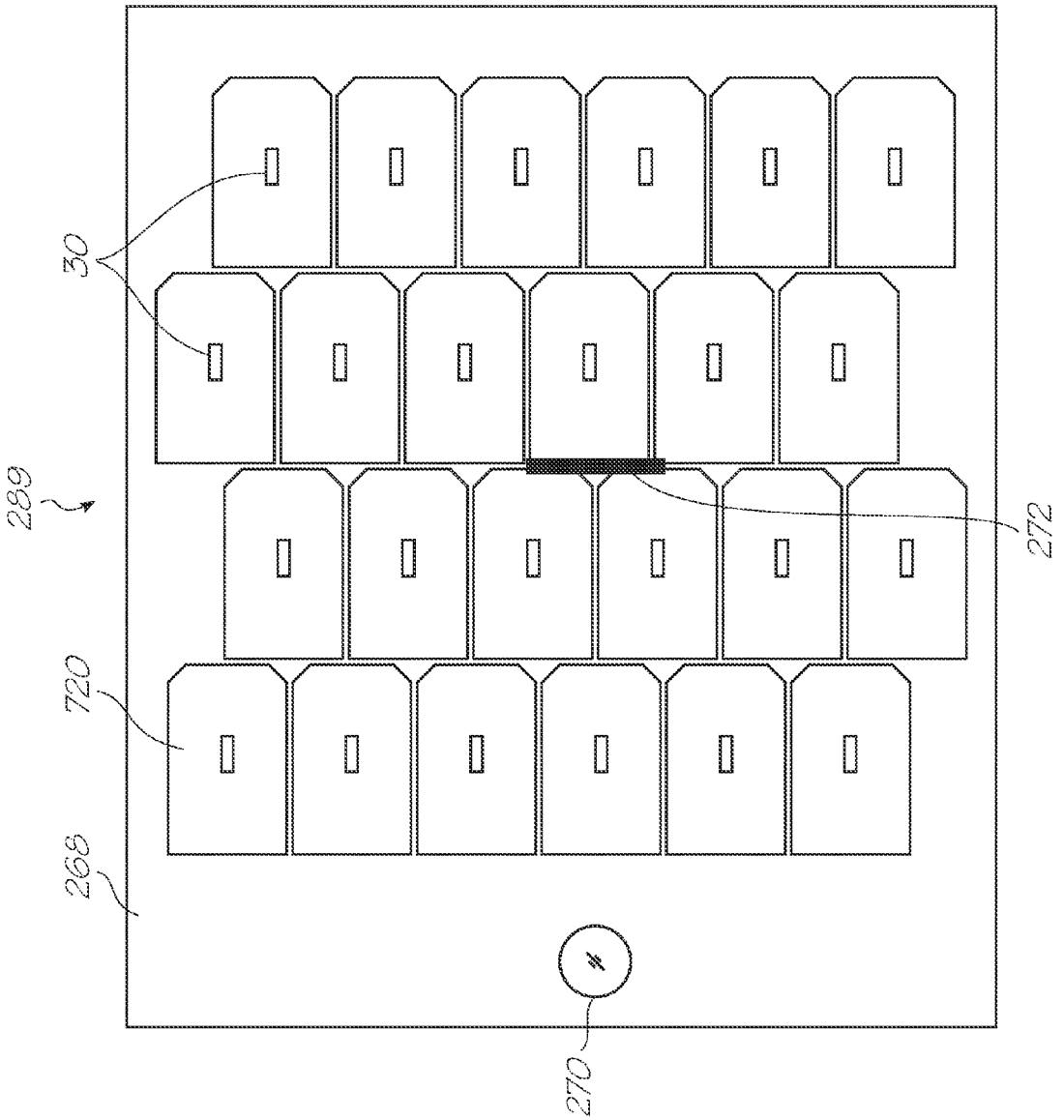


FIG. 91

FIG. 92



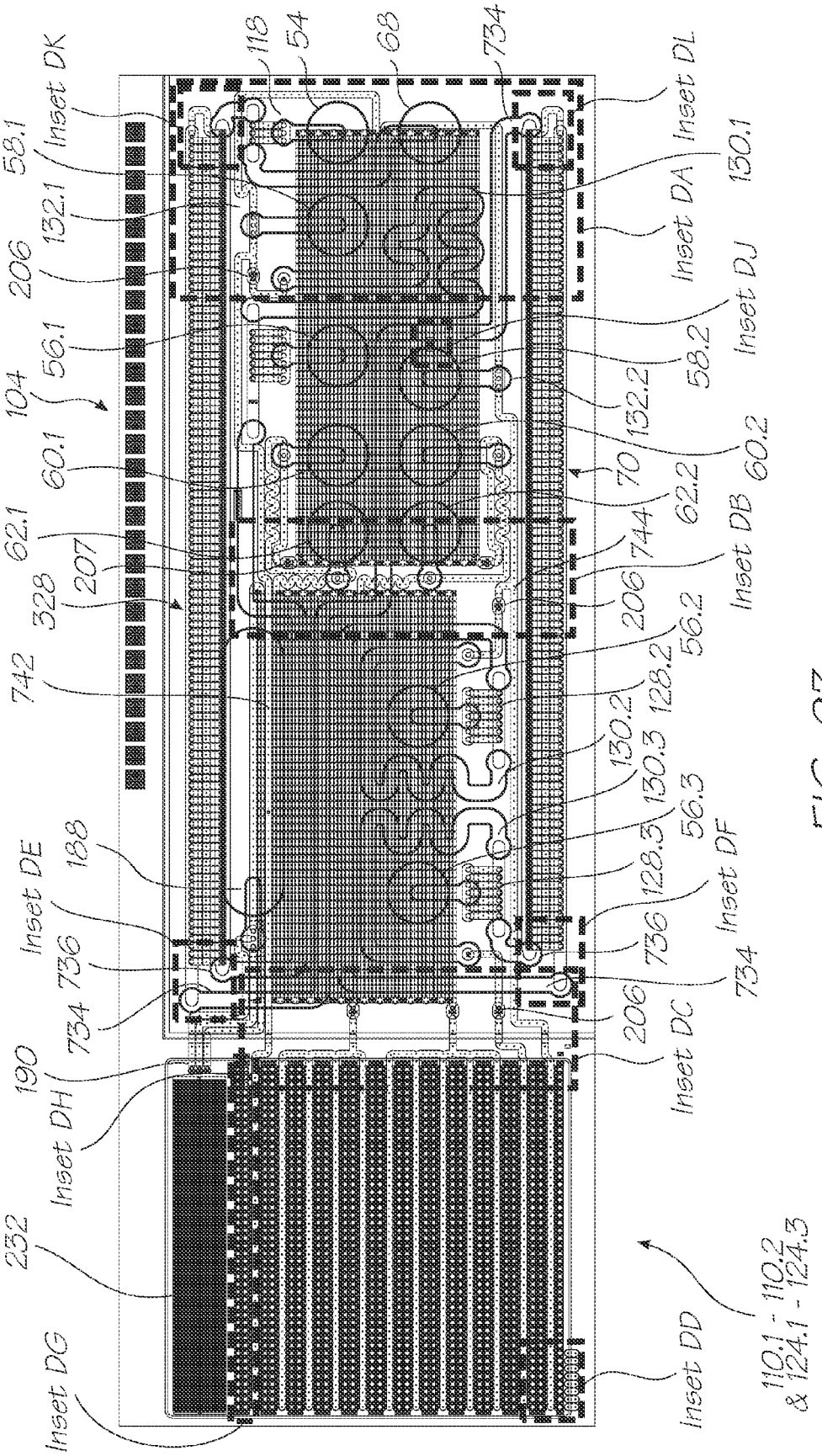

Inset DK
58.1
132.1
206
56.1
104
60.1
62.1
328
207
742
Inset DE
188
736
734
190
Inset DH
232
Inset DG
118
54
68
734
Inset DL
150.1
Inset DA
Inset DJ
58.2
132.2
70
62.2
744
206
56.2
128.2
130.2
130.3
56.3
128.3
736
734
206
Inset DC
Inset DF
Inset DB
60.2
Inset DD
110.1 - 110.2
& 124.1 - 124.3

FIG. 93

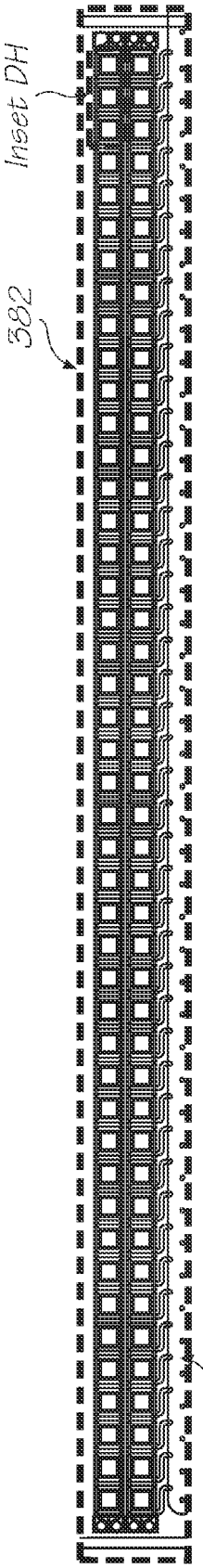


FIG. 94 (Inset DG)

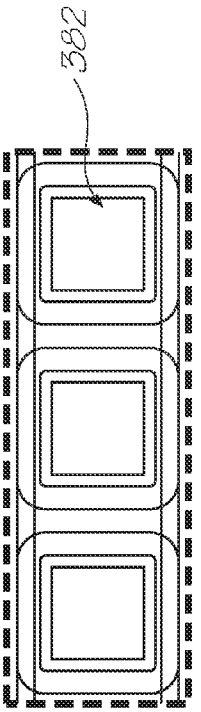


FIG. 95 (Inset DH)

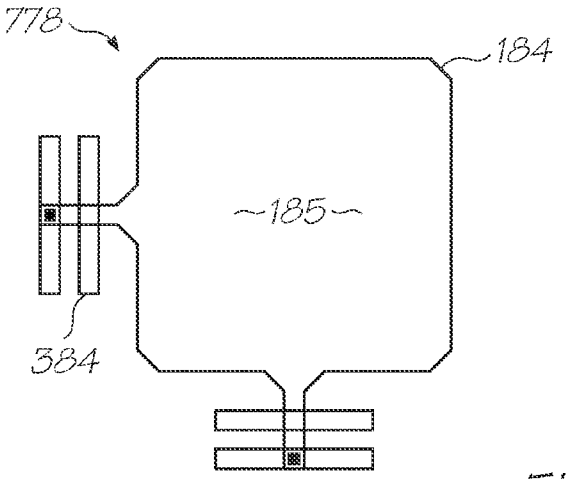


FIG. 96

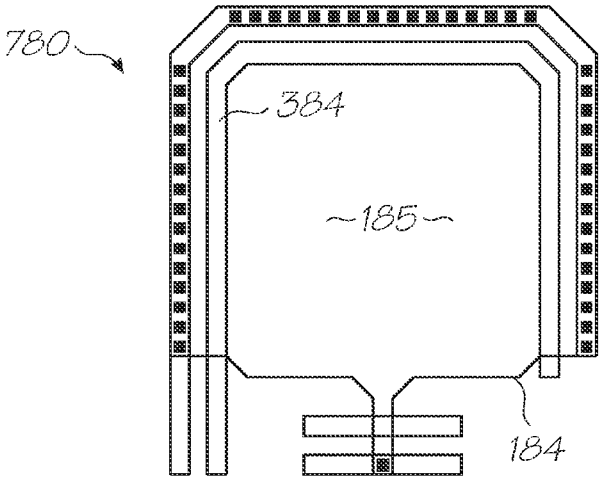


FIG. 97

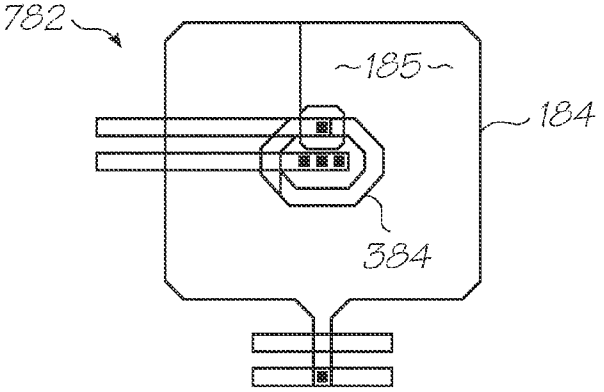


FIG. 98

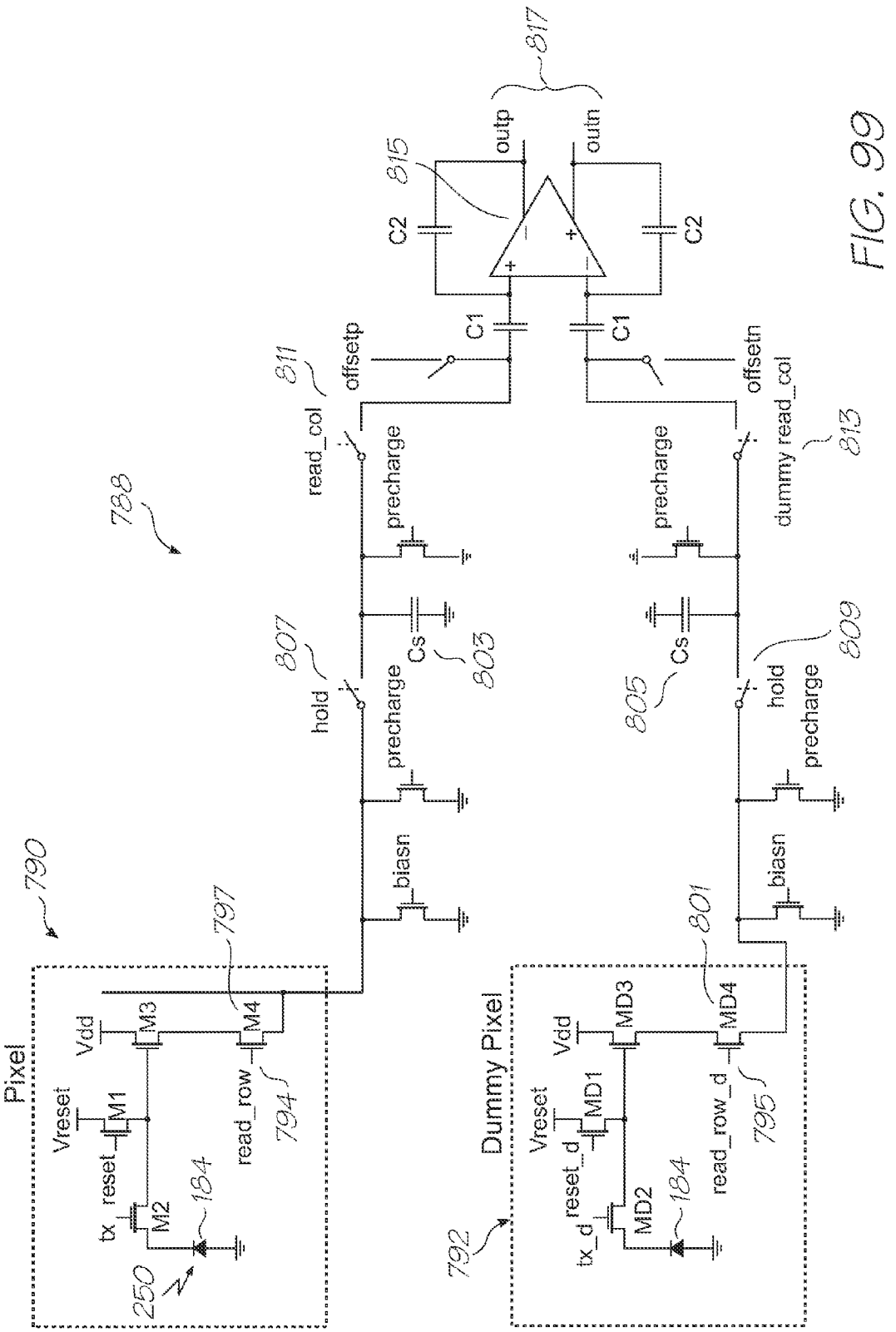

788
790
Pixel
Vreset
Vdd
M1
M3
M4
tx
reset
M2
184
250
read_row
794
797
792
Dummy Pixel
MD1
MD3
MD4
MD2
reset_d
tx_d
read_row_d
795
801
biasn
precharge
hold
807
Cs
803
805
809
read_col
offsetp
811
dummy read_col
offsetn
813
C1
C2
815
outp
outn
817

FIG. 99

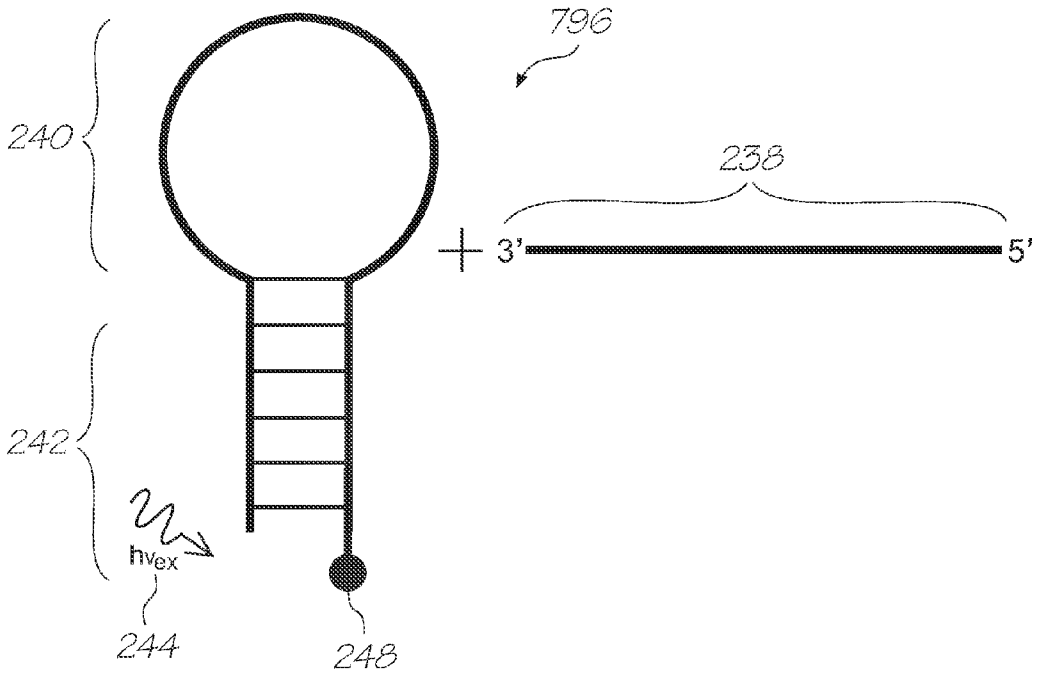


FIG. 100

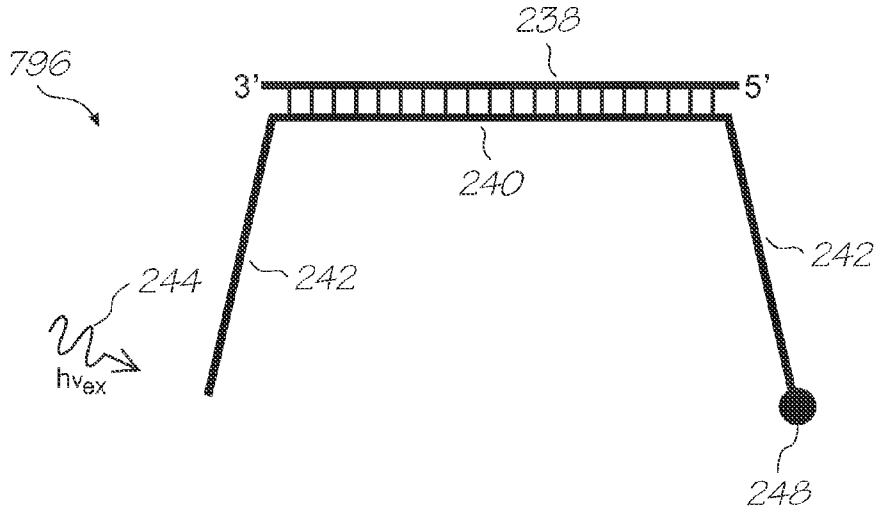


FIG. 101

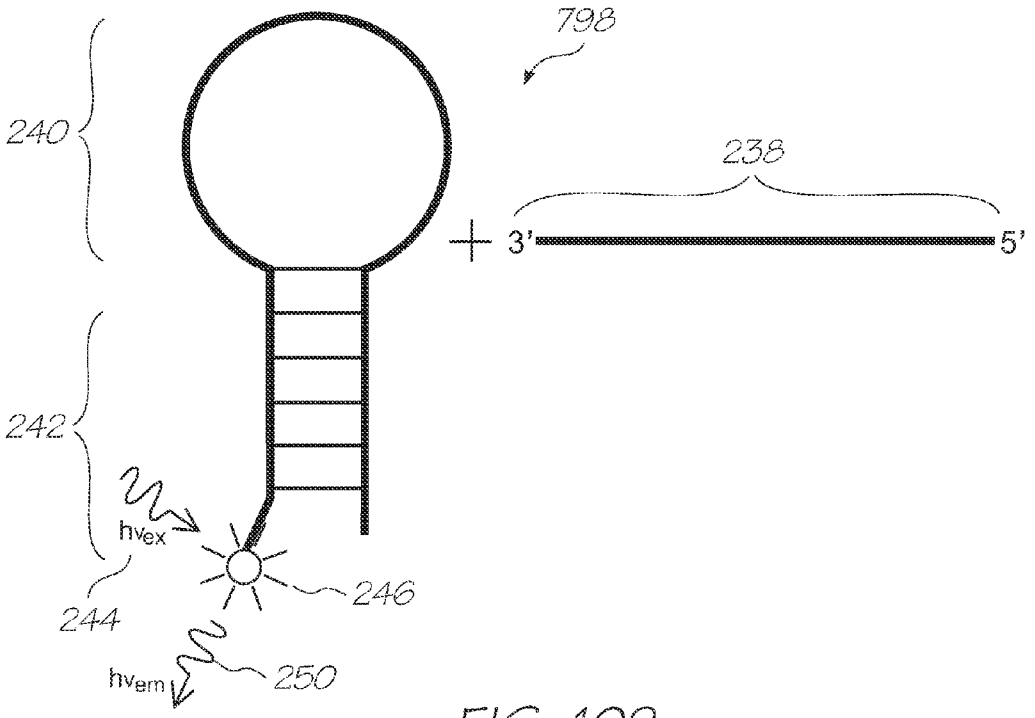


FIG. 102

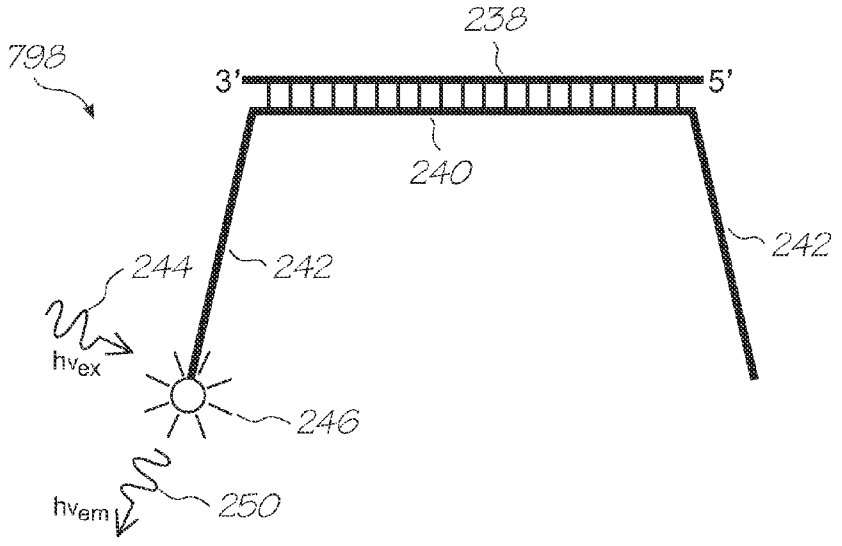


FIG. 103

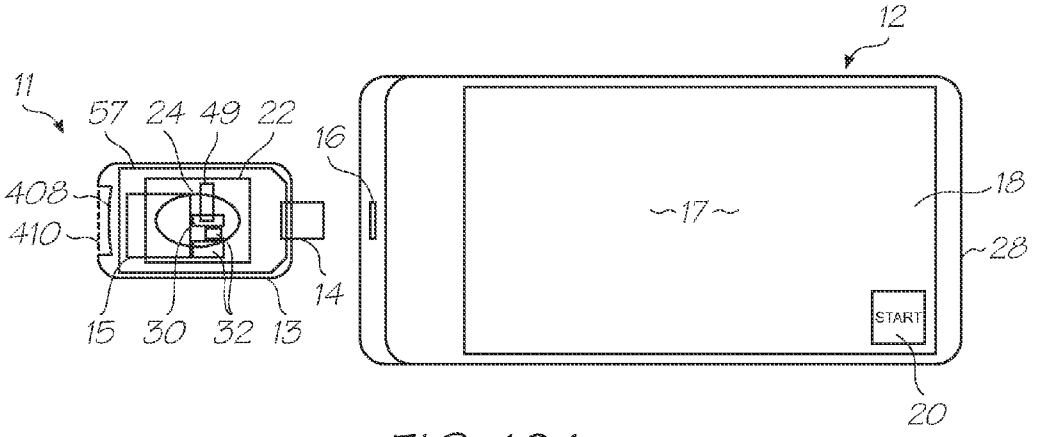


FIG. 104

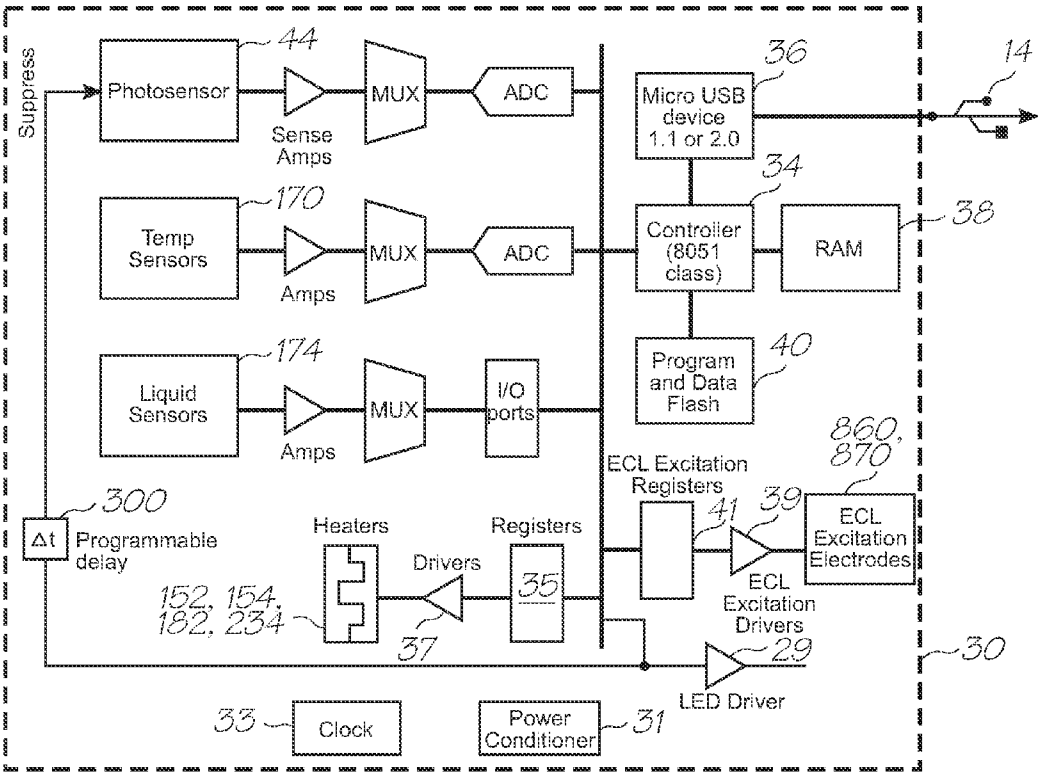


FIG. 105

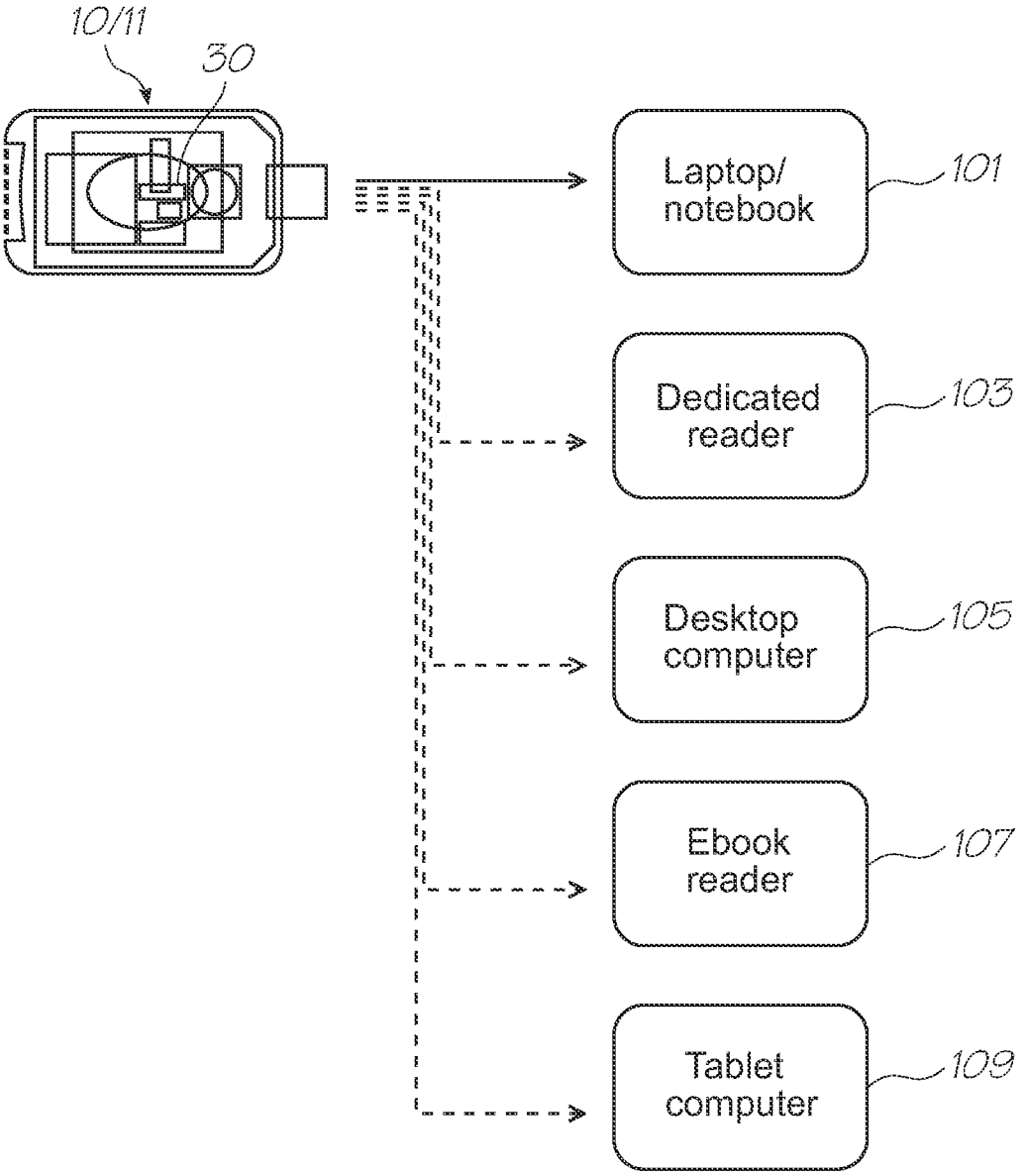

10/11
30
Laptop/ notebook
101
Dedicated reader
103
Desktop computer
105
Ebook reader
107
Tablet computer
109

FIG. 106

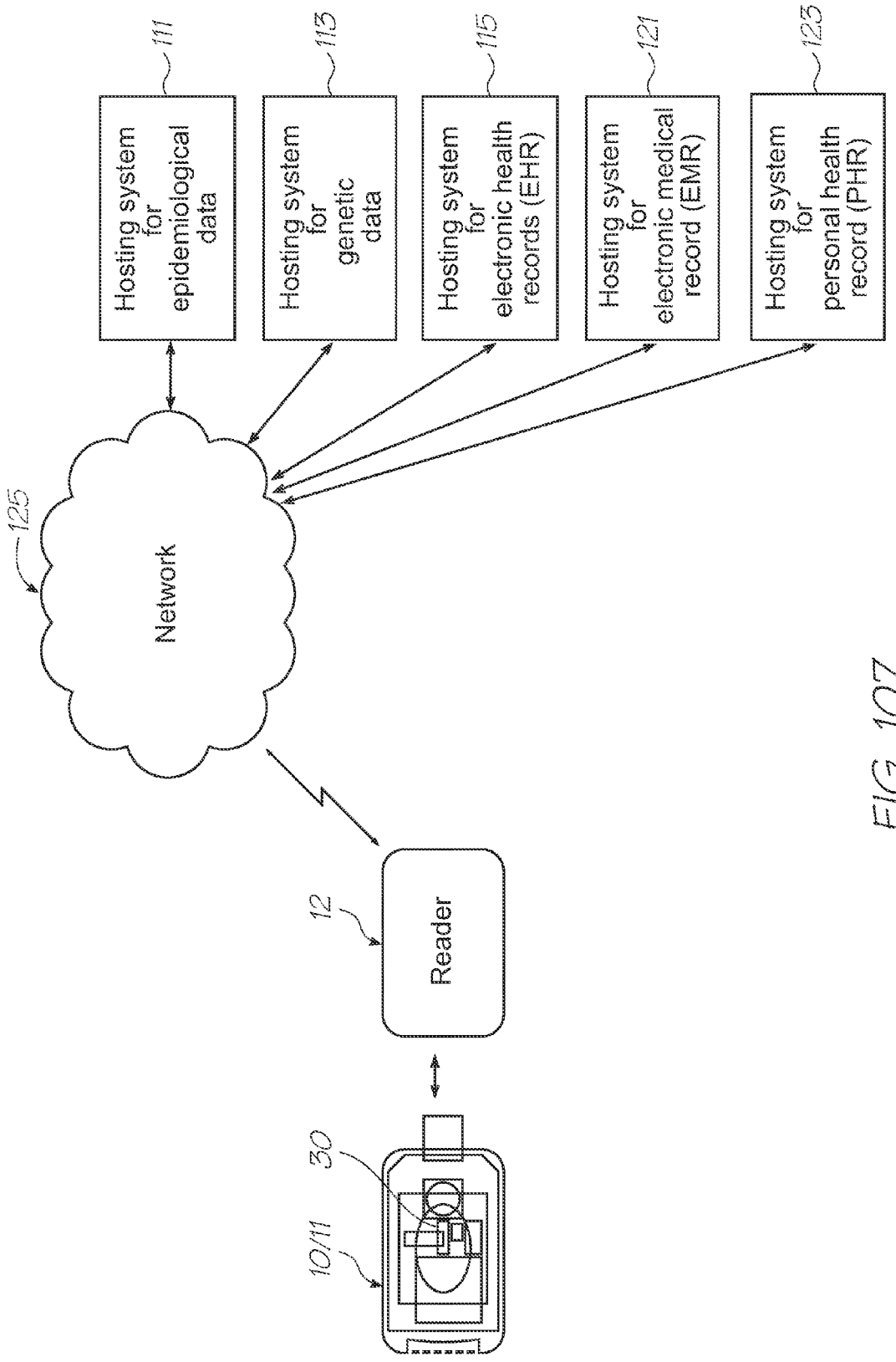

111
Hosting system for epidemiological data
113
Hosting system for genetic data
115
Hosting system for electronic health records (EHR)
121
Hosting system for electronic medical record (EMR)
123
Hosting system for personal health record (PHR)
125
Network
12
Reader
30
10/11

FIG. 107

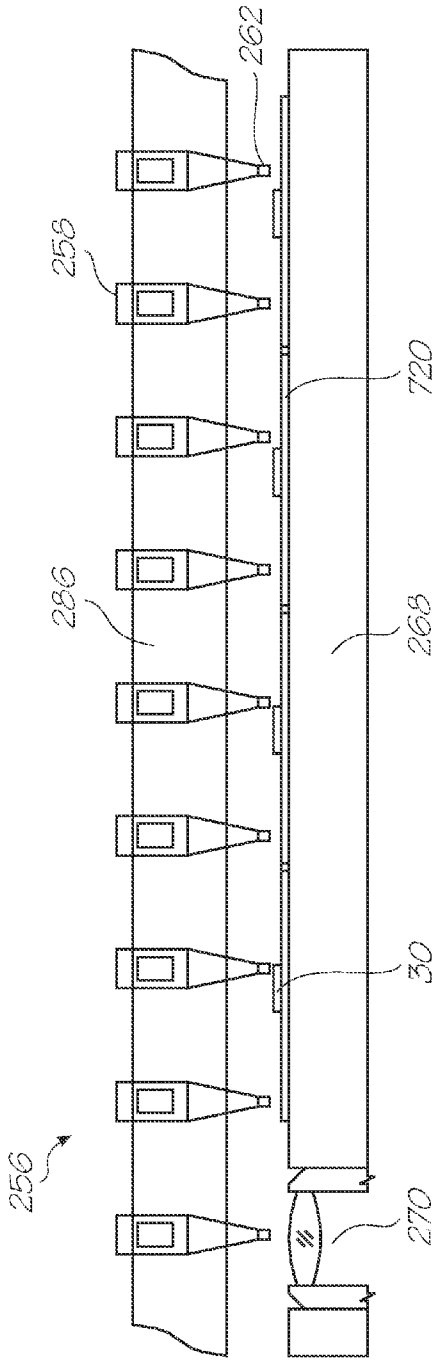


FIG. 108

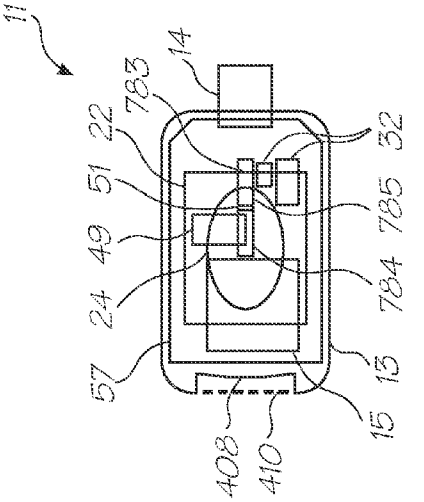


FIG. 109

MICROFLUIDIC TEST MODULE FOR INTERFACING WITH TABLET COMPUTER

FIELD OF THE INVENTION

[0001] The present invention relates to diagnostic devices that use microsystems technologies (MST). In particular, the invention relates to microfluidic and biochemical processing and analysis for molecular diagnostics.

CO-PENDING APPLICATIONS

[0002] The following applications have been filed by the Applicant which relate to the present application:

GBS001US	GBS002US	GBS003US	GBS005US	GBS006US
GSR001US	GSR002US	GAS001US	GAS002US	GAS003US
GAS004US	GAS006US	GAS007US	GAS008US	GAS009US
GAS010US	GAS012US	GAS013US	GAS014US	GAS015US
GAS016US	GAS017US	GAS018US	GAS019US	GAS020US
GAS021US	GAS022US	GAS023US	GAS024US	GAS025US
GAS026US	GAS027US	GAS028US	GAS030US	GAS031US
GAS032US	GAS033US	GAS034US	GAS035US	GAS036US
GAS037US	GAS038US	GAS039US	GAS040US	GAS041US
GAS042US	GAS043US	GAS044US	GAS045US	GAS046US
GAS047US	GAS048US	GAS049US	GAS050US	GAS054US
GAS055US	GAS056US	GAS057US	GAS058US	GAS059US
GAS060US	GAS061US	GAS062US	GAS063US	GAS065US
GAS066US	GAS067US	GAS068US	GAS069US	GAS070US
GAS080US	GAS081US	GAS082US	GAS083US	GAS084US
GAS085US	GAS086US	GAS087US	GAS088US	GAS089US
GAS090US	GAS091US	GAS092US	GAS093US	GAS094US
GAS095US	GAS096US	GAS097US	GAS098US	GAS099US
GAS100US	GAS101US	GAS102US	GAS103US	GAS104US
GAS105US	GAS106US	GAS108US	GAS109US	GAS110US
GAS111US	GAS112US	GAS113US	GAS114US	GAS115US
GAS117US	GAS118US	GAS119US	GAS120US	GAS121US
GAS122US	GAS123US	GAS124US	GAS125US	GAS126US
GAS127US	GAS128US	GAS129US	GAS130US	GAS131US
GAS132US	GAS133US	GAS134US	GAS135US	GAS136US
GAS137US	GAS138US	GAS139US	GAS140US	GAS141US
GAS142US	GAS143US	GAS144US	GAS146US	GAS147US
GRR001US	GRR002US	GRR003US	GRR004US	GRR005US
GRR006US	GRR007US	GRR008US	GRR009US	GRR010US
GVA001US	GVA002US	GVA004US	GVA005US	GVA006US
GVA007US	GVA008US	GVA009US	GVA010US	GVA011US
GVA012US	GVA013US	GVA014US	GVA015US	GVA016US
GVA017US	GVA018US	GVA019US	GVA020US	GVA021US
GVA022US	GHU001US	GHU002US	GHU003US	GHU004US
GHU006US	GHU007US	GHU008US	GWM001US	GWM002US
GDI001US	GDI002US	GDI003US	GDI004US	GDI005US
GDI006US	GDI007US	GDI009US	GDI010US	GDI011US
GDI013US	GDI014US	GDI015US	GDI016US	GDI017US
GDI019US	GDI023US	GDI028US	GDI030US	GDI039US
GDI040US	GDI041US	GPC001US	GPC002US	GPC003US
GPC004US	GPC005US	GPC006US	GPC007US	GPC008US
GPC009US	GPC010US	GPC011US	GPC012US	GPC014US
GPC017US	GPC018US	GPC019US	GPC023US	GPC027US
GPC028US	GPC029US	GPC030US	GPC031US	GPC033US
GPC034US	GPC035US	GPC036US	GPC037US	GPC038US
GPC039US	GPC040US	GPC041US	GPC042US	GPC043US
GLY001US	GLY002US	GLY003US	GLY004US	GLY005US
GLY006US	GIN001US	GIN002US	GIN003US	GIN004US
GIN005US	GIN006US	GIN007US	GIN008US	GMI001US
GMI002US	GMI005US	GMI008US	GLE001US	GLE002US
GLE003US	GLE004US	GLE005US	GLE006US	GLE007US
GLE008US	GLE009US	GLE010US	GLE011US	GLE012US
GLE013US	GLE014US	GLA001US	GGA001US	GGA003US
GRE001US	GRE002US	GRE003US	GRE004US	GRE005US
GRE006US	GCF001US	GCF002US	GCF003US	GCF004US
GCF005US	GCF006US	GCF007US	GCF008US	GCF009US
GCF010US	GCF011US	GCF012US	GCF013US	GCF014US
GCF015US	GCF016US	GCF020US	GCF021US	GCF022US
GCF023US	GCF024US	GCF025US	GCF027US	GCF028US
GCF029US	GCF030US	GCF031US	GCF032US	GCF033US

-continued

GCF034US	GCF035US	GCF036US	GCF037US	GSA001US
GSA002US	GSE001US	GSE002US	GSE003US	GSE004US
GDA001US	GDA002US	GDA003US	GDA004US	GDA005US
GDA006US	GDA007US	GPK001US	GMO001US	GMV001US
GMV002US	GMV003US	GMV004US	GRD001US	GRD002US
GRD003US	GRD004US	GPD001US	GPD003US	GPD004US
GPD005US	GPD006US	GPD007US	GPD008US	GPD009US
GPD010US	GPD011US	GPD012US	GPD013US	GPD014US
GPD015US	GPD016US	GPD017US	GAL001US	GPA001US
GPA003US	GPA004US	GPA005US	GSS001US	GSL001US
GCA001US	GCA002US	GCA003US		

[0003] The disclosures of these co-pending applications are incorporated herein by reference. The above applications have been identified by their filing docket number, which will be substituted with the corresponding application number, once assigned.

BACKGROUND OF THE INVENTION

[0004] Molecular diagnostics has emerged as a field that offers the promise of early disease detection, potentially before symptoms have manifested. Molecular diagnostic testing is used to detect:

[0005] Inherited disorders

[0006] Acquired disorders

[0007] Infectious diseases

[0008] Genetic predisposition to health-related conditions.

[0009] With high accuracy and fast turnaround times, molecular diagnostic tests have the potential to reduce the occurrence of ineffective health care services, enhance patient outcomes, improve disease management and individualize patient care. Many of the techniques in molecular diagnostics are based on the detection and identification of specific nucleic acids, both deoxyribonucleic acid (DNA) and ribonucleic acid (RNA), extracted and amplified from a biological specimen (such as blood or saliva). The complementary nature of the nucleic acid bases allows short sequences of synthesized DNA (oligonucleotides) to bond (hybridize) to specific nucleic acid sequences for use in nucleic acid tests. If hybridization occurs, then the complementary sequence is present in the sample. This makes it possible, for example, to predict the disease a person will contract in the future, determine the identity and virulence of an infectious pathogen, or determine the response a person will have to a drug.

Nucleic Acid Based Molecular Diagnostic Test

[0010] A nucleic acid based test has four distinct steps:

[0011] 1. Sample preparation

[0012] 2. Nucleic acid extraction

[0013] 3. Nucleic acid amplification (optional)

[0014] 4. Detection

[0015] Many sample types are used for genetic analysis, such as blood, urine, sputum and tissue samples. The diagnostic test determines the type of sample required as not all samples are representative of the disease process. These samples have a variety of constituents, but usually only one of these is of interest. For example, in blood, high concentrations of erythrocytes can inhibit the detection of a pathogenic organism. Therefore a purification and/or concentration step at the beginning of the nucleic acid test is often required.

[0016] Blood is one of the more commonly sought sample types. It has three major constituents: leukocytes (white blood cells), erythrocytes (red blood cells) and thrombocytes (platelets). The thrombocytes facilitate clotting and remain active in vitro. To inhibit coagulation, the specimen is mixed with an agent such as ethylenediaminetetraacetic acid (EDTA) prior to purification and concentration. Erythrocytes are usually removed from the sample in order to concentrate the target cells. In humans, erythrocytes account for approximately 99% of the cellular material but do not carry DNA as they have no nucleus. Furthermore, erythrocytes contain components such as haemoglobin that can interfere with the downstream nucleic acid amplification process (described below). Removal of erythrocytes can be achieved by differentially lysing the erythrocytes in a lysis solution, leaving remaining cellular material intact which can then be separated from the sample using centrifugation. This provides a concentration of the target cells from which the nucleic acids are extracted.

[0017] The exact protocol used to extract nucleic acids depends on the sample and the diagnostic assay to be performed. For example, the protocol for extracting viral RNA will vary considerably from the protocol to extract genomic DNA. However, extracting nucleic acids from target cells usually involves a cell lysis step followed by nucleic acid purification. The cell lysis step disrupts the cell and nuclear membranes, releasing the genetic material. This is often accomplished using a lysis detergent, such as sodium dodecyl sulfate, which also denatures the large amount of proteins present in the cells.

[0018] The nucleic acids are then purified with an alcohol precipitation step, usually ice-cold ethanol or isopropanol, or via a solid phase purification step, typically on a silica matrix in a column, resin or on paramagnetic beads in the presence of high concentrations of a chaotropic salt, prior to washing and then elution in a low ionic strength buffer. An optional step prior to nucleic acid precipitation is the addition of a protease which digests the proteins in order to further purify the sample.

[0019] Other lysis methods include mechanical lysis via ultrasonic vibration and thermal lysis where the sample is heated to 94° C. to disrupt cell membranes.

[0020] The target DNA or RNA may be present in the extracted material in very small amounts, particularly if the target is of pathogenic origin. Nucleic acid amplification provides the ability to selectively amplify (that is, replicate) specific targets present in low concentrations to detectable levels.

[0021] The most commonly used nucleic acid amplification technique is the polymerase chain reaction (PCR). PCR is well known in this field and comprehensive description of this type of reaction is provided in E. van Pelt-Verkuil et al., Principles and Technical Aspects of PCR Amplification, Springer, 2008.

[0022] PCR is a powerful technique that amplifies a target DNA sequence against a background of complex DNA. If RNA is to be amplified (by PCR), it must be first transcribed into cDNA (complementary DNA) using an enzyme called reverse transcriptase. Afterwards, the resulting cDNA is amplified by PCR.

[0023] PCR is an exponential process that proceeds as long as the conditions for sustaining the reaction are acceptable. The components of the reaction are:

[0024] 1. pair of primers—short single strands of DNA with around 10-30 nucleotides complementary to the regions flanking the target sequence

[0025] 2. DNA polymerase—a thermostable enzyme that synthesizes DNA

[0026] 3. deoxyribonucleoside triphosphates (dNTPs)—provide the nucleotides that are incorporated into the newly synthesized DNA strand

[0027] 4. buffer—to provide the optimal chemical environment for DNA synthesis

[0028] PCR typically involves placing these reactants in a small tube (~10-50 microlitres) containing the extracted nucleic acids. The tube is placed in a thermal cycler; an instrument that subjects the reaction to a series of different temperatures for varying amounts of time. The standard protocol for each thermal cycle involves a denaturation phase, an annealing phase, and an extension phase. The extension phase is sometimes referred to as the primer extension phase. In addition to such three-step protocols, two-step thermal protocols can be employed, in which the annealing and extension phases are combined. The denaturation phase typically involves raising the temperature of the reaction to 90-95° C. to denature the DNA strands; in the annealing phase, the temperature is lowered to ~50-60° C. for the primers to anneal; and then in the extension phase the temperature is raised to the optimal DNA polymerase activity temperature of 60-72° C. for primer extension. This process is repeated cyclically around 20-40 times, the end result being the creation of millions of copies of the target sequence between the primers.

[0029] There are a number of variants to the standard PCR protocol such as multiplex PCR, linker-primed PCR, direct PCR, tandem PCR, real-time PCR and reverse-transcriptase PCR, amongst others, which have been developed for molecular diagnostics.

[0030] Multiplex PCR uses multiple primer sets within a single PCR mixture to produce amplicons of varying sizes that are specific to different DNA sequences. By targeting multiple genes at once, additional information may be gained from a single test-run that otherwise would require several experiments. Optimization of multiplex PCR is more difficult though and requires selecting primers with similar annealing temperatures, and amplicons with similar lengths and base composition to ensure the amplification efficiency of each amplicon is equivalent.

[0031] Linker-primed PCR, also known as ligation adaptor PCR, is a method used to enable nucleic acid amplification of essentially all DNA sequences in a complex DNA mixture without the need for target-specific primers. The method firstly involves digesting the target DNA population with a suitable restriction endonuclease (enzyme). Double-stranded oligonucleotide linkers (also called adaptors) with a suitable overhanging end are then ligated to the ends of target DNA fragments using a ligase enzyme. Nucleic acid amplification is subsequently performed using oligonucleotide primers which are specific for the linker sequences. In this way, all fragments of the DNA source which are flanked by linker oligonucleotides can be amplified.

[0032] Direct PCR describes a system whereby PCR is performed directly on a sample without any, or with minimal, nucleic acid extraction. It has long been accepted that PCR reactions are inhibited by the presence of many components of unpurified biological samples, such as the haem component in blood. Traditionally, PCR has required extensive purification of the target nucleic acid prior to preparation of the

reaction mixture. With appropriate changes to the chemistry and sample concentration, however, it is possible to perform PCR with minimal DNA purification, or direct PCR. Adjustments to the PCR chemistry for direct PCR include increased buffer strength, the use of polymerases which have high activity and processivity, and additives which chelate with potential polymerase inhibitors.

[0033] Tandem PCR utilises two distinct rounds of nucleic acid amplification to increase the probability that the correct amplicon is amplified. One form of tandem PCR is nested PCR in which two pairs of PCR primers are used to amplify a single locus in separate rounds of nucleic acid amplification. The first pair of primers hybridize to the nucleic acid sequence at regions external to the target nucleic acid sequence. The second pair of primers (nested primers) used in the second round of amplification bind within the first PCR product and produce a second PCR product containing the target nucleic acid, that will be shorter than the first one. The logic behind this strategy is that if the wrong locus were amplified by mistake during the first round of nucleic acid amplification, the probability is very low that it would also be amplified a second time by a second pair of primers and thus ensures specificity.

[0034] Real-time PCR, or quantitative PCR, is used to measure the quantity of a PCR product in real time. By using a fluorophore-containing probe or fluorescent dyes along with a set of standards in the reaction, it is possible to quantitate the starting amount of nucleic acid in the sample. This is particularly useful in molecular diagnostics where treatment options may differ depending on the pathogen load in the sample.

[0035] Reverse-transcriptase PCR (RT-PCR) is used to amplify DNA from RNA. Reverse transcriptase is an enzyme that reverse transcribes RNA into complementary DNA (cDNA), which is then amplified by PCR. RT-PCR is widely used in expression profiling, to determine the expression of a gene or to identify the sequence of an RNA transcript, including transcription start and termination sites. It is also used to amplify RNA viruses such as human immunodeficiency virus or hepatitis C virus.

[0036] Isothermal amplification is another form of nucleic acid amplification which does not rely on the thermal denaturation of the target DNA during the amplification reaction and hence does not require sophisticated machinery. Isothermal nucleic acid amplification methods can therefore be carried out in primitive sites or operated easily outside of a laboratory environment. A number of isothermal nucleic acid amplification methods have been described, including Strand Displacement Amplification, Transcription Mediated Amplification, Nucleic Acid Sequence Based Amplification, Recombinase Polymerase Amplification, Rolling Circle Amplification, Ramification Amplification, Helicase-Dependent Isothermal DNA Amplification and Loop-Mediated Isothermal Amplification.

[0037] Isothermal nucleic acid amplification methods do not rely on the continuing heat denaturation of the template DNA to produce single stranded molecules to serve as templates for further amplification, but instead rely on alternative methods such as enzymatic nicking of DNA molecules by specific restriction endonucleases, or the use of an enzyme to separate the DNA strands, at a constant temperature.

[0038] Strand Displacement Amplification (SDA) relies on the ability of certain restriction enzymes to nick the unmodified strand of hemi-modified DNA and the ability of a 5'-3' exonuclease-deficient polymerase to extend and displace the downstream strand. Exponential nucleic acid amplification is then achieved by coupling sense and antisense reactions in which strand displacement from the sense reaction serves as a template for the antisense reaction. The use of nickase enzymes which do not cut DNA in the traditional manner but produce a nick on one of the DNA strands, such as N. Alw1, N. BstNB1 and Mly1, are useful in this reaction. SDA has been improved by the use of a combination of a heat-stable restriction enzyme (Ava1) and heat-stable Exo-polymerase (Bst polymerase). This combination has been shown to increase amplification efficiency of the reaction from 10^8 fold amplification to 10^{10} fold amplification so that it is possible using this technique to amplify unique single copy molecules.

[0039] Transcription Mediated Amplification (TMA) and Nucleic Acid Sequence Based Amplification (NASBA) use an RNA polymerase to copy RNA sequences but not corresponding genomic DNA. The technology uses two primers and two or three enzymes, RNA polymerase, reverse transcriptase and optionally RNase H (if the reverse transcriptase does not have RNase activity). One primer contains a promoter sequence for RNA polymerase. In the first step of nucleic acid amplification, this primer hybridizes to the target ribosomal RNA (rRNA) at a defined site. Reverse transcriptase creates a DNA copy of the target rRNA by extension from the 3' end of the promoter primer. The RNA in the resulting RNA:DNA duplex is degraded by the RNase activity of the reverse transcriptase if present or the additional RNase H. Next, a second primer binds to the DNA copy. A new strand of DNA is synthesized from the end of this primer by reverse transcriptase, creating a double-stranded DNA molecule. RNA polymerase recognizes the promoter sequence in the DNA template and initiates transcription. Each of the newly synthesized RNA amplicons re-enters the process and serves as a template for a new round of replication.

[0040] In Recombinase Polymerase Amplification (RPA), the isothermal amplification of specific DNA fragments is achieved by the binding of opposing oligonucleotide primers to template DNA and their extension by a DNA polymerase. Heat is not required to denature the double-stranded DNA (dsDNA) template. Instead, RPA employs recombinase-primer complexes to scan dsDNA and facilitate strand exchange at cognate sites. The resulting structures are stabilised by single-stranded DNA binding proteins interacting with the displaced template strand, thus preventing the ejection of the primer by branch migration. Recombinase disassembly leaves the 3' end of the oligonucleotide accessible to a strand displacing DNA polymerase, such as the large fragment of *Bacillus subtilis* Pol I (Bsu), and primer extension ensues. Exponential nucleic acid amplification is accomplished by the cyclic repetition of this process.

[0041] Helicase-dependent amplification (HDA) mimics the in vivo system in that it uses a DNA helicase enzyme to generate single-stranded templates for primer hybridization and subsequent primer extension by a DNA polymerase. In the first step of the HDA reaction, the helicase enzyme traverses along the target DNA, disrupting the hydrogen bonds linking the two strands which are then bound by single-stranded binding proteins. Exposure of the single-stranded target region by the helicase allows primers to anneal. The DNA polymerase then extends the 3' ends of each primer using free deoxyribonucleoside triphosphates (dNTPs) to produce two DNA replicates. The two replicated dsDNA

strands independently enter the next cycle of HDA, resulting in exponential nucleic acid amplification of the target sequence.

[0042] Other DNA-based isothermal techniques include Rolling Circle Amplification (RCA) in which a DNA polymerase extends a primer continuously around a circular DNA template, generating a long DNA product that consists of many repeated copies of the circle. By the end of the reaction, the polymerase generates many thousands of copies of the circular template, with the chain of copies tethered to the original target DNA. This allows for spatial resolution of target and rapid nucleic acid amplification of the signal. Up to 10^{12} copies of template can be generated in 1 hour. Ramification amplification is a variation of RCA and utilizes a closed circular probe (C-probe) or padlock probe and a DNA polymerase with a high processivity to exponentially amplify the C-probe under isothermal conditions.

[0043] Loop-mediated isothermal amplification (LAMP), offers high selectivity and employs a DNA polymerase and a set of four specially designed primers that recognize a total of six distinct sequences on the target DNA. An inner primer containing sequences of the sense and antisense strands of the target DNA initiates LAMP. The following strand displacement DNA synthesis primed by an outer primer releases a single-stranded DNA. This serves as template for DNA synthesis primed by the second inner and outer primers that hybridize to the other end of the target, which produces a stem-loop DNA structure. In subsequent LAMP cycling one inner primer hybridizes to the loop on the product and initiates displacement DNA synthesis, yielding the original stem-loop DNA and a new stem-loop DNA with a stem twice as long. The cycling reaction continues with accumulation of 10^9 copies of target in less than an hour. The final products are stem-loop DNAs with several inverted repeats of the target and cauliflower-like structures with multiple loops formed by annealing between alternately inverted repeats of the target in the same strand.

[0044] After completion of the nucleic acid amplification, the amplified product must be analysed to determine whether the anticipated amplicon (the amplified quantity of target nucleic acids) was generated. The methods of analyzing the product range from simply determining the size of the amplicon through gel electrophoresis, to identifying the nucleotide composition of the amplicon using DNA hybridization.

[0045] Gel electrophoresis is one of the simplest ways to check whether the nucleic acid amplification process generated the anticipated amplicon. Gel electrophoresis uses an electric field applied to a gel matrix to separate DNA fragments. The negatively charged DNA fragments will move through the matrix at different rates, determined largely by their size. After the electrophoresis is complete, the fragments in the gel can be stained to make them visible. Ethidium bromide is a commonly used stain which fluoresces under UV light.

[0046] The size of the fragments is determined by comparison with a DNA size marker (a DNA ladder), which contains DNA fragments of known sizes, run on the gel alongside the amplicon. Because the oligonucleotide primers bind to specific sites flanking the target DNA, the size of the amplified product can be anticipated and detected as a band of known size on the gel. To be certain of the identity of the amplicon, or if several amplicons have been generated, DNA probe hybridization to the amplicon is commonly employed.

[0047] DNA hybridization refers to the formation of double-stranded DNA by complementary base pairing. DNA hybridization for positive identification of a specific amplification product requires the use of a DNA probe around 20 nucleotides in length. If the probe has a sequence that is complementary to the amplicon (target) DNA sequence, hybridization will occur under favourable conditions of temperature, pH and ionic concentration. If hybridization occurs, then the gene or DNA sequence of interest was present in the original sample.

[0048] Optical detection is the most common method to detect hybridization. Either the amplicons or the probes are labelled to emit light through fluorescence or electrochemiluminescence. These processes differ in the means of producing excited states of the light-producing moieties, but both enable covalent labelling of nucleotide strands. In electrochemiluminescence (ECL), light is produced by luminophore molecules or complexes upon stimulation with an electric current. In fluorescence, it is illumination with excitation light which leads to emission.

[0049] Fluorescence is detected using an illumination source which provides excitation light at a wavelength absorbed by the fluorescent molecule, and a detection unit. The detection unit comprises a photosensor (such as a photomultiplier tube or charge-coupled device (CCD) array) to detect the emitted signal, and a mechanism (such as a wavelength-selective filter) to prevent the excitation light from being included in the photosensor output. The fluorescent molecules emit Stokes-shifted light in response to the excitation light, and this emitted light is collected by the detection unit. Stokes shift is the frequency difference or wavelength difference between emitted light and absorbed excitation light.

[0050] ECL emission is detected using a photosensor which is sensitive to the emission wavelength of the ECL species being employed. For example, transition metal-ligand complexes emit light at visible wavelengths, so conventional photodiodes and CCDs are employed as photosensors. An advantage of ECL is that, if ambient light is excluded, the ECL emission can be the only light present in the detection system, which improves sensitivity.

[0051] Microarrays allow for hundreds of thousands of DNA hybridization experiments to be performed simultaneously. Microarrays are powerful tools for molecular diagnostics with the potential to screen for thousands of genetic diseases or detect the presence of numerous infectious pathogens in a single test. A microarray consists of many different DNA probes immobilized as spots on a substrate. The target DNA (amplicon) is first labelled with a fluorescent or luminescent molecule (either during or after nucleic acid amplification) and then applied to the array of probes. The microarray is incubated in a temperature controlled, humid environment for a number of hours or days while hybridization between the probe and amplicon takes place. Following incubation, the microarray must be washed in a series of buffers to remove unbound strands. Once washed, the microarray surface is dried using a stream of air (often nitrogen). The stringency of the hybridization and washes is critical. Insufficient stringency can result in a high degree of nonspecific binding. Excessive stringency can lead to a failure of appropriate binding, which results in diminished sensitivity. Hybridization is recognized by detecting light emission from the labelled amplicons which have formed a hybrid with complementary probes.

[0052] Fluorescence from microarrays is detected using a microarray scanner which is generally a computer controlled inverted scanning fluorescence confocal microscope which typically uses a laser for excitation of the fluorescent dye and a photosensor (such as a photomultiplier tube or CCD) to detect the emitted signal. The fluorescent molecules emit Stokes-shifted light (described above) which is collected by the detection unit.

[0053] The emitted fluorescence must be collected, separated from the unabsorbed excitation wavelength, and transported to the detector. In microarray scanners, a confocal arrangement is commonly used to eliminate out-of-focus information by means of a confocal pinhole situated at an image plane. This allows only the in-focus portion of the light to be detected. Light from above and below the plane of focus of the object is prevented from entering the detector, thereby increasing the signal to noise ratio. The detected fluorescent photons are converted into electrical energy by the detector which is subsequently converted to a digital signal. This digital signal translates to a number representing the intensity of fluorescence from a given pixel. Each feature of the array is made up of one or more such pixels. The final result of a scan is an image of the array surface. The exact sequence and position of every probe on the microarray is known, and so the hybridized target sequences can be identified and analysed simultaneously.

[0054] More information regarding fluorescent probes can be found at: http://www.premierbiosoft.com/tech_notes/FRET_probe.html and http://www.invitrogen.com/site/us/en/home/References/Molecular-Probes-The-Handbook/Technical-Notes-and-Product-Highlights/Fluorescence-Resonance-Energy-Transfer-FRET.html

Point-of-Care Molecular Diagnostics

[0055] Despite the advantages that molecular diagnostic tests offer, the growth of this type of testing in the clinical laboratory has been slower than expected and remains a minor part of the practice of laboratory medicine. This is primarily due to the complexity and costs associated with nucleic acid testing compared with tests based on methods not involving nucleic acids. The widespread adaptation of molecular diagnostics testing to the clinical setting is intimately tied to the development of instrumentation that significantly reduces the cost, provides a rapid and automated assay from start (specimen processing) to finish (generating a result) and operates without major intervention by personnel.

[0056] A point-of-care technology serving the physician's office, the hospital bedside or even consumer-based, at home, would offer many advantages including:

[0057] rapid availability of results enabling immediate facilitation of treatment and improved quality of care.

[0058] ability to obtain laboratory values from testing very small samples.

[0059] reduced clinical workload.

[0060] reduced laboratory workload and improved office efficiency by reducing administrative work.

[0061] improved cost per patient through reduced length of stay of hospitalization, conclusion of outpatient consultation at the first visit, and reduced handling, storing and shipping of specimens.

[0062] facilitation of clinical management decisions such as infection control and antibiotic use.

Lab-on-a-Chip (LOC) Based Molecular Diagnostics

[0063] Molecular diagnostic systems based on microfluidic technologies provide the means to automate and speed up molecular diagnostic assays. The quicker detection times are primarily due to the extremely low volumes involved, automation, and the low-overhead inbuilt cascading of the diagnostic process steps within a microfluidic device. Volumes in the nanoliter and microliter scale also reduce reagent consumption and cost. Lab-on-a-chip (LOC) devices are a common form of microfluidic device. LOC devices have MST structures within a MST layer for fluid processing integrated onto a single supporting substrate (usually silicon). Fabrication using the VLSI (very large scale integrated) lithographic techniques of the semiconductor industry keeps the unit cost of each LOC device very low. However, controlling fluid flow through the LOC device, adding reagents, controlling reaction conditions and so on necessitate bulky external plumbing and electronics. Connecting a LOC device to these external devices effectively restricts the use of LOC devices for molecular diagnostics to the laboratory setting. The cost of the external equipment and complexity of its operation precludes LOC-based molecular diagnostics as a practical option for point-of-care settings.

[0064] In view of the above, there is a need for a molecular diagnostic system based on a LOC device for use at point-of-care.

SUMMARY OF THE INVENTION

[0065] Accordingly, the present invention provides a microfluidic test module for analyzing a sample fluid and communicating test results to a tablet computer, the microfluidic test module comprising:

[0066] an outer casing with a receptacle for receiving the sample;

[0067] functional sections for processing and analyzing the sample; a communication interface for communication with the tablet computer; and,

[0068] a controller for operative control of the communication interface.

[0069] Preferably, the communication interface is a universal serial bus (USB) device driver for operative control of a USB plug in the test module for communication with an external device.

[0070] Preferably, the USB device driver is configured to draw power from the tablet computer to power the controller and the functional sections.

[0071] Preferably, the controller is further configured for operative control of the functional sections during processing and analysis of the sample.

[0072] Preferably, the controller is configured to download data via the tablet computer.

[0073] Preferably, the microfluidic test module also has a plurality of reagent reservoirs containing reagents for processing the sample and digital memory for storing data relating to the reagent identities.

[0074] Preferably, the data stored in the digital memory is a unique identifier for microfluidic test module.

[0075] Preferably, the sample is a biological sample containing genetic material and one of the functional sections is

a nucleic acid amplification section for amplifying nucleic acid sequences in the genetic material.

[0076] Preferably, the nucleic acid amplification section is a polymerase chain reaction (PCR) section and the data stored in the digital memory includes thermal cycle times and cycle numbers.

[0077] Preferably, the functional sections include an incubation section upstream of the PCR section and one of the reagent reservoirs is a restriction enzyme reservoir, the incubation section having a heater for maintaining a mixture of the sample and restriction enzymes at an incubation temperature during restriction digestion of the nucleic acid sequences.

[0078] Preferably, the microfluidic test module also has an array of probes for hybridization with target nucleic acid sequences in the amplicon from the PCR section.

[0079] Preferably, the data stored in the digital memory includes probe identity data identifying the probe at each site within the array of probes.

[0080] Preferably, the microfluidic test module also has a photosensor wherein each of the probes are configured to form a probe-target hybrid with a complementary target nucleic acid sequence contained in the amplicon, each of the probe-target hybrids being configured to emit photons in response to an input, and the photosensor is configured for sensing the photons emitted by the probe-target hybrids.

[0081] Preferably, the data stored in the digital memory includes hybridization data generated from the photosensor output.

[0082] Preferably, the microfluidic test module also has a hybridization chamber array for containing the probes such that the probes within each hybridization chamber are configured to hybridize with one of the target nucleic acid sequences.

[0083] Preferably, the photosensor is an array of photodiodes positioned in registration with the hybridization chambers.

[0084] Preferably, the controller is configured for transmission of the hybridization data to the tablet computer.

[0085] Preferably, the sample is drawn from a patient and the controller is configured to download patient data via the tablet computer and store the patient data in the digital memory.

[0086] Preferably, the PCR section has an active valve for retaining liquid in the PCR section during thermal cycling and allowing flow to the hybridization chambers in response to an activation signal from the controller.

[0087] Preferably, the active valve is a boiling-initiated valve with a meniscus anchor configured to pin a meniscus that arrests capillary driven flow of the liquid, and a heater for boiling the liquid to unpin the meniscus from the meniscus anchor such that capillary driven flow resumes.

[0088] The easily usable, mass-producible, inexpensive, compact, light, and portable Microfluidic test module, with self-contained storage of required reagents, accepts a sample and processes and analyzes the sample material using the module's integral sensors, and provides the results electronically at its output port. The module's communications port is interfaced to a tablet computer which provides the module with power, computing, communications, and user interface support. Tablet computers are widely and inexpensively available, obviating the need for specialized, heavy, and expensive module support systems.

BRIEF DESCRIPTION OF THE DRAWINGS

[0089] Preferred embodiments of the present invention will now be described by way of example only with reference to the accompanying drawings, in which:

[0090] FIG. **1** shows a test module and test module reader configured for fluorescence detection;

[0091] FIG. **2** is a schematic overview of the electronic components in the test module configured for fluorescence detection;

[0092] FIG. **3** is a schematic overview of the electronic components in the test module reader;

[0093] FIG. **4** is a schematic representation of the architecture of the LOC device;

[0094] FIG. **5** is a perspective of the LOC device;

[0095] FIG. **6** is a plan view of the LOC device with features and structures from all layers superimposed on each other;

[0096] FIG. **7** is a plan view of the LOC device with the structures of the cap shown in isolation;

[0097] FIG. **8** is a top perspective of the cap with internal channels and reservoirs shown in dotted line;

[0098] FIG. **9** is an exploded top perspective of the cap with internal channels and reservoirs shown in dotted line;

[0099] FIG. **10** is a bottom perspective of the cap showing the configuration of the top channels;

[0100] FIG. **11** is a plan view of the LOC device showing the structures of the CMOS+MST device in isolation;

[0101] FIG. **12** is a schematic section view of the LOC device at the sample inlet;

[0102] FIG. **13** is an enlarged view of Inset AA shown in FIG. **6**;

[0103] FIG. **14** is an enlarged view of Inset AB shown in FIG. **6**;

[0104] FIG. **15** is an enlarged view of Inset AE shown in FIG. **13**;

[0105] FIG. **16** is a partial perspective illustrating the laminar structure of the LOC device within Inset AE;

[0106] FIG. **17** is a partial perspective illustrating the laminar structure of the LOC device within Inset AE;

[0107] FIG. **18** is a partial perspective illustrating the laminar structure of the LOC device within Inset AE;

[0108] FIG. **19** is a partial perspective illustrating the laminar structure of the LOC device within Inset AE;

[0109] FIG. **20** is a partial perspective illustrating the laminar structure of the LOC device within Inset AE;

[0110] FIG. **21** is a partial perspective illustrating the laminar structure of the LOC device within Inset AE;

[0111] FIG. **22** is schematic section view of the lysis reagent reservoir shown in FIG. **21**;

[0112] FIG. **23** is a partial perspective illustrating the laminar structure of the LOC device within Inset AB;

[0113] FIG. **24** is a partial perspective illustrating the laminar structure of the LOC device within Inset AB;

[0114] FIG. **25** is a partial perspective illustrating the laminar structure of the LOC device within Inset AI;

[0115] FIG. **26** is a partial perspective illustrating the laminar structure of the LOC device within Inset AB;

[0116] FIG. **27** is a partial perspective illustrating the laminar structure of the LOC device within Inset AB;

[0117] FIG. **28** is a partial perspective illustrating the laminar structure of the LOC device within Inset AB;

[0118] FIG. **29** is a partial perspective illustrating the laminar structure of the LOC device within Inset AB;
[0119] FIG. **30** is a schematic section view of the amplification mix reservoir and the polymerase reservoir;
[0120] FIG. **31** show the features of a boiling-initiated valve in isolation;
[0121] FIG. **32** is a schematic section view of the boiling-initiated valve taken through line **33-33** shown in FIG. **31**;
[0122] FIG. **33** is an enlarged view of Inset AF shown in FIG. **15**;
[0123] FIG. **34** is a schematic section view of the upstream end of the dialysis section taken through line **35-35** shown in FIG. **33**;
[0124] FIG. **35** is an enlarged view of Inset AC shown in FIG. **6**;
[0125] FIG. **36** is a further enlarged view within Inset AC showing the amplification section;
[0126] FIG. **37** is a further enlarged view within Inset AC showing the amplification section;
[0127] FIG. **38** is a further enlarged view within Inset AC showing the amplification section;
[0128] FIG. **39** is a further enlarged view within Inset AK shown in FIG. **38**;
[0129] FIG. **40** is a further enlarged view within Inset AC showing the amplification chamber;
[0130] FIG. **41** is a further enlarged view within Inset AC showing the amplification section;
[0131] FIG. **42** is a further enlarged view within Inset AC showing the amplification chamber;
[0132] FIG. **43** is a further enlarged view within Inset AL shown in FIG. **42**;
[0133] FIG. **44** is a further enlarged view within Inset AC showing the amplification section;
[0134] FIG. **45** is a further enlarged view within Inset AM shown in FIG. **44**;
[0135] FIG. **46** is a further enlarged view within Inset AC showing the amplification chamber;
[0136] FIG. **47** is a further enlarged view within Inset AN shown in FIG. **46**;
[0137] FIG. **48** is a further enlarged view within Inset AC showing the amplification chamber;
[0138] FIG. **49** is a further enlarged view within Inset AC showing the amplification chamber;
[0139] FIG. **50** is a further enlarged view within Inset AC showing the amplification section;
[0140] FIG. **51** is a schematic section view of the amplification section;
[0141] FIG. **52** is an enlarged plan view of the hybridization section;
[0142] FIG. **53** is a further enlarged plan view of two hybridization chambers in isolation;
[0143] FIG. **54** is schematic section view of a single hybridization chamber;
[0144] FIG. **55** is an enlarged view of the humidifier illustrated in Inset AG shown in FIG. **6**;
[0145] FIG. **56** is an enlarged view of Inset AD shown in FIG. **52**;
[0146] FIG. **57** is an exploded perspective view of the LOC device within Inset AD;
[0147] FIG. **58** is a diagram of a FRET probe in a closed configuration;
[0148] FIG. **59** is a diagram of a FRET probe in an open and hybridized configuration;
[0149] FIG. **60** is a graph of the intensity of an excitation light over time;
[0150] FIG. **61** is a diagram of the excitation illumination geometry of the hybridization chamber array;
[0151] FIG. **62** is a diagram of a Sensor Electronic Technology LED illumination geometry;
[0152] FIG. **63** is a schematic plan view of a reagent dispensing robot;
[0153] FIG. **64** is a perspective of a reagent microvial with inbuilt droplet generator;
[0154] FIG. **65** is a schematic plan view of an oligonucleotide ejector robot for loading selected probes into a probe ejector chip;
[0155] FIG. **66** is a schematic plan view of a probe spotting robot for loading probes into the LOC devices on a partial-depth sawn silicon wafer;
[0156] FIG. **67** is an enlarged plan view of the humidity sensor shown in Inset AH of FIG. **6**;
[0157] FIG. **68** is a schematic showing part of the photodiode array of the photo sensor;
[0158] FIG. **69** is a circuit diagram for a single photodiode;
[0159] FIG. **70** is a timing diagram for the photodiode control signals;
[0160] FIG. **71** shows an oligonucleotide ejector chip (ONEC);
[0161] FIG. **72** shows an array of droplet generators from the ONEC shown in Inset AO of FIG. **71**;
[0162] FIG. **73** is a schematic section of the array of droplet generators taken along line **91-91** shown in FIG. **72**;
[0163] FIG. **74** is an enlarged view of the evaporator shown in Inset AP of FIG. **55**;
[0164] FIG. **75** is a schematic section view through a hybridization chamber with a detection photodiode and trigger photodiode;
[0165] FIG. **76** is a diagram of linker-primed PCR;
[0166] FIG. **77** is a schematic representation of a test module with a lancet;
[0167] FIG. **78** is a diagrammatic representation of the architecture of LOC variant VII;
[0168] FIG. **79** is a diagrammatic representation of the architecture of LOC variant VIII;
[0169] FIG. **80** is a schematic illustration of the architecture of LOC variant XIV;
[0170] FIG. **81** is a schematic illustration of the architecture of LOC variant XLI;
[0171] FIG. **82** is a schematic illustration of the architecture of LOC variant XLIII;
[0172] FIG. **83** is a schematic illustration of the architecture of LOC variant XLIV;
[0173] FIG. **84** is a schematic illustration of the architecture of LOC variant XLVII;
[0174] FIG. **85** is a diagram of a primer-linked, linear fluorescent probe during the initial round of amplification;
[0175] FIG. **86** is a diagram of a primer-linked, linear fluorescent probe during a subsequent amplification cycle;
[0176] FIGS. **87**A to **87**F diagrammatically illustrate thermal cycling of a primer-linked fluorescent stem-and-loop probe;
[0177] FIG. **88** is a schematic illustration of the excitation LED relative to the hybridization chamber array and the photodiodes;
[0178] FIG. **89** is a schematic illustration of the excitation LED and optical lens for directing light onto the hybridization chamber array of the LOC device;

[0179] FIG. **90** is a schematic illustration of the excitation LED, optical lens, and optical prisms for directing light onto the hybridization chamber array of the LOC device;

[0180] FIG. **91** is a schematic illustration of the excitation LED, optical lens and mirror arrangement for directing light onto the hybridization chamber array of the LOC device;

[0181] FIG. **92** is a schematic plan view of a probe spotting robot for loading probes into the LOC devices on a separable PCB;

[0182] FIG. **93** is a plan view showing all the features superimposed on each other, and showing the location of Insets DA to DK;

[0183] FIG. **94** is an enlarged view of Inset DG shown in FIG. **93**;

[0184] FIG. **95** is an enlarged view of Inset DH shown in FIG. **93**;

[0185] FIG. **96** shows one embodiment of the shunt transistor for the photodiodes;

[0186] FIG. **97** shows one embodiment of the shunt transistor for the photodiodes;

[0187] FIG. **98** shows one embodiment of the shunt transistor for the photodiodes;

[0188] FIG. **99** is a circuit diagram of the differential imager;

[0189] FIG. **100** schematically illustrates a negative control fluorescent probe in its stem-and-loop configuration;

[0190] FIG. **101** schematically illustrates the negative control fluorescent probe of FIG. **100** in its open configuration;

[0191] FIG. **102** schematically illustrates a positive control fluorescent probe in its stem-and-loop configuration;

[0192] FIG. **103** schematically illustrates the positive control fluorescent probe of FIG. **102** in its open configuration;

[0193] FIG. **104** shows a test module and test module reader configured for use with ECL detection;

[0194] FIG. **105** is a schematic overview of the electronic components in the test module configured for use with ECL detection;

[0195] FIG. **106** shows a test module and alternative test module readers;

[0196] FIG. **107** shows a test module and test module reader along with the hosting system housing various databases;

[0197] FIG. **108** is a schematic side view of a reagent spotting robot;

[0198] FIG. **109** is a schematic representation of an electrochemiluminescence-based test module with multidevice microfluidic device;

DETAILED DESCRIPTION OF THE PREFERRED EMBODIMENTS

Overview

[0199] This overview identifies the main components of a molecular diagnostic system that incorporates embodiments of the present invention. Comprehensive details of the system architecture and operation are set out later in the specification.

[0200] Referring to FIGS. **1**, **2**, **3**, **104** and **105**, the system has the following top level components:

[0201] Test modules **10** and **11** are the size of a typical USB memory key and very cheap to produce. Test modules **10** and **11** each contain a microfluidic device, typically in the form of a lab-on-a-chip (LOC) device **30** preloaded with reagents and typically more than 1000 probes for the molecular diagnostic assay (see FIGS. **1** and **104**). Test module **10** schematically shown in FIG. **1** uses a fluorescence-based detection technique to identify target molecules, while test module **11** in FIG. **104** uses an electrochemiluminescence-based detection technique. The LOC device **30** has an integrated photosensor **44** for fluorescence or electrochemiluminescence detection (described in detail below). Both test modules **10** and **11** use a standard Micro-USB plug **14** for power, data and control, both have a printed circuit board (PCB) **57**, and both have external power supply capacitors **32** and an inductor **15**. The test modules **10** and **11** are both single-use only for mass production and distribution in sterile packaging ready for use.

[0202] The outer casing **13** has a macroreceptacle **24** for receiving the biological sample and a removable sterile sealing tape **22**, preferably with a low tack adhesive, to cover the macroreceptacle prior to use. A membrane seal **408** with a membrane guard **410** forms part of the outer casing **13** to reduce dehumidification within the test module while providing pressure relief from small air pressure fluctuations. The membrane guard **410** protects the membrane seal **408** from damage.

[0203] Test module reader **12** powers the test module **10** or **11** via Micro-USB port **16**. The test module reader **12** can adopt many different forms and a selection of these are described later. The version of the reader **12** shown in FIGS. **1**, **3** and **104** is a smart phone embodiment. A block diagram of this reader **12** is shown in FIG. **3**. Processor **42** runs application software from program storage **43**. The processor **42** also interfaces with the display screen **18** and user interface (UI) touch screen **17** and buttons **19**, a cellular radio **21**, wireless network connection **23**, and a satellite navigation system **25**. The cellular radio **21** and wireless network connection **23** are used for communications. Satellite navigation system **25** is used for updating epidemiological databases with location data. The location data can, alternatively, be entered manually via the touch screen **17** or buttons **19**. Data storage **27** holds genetic and diagnostic information, test results, patient information, assay and probe data for identifying each probe and its array position. Data storage **27** and program storage **43** may be shared in a common memory facility. Application software installed on the test module reader **12** provides analysis of results, along with additional test and diagnostic information.

[0204] To conduct a diagnostic test, the test module **10** (or test module **11**) is inserted into the Micro-USB port **16** on the test module reader **12**. The sterile sealing tape **22** is peeled back and the biological sample (in a liquid form) is loaded into the sample macroreceptacle **24**. Pressing start button **20** initiates testing via the application software. The sample flows into the LOC device **30** and the on-board assay extracts, incubates, amplifies and hybridizes the sample nucleic acids (the target) with presynthesized hybridization-responsive oligonucleotide probes. In the case of test module **10** (which uses fluorescence-based detection), the probes are fluorescently labelled and the LED **26** housed in the casing **13** provides the necessary excitation light to induce fluorescence emission from the hybridized probes (see FIGS. **1** and **2**). In test module **11** (which uses electrochemiluminescence (ECL) detection), the LOC device **30** is loaded with ECL probes (discussed above) and the LED **26** is not necessary for generating the luminescent emission. Instead, electrodes **860** and **870** provide the excitation electrical current (see FIG. **105**). The emission (fluorescent or luminescent) is detected using a photosensor **44** integrated into CMOS circuitry of each LOC device. The detected signal is amplified and converted to a

digital output which is analyzed by the test module reader **12**. The reader then displays the results.

[0205] The data may be saved locally and/or uploaded to a network server containing patient records. The test module **10** or **11** is removed from the test module reader **12** and disposed of appropriately.

[0206] FIGS. **1**, **3** and **104** show the test module reader **12** configured as a mobile phone/smart phone **28**. In other forms, the test module reader is a laptop/notebook **101**, a dedicated reader **103**, an ebook reader **107**, a tablet computer **109** or desktop computer **105** for use in hospitals, private practices or laboratories (see FIG. **106**). The reader can interface with a range of additional applications such as patient records, billing, online databases and multi-user environments. It can also be interfaced with a range of local or remote peripherals such as printers and patient smart cards.

[0207] Referring to FIG. **107**, the data generated by the test module **10** can be used to update, via the reader **12** and network **125**, the epidemiological databases hosted on the hosting system for epidemiological data **111**, the genetic databases hosted on the hosting system for genetic data **113**, the electronic health records hosted on the hosting system for electronic health records (EHR) **115**, the electronic medical records hosted on the hosting system for electronic medical records (EMR) **121**, and the personal health records hosted on the hosting system for personal health records (PHR) **123**. Conversely, the epidemiological data hosted on the hosting system for epidemiological data **111**, the genetic data hosted on the hosting system for genetic data **113**, the electronic health records hosted on the hosting system for electronic health records (EHR) **115**, the electronic medical records hosted on the hosting system for electronic medical records (EMR) **121**, and the personal health records hosted on the hosting system for personal health records (PHR) **123**, can be used to update, via network **125** and the reader **12**, the digital memory in the LOC **30** of the test module **10**.

[0208] Referring back to FIGS. **1**, **2**, **104** and **105** the reader **12** uses battery power in the mobile phone configuration. The mobile phone reader contains all test and diagnostic information preloaded. Data can also be loaded or updated via a number of wireless or contact interfaces to enable communications with peripheral devices, computers or online servers. A Micro-USB port **16** is provided for connection to a computer or mains power supply for battery recharge.

[0209] FIG. **77** shows an embodiment of the test module **10** used for tests that only require a positive or negative result for a particular target, such as testing whether a person is infected with, for example, H1N1 Influenza A virus. Only a purpose built USB power/indicator-only module **47** is adequate. No other reader or application software is necessary. An indicator **45** on the USB power/indicator-only module **47** signals positive or negative results. This configuration is well suited to mass screening.

[0210] Additional items supplied with the system may include a test tube containing reagents for pre-treatment of certain samples, along with spatula and lancet for sample collection. FIG. **77** shows an embodiment of the test module incorporating a spring-loaded, retractable lancet **390** and lancet release button **392** for convenience. A satellite phone can be used in remote areas.

Test Module Electronics

[0211] FIGS. **2** and **105** are block diagrams of the electronic components in the test modules **10** and **11**, respectively. The CMOS circuitry integrated in the LOC device **30** has a USB device driver **36**, a controller **34**, a USB-compatible LED driver **29**, clock **33**, power conditioner **31**, RAM **38** and program and data flash memory **40**. These provide the control and memory for the entire test module **10** or **11** including the photosensor **44**, the temperature sensors **170**, the liquid sensors **174**, and the various heaters **152**, **154**, **182**, **234**, together with associated drivers **37** and **39** and registers **35** and **41**. Only the LED **26** (in the case of test module **10**), external power supply capacitors **32** and the Micro-USB plug **14** are external to the LOC device **30**. The LOC devices **30** include bond-pads for making connections to these external components. The RAM **38** and the program and data flash memory **40** have the application software and the diagnostic and test information (Flash/Secure storage, e.g. via encryption) for over 1000 probes. In the case of test module **11** configured for ECL detection, there is no LED **26** (see FIGS. **104** and **105**). Data is encrypted by the LOC device **30** for secure storage and secure communication with an external device. The LOC devices **30** are loaded with electrochemiluminescent probes and the hybridization chambers each have a pair of ECL excitation electrodes **860** and **870**.

[0212] Many types of test modules **10** are manufactured in a number of test forms, ready for off-the-shelf use. The differences between the test forms lie in the on board assay of reagents and probes.

[0213] Some examples of infectious diseases rapidly identified with this system include:

[0214] Influenza—Influenza virus A, B, C, Isavirus, Thogotovirus

[0215] Pneumonia—respiratory syncytial virus (RSV), adenovirus, metapneumovirus, *Streptococcus pneumoniae, Staphylococcus aureus*

[0216] Tuberculosis—*Mycobacterium tuberculosis, bovis, africanum, canetti*, and *microti*

[0217] *Plasmodium falciparum, Toxoplasma gondii* and other protozoan parasites

[0218] Typhoid—*Salmonella enterica* serovar *typhi*

[0219] Ebola virus

[0220] Human immunodeficiency virus (HIV)

[0221] Dengue Fever—Flavivirus

[0222] Hepatitis (A through E)

[0223] Hospital acquired infections—for example *Clostridium difficile*, Vancomycin resistant *Enterococcus*, and Methicillin resistant *Staphylococcus aureus*

[0224] Herpes simplex virus (HSV)

[0225] Cytomegalovirus (CMV)

[0226] Epstein-Ban virus (EBV)

[0227] Encephalitis—Japanese Encephalitis virus, Chandipura virus

[0228] Whooping cough—*Bordetella pertussis*

[0229] Measles—paramyxovirus

[0230] Meningitis—*Streptococcus pneumoniae* and *Neisseria meningitidis*

[0231] Anthrax—*Bacillus anthracis*

[0232] Some examples of genetic disorders identified with this system include:

[0233] Cystic fibrosis

[0234] Haemophilia

[0235] Sickle cell disease

[0236] Tay-Sachs disease

[0237] Haemochromatosis

[0238] Cerebral arteriopathy

[0239] Crohn's disease

[0240] Polycistic kidney disease
[0241] Congential heart disease
[0242] Rett syndrome
[0243] A small selection of cancers identified by the diagnostic system include:
[0244] Ovarian
[0245] Colon carcinoma
[0246] Multiple endocrine neoplasia
[0247] Retinoblastoma
[0248] Turcot syndrome
[0249] The above lists are not exhaustive and the diagnostic system can be configured to detect a much greater variety of diseases and conditions using nucleic acid and proteomic analysis.

Detailed Architecture of System Components

LOC Device

[0250] The LOC device **30** is central to the diagnostic system. It rapidly performs the four major steps of a nucleic acid based molecular diagnostic assay, i.e. sample preparation, nucleic acid extraction, nucleic acid amplification, and detection, using a microfluidic platform. The LOC device also has alternative uses, and these are detailed later. As discussed above, test modules **10** and **11** can adopt many different configurations to detect different targets Likewise, the LOC device **30** has numerous different embodiments tailored to the target(s) of interest. One form of the LOC device **30** is LOC device **301** for fluorescent detection of target nucleic acid sequences in the pathogens of a whole blood sample. For the purposes of illustration, the structure and operation of LOC device **301** is now described in detail with reference to FIGS. **4** to **26** and **27** to **57**.
[0251] FIG. **4** is a schematic representation of the architecture of the LOC device **301**. For convenience, process stages shown in FIG. **4** are indicated with the reference numeral corresponding to the functional sections of the LOC device **301** that perform that process stage. The process stages associated with each of the major steps of a nucleic acid based molecular diagnostic assay are also indicated: sample input and preparation **288**, extraction **290**, incubation **291**, amplification **292** and detection **294**. The various reservoirs, chambers, valves and other components of the LOC device **301** will be described in more detail later.
[0252] FIG. **5** is a perspective view of the LOC device **301**. It is fabricated using high volume CMOS and MST (microsystems technology) manufacturing techniques. The laminar structure of the LOC device **301** is illustrated in the schematic (not to scale) partial section view of FIG. **12**. The LOC device **301** has a silicon substrate **84** which supports the CMOS+MST chip **48**, comprising CMOS circuitry **86** and an MST layer **87**, with a cap **46** overlaying the MST layer **87**. For the purposes of this patent specification, the term 'MST layer' is a reference to a collection of structures and layers that process the sample with various reagents. Accordingly, these structures and components are configured to define flow-paths with characteristic dimensions that will support capillary driven flow of liquids with physical characteristics similar to those of the sample during processing. In light of this, the MST layer and components are typically fabricated using surface micromachining techniques and/or bulk micromachining techniques. However, other fabrication methods can also produce structures and components dimensioned for capillary driven flows and processing very small volumes. The specific embodiments described in this specification show the MST layer as the structures and active components supported on the CMOS circuitry **86**, but excluding the features of the cap **46**. However, the skilled addressee will appreciate that the MST layer need not have underlying CMOS or indeed an overlying cap in order for it to process the sample.
[0253] The overall dimensions of the LOC device shown in the following figures are 1760 μm×5824 μm. Of course, LOC devices fabricated for different applications may have different dimensions.
[0254] FIG. **6** shows the features of the MST layer **87** superimposed with the features of the cap. Insets AA to AD, AG and AH shown in FIG. **6** are enlarged in FIGS. **13**, **14**, **35**, **56**, **55** and **67**, respectively, and described in detail below for a comprehensive understanding of each structure within the LOC device **301**. FIGS. **7** to **10** show the features of the cap **46** in isolation while FIG. **11** shows the CMOS+MST device **48** structures in isolation.

Laminar Structure

[0255] FIGS. **12** and **22** are sketches that diagrammatically show the laminar structure of the CMOS+MST device **48**, the cap **46** and the fluidic interaction between the two. The figures are not to scale for the purposes of illustration. FIG. **12** is a schematic section view through the sample inlet **68** and FIG. **22** is a schematic section through the reservoir **54**. As best shown in FIG. **12**, the CMOS+MST device **48** has a silicon substrate **84** which supports the CMOS circuitry **86** that operates the active elements within the MST layer **87** above. A passivation layer **88** seals and protects the CMOS layer **86** from the fluid flows through the MST layer **87**.
[0256] Fluid flows through both the cap channels **94** and the MST channels **90** (see for example FIGS. **7** and **16**) in the cap layer **46** and MST channel layer **100**, respectively. Cell transport occurs in the larger channels **94** fabricated in the cap **46**, while biochemical processes are carried out in the smaller MST channels **90**. Cell transport channels are sized so as to be able to transport cells in the sample to predetermined sites in the MST channels **90**. Transportation of cells with sizes greater than 20 microns (for example, certain leukocytes) requires channel dimensions greater than 20 microns, and therefore a cross sectional area transverse to the flow of greater than 400 square microns. MST channels, particularly at locations in the LOC where transport of cells is not required, can be significantly smaller.
[0257] It will be appreciated that cap channel **94** and MST channel **90** are generic references and particular MST channels **90** may also be referred to as (for example) heated microchannels or dialysis MST channels in light of their particular function. MST channels **90** are formed by etching through a MST channel layer **100** deposited on the passivation layer **88** and patterned with photoresist. The MST channels **90** are enclosed by a roof layer **66** which forms the top (with respect to the orientation shown in the figures) of the CMOS+MST device **48**.
[0258] Despite sometimes being shown as separate layers, the cap channel layer **80** and the reservoir layer **78** are formed from a unitary piece of material. Of course, the piece of material may also be non-unitary. This piece of material is etched from both sides in order to form a cap channel layer **80** in which the cap channels **94** are etched and the reservoir layer **78** in which the reservoirs **54**, **56**, **58**, **60** and **62** are etched. Alternatively, the reservoirs and the cap channels are formed by a micromolding process. Both etching and micro-

molding techniques are used to produce channels with cross sectional areas transverse to the flow as large as 20,000 square microns, and as small as 8 square microns.

[0259] At different locations in the LOC device, there can be a range of appropriate choices for the cross sectional area of the channel transverse to the flow. Where large quantities of sample, or samples with large constituents, are contained in the channel, a cross-sectional area of up to 20,000 square microns (for example, a 200 micron wide channel in a 100 micron thick layer) is suitable. Where small quantities of liquid, or mixtures without large cells present, are contained in the channel, a very small cross sectional area transverse to the flow is preferable.

[0260] A lower seal **64** encloses the cap channels **94** and the upper seal layer **82** encloses the reservoirs **54**, **56**, **58**, **60** and **62**.

[0261] The five reservoirs **54**, **56**, **58**, **60** and **62** are preloaded with assay-specific reagents. In the embodiment described here, the reservoirs are preloaded with the following reagents, but other reagents can easily be substituted:

[0262] reservoir **54**: anticoagulant with option to include erythrocyte lysis buffer

[0263] reservoir **56**: lysis reagent

[0264] reservoir **58**: restriction enzymes, ligase and linkers (for linker-primed PCR (see FIG. 76, extracted from T. Stachan et al., Human Molecular Genetics 2, Garland Science, NY and London, 1999))

[0265] reservoir **60**: amplification mix (dNTPs, primers, buffer) and

[0266] reservoir **62**: DNA polymerase.

[0267] The cap **46** and the CMOS+MST layers **48** are in fluid communication via corresponding openings in the lower seal **64** and the roof layer **66**. These openings are referred to as uptakes **96** and downtakes **92** depending on whether fluid is flowing from the MST channels **90** to the cap channels **94** or vice versa.

LOC Device Operation

[0268] The operation of the LOC device **301** is described below in a step-wise fashion with reference to analysing pathogenic DNA in a blood sample. Of course, other types of biological or non-biological fluid are also analysed using an appropriate set, or combination, of reagents, test protocols, LOC variants and detection systems. Referring back to FIG. **4**, there are five major steps involved in analysing a biological sample, comprising sample input and preparation **288**, nucleic acid extraction **290**, nucleic acid incubation **291**, nucleic acid amplification **292** and detection and analysis **294**.

[0269] The sample input and preparation step **288** involves mixing the blood with an anticoagulant **116** and then separating pathogens from the leukocytes and erythrocytes with the pathogen dialysis section **70**. As best shown in FIGS. **7** and **12**, the blood sample enters the device via the sample inlet **68**. Capillary action draws the blood sample along the cap channel **94** to the reservoir **54**. Anticoagulant is released from the reservoir **54** as the sample blood flow opens its surface tension valve **118** (see FIGS. **15** and **22**). The anticoagulant prevents the formation of clots which would block the flow.

[0270] As best shown in FIG. **22**, the anticoagulant **116** is drawn out of the reservoir **54** by capillary action and into the MST channel **90** via the downtake **92**. The downtake **92** has a capillary initiation feature (CIF) **102** to shape the geometry of the meniscus such that it does not anchor to the rim of the downtake **92**. Vent holes **122** in the upper seal **82** allows air to replace the anticoagulant **116** as it is drawn out of the reservoir **54**.

[0271] The MST channel **90** shown in FIG. **22** is part of a surface tension valve **118**. The anticoagulant **116** fills the surface tension valve **118** and pins a meniscus **120** to the uptake **96** to a meniscus anchor **98**. Prior to use, the meniscus **120** remains pinned at the uptake **96** so the anticoagulant does not flow into the cap channel **94**. When the blood flows through the cap channel **94** to the uptake **96**, the meniscus **120** is removed and the anticoagulant is drawn into the flow.

[0272] FIGS. **15** to **21** show Inset AE which is a portion of Inset AA shown in FIG. **13**. As shown in FIGS. **15**, **16** and **17**, the surface tension valve **118** has three separate MST channels **90** extending between respective downtakes **92** and uptakes **96**. The number of MST channels **90** in a surface tension valve can be varied to change the flow rate of the reagent into the sample mixture. As the sample mixture and the reagents mix together by diffusion, the flow rate out of the reservoir determines the concentration of the reagent in the sample flow. Hence, the surface tension valve for each of the reservoirs is configured to match the desired reagent concentration.

[0273] The blood passes into a pathogen dialysis section **70** (see FIGS. **4** and **15**) where target cells are concentrated from the sample using an array of apertures **164** sized according to a predetermined threshold. Cells smaller than the threshold pass through the apertures while larger cells do not pass through the apertures. Unwanted cells, which may be either the larger cells withheld by the array of apertures **164** or the smaller cells that pass through the apertures, are redirected to a waste unit **76** while the target cells continue as part of the assay.

[0274] In the pathogen dialysis section **70** described here, the pathogens from the whole blood sample are concentrated for microbial DNA analysis. The array of apertures is formed by a multitude of 3 micron diameter holes **164** fluidically connecting the input flow in the cap channel **94** to a target channel **74**. The 3 micron diameter apertures **164** and the dialysis uptake holes **168** for the target channel **74** are connected by a series of dialysis MST channels **204** (best shown in FIGS. **15** and **21**). Pathogens are small enough to pass through the 3 micron diameter apertures **164** and fill the target channel **74** via the dialysis MST channels **204**. Cells larger than 3 microns, such as erythrocytes and leukocytes, stay in the waste channel **72** in the cap **46** which leads to a waste reservoir **76** (see FIG. **7**).

[0275] Other aperture shapes, sizes and aspect ratios can be used to isolate specific pathogens or other target cells such as leukocytes for human DNA analysis. Greater detail on the dialysis section and dialysis variants is provided later.

[0276] Referring again to FIGS. **6** and **7**, the flow is drawn through the target channel **74** to the surface tension valve **128** of the lysis reagent reservoir **56**. The surface tension valve **128** has seven MST channels **90** extending between the lysis reagent reservoir **56** and the target channel **74**. When the menisci are unpinned by the sample flow, the flow rate from all seven of the MST channels **90** will be greater than the flow rate from the anticoagulant reservoir **54** where the surface tension valve **118** has three MST channels **90** (assuming the physical characteristics of the fluids are roughly equivalent). Hence the proportion of lysis reagent in the sample mixture is greater than that of the anticoagulant.

[0277] The lysis reagent and target cells mix by diffusion in the target channel **74** within the chemical lysis section **130**. A boiling-initiated valve **126** stops the flow until sufficient time has passed for diffusion and lysis to take place, releasing the genetic material from the target cells (see FIGS. **6** and **7**). The structure and operation of the boiling-initiated valves are described in greater detail below with reference to FIGS. **31** and **32**. Other active valve types (as opposed to passive valves such as the surface tension valve **118**) have also been developed by the Applicant which may be used here instead of the boiling-initiated valve. These alternative valve designs are also described later.

[0278] When the boiling-initiated valve **126** opens, the lysed cells flow into a mixing section **131** for pre-amplification restriction digestion and linker ligation.

[0279] Referring to FIG. **13**, restriction enzymes, linkers and ligase are released from the reservoir **58** when the flow unpins the menisci at the surface tension valve **132** at the start of the mixing section **131**. The mixture flows the length of the mixing section **131** for diffusion mixing. At the end of the mixing section **131** is downtake **134** leading into the incubator inlet channel **133** of the incubation section **114** (see FIG. **13**). The incubator inlet channel **133** feeds the mixture into a serpentine configuration of heated microchannels **210** which provides an incubation chamber for holding the sample during restriction digestion and ligation of the linkers (see FIGS. **13** and **14**).

[0280] FIGS. **23**, **24**, **25**, **26**, **27**, **28** and **29** show the layers of the LOC device **301** within Inset AB of FIG. **6**. Each figure shows the sequential addition of layers forming the structures of the CMOS+MST layer **48** and the cap **46**. Inset AB shows the end of the incubation section **114** and the start of the amplification section **112**. As best shown in FIGS. **14** and **23**, the flow fills the microchannels **210** of the incubation section **114** until reaching the boiling-initiated valve **106** where the flow stops while diffusion takes place. As discussed above, the microchannel **210** upstream of the boiling-initiated valve **106** becomes an incubation chamber containing the sample, restriction enzymes, ligase and linkers. The heaters **154** are then activated and held at constant temperature for a specified time for restriction digestion and linker ligation to occur.

[0281] The skilled worker will appreciate that this incubation step **291** (see FIG. **4**) is optional and only required for some nucleic acid amplification assay types. Furthermore, in some instances, it may be necessary to have a heating step at the end of the incubation period to spike the temperature above the incubation temperature. The temperature spike inactivates the restriction enzymes and ligase prior to entering the amplification section **112**. Inactivation of the restriction enzymes and ligase has particular relevance when isothermal nucleic acid amplification is being employed.

[0282] Following incubation, the boiling-initiated valve **106** is activated (opened) and the flow resumes into the amplification section **112**. Referring to FIGS. **31** and **32**, the mixture fills the serpentine configuration of heated microchannels **158**, which form one or more amplification chambers, until it reaches the boiling-initiated valve **108**. As best shown in the schematic section view of FIG. **30**, amplification mix (dNTPs, primers, buffer) is released from reservoir **60** and polymerase is subsequently released from reservoir **62** into the intermediate MST channel **212** connecting the incubation and amplification sections (**114** and **112** respectively).

[0283] FIGS. **35** to **51** show the layers of the LOC device **301** within Inset AC of FIG. **6**. Each figure shows the sequential addition of layers forming the structures of the CMOS+MST device **48** and the cap **46**. Inset AC is at the end of the amplification section **112** and the start of the hybridization and detection section **52**. The incubated sample, amplification mix and polymerase flow through the microchannels **158** to the boiling-initiated valve **108**. After sufficient time for diffusion mixing, the heaters **154** in the microchannels **158** are activated for thermal cycling or isothermal amplification. The amplification mix goes through a predetermined number of thermal cycles or a preset amplification time to amplify sufficient target DNA. After the nucleic acid amplification process, the boiling-initiated valve **108** opens and flow resumes into the hybridization and detection section **52**. The operation of boiling-initiated valves is described in more detail later.

[0284] As shown in FIG. **52**, the hybridization and detection section **52** has an array of hybridization chambers **110**. FIGS. **52**, **53**, **54** and **56** show the hybridization chamber array **110** and individual hybridization chambers **180** in detail. At the entrance to the hybridization chamber **180** is a diffusion barrier **175** which prevents diffusion of the target nucleic acid, probe strands and hybridized probes between the hybridization chambers **180** during hybridization so as to prevent erroneous hybridization detection results. The diffusion barriers **175** present a flow-path-length that is long enough to prevent the target sequences and probes diffusing out of one chamber and contaminating another chamber within the time taken for the probes and nucleic acids to hybridize and the signal to be detected, thus avoiding an erroneous result.

[0285] Another mechanism to prevent erroneous readings is to have identical probes in a number of the hybridization chambers. The CMOS circuitry **86** derives a single result from the photodiodes **184** corresponding to the hybridization chambers **180** that contain identical probes. Anomalous results can be disregarded or weighted differently in the derivation of the single result.

[0286] The thermal energy required for hybridization is provided by CMOS-controlled heaters **182** (described in more detail below). After the heater is activated, hybridization occurs between complementary target-probe sequences. The LED driver **29** in the CMOS circuitry **86** signals the LED **26** located in the test module **10** to illuminate. These probes only fluoresce when hybridization has occurred thereby avoiding washing and drying steps that are typically required to remove unbound strands. Hybridization forces the stem-and-loop structure of the FRET probes **186** to open, which allows the fluorophore to emit fluorescent energy in response to the LED excitation light, as discussed in greater detail later. Fluorescence is detected by a photodiode **184** in the CMOS circuitry **86** underlying each hybridization chamber **180** (see hybridization chamber description below). The photodiodes **184** for all hybridization chambers and associated electronics collectively form the photosensor **44** (see FIG. **68**). In other embodiments, the photosensor may be an array of charge coupled devices (CCD array). The detected signal from the photodiodes **184** is amplified and converted to a digital output which is analyzed by the test module reader **12**. Further details of the detection method are described later.

Additional Details for the LOC Device

Modularity of the Design

[0287] The LOC device **301** has many functional sections, including the reagent reservoirs **54**, **56**, **58**, **60** and **62**, the dialysis section **70**, lysis section **130**, incubation section **114**, and amplification section **112**, valve types, the humidifier and humidity sensor. In other embodiments of the LOC device, these functional sections can be omitted, additional functional sections can be added or the functional sections can be used for alternative purposes to those described above.

[0288] For example, the incubation section **114** can be used as the first amplification section **112** of a tandem amplification assay system, with the chemical lysis reagent reservoir **56** being used to add the first amplification mix of primers, dNTPs and buffer and reagent reservoir **58** being used for adding the reverse transcriptase and/or polymerase. A chemical lysis reagent can also be added to the reservoir **56** along with the amplification mix if chemical lysis of the sample is desired or, alternatively, thermal lysis can occur in the incubation section by heating the sample for a predetermined time. In some embodiments, an additional reservoir can be incorporated immediately upstream of reservoir **58** for the mix of primers, dNTPs and buffer if there is a requirement for chemical lysis and a separation of this mix from the chemical lysis reagent is desired.

[0289] In some circumstances it may be desirable to omit a step, such as the incubation step **291**. In this case, a LOC device can be specifically fabricated to omit the reagent reservoir **58** and incubation section **114**, or the reservoir can simply not be loaded with reagents or the active valves, if present, not activated to dispense the reagents into the sample flow, and the incubation section then simply becomes a channel to transport the sample from the lysis section **130** to the amplification section **112**. The heaters are independently operable and therefore, where reactions are dependent on heat, such as thermal lysis, programming the heaters not to activate during this step ensures thermal lysis does not occur in LOC devices that do not require it. The dialysis section **70** can be located at the beginning of the fluidic system within the microfluidic device as shown in FIG. **4** or can be located anywhere else within the microfluidic device. For example, dialysis after the amplification phase **292** to remove cellular debris prior to the hybridization and detection step **294** may be beneficial in some circumstances. Alternatively, two or more dialysis sections can be incorporated at any location throughout the LOC device. Similarly, it is possible to incorporate additional amplification sections **112** to enable multiple targets to be amplified in parallel or in series prior to being detected in the hybridization chamber arrays **110** with specific nucleic acid probes. For analysis of samples like whole blood, in which dialysis is not required, the dialysis section **70** is simply omitted from the sample input and preparation section **288** of the LOC design. In some cases, it is not necessary to omit the dialysis section **70** from the LOC device even if the analysis does not require dialysis. If there is no geometric hindrance to the assay by the existence of a dialysis section, a LOC with the dialysis section **70** in the sample input and preparation section can still be used without a loss of the required functionality.

[0290] Furthermore, the detection section **294** may encompass proteomic chamber arrays which are identical to the hybridization chamber arrays but are loaded with probes designed to conjugate or hybridize with sample target proteins present in non-amplified sample instead of nucleic acid probes designed to hybridize to target nucleic acid sequences.

[0291] It will be appreciated that the LOC devices fabricated for use in this diagnostic system are different combinations of functional sections selected in accordance with the particular LOC application. The vast majority of functional sections are common to many of the LOC devices and the design of additional LOC devices for new application is a matter of compiling an appropriate combination of functional sections from the extensive selection of functional sections used in the existing LOC devices.

[0292] Only a small number of the LOC devices are shown in this description and some more are shown schematically to illustrate the design flexibility of the LOC devices fabricated for this system. The person skilled in the art will readily recognise that the LOC devices shown in this description are not an exhaustive list and many additional LOC designs are a matter of compiling the appropriate combination of functional sections.

Sample Types

[0293] LOC variants can accept and analyze the nucleic acid or protein content of a variety of sample types in liquid form including, but not limited to, blood and blood products, saliva, cerebrospinal fluid, urine, semen, amniotic fluid, umbilical cord blood, breast milk, sweat, pleural effusion, tear, pericardial fluid, peritoneal fluid, environmental water samples and drink samples. Amplicon obtained from macroscopic nucleic acid amplification can also be analysed using the LOC device; in this case, all the reagent reservoirs will be empty or configured not to release their contents, and the dialysis, lysis, incubation and amplification sections will be used solely to transport the sample from the sample inlet **68** to the hybridization chambers **180** for nucleic acid detection, as described above.

[0294] For some sample types, a pre-processing step is required, for example semen may need to be liquefied and mucus may need to be pre-treated with an enzyme to reduce the viscosity prior to input into the LOC device.

Sample Input

[0295] Referring to FIGS. **1** and **12**, the sample is added to the macroreceptacle **24** of the test module **10**. The macroreceptacle **24** is a truncated cone which feeds into the inlet **68** of the LOC device **301** by capillary action. Here it flows into the 64 μm wide×60 μm deep cap channel **94** where it is drawn towards the anticoagulant reservoir **54**, also by capillary action.

Reagent Reservoirs

[0296] The small volumes of reagents required by the assay systems using microfluidic devices, such as LOC device **301**, permit the reagent reservoirs to contain all reagents necessary for the biochemical processing with each of the reagent reservoirs having a small volume. This volume is easily less than 1,000,000,000 cubic microns, in the vast majority of cases less than 300,000,000 cubic microns, typically less than 70,000,000 cubic microns and in the case of the LOC device **301** shown in the drawings, less than 20,000,000 cubic microns.

Dialysis Section

[0297] Referring to FIGS. **15** to **21**, **33** and **34**, the pathogen dialysis section **70** is designed to concentrate pathogenic

target cells from the sample. As previously described, a plurality of apertures in the form of 3 micron diameter holes **164** in the roof layer **66** filter the target cells from the bulk of the sample. As the sample flows past the 3 micron diameter apertures **164**, microbial pathogens pass through the holes into a series of dialysis MST channels **204** and flow back up into the target channel **74** via 16 μm dialysis uptake holes **168** (see FIGS. **33** and **34**). The remainder of the sample (erythrocytes and so on) stay in the cap channel **94**. Downstream of the pathogen dialysis section **70**, the cap channel **94** becomes the waste channel **72** leading to the waste reservoir **76**. For biological samples of the type that generate a substantial amount of waste, a foam insert or other porous element **49** within the outer casing **13** of the test module **10** is configured to be in fluid communication with the waste reservoir **76** (see FIG. **1**).

[0298] The pathogen dialysis section **70** functions entirely on capillary action of the fluid sample. The 3 micron diameter apertures **164** at the upstream end of the pathogen dialysis section **70** have capillary initiation features (CIFs) **166** (see FIG. **33**) so that the fluid is drawn down into the dialysis MST channel **204** beneath. The first uptake hole **198** for the target channel **74** also has a CIF **202** (see FIG. **15**) to avoid the flow simply pinning a meniscus across the dialysis uptake holes **168**.

[0299] The small constituents dialysis section **682** schematically shown in FIG. **81** can have a similar structure to the pathogen dialysis section **70**. The small constituents dialysis section separates any small target cells or molecules from a sample by sizing (and, if necessary, shaping) apertures suitable for allowing the small target cells or molecules to pass into the target channel and continue for further analysis. Larger sized cells or molecules are removed to a waste reservoir **766**. Thus, the LOC device **30** (see FIGS. **1** and **104**) is not limited to separating pathogens that are less than 3 μm in size, but can be used to separate cells or molecules of any size desired.

Lysis Section

[0300] Referring back to FIGS. **7**, **11** and **13**, the genetic material in the sample is released from the cells by a chemical lysis process. As described above, a lysis reagent from the lysis reservoir **56** mixes with the sample flow in the target channel **74** downstream of the surface tension valve **128** for the lysis reservoir **56**. However, some diagnostic assays are better suited to a thermal lysis process, or even a combination of chemical and thermal lysis of the target cells. The LOC device **301** accommodates this with the heated microchannels **210** of the incubation section **114**. The sample flow fills the incubation section **114** and stops at the boiling-initiated valve **106**. The incubation microchannels **210** heat the sample to a temperature at which the cellular membranes are disrupted.

[0301] In some thermal lysis applications, an enzymatic reaction in the chemical lysis section **130** is not necessary and the thermal lysis completely replaces the enzymatic reaction in the chemical lysis section **130**.

Boiling-Initiated Valve

[0302] As discussed above, the LOC device **301** has three boiling-initiated valves **126**, **106** and **108**. The location of these valves is shown in FIG. **6**. FIG. **31** is an enlarged plan view of the boiling-initiated valve **108** in isolation at the end of the heated microchannels **158** of the amplification section **112**.

[0303] The sample flow **119** is drawn along the heated microchannels **158** by capillary action until it reaches the boiling-initiated valve **108**. The leading meniscus **120** of the sample flow pins at a meniscus anchor **98** at the valve inlet **146**. The geometry of the meniscus anchor **98** stops the advancing meniscus to arrest the capillary flow. As shown in FIGS. **31** and **32**, the meniscus anchor **98** is an aperture provided by an uptake opening from the MST channel **90** to the cap channel **94**. Surface tension in the meniscus **120** keeps the valve closed. An annular heater **152** is at the periphery of the valve inlet **146**. The annular heater **152** is CMOS-controlled via the boiling-initiated valve heater contacts **153**.

[0304] To open the valve, the CMOS circuitry **86** sends an electrical pulse to the valve heater contacts **153**. The annular heater **152** resistively heats until the liquid sample **119** boils. The boiling unpins the meniscus **120** from the valve inlet **146** and initiates wetting of the cap channel **94**. Once wetting the cap channel **94** begins, capillary flow resumes. The fluid sample **119** fills the cap channel **94** and flows through the valve downtake **150** to the valve outlet **148** where capillary driven flow continues along the amplification section exit channel **160** into the hybridization and detection section **52**. Liquid sensors **174** are placed before and after the valve for diagnostics.

[0305] It will be appreciated that once the boiling-initiated valves are opened, they cannot be re-closed. However, as the LOC device **301** and the test module **10** are single-use devices, re-closing the valves is unnecessary.

Incubation Section and Nucleic Acid Amplification Section

[0306] FIGS. **6**, **7**, **13**, **14**, **23**, **24**, **25**, **35** to **45**, **50** and **51** show the incubation section **114** and the amplification section **112**. The incubation section **114** has a single, heated incubation microchannel **210** etched in a serpentine pattern in the MST channel layer **100** from the downtake opening **134** to the boiling-initiated valve **106** (see FIGS. **13** and **14**). Control over the temperature of the incubation section **114** enables enzymatic reactions to take place with greater efficiency. Similarly, the amplification section **112** has a heated amplification microchannel **158** in a serpentine configuration leading from the boiling-initiated valve **106** to the boiling-initiated valve **108** (see FIGS. **6** and **14**). These valves arrest the flow to retain the target cells in the heated incubation or amplification microchannels **210** or **158** while mixing, incubation and nucleic acid amplification takes place. The serpentine pattern of the microchannels also facilitates (to some extent) mixing of the target cells with reagents.

[0307] In the incubation section **114** and the amplification section **112**, the sample cells and the reagents are heated by the heaters **154** controlled by the CMOS circuitry **86** using pulse width modulation (PWM). Each meander of the serpentine configuration of the heated incubation microchannel **210** and amplification microchannel **158** has three separately operable heaters **154** extending between their respective heater contacts **156** (see FIG. **14**) which provides for the two-dimensional control of input heat flux density. As best shown in FIG. **51**, the heaters **154** are supported on the roof layer **66** and embedded in the lower seal **64**. The heater material is TiAl but many other conductive metals would be suitable. The elongate heaters **154** are parallel with the longitudinal extent of each channel section that forms the wide

meanders of the serpentine shape. In the amplification section **112**, each of the wide meanders can operate as separate PCR chambers via individual heater control.

[0308] The small volumes of amplicon required by the assay systems using microfluidic devices, such as LOC device **301**, permit low amplification mixture volumes for amplification in amplification section **112**. This volume is easily less than 400 nanoliters, in the vast majority of cases less than 170 nanoliters, typically less than 70 nanoliters and in the case of the LOC device **301**, between 2 nanoliters and 30 nanoliters.

Increased Rates of Heating and Greater Diffusive Mixing

[0309] The small cross section of each channel section increases the heating rate of the amplification fluid mix. All the fluid is kept a relatively short distance from the heater **154**. Reducing the channel cross section (that is the amplification microchannel **158** cross section) to less than 100,000 square microns achieves appreciably higher heating rates than that provided by more 'macro-scale' equipment. Lithographic fabrication techniques allow the amplification microchannel **158** to have a cross sectional area transverse to the flow-path less than 16,000 square microns which gives substantially higher heating rates. Feature sizes on the order of 1 micron are readily achievable with lithographic techniques. If very little amplicon is needed (as is the case in the LOC device **301**), the cross sectional area can be reduced to less than 2,500 square microns. For diagnostic assays with 1,000 to 2,000 probes on the LOC device, and a requirement of 'sample-in, answer out' in less than 1 minute, a cross sectional area transverse to the flow of between 400 square microns and 1 square micron is adequate.

[0310] The heater element in the amplification microchannel **158** heats the nucleic acid sequences at a rate more than 80 Kelvin (K) per second, in the vast majority of cases at a rate greater than 100 K per second. Typically, the heater element heats the nucleic acid sequences at a rate more than 1,000 K per second and in many cases, the heater element heats the nucleic acid sequences at a rate more than 10,000 K per second. Commonly, based on the demands of the assay system, the heater element heats the nucleic acid sequences at a rate more than 100,000 K per second, more than 1,000,000 K per second more than 10,000,000 K per second, more than 20,000,000 K per second, more than 40,000,000 K per second, more than 80,000,000 K per second and more than 160,000,000 K per second.

[0311] A small cross-sectional area channel is also beneficial for diffusive mixing of any reagents with the sample fluid. Before diffusive mixing is complete, diffusion of one liquid into the other is greatest near the interface between the two. Concentration decreases with distance from the interface. Using microchannels with relatively small cross sections transverse to the flow direction, keeps both fluid flows close to the interface for more rapid diffusive mixing. Reducing the channel cross section to less than 100,000 square microns achieves appreciably higher mixing rates than that provided by more 'macro-scale' equipment. Lithographic fabrication techniques allows microchannels with a cross sectional area transverse to the flow-path less than 16000 square microns which gives significantly higher mixing rates. If small volumes are needed (as is the case in the LOC device **301**), the cross sectional area can be reduced to less than 2500 square microns. For diagnostic assays with 1000 to 2000 probes on the LOC device, and a requirement of 'sample-in, answer out' in less than 1 minute, a cross sectional area transverse to the flow of between 400 square microns and 1 square micron is adequate.

Short Thermal Cycle Times

[0312] Keeping the sample mixture proximate to the heaters, and using very small fluid volumes allows rapid thermal cycling during the nucleic acid amplification process. Each thermal cycle (i.e. denaturing, annealing and primer extension) is completed in less than 30 seconds for target sequences up to 150 base pairs (bp) long. In the vast majority of diagnostic assays, the individual thermal cycle times are less than 11 seconds, and a large proportion are less than 4 seconds. LOC devices **30** with some of the most common diagnostic assays have thermal cycles time between 0.45 seconds to 1.5 seconds for target sequences up to 150 bp long. Thermal cycling at this rate allows the test module to complete the nucleic acid amplification process in much less than 10 minutes; often less than 220 seconds. For most assays, the amplification section generates sufficient amplicon in less than 80 seconds from the sample fluid entering the sample inlet. For a great many assays, sufficient amplicon is generated in 30 seconds.

[0313] Upon completion of a preset number of amplification cycles, the amplicon is fed into the hybridization and detection section **52** via the boiling-initiated valve **108**.

Hybridization Chambers

[0314] FIGS. **52**, **53**, **54**, **56** and **57** show the hybridization chambers **180** in the hybridization chamber array **110**. The hybridization and detection section **52** has a 24×45 array **110** of hybridization chambers **180**, each with hybridization-responsive FRET probes **186**, heater element **182** and an integrated photodiode **184**. The photodiode **184** is incorporated for detection of fluorescence resulting from the hybridization of a target nucleic acid sequence or protein with the FRET probes **186**. Each photodiode **184** is independently controlled by the CMOS circuitry **86**. Any material between the FRET probes **186** and the photodiode **184** must be transparent to the emitted light. Accordingly, the wall section **97** between the probes **186** and the photodiode **184** is also optically transparent to the emitted light. In the LOC device **301**, the wall section **97** is a thin (approximately 0.5 micron) layer of silicon dioxide.

[0315] Incorporation of a photodiode **184** directly beneath each hybridization chamber **180** allows the volume of probe-target hybrids to be very small while still generating a detectable fluorescence signal (see FIG. **54**). The small amounts permit small volume hybridization chambers. A detectable amount of probe-target hybrid requires a quantity of probe, prior to hybridization, which is easily less than 270 picograms (corresponding to 900,000 cubic microns), in the vast majority of cases less than 60 picograms (corresponding to 200,000 cubic microns), typically less than 12 picograms (corresponding to 40,000 cubic microns) and in the case of the LOC device **301** shown in the accompanying figures, less than 2.7 picograms (corresponding to a chamber volume of 9,000 cubic microns). Of course, reducing the size of the hybridization chambers allows a higher density of chambers and therefore more probes on the LOC device. In LOC device **301**, the hybridization section has more than 1,000 chambers in an area of 1,500 microns by 1,500 microns (i.e. less than 2,250 square microns per chamber). Smaller volumes also reduce

the reaction times so that hybridization and detection is faster. An additional advantage of the small amount of probe required in each chamber is that only very small quantities of probe solution need to be spotted into each chamber during production of the LOC device. Embodiments of the LOC device according to the invention can be spotted using a probe solution volume of 1 picoliter or less.

[0316] After nucleic acid amplification, boiling-initiated valve **108** is activated and the amplicon flows along the flow-path **176** and into each of the hybridization chambers **180** (see FIGS. **52** and **56**). An end-point liquid sensor **178** indicates when the hybridization chambers **180** are filled with amplicon and the heaters **182** can be activated.

[0317] After sufficient hybridization time, the LED **26** (see FIG. **2**) is activated. The opening in each of the hybridization chambers **180** provides an optical window **136** for exposing the FRET probes **186** to the excitation radiation (see FIGS. **52**, **54** and **56**). The LED **26** is illuminated for a sufficiently long time in order to induce a fluorescence signal from the probes with high intensity. During excitation, the photodiode **184** is shorted. After a pre-programmed delay **300** (see FIG. **2**), the photodiode **184** is enabled and fluorescence emission is detected in the absence of the excitation light. The incident light on the active area **185** of the photodiode **184** (see FIG. **54**) is converted into a photocurrent which can then be measured using CMOS circuitry **86**.

[0318] The hybridization chambers **180** are each loaded with probes for detecting a single target nucleic acid sequence. Each hybridization chambers **180** can be loaded with probes to detect over 1,000 different targets if desired. Alternatively, many or all the hybridization chambers can be loaded with the same probes to detect the same target nucleic acid repeatedly. Replicating the probes in this way throughout the hybridization chamber array **110** leads to increased confidence in the results obtained and the results can be combined by the photodiodes adjacent those hybridization chambers to provide a single result if desired. The person skilled in the art will recognise that it is possible to have from one to over 1,000 different probes on the hybridization chamber array **110**, depending on the assay specification.

Humidifier and Humidity Sensor

[0319] Inset AG of FIG. **6** indicates the position of the humidifier **196**. The humidifier prevents evaporation of the reagents and probes during operation of the LOC device **301**. As best shown in the enlarged view of FIG. **55**, a water reservoir **188** is fluidically connected to three evaporators **190**. The water reservoir **188** is filled with molecular biology-grade water and sealed during manufacturing. As best shown in FIGS. **55** and **74**, water is drawn into three downtakes **194** and along respective water supply channels **192** by capillary action to a set of three uptakes **193** at the evaporators **190**. A meniscus pins at each uptake **193** to retain the water. The evaporators have annular shaped heaters **191** which encircle the uptakes **193**. The annular heaters **191** are connected to the CMOS circuitry **86** by the conductive columns **376** to the top metal layer **195** (see FIG. **37**). Upon activation, the annular heaters **191** heat the water causing evaporation and humidifying the device surrounds.

[0320] The position of the humidity sensor **232** is also shown in FIG. **6**. However, as best shown in the enlarged view of Inset AH in FIG. **67**, the humidity sensor has a capacitive comb structure. A lithographically etched first electrode **296** and a lithographically etched second electrode **298** face each other such that their teeth are interleaved. The opposed electrodes form a capacitor with a capacitance that can be monitored by the CMOS circuitry **86**. As the humidity increases, the permittivity of the air gap between the electrodes increases, so that the capacitance also increases. The humidity sensor **232** is adjacent the hybridization chamber array **110** where humidity measurement is most important to slow evaporation from the solution containing the exposed probes.

Feedback Sensors

[0321] Temperature and liquid sensors are incorporated throughout the LOC device **301** to provide feedback and diagnostics during device operation. Referring to FIG. **35**, nine temperature sensors **170** are distributed throughout the amplification section **112** Likewise, the incubation section **114** also has nine temperature sensors **170**. These sensors each use a 2×2 array of bipolar junction transistors (BJTs) to monitor the fluid temperature and provide feedback to the CMOS circuitry **86**. The CMOS circuitry **86** uses this to precisely control the thermal cycling during the nucleic acid amplification process and any heating during thermal lysis and incubation.

[0322] In the hybridization chambers **180**, the CMOS circuitry **86** uses the hybridization heaters **182** as temperature sensors (see FIG. **56**). The electrical resistance of the hybridization heaters **182** is temperature dependent and the CMOS circuitry **86** uses this to derive a temperature reading for each of the hybridization chambers **180**.

[0323] The LOC device **301** also has a number of MST channel liquid sensors **174** and cap channel liquid sensors **208**. FIG. **35** shows a line of MST channel liquid sensors **174** at one end of every other meander in the heated microchannel **158**. As best shown in FIG. **37**, the MST channel liquid sensors **174** are a pair of electrodes formed by exposed areas of the top metal layer **195** in the CMOS structure **86**. Liquid closes the circuit between the electrodes to indicate its presence at the sensor's location.

[0324] FIG. **25** shows an enlarged perspective of cap channel liquid sensors **208**. Opposing pairs of TiAl electrodes **218** and **220** are deposited on the roof layer **66**. Between the electrodes **218** and **220** is a gap **222** to hold the circuit open in the absence of liquid. The presence of liquid closes the circuit and the CMOS circuitry **86** uses this feedback to monitor the flow.

Gravitational Independence

[0325] The test modules **10** are orientation independent. They do not need to be secured to a flat stable surface in order to operate. Capillary driven fluid flows and a lack of external plumbing into ancillary equipment allow the modules to be truly portable and simply plugged into a similarly portable hand held reader such as a mobile telephone. Having a gravitationally independent operation means the test modules are also accelerationally independent to all practical extents. They are resistant to shock and vibration and will operate on moving vehicles or while the mobile telephone is being carried around.

Nucleic Acid Amplification Variants

Direct PCR

[0326] Traditionally, PCR requires extensive purification of the target DNA prior to preparation of the reaction mixture.

However, with appropriate changes to the chemistry and sample concentration, it is possible to perform nucleic acid amplification with minimal DNA purification, or direct amplification. When the nucleic acid amplification process is PCR, this approach is called direct PCR. In LOC devices where nucleic acid amplification is performed at a controlled, constant temperature, the approach is direct isothermal amplification. Direct nucleic acid amplification techniques have considerable advantages for use in LOC devices, particularly relating to simplification of the required fluidic design. Adjustments to the amplification chemistry for direct PCR or direct isothermal amplification include increased buffer strength, the use of polymerases which have high activity and processivity, and additives which chelate with potential polymerase inhibitors. Dilution of inhibitors present in the sample is also important.

[0327] To take advantage of direct nucleic acid amplification techniques, the LOC device designs incorporate two additional features. The first feature is reagent reservoirs (for example reservoir **58** in FIG. **8**) which are appropriately dimensioned to supply a sufficient quantity of amplification reaction mix, or diluent, so that the final concentrations of sample components which might interfere with amplification chemistry are low enough to permit successful nucleic acid amplification. The desired dilution of non-cellular sample components is in the range of 5× to 20×. Different LOC structures, for example the pathogen dialysis section **70** in FIG. **4**, are used when appropriate to ensure that the concentration of target nucleic acid sequences is maintained at a high enough level for amplification and detection. In this embodiment, further illustrated in FIG. **6**, a dialysis section which effectively concentrates pathogens small enough to be passed into the amplification section **292** is employed upstream of the sample extraction section **290**, and rejects larger cells to a waste receptacle **76**. In another embodiment, a dialysis section is used to selectively deplete proteins and salts in blood plasma while retaining cells of interest.

[0328] The second LOC structural feature which supports direct nucleic acid amplification is design of channel aspect ratios to adjust the mixing ratio between the sample and the amplification mix components. For example, to ensure dilution of inhibitors associated with the sample in the preferred 5×-20× range through a single mixing step, the length and cross-section of the sample and reagent channels are designed such that the sample channel, upstream of the location where mixing is initiated, constitutes a flow impedance 4×-19× higher than the flow impedance of the channels through which the reagent mixture flows. Control over flow impedances in microchannels is readily achieved through control over the design geometry. The flow impedance of a microchannel increases linearly with the channel length, for a constant cross-section. Importantly for mixing designs, flow impedance in microchannels depends more strongly on the smallest cross-sectional dimension. For example, the flow impedance of a microchannel with rectangular cross-section is inversely proportional to the cube of the smallest perpendicular dimension, when the aspect ratio is far from unity.

Reverse-Transcriptase PCR (RT-PCR)

[0329] Where the sample nucleic acid species being analysed or extracted is RNA, such as from RNA viruses or messenger RNA, it is first necessary to reverse transcribe the RNA into complementary DNA (cDNA) prior to PCR amplification. The reverse transcription reaction can be performed in the same chamber as the PCR (one-step RT-PCR) or it can be performed as a separate, initial reaction (two-step RT-PCR). In the LOC variants described herein, a one-step RT-PCR can be performed simply by adding the reverse transcriptase to reagent reservoir **62** along with the polymerase and programming the heaters **154** to cycle firstly for the reverse transcription step and then progress onto the nucleic acid amplification step. A two-step RT-PCR could also be easily achieved by utilizing the reagent reservoir **58** to store and dispense the buffers, primers, dNTPs and reverse transcriptase and the incubation section **114** for the reverse transcription step followed by amplification in the normal way in the amplification section **112**.

Isothermal Nucleic Acid Amplification

[0330] For some applications, isothermal nucleic acid amplification is the preferred method of nucleic acid amplification, thus avoiding the need to repetitively cycle the reaction components through various temperature cycles but instead maintaining the amplification section at a constant temperature, typically around 37° C. to 41° C. A number of isothermal nucleic acid amplification methods have been described, including Strand Displacement Amplification (SDA), Transcription Mediated Amplification (TMA), Nucleic Acid Sequence Based Amplification (NASBA), Recombinase Polymerase Amplification (RPA), Helicase-Dependent isothermal DNA Amplification (HDA), Rolling Circle Amplification (RCA), Ramification Amplification (RAM) and Loop-mediated Isothermal Amplification (LAMP), and any of these, or other isothermal amplification methods, can be employed in particular embodiments of the LOC device described herein.

[0331] In order to perform isothermal nucleic acid amplification, the reagent reservoirs **60** and **62** adjoining the amplification section will be loaded with the appropriate reagents for the specified isothermal method instead of PCR amplification mix and polymerase. For example, for SDA, reagent reservoir **60** contains amplification buffer, primers and dNTPs and reagent reservoir **62** contains an appropriate nickase enzyme and Exo-DNA polymerase. For RPA, reagent reservoir **60** contains the amplification buffer, primers, dNTPs and recombinase proteins, with reagent reservoir **62** containing a strand displacing DNA polymerase such as Bsu. Similarly, for HDA, reagent reservoir **60** contains amplification buffer, primers and dNTPs and reagent reservoir **62** contains an appropriate DNA polymerase and a helicase enzyme to unwind the double stranded DNA strand instead of using heat. The skilled person will appreciate that the necessary reagents can be split between the two reagent reservoirs in any manner appropriate for the nucleic acid amplification process.

[0332] For amplification of viral nucleic acids from RNA viruses such as HIV or hepatitis C virus, NASBA or TMA is appropriate as it is unnecessary to first transcribe the RNA to cDNA. In this example, reagent reservoir **60** is filled with amplification buffer, primers and dNTPs and reagent reservoir **62** is filled with RNA polymerase, reverse transcriptase and, optionally, RNase H.

[0333] For some forms of isothermal nucleic acid amplification it may be necessary to have an initial denaturation cycle to separate the double stranded DNA template, prior to maintaining the temperature for the isothermal nucleic acid amplification to proceed. This is readily achievable in all embodiments of the LOC device described herein, as the

temperature of the mix in the amplification section **112** can be carefully controlled by the heaters **154** in the amplification microchannels **158** (see FIG. **14**).

[0334] Isothermal nucleic acid amplification is more tolerant of potential inhibitors in the sample and, as such, is generally suitable for use where direct nucleic acid amplification from the sample is desired. Therefore, isothermal nucleic acid amplification is sometimes useful in LOC variant XLIII **673**, LOC variant XLIV **674** and LOC variant XLVII **677**, amongst others, shown in FIGS. **82**, **83** and **84**, respectively. Direct isothermal amplification may also be combined with one or more pre-amplification dialysis steps **70**, **686** or **682** as shown in FIGS. **82** and **84** and/or a pre-hybridization dialysis step **682** as indicated in FIG. **83** to help partially concentrate the target cells in the sample before nucleic acid amplification or remove unwanted cellular debris prior to the sample entering the hybridization chamber array **110**, respectively. The person skilled in the art will appreciate that any combination of pre-amplification dialysis and pre-hybridization dialysis can be used.

[0335] Isothermal nucleic acid amplification can also be performed in parallel amplification sections such as those schematically represented in FIGS. **78**, **79** and **80**, multiplexed and some methods of isothermal nucleic acid amplification, such as LAMP, are compatible with an initial reverse transcription step to amplify RNA.

Additional Details on the Fluorescence Detection System

[0336] FIGS. **58** and **59** show the hybridization-responsive FRET probes **236**. These are often referred to as molecular beacons and are stem-and-loop probes, generated from a single strand of nucleic acid, that fluoresce upon hybridization to complementary nucleic acids. FIG. **58** shows a single FRET probe **236** prior to hybridization with a target nucleic acid sequence **238**. The probe has a loop **240**, stem **242**, a fluorophore **246** at the 5' end, and a quencher **248** at the 3' end. The loop **240** consists of a sequence complementary to the target nucleic acid sequence **238**. Complementary sequences on either side of the probe sequence anneal together to form the stem **242**.

[0337] In the absence of a complementary target sequence, the probe remains closed as shown in FIG. **58**. The stem **242** keeps the fluorophore-quencher pair in close proximity to each other, such that significant resonant energy transfer can occur between them, substantially eliminating the ability of the fluorophore to fluoresce when illuminated with the excitation light **244**.

[0338] FIG. **59** shows the FRET probe **236** in an open or hybridized configuration. Upon hybridization to a complementary target nucleic acid sequence **238**, the stem-and-loop structure is disrupted, the fluorophore and quencher are spatially separated, thus restoring the ability of the fluorophore **246** to fluoresce. The fluorescence emission **250** is optically detected as an indication that the probe has hybridized.

[0339] The probes hybridize with very high specificity with complementary targets, since the stem helix of the probe is designed to be more stable than a probe-target helix with a single nucleotide that is not complementary. Since double-stranded DNA is relatively rigid, it is sterically impossible for the probe-target helix and the stem helix to coexist.

Primer-Linked Probes

[0340] Primer-linked, stem-and-loop probes and primer-linked, linear probes, otherwise known as scorpion probes, are an alternative to molecular beacons and can be used for real-time and quantitative nucleic acid amplification in the LOC device. Real-time amplification could be performed directly in the hybridization chambers of the LOC device. The benefit of using primer-linked probes is that the probe element is physically linked to the primer, thus only requiring a single hybridization event to occur during the nucleic acid amplification rather than separate hybridizations of the primers and probes being required. This ensures that the reaction is effectively instantaneous and results in stronger signals, shorter reaction times and better discrimination than when using separate primers and probes. The probes (along with polymerase and the amplification mix) would be deposited into the hybridization chambers **180** during fabrication and there would be no need for a separate amplification section on the LOC device. Alternatively, the amplification section is left unused or used for other reactions.

Primer-Linked Linear Probe

[0341] FIGS. **85** and **86** show a primer-linked linear probe **692** during the initial round of nucleic acid amplification and in its hybridized configuration during subsequent rounds of nucleic acid amplification, respectively. Referring to FIG. **85**, the primer-linked linear probe **692** has a double-stranded stem segment **242**. One of the strands incorporates the primer linked probe sequence **696** which is homologous to a region on the target nucleic acid **696** and is labelled on its 5' end with fluorophore **246**, and linked on its 3' end to an oligonucleotide primer **700** via an amplification blocker **694**. The other strand of the stem **242** is labelled at its 3 end with a quencher moiety **248**. After an initial round of nucleic acid amplification has completed, the probe can loop around and hybridize to the extended strand with the, now complementary, sequence **698**. During the initial round of nucleic acid amplification, the oligonucleotide primer **700** anneals to the target DNA **238** (FIG. **85**) and is then extended, forming a DNA strand containing both the probe sequence and the amplification product. The amplification blocker **694** prevents the polymerase from reading through and copying the probe region **696**. Upon subsequent denaturation, the extended oligonucleotide primer **700**/template hybrid is dissociated and so is the double stranded stem **242** of the primer-linked linear probe, thus releasing the quencher **248**. Once the temperature decreases for the annealing and extension steps, the primer linked probe sequence **696** of the primer-linked linear probe curls around and hybridizes to the amplified complementary sequence **698** on the extended strand and fluorescence is detected indicating the presence of the target DNA. Non-extended primer-linked linear probes retain their double-stranded stem and fluorescence remains quenched. This detection method is particularly well suited for fast detection systems as it relies on a single-molecule process.

Primer-Linked Stem-and-Loop Probes

[0342] FIGS. **87**A to **87**F show the operation of a primer-linked stem-and-loop probe **704**. Referring to FIG. **87**A, the primer-linked stem-and-loop probe **704** has a stem **242** of complementary double-stranded DNA and a loop **240** which incorporates the probe sequence. One of the stem strands **708** is labelled at its 5' end with fluorophore **246**. The other strand **710** is labelled with a 3'-end quencher **248** and carries both the amplification blocker **694** and oligonucleotide primer **700**. During the initial denaturation phase (see FIG. **87**B), the

strands of the target nucleic acid **238** separate, as does the stem **242** of the primer-linked, stem-and-loop probe **704**. When the temperature cools for the annealing phase (see FIG. **87**C), the oligonucleotide primer **700** on the primer-linked stem-and-loop probe **704** hybridizes to the target nucleic acid sequence **238**. During extension (see FIG. **87**D) the complement **706** to the target nucleic acid sequence **238** is synthesized forming a DNA strand containing both the probe sequence **704** and the amplified product. The amplification blocker **694** prevents the polymerase from reading through and copying the probe region **704**. When the probe next anneals, following denaturation, the probe sequence of the loop segment **240** of the primer-linked stem-and-loop probe (see FIG. **87**F) anneals to the complementary sequence **706** on the extended strand. This configuration leaves the fluorophore **246** relatively remote from the quencher **248**, resulting in a significant increase in fluorescence emission.

Control Probes

[0343] The hybridization chamber array **110** includes some hybridization chambers **180** with positive and negative control probes used for assay quality control. FIGS. **100** and **101** schematically illustrate negative control probes without a fluorophore **796**, and FIGS. **102** and **103** are sketches of positive control probes without a quencher **798**. The positive and negative control probes have a stem-and-loop structure like the FRET probes described above. However, a fluorescence signal **250** will always be emitted from positive control probes **798** and no fluorescence signal **250** is ever emitted from negative control probes **796**, regardless of whether the probes hybridize into an open configuration or remain closed.

[0344] Referring to FIGS. **100** and **101**, the negative control probe **796** has no fluorophore (and may or may not have a quencher **248**). Hence, whether the target nucleic acid sequence **238** hybridizes with the probe (see FIG. **101**), or the probe remains in its stem-and-loop configuration (see FIG. **100**), the response to the excitation light **244** is negligible. Alternatively, the negative control probe **796** could be designed so that it always remains quenched. For example, by synthesizing the loop **240** to have a probe sequence that will not hybridize to any nucleic acid sequence within the sample under investigation, the stem **242** of the probe molecule will re-hybridize to itself and the fluorophore and quencher will remain in close proximity and no appreciable fluorescence signal will be emitted. This negative control signal would correspond to low level emissions from hybridization chambers **180** in which the probes has not hybridized but the quencher does not quench all emissions from the reporter.

[0345] Conversely, the positive control probe **798** is constructed without a quencher as illustrated in FIGS. **102** and **103**. Nothing quenches the fluorescence emission **250** from the fluorophore **246** in response to the excitation light **244** regardless of whether the positive control probe **798** hybridizes with the target nucleic acid sequence **238**.

[0346] FIG. **52** shows a possible distribution of the positive and negative control probes (**378** and **380** respectively) throughout the hybridization chamber array **110**. The control probes **378** and **380** are placed in hybridization chambers **180** positioned in a line across the hybridization chamber array **110**. However, the arrangement of the control probes within the array is arbitrary (as is the configuration of the hybridization chamber array **110**).

Fluorophore Design

[0347] Fluorophores with long fluorescence lifetimes are required in order to allow enough time for the excitation light to decay to an intensity below that of the fluorescence emission at which time the photosensor **44** is enabled, thereby providing a sufficient signal to noise ratio. Also, longer fluorescence lifetime translates into larger integrated fluorescence photon count.

[0348] The fluorophores **246** (see FIG. **59**) have a fluorescence lifetime greater than 100 nanoseconds, often greater than 200 nanoseconds, more commonly greater than 300 nanoseconds and in most cases greater than 400 nanoseconds.

[0349] The metal-ligand complexes based on the transition metals or lanthanides have long lifetimes (from hundreds of nanoseconds to milliseconds), adequate quantum yields, and high thermal, chemical and photochemical stability, which are all favourable properties with respect to the fluorescence detection system requirements.

[0350] A particularly well-studied metal-ligand complex based on the transition metal ion Ruthenium (Ru (II)) is tris(2,2'-bipyridine) ruthenium (II) ($[Ru(bpy)_3]^{2+}$) which has a lifetime of approximately 1 μs. This complex is available commercially from Biosearch Technologies under the brand name Pulsar 650.

TABLE 1

Photophysical properties of Pulsar 650 (Ruthenium chelate)

Parameter	Symbol	Value	Unit
Absorption Wavelength	λ_{abs}	460	nm
Emission Wavelength	λ_{em}	650	nm
Extinction Coefficient	E	14800	$M^{-1}cm^{-1}$
Fluorescence Lifetime	τ_f	1.0	μs
Quantum Yield	H	1 (deoxygenated)	N/A

[0351] Terbium chelate, a lanthanide metal-ligand complex has been successfully demonstrated as a fluorescent reporter in a FRET probe system, and also has a long lifetime of 1600 μs.

TABLE 2

Photophysical properties of terbium chelate

Parameter	Symbol	Value	Unit
Absorption Wavelength	λ_{abs}	330-350	nm
Emission Wavelength	λ_{em}	548	nm
Extinction Coefficient	E	13800 (λ_{abs} and ligand dependent, can be up to 30000 @ $\lambda_{e-340\,nm}$)	$M^{-1}cm^{-1}$
Fluorescence Lifetime	τ_f	1600 (hybridized probe)	μs
Quantum Yield	H	1 (ligand dependent)	N/A

[0352] The fluorescence detection system used by the LOC device **301** does not utilize filters to remove unwanted background fluorescence. It is therefore advantageous if the quencher **248** has no native emission in order to increase the signal-to-noise ratio. With no native emission, there is no contribution to background fluorescence from the quencher **248**. High quenching efficiency is also important so that fluorescence is prevented until a hybridization event occurs. The Black Hole Quenchers (BHQ), available from Biosearch Technologies, Inc. of Novato Calif., have no native emission and high quenching efficiency, and are suitable quenchers for the system. BHQ-1 has an absorption maximum at 534 nm,

and a quenching range of 480-580 nm, making it a suitable quencher for the Tb-chelate fluorophore. BHQ-2 has an absorption maximum at 579 nm, and a quenching range of 560-670 nm, making it a suitable quencher for Pulsar 650.

[0353] Iowa Black Quenchers (Iowa Black FQ and RQ), available from Integrated DNA Technologies of Coralville, Iowa, are suitable alternative quenchers with little or no background emission. Iowa Black FQ has a quenching range from 420-620 nm, with an absorption maximum at 531 nm and would therefore be a suitable quencher for the Tb-chelate fluorophore. Iowa Black RQ has an absorption maximum at 656 nm, and a quenching range of 500-700 nm, making it an ideal quencher for Pulsar 650.

[0354] In the embodiments described here, the quencher **248** is a functional moiety which is initially attached to the probe, but other embodiments are possible in which the quencher is a separate molecule free in solution.

Excitation Source

[0355] In the fluorescence detection based embodiments described herein, a LED is chosen as the excitation source instead of a laser diode, high power lamp or laser due to the low power consumption, low cost and small size. Referring to FIG. **88**, the LED **26** is positioned directly above the hybridization chamber array **110** on an external surface of the LOC device **301**. On the opposing side of the hybridization chamber array **110**, is the photosensor **44**, made up of an array of photodiodes **184** (see FIGS. **53**, **54** and **68**) for detection of fluorescence signals from each of the chambers.

[0356] FIGS. **89**, **90** and **91** schematically illustrate other embodiments for exposing the probes to excitation light. In the LOC device **30** shown in FIG. **89**, the excitation light **244** generated by the excitation LED **26** is directed onto the hybridization chamber array **110** by the lens **254**. The excitation LED **26** is pulsed and the fluorescence emissions are detected by the photosensor **44**.

[0357] In the LOC device **30** shown in FIG. **90**, the excitation light **244** generated by the excitation LED **26** is directed onto the hybridization chamber array **110** by the lens **254**, a first optical prism **712** and second optical prism **714**. The excitation LED **26** is pulsed and the fluorescence emissions are detected by the photosensor **44**.

[0358] Similarly, the LOC device **30** shown in FIG. **91**, the excitation light **244** generated by the excitation LED **26** is directed onto the hybridization chamber array **110** by the lens **254**, a first minor **716** and second minor **718**. Again, the excitation LED **26** is pulsed and the fluorescence emissions are detected by the photosensor **44**.

[0359] The excitation wavelength of the LED **26** is dependent on the choice of fluorescent dye. The Philips LXK2-PR14-R00 is a suitable excitation source for the Pulsar 650 dye. The SET UVTOP335TO39BL LED is a suitable excitation source for the Tb-chelate label.

TABLE 3

Philips LXK2-PR14-R00 LED specifications

Parameter	Symbol	Value	Unit
Wavelength	λ_{ex}	460	nm
Emission Frequency	ν_{em}	$6.52(10)^{14}$	Hz
Output Power	p_l	0.515 (min) @ 1 A	W
Radiation pattern		Lambertian profile	N/A

TABLE 4

SET UVTOP334TO39BL LED Specifications

Parameter	Symbol	Value	Unit
Wavelength	λ_e	340	nm
Emission Frequency	ν_e	$8.82(10)^{14}$	Hz
Power	p_l	0.000240 (min) @ 20 mA	W
Pulse Forward Current	I	200	mA
Radiation pattern		Lambertian	N/A

Ultra Violet Excitation Light

[0360] Silicon absorbs little light in the UV spectrum. Accordingly, it is advantageous to use UV excitation light. A UV LED excitation source can be used but the broad spectrum of the LED **26** reduces the effectiveness of this method. To address this, a filtered UV LED can be used. Optionally, a UV laser can be the excitation source unless the relatively high cost of the laser is impractical for the particular test module market.

LED Driver

[0361] The LED driver **29** drives the LED **26** at a constant current for the required duration. A lower power USB 2.0-certifiable device can draw at most 1 unit load (100 mA), with a minimum operating voltage of 4.4 V. A standard power conditioning circuit is used for this purpose.

Photodiode

[0362] FIG. **54** shows the photodiode **184** integrated into the CMOS circuitry **86** of the LOC device **301**. The photodiode **184** is fabricated as part of the CMOS circuitry **86** without additional masks or steps. This is one significant advantage of a CMOS photodiode over a CCD, an alternate sensing technology which could be integrated on the same chip using non-standard processing steps, or fabricated on an adjacent chip. On-chip detection is low cost and reduces the size of the assay system. The shorter optical path length reduces noise from the surrounding environment for efficient collection of the fluorescence signal and eliminates the need for a conventional optical assembly of lenses and filters.

[0363] Quantum efficiency of the photodiode **184** is the fraction of photons impinging on its active area **185** that are effectively converted to photo-electrons. For standard silicon processes, the quantum efficiency is in the range of 0.3 to 0.5 for visible light, depending on process parameters such as the amount and absorption properties of the cover layers.

[0364] The detection threshold of the photodiode **184** determines the smallest intensity of the fluorescence signal that can be detected. The detection threshold also determines the size of the photodiode **184** and hence the number of hybridization chambers **180** in the hybridization and detection section **52** (see FIG. **52**). The size and number of chambers are technical parameters that are limited by the dimensions of the LOC device (in the case of the LOC device **301**, the dimensions are 1760 μm×5824 μm) and the real estate available after other functional modules such as the pathogen dialysis section **70** and amplification section(s) **112** are incorporated.

[0365] For standard silicon processes, the photodiode **184** detects a minimum of 5 photons. However, to ensure reliable detection, the minimum can be set to 10 photons. Therefore

with the quantum efficiency range being 0.3 to 0.5 (as discussed above), the fluorescence emission from the probes should be a minimum of 17 photons but 30 photons would incorporate a suitable margin of error for reliable detection.

Calibration Chambers

[0366] The non-uniformity of the electrical characteristic of the photodiode **184**, autofluorescence, and residual excitation photon flux that has not yet completely decayed, introduce background noise and offset into the output signal. This background is removed from each output signal using one or more calibration signals. Calibration signals are generated by exposing one or more calibration photodiodes **184** in the array to respective calibration sources. A low calibration source is used for determining a negative result in which a target has not reacted with a probe. A high calibration source is indicative of a positive result from a probe-target complex. In the embodiment described here, the low calibration light source is provided by calibration chambers **382** in the hybridization chamber array **110** which:

[0367] do not contain any probes;

[0368] contain probes that have no fluorescent reporter; or,

[0369] contain probes with a reporter and quencher configured such that quenching is always expected to occur.

[0370] The output signal from such calibration chambers **382** closely approximates the noise and offset in the output signal from all the hybridization chambers in the LOC device. Subtracting the calibration signal from the output signals generated by the other hybridization chambers substantially removes the background and leaves the signal generated by the fluorescence emission (if any). Signals arising from ambient light in the region of the chamber array are also subtracted.

[0371] It will be appreciated that the negative control probes described above with reference to FIGS. **100** to **103** can be be used in calibration chambers. However, as shown in FIGS. **94** and **95**, which are enlarged views of insets DG and DH of LOC variant X **728** shown in FIG. **93**, another option is to fluidically isolate the calibration chambers **382** from the amplicon. The background noise and offset can be determined by leaving the fluidically isolated chambers empty, or containing reporterless probes, or indeed any of the 'normal' probes with both reporter and quencher as hybridization is precluded by fluidic isolation.

[0372] The calibration chambers **382** can provide a high calibration source to generate a high signal in the corresponding photodiodes. The high signal corresponds to all probes in a chamber having hybridized. Spotting probes with reporters and no quenchers, or just reporters will consistently provide a signal approximating that of a hybridization chamber in which a predominant number of the probes have hybridized. It will also be appreciated that calibration chambers **382** can be used instead of control probes, or in addition to control probes.

[0373] The number and arrangement of the calibration chambers **382** throughout the hybridization chamber array is arbitrary. However, the calibration is more accurate if photodiodes **184** are calibrated by a calibration chamber **382** that is relatively proximate. Referring to FIG. **56**, the hybridization chamber array **110** has one calibration chamber **382** for every eight hybridization chambers **180**. That is, a calibration chamber **382** is positioned in the middle of every three by three square of hybridization chambers **180**. In this configuration, the hybridization chambers **180** are calibrated by a calibration chamber **382** that is immediately adjacent.

[0374] FIG. **99** shows a differential imager circuit **788** used to substract the signal from the photodiode **184** corresponding to the calibration chamber **382** as a result of excitation light, from the fluorescence signal from the surrounding hybridization chambers **180**. The differential imager circuit **788** samples the signal from the pixel **790** and a "dummy" pixel **792**. In one embodiment, the "dummy" pixel **792** is shielded from light, so its output signal provides a dark reference. Alternatively, the "dummy" pixel **792** can be exposed to the excitation light along with the rest of the array. In the embodiment where the "dummy" pixel **792** is open to light, signals arising from ambient light in the region of the chamber array are also subtracted. The signals from the pixel **790** are small (i.e. close to dark signal), and without a reference to a dark level it is hard to differentiate between the background and a very small signal.

[0375] During use, the "read_row" **794** and "read_row_d" **795** are activated and M**4** **797** and MD**4** **801** transistors are turned on. Switches **807** and **809** are closed such that the outputs from the pixel **790** and "dummy" pixel **792** are stored on pixel capacitor **803** and dummy pixel capacitor **805** respectively. After the pixel signals have been stored, switches **807** and **809** are deactivated. Then the "read_col" switch **811** and dummy "read_col" switch **813** are closed, and the switched capacitor amplifier **815** at the output amplifies the differential signal **817**.

Suppression and Enablement of the Photodiode

[0376] The photodiode **184** needs to be suppressed during excitation by the LED **26** and enabled during fluorescence. FIG. **69** is a circuit diagram for a single photodiode **184** and FIG. **70** is a timing diagram for the photodiode control signals. The circuit has photodiode **184** and six MOS transistors, M_{shunt} **394**, M_{tx} **396**, M_{reset} **398**, M_{sf} **400**, M_{read} **402** and M_{bias} **404**. At the beginning of the excitation cycle, t**1**, the transistors M_{shunt} **394**, and M_{reset} **398** are turned on by pulling the M_{shunt} gate **384** and the reset gate **388** high. During this period, the excitation photons generate carriers in the photodiode **184**. These carriers have to be removed, as the amount of generated carriers can be sufficient to saturate the photodiode **184**. During this cycle, M_{shunt} **394** directly removes the carriers generated in photodiode **184**, while M_{reset} **398** resets any carriers that have accumulated on node 'NS' **406** due to leakage in transistors or due to diffusion of excitation-produced carriers in the substrate. After excitation, a capture cycle commences at t**4**. During this cycle, the emitted response from the fluorophore is captured and integrated in the circuit on node 'NS' **406**. This is achieved by pulling tx gate **386** high, which turns on the transistor M_{tx} **396** and transfers any accumulated carriers on the photodiode **184** to node 'NS' **406**. The duration of the capture cycle can be as long as the fluorophore emits. The outputs from all photodiodes **184** in the hybridization chamber array **110** are captured simultaneously.

[0377] There is a delay between the end of the capture cycle t**5** and the start of the read cycle t**6**. This delay is due to the requirement to read each photodiode **184** in the hybridization chamber array **110** (see FIG. **52**) separately following the capture cycle. The first photodiode **184** to be read will have the shortest delay before the read cycle, while the last photodiode **184** will have the longest delay before the read cycle. During the read cycle, transistor M_{read} **402** is turned on by

pulling the read gate **393** high. The 'NS' node **406** voltage is buffered and read out using the source-follower transistor M_{sf} **400**.

[0378] There are additional, optional methods of enabling or suppressing the photodiode as discussed below:

1. Suppression Methods

[0379] FIGS. **96**, **97** and **98** show three possible configurations **778**, **780**, **782** for the M_{shunt} transistor **394**. The M_{shunt} transistor **394** has a very high off ratio at maximum $|V_{Gs}|=5$ V which is enabled during excitation. As shown in FIG. **96**, the M_{shunt} gate **384** is configured to be on the edge of the photodiode **184**. Optionally, as shown in FIG. **97**, the M_{shunt} gate **384** may be configured to surround the photodiode **184**. A third option is to configure the M_{shunt} gate **384** inside the photodiode **184**, as shown in FIG. **98**. Under this third option there would be less photodiode active area **185**.

[0380] These three configurations **778**, **780** and **782** reduce the average path length from all locations in the photodiode **184** to the M_{shunt} gate **384**. In FIG. **96**, the M_{shunt} gate **384** is on one side of the photodiode **184**. This configuration is simplest to fabricate and impinges the least on the photodiode active area **185**. However, any carriers lingering on the remote side of the photodiode **184** would take longer to propagate through to the M_{shunt} gate **384**.

[0381] In FIG. **97**, the M_{shunt} gate **384** surrounds the photodiode **184**. This further reduces the average path length for carriers in the photodiode **184** to the M_{shunt} gate **384**. However, extending the M_{shunt} gate **384** about the periphery of the photodiode **184** imposes a greater reduction of the photodiode active area **185**. The configuration **782** in FIG. **98** positions the M_{shunt} gate **384** within the active area **185**. This provides the shortest average path length to the M_{shunt} gate **384** and hence the shortest transition time. However, the impingement on the active area **185** is greatest. It also poses a wider leakage path.

2. Enabling Methods

[0382] a. A trigger photodiode drives the shunt transistor with a fixed delay.
b. A trigger photodiode drives the shunt transistor with programmable delay.
c. The shunt transistor is driven from the LED drive pulse with a fixed delay.
d. The shunt transistor is driven as in 2c but with programmable delay.

[0383] FIG. **75** is a schematic section view through a hybridization chamber **180** showing a photodiode **184** and trigger photodiode **187** embedded in the CMOS circuitry **86**. A small area in the corner of the photodiode **184** is replaced with the trigger photodiode **187**. A trigger photodiode **187** with a small area is sufficient as the intensity of the excitation light will be high in comparison with the fluorescence emission. The trigger photodiode **187** is sensitive to the excitation light **244**. The trigger photodiode **187** registers that the excitation light **244** has extinguished and activates the photodiode **184** after a short time delay Δt **300** (see FIG. **2**). This delay allows the fluorescence photodiode **184** to detect the fluorescence emission from the FRET probes **186** in the absence of the excitation light **244**. This enables detection and improves the signal to noise ratio.

[0384] Both photodiodes **184** and trigger photodiodes **187** are located in the CMOS circuitry **86** under each hybridization chamber **180**. The array of photodiodes combines, along with appropriate electronics, to form the photosensor **44** (see FIG. **68**). The photodiodes **184** are pn-junction fabricated during CMOS structure manufacturing without additional masks or steps. During MST fabrication, the dielectric layer (not shown) above the photodiodes **184** is optionally thinned using the standard MST photolithography techniques to allow more fluorescent light to illuminate the active area **185** of the photodiode **184**. The photodiode **184** has a field of view such that the fluorescence signal from the probe-target hybrids within the hybridization chamber **180** is incident on the sensor face. The fluorescent light is converted into a photocurrent which can then be measured using CMOS circuitry **86**.

[0385] Alternatively, one or more hybridization chambers **180** can be dedicated to a trigger photodiode **187** only. These options can be used in these in combination with 2a and 2b above.

Delayed Detection of Fluorescence

[0386] The following derivations elucidate the delayed detection of fluorescence using a long-lifetime fluorophore for the LED/fluorophore combinations described above. The fluorescence intensity is derived as a function of time after excitation by an ideal pulse of constant intensity I, between time t_1 and t_2 as shown in FIG. **60**.

[0387] Let [S1](t) equal the density of excited states at time t, then during and after excitation, the number of excited states per unit time per unit volume is described by the following differential equation:

$$\frac{d[S1]}{dt}(t)+\frac{[S1](t)}{\tau_F}=\frac{I_e\varepsilon c}{h\nu_e} \tag{1}$$

where c is the molar concentration of fluorophores, E is the molar extinction coefficient, ν_e is the excitation frequency, and $h=6.62606896(10)^{-34}$ Js is the Planck constant.

This differential equation has the general form:

$$\frac{dy}{dx}+p(x)y=q(x)$$

which has the solution:

$$y(x)=\frac{\int e^{\int p(x)dx}q(x)dx+k}{e^{\int p(x)dx}} \tag{2}$$

[0388] Using this now to solve equation (1),

$$[S1](t)=\frac{I_e\varepsilon c\tau_f}{h\nu_e}+ke^{-t/\tau_f} \tag{3}$$

[0389] Now at time t_1, $[S1](t_1)=0$, and from (3):

$$k = -\frac{I_e \varepsilon c \tau_f}{h\nu_e} e^{t_1/\tau_f} \tag{4}$$

[0390] Substituting (4) into (3):

$$[S1](t) = \frac{I_e \varepsilon c \tau_f}{h\nu_e} - \frac{I_e \varepsilon c \tau_f}{h\nu_e} e^{-(t-t_1)/\tau_f}$$

[0391] At time t_2:

$$[S1](t_2) = \frac{I_e \varepsilon c \tau_f}{h\nu_e} - \frac{I_e \varepsilon c \tau_f}{h\nu_e} e^{-(t_2-t_1)/\tau_f} \tag{5}$$

[0392] For $t \geqq t_2$, the excited states decay exponentially and this is described by:

$$[S1](t)=[S1](t_2)e^{-(t-t_2)/\tau_f} \tag{6}$$

[0393] Substituting (5) into (6):

$$[S1](t) = \frac{I_e \varepsilon c \tau_f}{h\nu_e}\left[1 - e^{-(t_2-t_1)/\tau_f}\right]e^{-(t-t_1)/\tau_f} \tag{7}$$

[0394] The fluorescence intensity is given by the following equation:

$$I_f(t) = -\frac{d[S1](t)}{dx} h\nu_f \eta l \tag{8}$$

where ν_f is the fluorescence frequency, η is the quantum yield and l is the optical path length.

[0395] Now from (7):

$$\frac{d[S1](t)}{dt} = -\frac{I_e \varepsilon c}{h\nu_e}\left[1 - e^{-(t_2-t_1)/\tau_f}\right]e^{-(t-t_2)/\tau_f} \tag{9}$$

[0396] Substituting (9) into (8):

$$I_f(t) = I_e \varepsilon c l \eta \frac{\nu_f}{\nu_e}\left[1 - e^{-(t_2-t_1)/\tau_f}\right]e^{-(t-t_2)/\tau_f} \tag{10}$$

$$\text{For } \frac{t_2 - t_1}{\tau_f} \to \infty,\ I_f(t) \to I_e \varepsilon c l \eta \frac{\nu_f}{\nu_e} e^{-(t-t_2)/\tau_f}$$

[0397] Therefore, we can write the following approximate equation which describes the fluorescence intensity decay after a sufficiently long excitation pulse ($t_2-t_1 \gg \tau_f$):

$$I_f(t) = I_e \varepsilon c l \eta \frac{\nu_f}{\nu_e} e^{-(t-t_2)/\tau_f} \quad \text{for } t \geq t_2 \tag{11}$$

[0398] In the previous section, we concluded that for $t_2-t_1 \gg \tau_f$,

$$I_f(t) = I_e \varepsilon c l \eta \frac{\nu_f}{\nu_e} e^{-(t-t_2)/\tau_f} \quad \text{for } t \geq t_2.$$

[0399] From the above equation, we can derive the following:

$$\ddot{n}_f(t) = \ddot{n}_e \varepsilon c l \eta e^{-(t-t_2)/\tau_f} \tag{12}$$

where

$$\ddot{n}_f(t) = \frac{I_f(t)}{h\nu_f}$$

is the number of fluorescent photons per unit time per unit area and

$$\ddot{n}_e = \frac{I_e}{h\nu_e}$$

is the number of excitation photons per unit time per unit area.

[0400] Consequently,

$$\ddot{n}_f(t) = \int_{t_3}^{\infty} \ddot{n}_f(t) dt \tag{13}$$

where $\ddot{n}_f$ is the number of fluorescent photons per unit area and t_3 is the instant of time at which the photodiode is turned on. Substituting (12) into (13):

$$\ddot{n}_f = \int_{t_3}^{\infty} \ddot{n}_e \varepsilon c l \eta e^{-(t-t_2)/\tau_f} dt \tag{14}$$

[0401] Now, the number of fluorescent photons that reach the photodiode per unit time per unit area, $\ddot{n}_s(t)$, is given by the following:

$$\ddot{n}_s(t) = \ddot{n}_f(t)\phi_0 \tag{15}$$

where ϕ_0 is the light gathering efficiency of the optical system.

[0402] Substituting (12) into (15) we find

$$\ddot{n}_s(t) = \phi_0 \ddot{n}_e \varepsilon c l \eta e^{-(t-t_2)/\tau_f} \tag{16}$$

[0403] Similarly, the number of fluorescence photons that reach the photodiode per unit fluorescent area $\ddot{n}_s$, will be as follows:

$$\ddot{n}_s = \int_{t_3}^{\infty} \ddot{n}_s(t) dt$$

and substituting in (16) and integrating:

$$\ddot{n}_s = \phi_0 \ddot{n}_e \varepsilon c l \eta \tau_f e^{-(t_3-t_2)/\tau_f}$$

[0404] Therefore,

$$n_s = \phi_0 \dot{n}_e \in c l \eta \tau_f e^{-\Delta t/\tau_f} \quad (17)$$

[0405] The optimal value of t_3 is when the rate of electrons generated in the photodiode **184** due to fluorescence photons becomes equal to the rate of electrons generated in the photodiode **184** by the excitation photons, as the flux of the excitation photons decays much faster than that of the fluorescence photons.

[0406] The rate of sensor output electrons per unit fluorescent area due to fluorescence is:

$$\ddot{e}_f(t) = \phi_f \ddot{n}_s(t)$$

where ϕ_f is the quantum efficiency of the sensor at the fluorescence wavelength.

[0407] Substituting in (17) we have:

$$\ddot{e}_f(t) = \phi_f \phi_0 \ddot{n}_e \varepsilon c l \eta e^{-(t-t_2)/\tau_f} \quad (18)$$

[0408] Similarly, the rate of sensor output electrons per unit fluorescent area due to the excitation photons is:

$$\ddot{e}_e(t) = \phi_e \ddot{n}_e e^{-(t-t_2)/\tau_e} \quad (19)$$

where ϕ_e is the quantum efficiency of the sensor at the excitation wavelength, and τ_e is the time-constant corresponding to the "off" characteristics of the excitation LED. After time t_2, the LED's decaying photon flux would increase the intensity of the fluorescence signal and extend its decay time, but we are assuming that this has a negligible effect on $I_f(t)$, thus we are taking a conservative approach.

[0409] Now, as mentioned earlier, the optimal value of t_3 is when:

$$\ddot{e}_f(t_3) = \ddot{e}_e(t_3)$$

[0410] Therefore, from (18) and (19) we have:

$$\phi_f \phi_0 \ddot{n}_e \varepsilon c l \eta e^{-(t_3-t_2)/\tau_f} = \phi_e \ddot{n}_e e^{-(t_3-t_2)/\tau_e}$$

and rearranging we find:

$$t_3 - t_2 = \frac{\ln\left(\varepsilon c l \eta \frac{\phi_f \phi_0}{\phi_e}\right)}{\frac{1}{\tau_f} - \frac{1}{\tau_e}} \quad (20)$$

[0411] From the previous two sections, we have the following two working equations:

$$n_s = \phi_0 \dot{n}_e F \tau_f e^{-\Delta t/\tau_f} \quad (21)$$

$$\Delta t = \frac{\ln\left(F \frac{\phi_f \phi_0}{\phi_e}\right)}{\frac{1}{\tau_f} - \frac{1}{\tau_e}} \quad (22)$$

where $F = \in c l \eta$ and $\Delta t = t_3 - t_2$. We also know that, in practice, $t_2 - t_1 >> \tau_f$.

[0412] The optimal time for fluorescence detection and the number of fluorescence photons detected using the Philips LXK2-PR14-R00 LED and Pulsar 650 dye are determined as follows. The optimum detection time is determined using equation (22):

[0413] Recalling the concentration of amplicon, and assuming that all amplicons hybridize, then the concentration of fluorescent fluorophores is: $c = 2.89(10)^{-6}$ mol/L

[0414] The height of the chamber is the optical path length $l = 8(10)^{-6}$ m.

[0415] We have taken the fluorescence area to be equal to our photodiode area, yet our actual fluorescence area is substantially larger than our photodiode area; consequently we can approximately assume $\phi_0 = 0.5$ for the light gathering efficiency of our optical system. From the photodiode characteristics,

$$\frac{\phi_f}{\phi_e} = 10$$

is a very conservative value for the ratio of the photodiode quantum efficiency at the fluorescence wavelength to its quantum efficiency at the excitation wavelength.

[0416] With a typical LED decay lifetime of $\tau_e = 0.5$ ns and using Pulsar 650 specifications, Δt can be determined:

$$F = [1.48(10)^6][2.89(10)^{-6}][8(10)^{-6}](1)$$
$$= 3.42(10)^{-5}$$

$$\Delta t = \frac{\ln([3.42(10)^{-5}](10)(0.5))}{\frac{1}{1(10)^{-6}} - \frac{1}{0.5(10)^{-9}}}$$
$$= 4.34(10)^{-9} \text{ s}$$

[0417] The number of photons detected is determined using equation (21). First, the number of excitation photons emitted per unit time $\dot{n}_e$ is determined by examining the illumination geometry.

[0418] The Philips LXK2-PR14-R00 LED has a Lambertian radiation pattern, therefore:

$$\ddot{n}_l = \ddot{n}_{l0}\cos(\theta) \tag{23}$$

where $\ddot{n}_l$ is the number of photons emitted per unit time per unit solid angle at an angle of θ off the LED's forward axial direction, and $\ddot{n}_{l0}$ is the valve of $\ddot{n}_l$ in the forward axial direction.

[0419] The total number of photons emitted by the LED per unit time is:

$$\begin{aligned}\dot{n}_l &= \int_\Omega \ddot{n}_l d\Omega \\ &= \int_\Omega \ddot{n}_{l0}\cos(\theta) d\Omega\end{aligned} \tag{24}$$

[0420] Now,

$$\Delta\Omega = 2\pi[1-\cos(\theta+\Delta\theta)] - 2\pi[1-\cos(\theta)]$$

$$\Delta\Omega = 2\pi[\cos(\theta)-\cos(\theta+\Delta\theta)]$$

$$= 4\pi\sin(\theta)\cos\left(\frac{\Delta\theta}{2}\right)\sin\left(\frac{\Delta\theta}{2}\right) + 4\pi\cos(\theta)\sin^2\left(\frac{\Delta\theta}{2}\right)$$

$$d\Omega = 2\pi\sin(\theta)d\theta$$

[0421] Substituting this into (24):

$$\begin{aligned}\dot{n}_l &= \int_0^{\frac{\pi}{2}} 2\pi\ddot{n}_{l0}\cos(\theta)\sin(\theta)d\theta \\ &= \pi\ddot{n}_{l0}\end{aligned}$$

[0422] Rearranging, we have:

$$\ddot{n}_{l0} = \frac{\dot{n}_l}{\pi} \tag{26}$$

[0423] The LED's output power is 0.515 W and ν_e=6.52 $(10)^{14}$ Hz, therefore:

$$\begin{aligned}\dot{n}_l &= \frac{p_l}{h\nu_e} \\ &= \frac{0.515}{[6.63(10)^{-34}][6.52(10)^{14}]} \\ &= 1.19(10)^{18}\ \text{photons/s}\end{aligned} \tag{27}$$

[0424] Substituting this value into (26) we have:

$$\begin{aligned}\ddot{n}_{l0} &= \frac{1.19(10)^{18}}{\pi} \\ &= 3.79(10)^{17}\ \text{photons/s/sr}\end{aligned}$$

[0425] Referring to FIG. **61**, the optical centre **252** and the lens **254** of the LED **26** are schematically shown. The photodiodes are 16 μm×16 μm, and for the photodiode in the middle of the array, the solid angle (Ω) of the cone of light emitted from the LED **26** to the photodiode **184** is approximately:

$$\begin{aligned}\Omega &= \text{area of sensor}/r^2 \\ &= \frac{[16(10)^{-6}][16(10)^{-6}]}{[2.825(10)^{-3}]^2} \\ &= 3.21(10)^{-5}sr\end{aligned}$$

[0426] It will be appreciated that the central photodiode **184** of the photodiode array **44** is used for the purpose of these calculations. A sensor located at the edge of the array would only receive 2% less photons upon a hybridization event for a Lambertian excitation source intensity distribution.

[0427] The number of excitation photons emitted per unit time is:

$$\begin{aligned}\dot{n}_e &= \ddot{n}_l\Omega \\ &= [3.79(10)^{17}][3.21(10)^{-5}] \\ &= 1.22(10)^{13}\ \text{photons/s}\end{aligned} \tag{28}$$

[0428] Now referring to equation (29):

$$n_s = \phi_0\dot{n}_e F\tau_f e^{-\Delta t/\tau_f}$$

$$\begin{aligned}n_s &= (0.5)[1.22(10)^{13}][3.42(10)^{-5}][1(10)^{-6}]e^{-4.34(10)^{-9}/1(10)^{-6}} \\ &= 208\ \text{photons per sensor.}\end{aligned}$$

[0429] Therefore, using the Philips LXK2-PR14-R00 LED and Pulsar 650 fluorophore, we can easily detect any hybridization events which results in this number of photons being emitted.

[0430] The SET LED illumination geometry is shown in FIG. **62**. At I_D=20 mA, the LED has a minimum optical power output of p_1=240 μW centred at λ_e=340 nm (the absorption wavelength of the terbium chelate). Driving the LED at I_D=200 mA would increase the output power linearly to p_1=2.4 mW. By placing the LED's optical centre **252**, 17.5 mm away from the hybridization chamber array **110**, we would approximately concentrate this output flux in a circular spot size which has a maximum diameter of 2 mm.

[0431] The photon flux in the 2 mm-diameter spot at the hybridization away plane is given by equation 27.

$$\begin{aligned}\dot{n}_l &= \frac{p_l}{h\nu_e} \\ &= \frac{2.4(10)^{-3}}{[6.63(10)^{-34}][8.82(10)^{14}]} \\ &= 4.10(10)^{15}\ \text{photons/s}\end{aligned}$$

[0432] Using equation 28, we have:

$$\begin{aligned}\dot{n}_e &= \ddot{n}_l\Omega \\ &= 4.10(10)15\frac{[16(10)^{-6}]^2}{\pi[1(10)^{-3}]^2} \\ &= 3.34(10)^{11}\ \text{photons/s}\end{aligned}$$

[0433] Now, recalling equation 22 and using the Tb chelate properties listed previously,

$$\Delta t = \frac{\ln[(6.94(10)^{-5})(10)(0.5)]}{\frac{1}{1(10)^{-3}} - \frac{1}{0.5(10)^{-9}}}$$

$$= 3.98(10)^{-9}s$$

[0434] Now from equation 21:

$$n_s = (0.5)[3.34(10)^{11}][6.94(10)^{-5}][1(10)^{-3}]e^{-3.98(10)^{-9}/1(10)^{-3}}$$

$$= 11{,}600 \text{ photons per sensor.}$$

[0435] The theoretical number of photons emitted by hybridization events using the SET LED and terbium chelate system are easily detectable and well over the minimum of 30 photons required for reliable detection by the photosensor as indicated above.

Maximum Spacing Between Probes and Photodiode

[0436] The on-chip detection of hybridization avoids the needs for detection via confocal microscopy (see Background of the Invention). This departure from traditional detection techniques is a significant factor in the time and cost savings associated with this system. Traditional detection requires imaging optics which necessarily uses lenses or curved mirrors. By adopting non-imaging optics, the diagnostic system avoids the need for a complex and bulky optical train. Positioning the photodiode very close to the probes has the advantage of extremely high collection efficiency: when the thickness of the material between the probes and the photodiode is of the order of 1 micron, the angle of collection of emission light is up to 173°. This angle is calculated by considering light emitted from a probe at the centroid of the face of the hybridization chamber closest to the photodiode, which has a planar active surface area parallel to that chamber face. The cone of emission angles within which light is able to be absorbed by the photodiode is defined as having the emitting probe at its vertex and the corner of the sensor on the perimeter of its planar face. For a 16 micron×16 micron sensor, the vertex angle of this cone is 170°; in the limiting case where the photodiode is expanded so that its area matches that of the 29 micron×19.75 micron hybridization chamber, the vertex angle is 173°. A separation between the chamber face and the photodiode active surface of 1 micron or less is readily achievable.

[0437] Employing a non-imaging optics scheme does require the photodiode **184** to be very close to the hybridization chamber in order to collect sufficient photons of fluorescence emission. The maximum spacing between the photodiode and probes is determined as follows with reference to FIG. **54**.

[0438] Utilizing a terbium chelate fluorophore and a SET UVTOP335TO39BL LED, we calculated **11600** photons reaching our 16 micron×16 micron photodiode **184** from the respective hybridization chamber **180**. In performing this calculation we assumed that the light-collecting region of our hybridization chamber **180** has a base area which is the same as our photodiode active area **185**, and half of the total number of the hybridization photons reaches the photodiode **184**. That is, the light gathering efficiency of the optical system is ϕ_0=0.5.

[0439] More accurately we can write ϕ_0=[(base area of the light-collecting region of the hybridization chamber)/(photodiode area)][$\Omega/4\pi$], where Ω=solid angle subtended by the photodiode at a representative point on the base of the hybridization chamber. For a right square pyramid geometry: $\Omega=4\arcsin(a^2/(4d_0^2+a^2))$, where d_0=distance between the chamber and the photodiode, and a is the photodiode dimension.

[0440] Each hybridization chamber releases 23200 photons. The selected photodiode has a detection threshold of 17 photons; therefore, the minimum optical efficiency required is:

$$\phi_0 = 17/23200 = 7.33\times10^{-4}$$

[0441] The base area of the light-collecting region of the hybridization chamber **180** is 29 micron×19.75 micron.

[0442] Solving for d_0, we will get the maximum limiting distance between the bottom of our hybridization chamber and our photodiode **184** to be d_0=249 microns. In this limit, the collection cone angle as defined above is only 0.8°. It should be noted this analysis ignores the negligible effect of refraction.

Test Module with Microfluidic Device Having Dialysis Device, LOC and Interconnecting Cap

[0443] A test module **11** for analysing a sample fluid containing target molecules is shown in FIG. **109**. The test module **11** comprises an outer casing **13** with a receptacle **24** for receiving the sample fluid, a removable sterile sealing tape **22** to cover the receptacle **24** prior to use, a membrane seal **408** with a membrane guard **410** forming part of the outer casing **13** to reduce dehumidification within the test module while providing pressure relief from small air pressure fluctuations with the membrane guard **410** protecting the membrane seal **408** from damage, a printed circuit board (PCB) **57**, a microfluidic device **783**, a porous element **49**, a standard Micro-USB plug **14** for power, data and control, external power supply capacitors **32**, and inductor **15**.

[0444] The microfluidic device **783** has a dialysis device **784** in fluid communication with the receptacle **24** and configured to separate the target molecules from other constituents of the sample, a LOC device **785** for analysing the target molecules and a cap **51** overlaying the LOC device **785** and the dialysis device **784** for establishing fluid communication between the LOC device **785** and the dialysis device **784**.

Reagent Loading and Probe Spotting System

[0445] Reagent reservoirs **54**, **56**, **58**, **60** and **62** (see FIG. **6**) are filled with reagents and water from a robotic, droplet ejection system shown in FIGS. **63** to **66**. The robotic system also spots the oligonucleotide FRET probes **186** or ECL probes **237** into the hybridization chambers **180**. Droplet dispensing technology is an inexpensive spotting technique, delivers small droplets with reproducible volumes and many droplets of different solutions can be dispensed simultaneously. This allows the LOC devices to be mass produced at extremely high throughput and low cost.

[0446] The reagent and probe spotting system includes three robotic subsystems:

[0447] 1. Reagent dispensing robot **256** (see FIG. **63**)—microvials **258** (see FIG. **64**), each with a droplet dispenser **262**, dispense reagents into the reservoirs **54**, **56**, **58**, **60** and

62 and water into the water reservoir 188 (see FIG. 6). It then applies the patterned upper seal 82 (if necessary) to the cap 46.

[0448] 2. ONEC refill robot 274 (see FIG. 65)—microvials 258 with a droplet dispenser 262 dispense probes into the reservoirs 278 of an oligonucleotide ejector chip (ONEC) 272 (see FIGS. 71 and 72). The ONEC reservoirs 278 feed an array of thermal droplet generators 271. The ONEC is then used in the third robotic subsystem, the LOC spotting robot.

[0449] 3. LOC spotting robot 289 (schematically shown in FIG. 66)—ONEC 272 spots each hybridization chamber 180 of the LOC device 30 with probes using a thermal droplet generator 271 (see FIG. 72).

Microvials

[0450] The reagent dispensing robot 256 and the ONEC refill robot 274 both use microvials 258 as shown schematically in FIG. 64. Probes and reagents are ordered directly from the suppliers in macrovials (not shown). Liquids are micropipetted from the macrovials into a container 259 on each of the microvials 258 to form small aliquots (typically between 282 microliters and 400 microliters) that can be refrigerated along with the macrovials until required. Each microvial 258 has a piezoelectric droplet dispenser 262 and an enclosed quality assurance chip (i.e. integrated circuit) 266 with flash memory and electrical contacts 264 for power and data transmission. The droplet dispenser 262 has a piezoelectric actuator 261 configured to eject drops with a volume between 50 picoliters and 150 picoliters for reasonably quick reagent loading while maintaining accurate drop placement.

Probe and Reagent Identification Scheme

[0451] The quality assurance chip 266 (see FIG. 64) has digital memory used to store, identify and track the specification data characterizing the reagent or oligonucleotide probe solution within the microvial 258. At the end of the spot and load process, the data from each microvial 258, along with other loading and spotting data, is downloaded and stored in the program and data flash memory 40 of the LOC device 30 via the control microprocessor 263 controlling the reagent dispensing robot or probe dispensing robot. This data is used for diagnostic information and processing tasks, quality control and auditing.

[0452] Referring to FIG. 73, ONEC 272 also has digital memory such as flash memory 281 in the ONEC CMOS structure 285 to store oligonucleotide specification data such as probe identities, batch numbers and so on. As with the LOC device, the ONEC refill robot 274 downloads the specification data to the ONEC flash memory 281 from the quality assurance chips 266 on the microvials 258.

[0453] Automated information transfer minimizes the possibility of errors occurring and in the event an incorrect microvial is used, the test module reader 12 or other system component identifies this error when processing the diagnostic information.

Reagent Dispensing Robot

[0454] A simplified top and side view of the reagent dispensing robot 256 are shown in FIGS. 63 and 108. It includes:

[0455] microvials 258 containing reagents and molecular biology grade water (only some of the microvials are shown)

[0456] mechanical/electrical rack 286 (shown only in outline) which holds and provides electrical connectivity to microvials 258

[0457] XY stage 268 providing a surface for detachably mounting a partial-depth sawn silicon wafer 260 or other fixed array such as separable PCB wafer 720

[0458] Registration camera 270 providing feedback to the control microprocessor 263 for mapping the exact location of the piezoelectric droplet dispensers 262

[0459] The piezoelectric droplet dispensers 262 on the microvials 258 are used to dispense the reagents and water directly into the LOC device reservoirs 54, 56, 58, 60 and 62 and the humidifier water reservoir 188 respectively.

ONEC Refill Robot

[0460] The ONEC refill robot 274 is shown in FIG. 65. It is similar to the reagent dispensing robot 256 and includes:

[0461] 1080 microvials 258 containing solutions of oligonucleotide probes (for the purposes of illustration, not all microvials are shown)

[0462] mechanical/electrical rack 286 (shown only in outline)—holds and provides electrical connectivity to microvials 258

[0463] oligonucleotide ejector chip (ONEC) 272—with 1080 ONEC reservoirs 278 supplying respective ejectors 287 with four ONEC thermal droplet generators 271 each (see FIGS. 71 and 72)

[0464] XY stage 268: holds the oligonucleotide ejector chip/s (ONEC/s) 272

[0465] Registration camera 270 providing feedback to the control microprocessor 263 for mapping the exact location of the thermal droplet generators 271

[0466] The ONEC 272 is moved under the mechanical/electrical rack 286. A unique probe solution is dispensed from each microvial 258 into each ONEC reservoir 278. The ONEC 272 is then used in the probe spotting robot 273 to spot the LOC device hybridization chambers 180 with a single droplet of probe solution.

ONEC

[0467] FIGS. 71, 72 and 73 show the ONEC 272 in detail. The ONEC 272 is an oligonucleotide spotting device for contactless spotting of probes onto a surface such as the hybridization chamber array in any of the LOC devices. It has overall dimensions of 23,296 μm×1,760 μm and is fabricated using well-established high volume photolithography fabrication techniques. Each ONEC has 1080 reservoirs 278 etched into the reservoir side 277 of a monolithic silicon substrate 275 (see FIG. 73). With more than 1000 reservoirs 278, each ONEC has the complete assay of probes needed to spot the LOC devices described herein. This allows the spotting process of each LOC to be one-step in the sense that there is no need to use more than one ONEC to spot LOCs configured for each particular analysis. The ONEC reservoirs 278 have a rectangular base (96 μm×208 μm) with a depth of 200 μm. Each ONEC reservoir 278 feeds a probe suspension to a respective ejector 287. The liquid suspension of probes fill a common chamber 282 via a pair of chamber inlets 284 (see FIG. 72). The chamber inlets 284 are two 21 μm diameter holes from the reservoir 278 to the common chamber 282. One of four thermal droplet generators 271 ejects probe droplets through nozzles 283 in the ejector side 279 into the hybridization chambers 180 by heating the actuator 280 to

generate a vapor bubble. Having four thermal droplet generators **271** allows for redundancy if there is a droplet generator failure.

LOC Probe Spotting Robot

[0468] The LOC probe spotting robot **289** is shown in FIGS. **66** and **92**. For clarity, components other than the LOC device **30** on the PCB wafer **720** are not shown. It includes the following:

[0469] ONEC **272**—oligonucleotide ejector chip with 1080 reservoirs **278**, each filled with a probe solution (see FIGS. **71** and **72**)

[0470] XY stage **268**: holds the partial-depth sawn silicon LOC wafer **260** (see FIG. **66**) or alternatively the separable PCB wafer **720** (see FIG. **92**)

[0471] Registration camera **270** providing feedback to the control processor **263** for mapping the exact location of the ONEC thermal droplet generators **271**

[0472] The LOC silicon wafer **260** or the separable PCB wafer **720** is detachably mounted to a stage that can translate along two orthogonal axes. The ONEC **272** is detachably held in a chuck **265** that is closely adjacent the stage with the ejectors **287** facing the stage (see FIG. **66**). The LOC silicon wafer **260** or the separable PCB wafer **720** is moved relative to the ONEC **272** by the control processor **263**. Each LOC device hybridization chamber **180** is spotted by the ejectors under the operative control of the control processor **263**. Using volumes less than 100 picoliters reduces the reaction times and allows the density of the hybridization chamber array to increase. Spotting low-volume probe droplets has not been previously adopted because of the difficulty associated with ejecting very small droplets precisely and reliably. Misdirected drops can fail to spot the correct chamber and may contaminate an adjacent chamber.

[0473] The ONEC **272** can be driven to generate a range of droplet volumes. For accurate dispensing, the droplets generated by the ONEC **272** would be less than 100 picoliters. To improve the accuracy of the probes and reagents dispensed (in terms of volume and position on the LOC device), the droplets generated by the ONEC can be reduced to less than 25 picoliters, and preferably less than 6 picoliters. The ONEC **272** dispenses probe solution into the 1080 hybridization chambers **180** in droplets with volumes between 0.1 picoliters and 1.6 picoliters and a high degree of positional accuracy.

[0474] The hybridization chamber array **110** is configured as 24 rows with 45 adjacent chambers in each row (see FIG. **52**). The sample flow-path **176** extends between every second row such that the overall array has a substantially square shape for approximately uniform illumination by the LED **26**. As the hybridization chamber array **110** is confined to an area less than 1500 microns by 1500 microns, the spotting accuracy of the ONEC **272** is necessarily high. A registration camera **270** is used by the control processor **263** to determine the exact position of the ONEC thermal droplet generators **271** and the droplet generator drive pulses are synchronized with the XY stage **268** via the ONEC bond-pads **276**.

[0475] The LOC probe spotting robot **273** using the ONEC **272** and camera **270** can easily spot probes onto a surface (such as the hybridization chamber array **110**) at a rate greater than 100 probes per second; in the vast majority of cases at a rate greater than 1,400 probes per second. Typically, the array of droplet generators spot the probes onto the surface at a rate greater than 20,000 probes per second and in many cases, the array of droplet generators spot the probes onto the surface at a rate between 300,000 probes per second and 1,000,000 probes per second.

[0476] The array of droplet generators lithographically fabricated on a silicon substrate allows the ONEC **272** to spot oligonucleotides onto a surface at a density far greater than existing probe spotters. ONEC **272** easily spots at a density of more than 1 probe per square millimetre. In the vast majority of cases, the spotting density is greater than 8 probes per square millimetre. In most cases, the spotting density is more than 60 probes per square millimetre, and typically the density is between 500 probes per square millimetre and 1,500 probes per square millimetre.

[0477] The LOC probe spotting robot **273**, using the ONEC **272** as a biochemical deposition device, can easily deposit biochemicals onto a surface at a rate greater than 100 droplets per second, in the vast majority of cases at a rate greater than 1,400 droplets per second. Typically, the array of droplet generators spot the droplets onto the surface at a rate greater than 20,000 droplets per second, and in many cases, the array of droplet generators spot the droplets onto the surface at a rate between 300,000 droplets per second and 1,000,000 droplets per second.

[0478] The LOC probe spotting robot **273**, using the ONEC **272** as a biochemical deposition device, can easily deposit biochemicals onto a surface at a density of more than 1 droplet per square millimetre. In the vast majority of cases, the spotting density is greater than 8 droplets per square millimetre. In most cases, the spotting density is more than 60 droplets per square millimetre, and typically the density is between 500 droplets per square millimetre and 1,500 droplets per square millimetre.

CONCLUSION

[0479] The devices, systems and methods described here facilitate molecular diagnostic tests at low cost with high speed and at the point-of-care.

The system and its components described above are purely illustrative and the skilled worker in this field will readily recognize many variations and modifications which do not depart from the spirit and scope of the broad inventive concept.

1. A microfluidic test module for analyzing a sample fluid and communicating test results to a tablet computer, the microfluidic test module comprising:

an outer casing with a receptacle for receiving the sample;

functional sections for processing and analyzing the sample;

a communication interface for communication with the tablet computer; and,

a controller for operative control of the communication interface.

2. The microfluidic test module according to claim **1** wherein the communication interface is a universal serial bus (USB) device driver for operative control of a USB plug in the test module for communication with an external device.

3. The microfluidic test module according to claim **2** wherein the USB device driver is configured to draw power from the tablet computer to power the controller and the functional sections.

4. The microfluidic test module according to claim **3** wherein the controller is further configured for operative control of the functional sections during processing and analysis of the sample.

5. The microfluidic test module according to claim **4** wherein the controller is configured to download data via the tablet computer.

6. The microfluidic test module according to claim **1** further comprising a plurality of reagent reservoirs containing reagents for processing the sample and digital memory for storing data relating to the reagent identities.

7. The microfluidic test module according to claim **6** wherein the data stored in the digital memory is a unique identifier for microfluidic test module.

8. The microfluidic test module according to claim **7** wherein the sample is a biological sample containing genetic material and one of the functional sections is a nucleic acid amplification section for amplifying nucleic acid sequences in the genetic material.

9. The microfluidic test module according to claim **8** wherein the nucleic acid amplification section is a polymerase chain reaction (PCR) section and the data stored in the digital memory includes thermal cycle times and cycle numbers.

10. The microfluidic test module according to claim **9** wherein the functional sections include an incubation section upstream of the PCR section and one of the reagent reservoirs is a restriction enzyme reservoir, the incubation section having a heater for maintaining a mixture of the sample and restriction enzymes at an incubation temperature during restriction digestion of the nucleic acid sequences.

11. The microfluidic test module according to claim **9** further comprising an array of probes for hybridization with target nucleic acid sequences in the amplicon from the PCR section.

12. The microfluidic test module according to claim **11** wherein the data stored in the digital memory includes probe identity data identifying the probe at each site within the array of probes.

13. The microfluidic test module according to claim **11** further comprising a photosensor wherein each of the probes are configured to form a probe-target hybrid with a complementary target nucleic acid sequence contained in the amplicon, each of the probe-target hybrids being configured to emit photons in response to an input, and the photosensor is configured for sensing the photons emitted by the probe-target hybrids.

14. The microfluidic test module according to claim **13** wherein the data stored in the digital memory includes hybridization data generated from the photosensor output.

15. The microfluidic test module according to claim **14** further comprising a hybridization chamber array for containing the probes such that the probes within each hybridization chamber are configured to hybridize with one of the target nucleic acid sequences.

16. The microfluidic test module according to claim **15** wherein the photosensor is an array of photodiodes positioned in registration with the hybridization chambers.

17. The microfluidic test module according to claim **16** wherein the controller is configured for transmission of the hybridization data to the tablet computer.

18. The microfluidic test module according to claim **15** wherein the sample is drawn from a patient and the controller is configured to download patient data via the tablet computer and store the patient data in the digital memory.

19. The microfluidic test module according to claim **15** wherein the PCR section has an active valve for retaining liquid in the PCR section during thermal cycling and allowing flow to the hybridization chambers in response to an activation signal from the controller.

20. The microfluidic test module according to claim **19** wherein the active valve is a boiling-initiated valve with a meniscus anchor configured to pin a meniscus that arrests capillary driven flow of the liquid, and a heater for boiling the liquid to unpin the meniscus from the meniscus anchor such that capillary driven flow resumes.

* * * * *